ADVANCES IN DRUG FORMULATION

EDITED BY: Biswajit Mukherjee, Johan Engblom, Paul Chi-Lui Ho and Veranja Karunaratne

PUBLISHED IN: Frontiers in Pharmacology

frontiers Research Topics

ISSN 1664-8714
ISBN 978-2-88966-369-9
DOI 10.3389/978-2-88966-369-9

About Frontiers

Frontiers is more than just an open-access publisher of scholarly articles: it is a pioneering approach to the world of academia, radically improving the way scholarly research is managed. The grand vision of Frontiers is a world where all people have an equal opportunity to seek, share and generate knowledge. Frontiers provides immediate and permanent online open access to all its publications, but this alone is not enough to realize our grand goals.

Frontiers Journal Series

The Frontiers Journal Series is a multi-tier and interdisciplinary set of open-access, online journals, promising a paradigm shift from the current review, selection and dissemination processes in academic publishing. All Frontiers journals are driven by researchers for researchers; therefore, they constitute a service to the scholarly community. At the same time, the Frontiers Journal Series operates on a revolutionary invention, the tiered publishing system, initially addressing specific communities of scholars, and gradually climbing up to broader public understanding, thus serving the interests of the lay society, too.

Dedication to Quality

Each Frontiers article is a landmark of the highest quality, thanks to genuinely collaborative interactions between authors and review editors, who include some of the world's best academicians. Research must be certified by peers before entering a stream of knowledge that may eventually reach the public - and shape society; therefore, Frontiers only applies the most rigorous and unbiased reviews.
Frontiers revolutionizes research publishing by freely delivering the most outstanding research, evaluated with no bias from both the academic and social point of view. By applying the most advanced information technologies, Frontiers is catapulting scholarly publishing into a new generation.

What are Frontiers Research Topics?

Frontiers Research Topics are very popular trademarks of the Frontiers Journals Series: they are collections of at least ten articles, all centered on a particular subject. With their unique mix of varied contributions from Original Research to Review Articles, Frontiers Research Topics unify the most influential researchers, the latest key findings and historical advances in a hot research area! Find out more on how to host your own Frontiers Research Topic or contribute to one as an author by contacting the Frontiers Editorial Office: researchtopics@frontiersin.org

ADVANCES IN DRUG FORMULATION

Topic Editors:
Biswajit Mukherjee, Jadavpur University, India
Johan Engblom, Malmö University, Sweden
Paul Chi-Lui Ho, National University of Singapore, Singapore
Veranja Karunaratne, University of Peradeniya, Sri Lanka

Citation: Mukherjee, B., Engblom, J., Ho, P. C.-L., Karunaratne, V., eds. (2021). Advances in Drug Formulation. Lausanne: Frontiers Media SA.
doi: 10.3389/978-2-88966-369-9

Table of Contents

frontiers in Pharmacology

EDITORIAL
published: 27 November 2020
doi: 10.3389/fphar.2020.608771

Editorial: Advances in Drug Formulation

Biswajit Mukherjee[1]*, *Johan Engblom*[2], *Paul Chi-Lui Ho*[3] and *Veranja Karunaratne*[4]

[1]Department of Pharmaceutical Technology, Jadavpur University, Kolkata, India, [2]Department of Biomedical Science, Malmö University, Malmö, Sweden, [3]Department of Pharmacy, National University of Singapore, Singapore, [4]Department of Chemistry, University of Peradeniya, Peradeniya, Sri Lanka

Keywords: editorial, nanoliposomes, microwave ablation, nanoparticles, colon cancer, gastrointestinal tract

Editorial on the Research Topic

Advances in Drug Formulation

Advancement instils no ceiling. With vast amelioration of technology and blooming of biomedical information, a tremendous effort for improvement in drug delivery technology has been observed. The advancement of drug formulation has also been leading more toward further sophistication of drug transport systems that could deliver drug to site-specific cells/tissues/organs *in vivo*. Such target–specific drug delivery systems are needed because they can decrease dose and frequency of administration of drugs and thereby, reduce drug-related toxicity (Chakraborty et al., 2020). The present issue has highlighted several current areas related to the advancement of drug formulations.

In an interesting study, Wu et al. (2020) showed that doxorubicin-loaded liposomes enhanced the efficiency of electromagnetic waves (Microwave ablation, MWA) at solid tumors during hepatocellular carcinoma therapy. The investigators showed that doxorubicin-loaded nanoliposomes robustly enhanced mild MWA therapy in hepatocellular carcinoma, indicating their substantial tumor sensitizing ability. The researchers have claimed that the chemoablation therapy improved survival rates by enhancing the targeting efficiency. The formulations showed considerable promise for clinical HCC therapy.

Li et al. (2019) described the potentials of tocopherol polyethylene glycol 1,000 succinate (TPGS)/curcumin (CCM) micellar nanoparticles as a drug delivery system against colon cancer. The investigation showed that loading CCM into TPGS nanoparticles significantly enhanced its systemic absorption, increasing its Cmax, and producing a more sustained release profile, and increased apoptosis, and inhibited migration of HT-29 colon cancer cells. The nanoparticles efficiently released CCM in simulated colonic fluid and were significantly more efficacious than free CCM in reducing ROS concentration. Thus, the findings of the investigation shed light to test the nanoparticles against colon cancer in animal model in future study.

Moles et al. (2019) showed how malaria can be potentially managed with liposomal systems of diprotic basic drugs. The researchers have theorized novel distribution models to describe the partitioning behavior of diprotic basic drugs in 1,2-dioleoyl-sn-glycero-3-phosphocholine-based and red blood cell-analogous liposome suspensions. They further directed stable internalization of ionized drug microspecies into neutrally charged and anionic lipid bilayer leaflets in the form of ion pairs in association with anionic lipids. They have further claimed RBC as a clinically safe long-circulating carrier for polyprotic drugs, and the optimization of antimalarial therapies using RBC-targeted liposomal drug formulations.

Wang et al. (2019) showed that hepatic inflammatory proteins, CRP and TNF-α, and serum levels of IL1α were significantly increased in 5-PAHSA (palmitic acid esterified at the fifth carbon of hydroxy stearic acid)-treated db/db mice compared to the control mice. However, the effects of 5-PAHSA were not dose-dependent. Likewise, 5-PAHSA did not produce inflammatory factors in the

OPEN ACCESS

Edited and reviewed by:
Salvatore Salomone, University of Catania, Italy

***Correspondence:**
Biswajit Mukherjee
biswajit.mukherjee@jadavpuruniversity.in; biswajit55@yahoo.com

Specialty section:
This article was submitted to Experimental Pharmacology and Drug Discovery, a section of the journal Frontiers in Pharmacology

Received: *21 September 2020*
Accepted: *15 October 2020*
Published: *27 November 2020*

Citation:
Mukherjee B, Engblom J, Ho PC-L and Karunaratne V (2020) Editorial: Advances in Drug Formulation. Front. Pharmacol. 11:608771. doi: 10.3389/fphar.2020.608771

experimental mice, suggesting chronic 5-PAHSA administration may induce systemic inflammatory responses. The researchers also showed that 5-PAHSA treatment improved glucose tolerance and insulin sensitivity in mice that received a high fat diet. But simultaneously, 5-PAHSA treatment showed no metabolic benefit in db/db mice. Thus, hyperglycemia condition in db/db mice may impair 5-PAHSA effects on metabolism. Finally, they postulated that the hyperglycemic conditions might impair 5-PAHSA action by inhibiting AMPKα mediated signals and promoting NF-κB-mediated inflammation.

Hua (2019a) presented two interesting reviews and a mini-review article. In her first review Hua described the physiological and pharmaceutical considerations for rectal drug formulations. Her profound scientific insights on the rectal route for drug delivery as a preferred route for drug administration with pronounced clinical or pharmaceutical perspectives are worth-mentioning. The rectal route may represent a practical alternative and drugs can be administered for both local and systemic action. The oral route of administration is the most preferred route by patients for gastrointestinal diseases. In her another review, she has provided a vivid understanding of the physiology of the gastrointestinal tract in healthy and diseased states and the use of it in drug delivery by modulating various physiological factors. Hua has opined for multiparticulate dosage systems to improve gastrointestinal drug delivery compared to single-unit dose common formulations (Hua, 2012). In her next erudite article (minireview), Hua showed her prudence describing significant advantages for the sublingual and buccal routes of systemic drug administration, substantiated by many current and focused research works in the areas (Hua, 2019b).

Many new thoughts and ideas along with their implementation have been enriching formulation development. Among the most recent approaches in the research of drug formulations, idea of nanorobots has emerged as a powerful therapeutic tool to develop highly efficacious precision medicines to localize the drug at the target site (da Silva Luz et al., 2016). The nanorobots have the ability to convert the minimum levels of physiological energy into propulsion and movement and can be steered to a target location under physiological environment and conditions leading to predominant improvement in therapeutic efficacy and reduction of systemic side-effects. They can also be programmed to release the therapeutic payloads with a precise release mechanism. Laser-driven nanoformulation for drug delivery is also another novel approach that needs attention.

In summary, drug-targets have already been preset in many diseases. Many sophisticated technologies, unique and powerful methodologies, and many novel pharmaceutical materials are available. Formulation scientists simply need to assemble them to develop smart and intelligent drug consignments that can accurately deliver the drug loads to preset targets. Successful development of many such accurate drug targeting-systems can bring a revolutionary change in drug formulations and human health care.

AUTHOR CONTRIBUTIONS

All authors listed have made a substantial, direct, and intellectual contribution to the work and approved it for publication.

REFERENCES

Chakraborty, S., Dlie, Z. Y., Chakraborty, S., Roy, S., Mukherjee, B., Besra, S. E., et al. (2020). Aptamer-functionalized drug nanocarrier improves hepatocellular carcinoma toward normal by targeting neoplastic hepatocytes. *Mol. Ther. Nucleic Acids* 20, 34–49. doi:10.1016/j.omtn.2020.01.034

da Silva Luz, G. V., Barros, K. V. G., de Araújo, F. V. C., da Silva, G. B., da Silva, P. A. F., Condori, R. C. I., et al. (2016). Nanorobotics in drug delivery systems for treatment of cancer: a review. *J. Mater. Sci. Eng.* 6 (5–6), 167–180. doi:10.17265/2161-6213/2016.5-6.005

Conflict of Interest: The authors declare that the research was conducted in the absence of any commercial or financial relationships that could be construed as a potential conflict of interest.

frontiers in Pharmacology

ORIGINAL RESEARCH
published: 07 January 2019
doi: 10.3389/fphar.2018.01491

High Glucose Concentration Impairs 5-PAHSA Activity by Inhibiting AMP-Activated Protein Kinase Activation and Promoting Nuclear Factor-Kappa-B-Mediated Inflammation

*Yan-Mei Wang, Hong-Xia Liu and Ning-Yuan Fang**

Department of Geriatrics, Renji Hospital, School of Medicine, Shanghai Jiao Tong University, Shanghai, China

OPEN ACCESS

Edited by:
Salvatore Salomone,
Università degli Studi di Catania, Italy

Reviewed by:
Zecharia Madar,
Hebrew University of Jerusalem, Israel
Elisa Pagnin,
Università degli Studi di Padova, Italy

****Correspondence:***
Ning-Yuan Fang
fnyuan123@163.com

Specialty section:
This article was submitted to Experimental Pharmacology and Drug Discovery, a section of the journal Frontiers in Pharmacology

Received: *29 September 2018*
Accepted: *05 December 2018*
Published: *07 January 2019*

Citation:
Wang Y-M, Liu H-X and Fang N-Y (2019) High Glucose Concentration Impairs 5-PAHSA Activity by Inhibiting AMP-Activated Protein Kinase Activation and Promoting Nuclear Factor-Kappa-B-Mediated Inflammation. Front. Pharmacol. 9:1491. doi: 10.3389/fphar.2018.01491

Recently, the endogenous fatty acid palmitic acid-5-hydroxystearic acid (5-PAHSA) was found to increase insulin sensitivity and have anti-inflammatory effects in mice with high-fat diet (HFD)-induced diabetes. However, it is unknown if 5-PAHSA affects glucose and lipid metabolism in db/db mice, which are characterized by extreme hyperglycemia. Here, we aim to determine the effect of continued 5-PAHSA administration on glucose and lipid metabolism in db/db mice. We also used 3T3-L1 cells and HepG2 cells to investigate the mechanism behind this effect. HepG2 cells and 3T3-L1 cells were induced to become models of insulin resistance. The models were used to test the effect of 5-PAHSA on insulin signaling. 5-PAHSA was administered orally to db/db mice for 1 month to assess its effects on glucose and lipid metabolism. We also exposed HepG2 cells to high glucose concentrations to investigate the influence on 5-PAHSA's effects on hepatic lipid metabolism and inflammation. 5-PAHSA improved glucose uptake and insulin signaling in HepG2 cells and 3T3-L1 cells. However, after 1 month of treatment, 5-PAHSA did not reduce blood glucose levels, but increased inflammation and promoted fatty liver in db/db mice. In HepG2 cells under normal glucose conditions, 5-PAHSA treatment reduced lipogenesis and increased lipid oxidation. Notably, a high glucose concentration in cell media abolished the positive effects of 5-PAHSA treatment. These changes were associated with: decreased phosphorylation of AMP-activated protein kinase (AMPK) and acetyl-CoA carboxylase (ACC); upregulation of sterol-regulatory element-binding protein 1c (SREBP1c), and fatty acid synthase (FAS); and downregulation of carnitine palmitoyltransferase 1 (CPT1). Besides, the anti-inflammatory effect of 5-PAHSA was also impaired by high glucose conditions. Thus, high glucose concentrations impaired 5-PAHSA action by inhibiting the AMPK signaling pathway and promoting nuclear factor-kappa-B (NF-κB) mediated inflammation.

Keywords: 5-PAHSA, insulin resistance, inflammation, fatty liver, high glucose

INTRODUCTION

Type 2 diabetes mellitus (T2DM) is a disease that affects more than 400 million people worldwide (Nathan, 2015). The medical and economic burdens of diabetes present an important public health challenge for the developed and the developing world (American Diabetes Association, 2013; Le et al., 2013; Seuring et al., 2015; Bao et al., 2017). Further, there is an urgent need for safe and effective interventions for T2DM because most currently used medications for long-term T2DM treatment have side effects, such as hypoglycemia, weight gain, and gastrointestinal reactions (Stein et al., 2013).

There is a strong association between T2DM and dyslipidemia, as >70% of patients with T2DM develop non-alcoholic fatty liver disease (NAFLD) with the inflammatory complication, non-alcoholic steatohepatitis (NASH) (Williams et al., 2011; Loomba et al., 2012). Several studies have demonstrated that elevated levels of free fatty acids play a causative role in metabolic syndrome (Devaraj et al., 2008; Sun and Chen, 2010; Perry et al., 2015). However, Yore et al. (2014) reported recently that the endogenous fatty acid, 5-PAHSA, had favorable metabolic effects via binding and activating its G-protein-coupled receptor 120 (GPR120). Consistent downregulation of 5-PAHSA was found in all adipose depots and the serum of insulin-resistant mice, as well as in the white adipose tissue and serum of insulin-resistant humans. Acute oral administration of 5-PAHSA in insulin-resistant high-fat diet (HFD)-fed mice lowered basal glycemia and improved glucose tolerance (Yore et al., 2014). Moreover, chronic 5-PAHSA treatment improved insulin sensitivity in chow- and HFD-fed mice (Syed et al., 2018). Besides, 5-PAHSA might also reduce inflammatory cytokine production from immune cells and ameliorate adipose inflammation in obesity.

Discovery of the anti-diabetic and anti-inflammatory effects of 5-PAHSA make it a promising candidate for further research and drug development. However, when considering clinical applications, the effect of repeated and continuous administration of 5-PAHSA for diabetic metabolic disorders should be better understood.

Leptin receptor deficient db/db mice are widely used as a diabetic model for T2DM research (Wang et al., 2014). The db/db mouse is the most popular animal model used by pharmaceutical companies to test blood glucose lowering agents, insulin sensitizers, insulin secretagogues, and anti-obesity agents (Reed and Scribner, 1999). Since the effect of 5-PAHSA treatment on db/db mice has not been characterized, one aim of this study was to investigate the effects of repeated 5-PAHSA treatment on glucose and lipid metabolism in db/db mice. We found that 1 month of 5-PAHSA administration had no beneficial effect on glucose metabolism in db/db mice. Moreover, we found that the course of 5-PAHSA treatment promoted hepatic fatty infiltration and inflammatory responses in these mice. The mechanisms governing these negative effects of 5-PAHSA treatment, particularly in the liver, are not fully understood. Given that high blood glucose levels are characteristic of db/db mice, we hypothesized that hyperglycemia may alter the effects of 5-PAHSA treatment and tested this hypothesis in human liver-derived HepG2 cells. Thus, the other aim of this study was to study the role of hyperglycemia in the impairment of 5-PAHSA action.

MATERIALS AND METHODS

Reagents

Radio-immunoprecipitation assay (RIPA) buffer, Dulbecco's Modified Eagle's Medium (DMEM), TRIzol reagent, fetal bovine serum (FBS), penicillin/streptomycin, phenylmethylsulfonyl fluoride (PMSF), and Halt protease and phosphatase inhibitor cocktail were obtained from Thermo Fisher Scientific (Waltham, MA, United States). D-glucose, bovine serum albumin (BSA), insulin and Dimethylsulfoxide (DMSO) were obtained from Sigma-Aldrich (St. Louis, MO, United States). Phosphate-buffered saline (PBS) was obtained from GE Healthcare Life Sciences (Beijing, China). The bicinchoninic acid (BCA) protein assay and primary antibody dilution buffer were obtained from Beyotime (Nanjing, China). Antibodies against insulin receptor substrate 1 (IRS1), pThr896-IRS1, insulin receptor substrate 2 (IRS2), pSer731-IRS2, protein kinase B (Akt), pSer473-Akt, GPADH, AMP-activated protein kinase alpha (AMPKα), pThr172-AMPKα, acetyl-CoA carboxylase (ACC), pSer79-ACC, carnitine palmitoyltransferase 1 (CPT1), fatty acid synthase (FAS), IκB alpha, pSer36-IκB alpha, NF-κB, pSer536-NF-κB, and β-actin were obtained from Abcam (Cambridge, MA, United States), and the antibody against sterol-regulatory element-binding protein 1c (SREBP1c) was obtained from Santa Cruz (Dallas, TX, United States).

Synthesis and Verification of 5-PAHSA

Detailed information on synthesis and verification of 5-PAHSA is outlined in the **Supplementary Information**.

Cell Culture and Treatments

3T3-L1 cells and human hepatoma HepG2 cell line were obtained from the Chinese Academy of Medical Sciences and Peking Union Medical College (Beijing, China). 3T3-L1 cells were grown in DMEM supplemented with 10% FBS, 200 U/ml penicillin, and 200 U/ml streptomycin in 5% CO_2 humidified atmosphere at 37°C until confluence. Two days after confluence, to induce adipocyte differentiation, cells were incubated for 48 h in DMEM supplemented with 10% FBS containing 500 μM 3-isobutyl-1-methylxanthine (IBMX), 0.25 μM dexamethasone, and 10 μg/ml insulin. Then the cells were maintained in culture medium supplemented with insulin only, which were changed every 2 days until complete differentiation. To induce insulin resistance, mature 3T3-L1 cells were treated with recombinant mouse tumor necrosis factor (TNF)-α (4 ng/ml). Media was changed daily for TNF-α treatment, for a total incubation time of 4 days. For 5-PAHSA treatment, 3T3-L1 cells were treatment with 5-PAHSA (20 μM) for 2 days, and then harvested for RNA or protein isolation.

We cultured HepG2 cells in DMEM, with either a normal glucose concentration (5.5 mM D-glucose) or a high glucose concentration (30 mM). To induce insulin resistance, HepG2 cells were treatment with high insulin (100 nM). Media was

changed daily for a total incubation time of 3 days. For 5-PAHSA treatment, HepG2 cells were treated with 5-PAHSA (20 μM) for 2 days, and then harvested for RNA or protein isolation.

Immunofluorescence Staining

Immunofluorescence staining was conducted based on standard procedures for the Glut4 membrane translocation analysis. Briefly, cells were blocked with 5% BSA for 30 min at room temperature with membrane rupture treatment by Triton to detect total Glut4 or without membrane rupture to determine membrane distribution. Cells were incubated at 4°C with anti-Glut4 antibody overnight. Equal PBS was added instead of Glut4 as a negative control. The Cy3-conjugated secondary antibody was applied to the samples at room temperature for 1 h. After washing with PBS, images were immediately captured under an immunofluorescence microscope.

Glucose Uptake Assay

Cells in 96 well dishes were washed twice with PBS and incubated with 100 μl KRPH/2% BSA for 40 min. Prepare sample background controls, insulin stimulated cells and non-stimulated control samples. (1) Sample background control (untreated) cells: Do not add insulin and 2-deoxyglucose (2-DG). (2) Insulin stimulated cells: KRPH/2% BSA contained with 10 μM insulin for 20 min and add 10 μl of 10 mM 2-DG for 20 min. (3) Non-stimulated control samples: Non-insulin stimulated cells, but add 10 μl of 10mM 2-DG for 20 min. Prepare Reaction Mix A and add in all samples. And incubate for 1 h. Add 90 μl Extraction buffer in each well and heat at 90°C for 40 min. Prepare Reaction Mix B fresh and add 38 μl in all wells. Measure output OD at 412 nm wavelength on a microplate reader in a kinetic mode, every 2–3 min, at 37°C protected from light.

Animals

All animal experiments were approved by Fudan University Animal Care and Use Committee. Male db/db and wild-type (WT) C57BL6/J mice were purchased from the Model Animal Research Center of Nanjing University (Nanjing, China). At 3 weeks of age, the C57BL/6 mice were given high fat diet (HFD, Shanghai SLAC Company) for 20 weeks. Mice with random blood glucose > 11.1 mmol/L were considered as insulin-resistant mice. Individual db/db mouse weighed 40 ± 5 g, WT mouse weighed 28 ± 2 g and HFD-induced insulin-resistant mouse weighed 32 ± 2 g. All mice were housed in colony cages with *ad libitum* access to food and water. Mice were kept on a 12/12 h light/dark cycle in a temperature-controlled environment.

Groups and Intervention

Mice were divided into six groups: db/db control group (db/db/C); db/db+5-PAHSA (50 mg/kg per day) group (db/db/L); db/db+5-PAHSA (150 mg/kg per day) group (db/db/H); WT control group (WT/C); WT+5-PAHSA (50 mg/kg per day) group (WT/L). WT+5-PAHSA (150 mg/kg per day) group (WT/H) (n = 5 for each group). For glucose metabolism studies, we added HFD-induced diabetic mice (control; HFD plus 50 mg/kg 5-PAHSA, n = 5 mice) to the above two groups.

We administered 5-PAHSA by gavage once a day for 1 month. The control mice were given with the same volume of vehicle [50% polyethylene glycol (PEG) 400, 0.5% Tween-80, 49.5% H_2O] at the corresponding time points.

Oral Glucose Tolerance Tests (OGTT)

We performed OGTT 5 h after food removal in awake mice. At 4.5 h after food removal (0.5 h before initiation of the OGTT), we gavaged mice with 50 mg/kg/150 mg/kg 5-PAHSA, or with an equivalent volume of vehicle. We gave mice 1 g/kg glucose by gavage 30 min after administration of 5-PAHSA or vehicle and monitored blood glucose over a 2 h period. Before the 5-PAHSA gavage and 5 min after the glucose gavage, we bled mice from the tail vein using heparin coated capillary tubes and determined blood glucose by Accu-Check active bands (Roche Diagnostics) (n = 5 mice for each group).

Measurement of Blood Glucose

We collected blood from the tail vein of each mouse using heparin coated capillary tubes. We measured blood glucose with Accu-Check active bands (Roche Diagnostics) (n = 5 mice for each group).

Staining of Mice Liver Specimens

We fixed liver specimens in 10% formalin, embedded in paraffin, sectioned the tissue (4 μm), and then stained sections with hematoxylin-eosin. We blindly assessed infiltration of inflammatory cells in liver on four random fragments from different areas of each liver (n = 5 mice for each group).

Enzyme-Linked Immunosorbent Assay (ELISA)

We collected blood from the abdominal aorta of mice at the time of sacrifice. Serum C-reactive protein (CRP), TNF-α, interleukin (IL)-1α, and insulin levels were measured by ELISA kit (Sigma-Aldrich, St. Louis, MO, United States), according to the manufacturer's instructions (n = 5 mice for each group).

We extracted hepatic proteins from 50 mg of mouse liver homogenate by homogenization in 1.5 mL of phosphate-buffered saline (PBS) using TissueLyser (Qiagen, CA, United States). We centrifuged the homogenate for 10 min at 1000 g and collected the protein from the lower phase. We quantified CRP and TNF-α in the liver with ELISA (Sigma-Aldrich, St. Louis, MO, United States) (n = 5 mice for each group).

Levels of interleukin 6 (IL-6) and monocyte chemotactic protein 1 (MCP1) in HepG2 cells-conditioned medium were measured using ELISA (Sigma-Aldrich, St. Louis, MO, United States).

Gene Expression Analysis

TRIzol reagent was used to extract total RNA from HepG2 cells. A total of 1 μg RNA was subjected to reverse transcription using the PrimeScript™ RT Reagent kit (Takara, Shiga, Japan). Gene expression was evaluated by Quantitative reverse transcription PCR (qPCR) analysis using SYBR Green reagents (SYBR® Premix Ex Taq™) and the LightCycler®

480 Real-Time PCR System (Roche Diagnostics, Basel, Switzerland). The primers for qPCR of HepG2 cells are shown in **Table 1**.

Oil Red O Staining

Cells were washed with PBS, fixation in 10% formalin for 20 min at room temperature, and further washing with PBS. A mixture of Oil Red O solution and water with ratio of 3:2 was layered onto cells for 60 min, followed by washing three times with deionized water. Images were subsequently captured under a microscope.

Intracellular Triglyceride and Cholesterol Content Assay

We pre-incubated HepG2 cells in a 6-well cell culture plate for 72 h. The cells were cultured in DMEM containing either normal glucose or high glucose, supplemented with 5-PAHSA or vehicle control. After a 72 h incubation, we collected and centrifuged cells at 1000 rpm for 10 min. Cell pellets were washed once with PBS, resuspended in 400 μL PBS buffer, and transferred to a microsmashing tube for ultrasonication (ultrasonic output power of 400 w, intermission/ultrasonication time of 30 s/5 s, total extraction time of 15 s). After ultrasonication, we determined the concentration of cellular triglyceride using an EnzyChrom^{TM} triglyceride assay kit (Bioassay Systems, Hayward, CA, United States) and normalized the measured value to the protein concentration, according to the manufacturer's protocol.

Western Blot Analysis

We applied equal amounts of protein (15 μg/lane) to a 10% SDS-polyacrylamide gel electrophoresis and transferred to a polyvinylidene fluoride (PVDF) membrane (Bio-Rad, CA, United States). We blocked membranes with 5% non-fat dry milk in Tris-buffered saline (TBS) (Amersham Biosciences, Uppsala, Sweden) containing 0.05% Tween-20 (T-TBS) (Bio-Rad, CA, United States) and then incubated overnight at 4°C with antibodies to reveal the expression of them. Then we washed the membranes with T-TBS and incubated with specific secondary antibodies for 1 h. We visualized peroxidase activity with an enhanced chemiluminescence substrate system (ECL; Santa Cruz Biotechnology, Santa Cruz, CA, United States) and quantified the bands using Quantity One (Bio-Rad, CA, United States).

TABLE 1 | The primers for qPCR of HepG2 cells.

Primer	Direction	Sequence (5′–3′)
β-actin	Forward	AGC CTT GTA GGT ACC CAA CC
	Reverse	TCC CAC TCA CCT GAG GTG CTG AA
FAS	Forward	AGG TGG TGA TAG CCGGTA TGT
	Reverse	TGG GTA ATC CAT AGA GCC CAG
CPT1	Forward	CGA TCA TCA TGA CTA TGC GCT ACT
	Reverse	GCC GTG CTC TGC AAA CAT C
SREBPlc	Forward	CAC CGT TTC TTC GTG GAT GG
	Reverse	CCC GCA GCA TCA GAA CAG C
MCP1	Forward	CGC CTC CAG CAT GAA AGT CT
	Reverse	GGA ATG AAG GTG GCT GCT ATG
IL-6	Forward	GGT ACA TCC TCG ACG GCA TCT
	Reverse	GTG CCT CTT TGC TGC TTT CAC

Statistical Analysis

All data are representative of at least three different experiments and are expressed as the mean ± standard error (SE). All data were analyzed using GraphPad Prism software (GraphPad Software Inc., San Diego, CA, United States). We used the analysis of variance (ANOVA) to compare the differences between multiple groups. The non-paired *t*-test was used to analyze two groups after the homogeneity of variance test. We considered differences to be statistically significant at $p < 0.05$.

RESULTS

Effects of 5-PAHSA on Insulin Resistance *in vitro*

To test the effects of 5-PAHSA on insulin resistance, HepG2 cells and 3T3-L1 cells were treated with high insulin and TNF-α, respectively, to become experimental models of insulin resistance (IR). The models were assessed by the ability of insulin to stimulate glucose uptakes. In HepG2 cells, high insulin treatment impaired the action of insulin to stimulate glucose uptake, indicating the successful establishment of IR model using HepG2 cells. However, the defect could be rescued by 5-PAHSA treatment (**Figure 1A**). We also examined the effect of 5-PAHSA on various parameters of insulin signaling. The results showed that treatment with high insulin decreased levels of insulin-stimulated IRS1 phosphorylation at Thr896 and Akt phosphorylation at Ser473, increased IRS2 phosphorylation at Ser731, whereas co-treatment with 5-PAHSA largely prevented this actions (**Figures 1B,C**).

In 3T3-L1 adipocytes, insulin-dependent glucose uptake was decreased by TNF-α treatment. The results showed the successful establishment of IR model using 3T3-L1 adipocytes. However, the defect in insulin action was reversible by 5-PAHSA treatment (**Figure 2A**). TNF-α treatment decreased levels of insulin-stimulated phosphorylation on IRS1 (Thr896) and Akt (Ser473), increased phosphorylation on IRS2 (Ser731), but 5-PAHSA treatment largely prevented this effects (**Figures 2B,C**). TNF-α alone or together with 5-PAHSA had no effect on total Glut4 levels (**Figures 2B–D**). However, the expression levels of Glut4 on cell surface were decreased in TNF-α treated 3T3-L1 adipocytes compared with control based on immunofluorescence detection. In contrast, 5-PAHSA treatment significantly increased Glut4 plasma membrane translocation (**Figure 2E**). Together, our results indicated that 5-PAHSA can significantly reduce high insulin- and TNF-α-induced insulin resistance in HepG2 cells and 3T3-L1 cells.

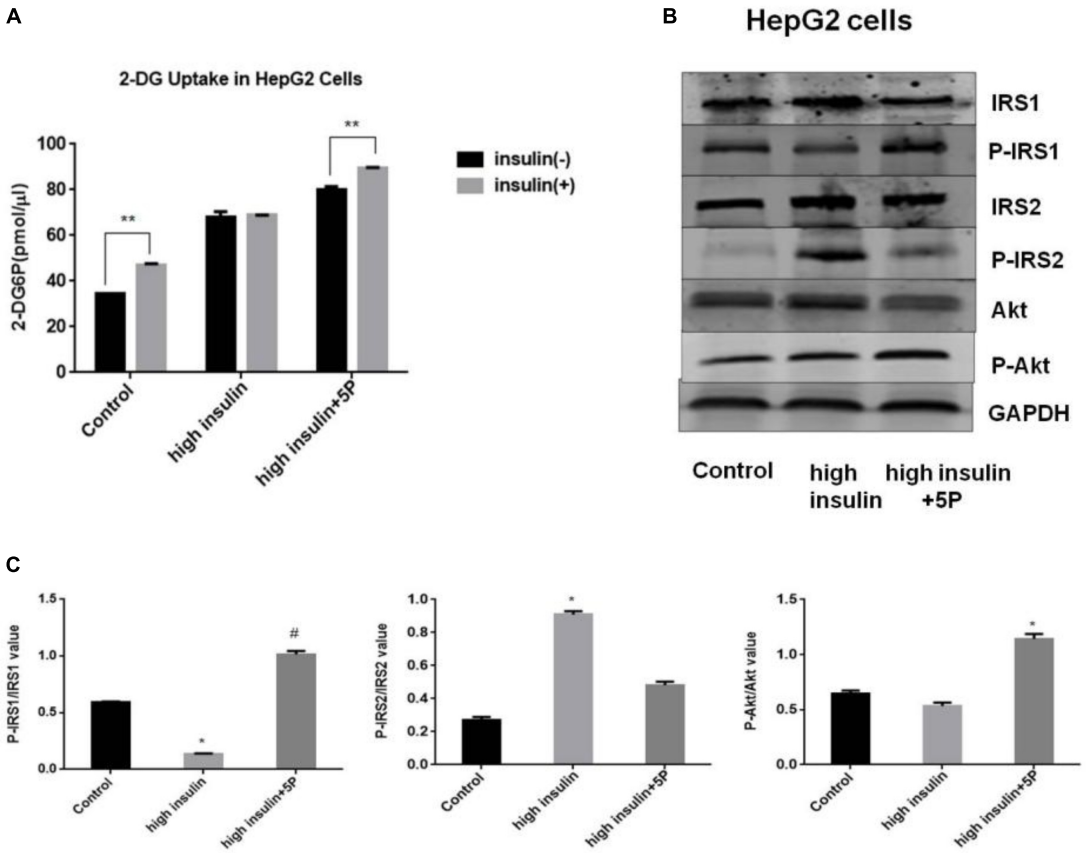

FIGURE 1 | Effects of 5-PAHSA treatment on glucose uptake and insulin signaling pathway in HepG2 cells. **(A)** Rates of glucose transport in HepG2 cells. Basal glucose transport (black) and insulin stimulated glucose transport (gray) are shown. Cells were untreated, treated with high insulin or high insulin plus 5-PAHSA. Basal rate refers to the rate of glucose transport in the absence of insulin. Insulin-stimulated rate was calculated as the rate of transport in the presence of insulin minus the basal rate. $^{**}p < 0.01$ versus basal rate (*t*-test). **(B)** Insulin signaling was examined by western blot analysis in HepG2 cells. Cells were untreated, treated with high insulin or high insulin plus 5-PAHSA. **(C)** Quantification of western blotting. $^{*}p < 0.05$ versus control, $^{\#}p < 0.05$ versus high insulin (one-way ANOVA). Data are representative of at least three different experiments. All data represent means ± standard error (SE).

5-PAHSA Treatment Improved Glucose Tolerance in HFD-Induced Insulin-Resistant Mice, While Had No Effect on Glucose Tolerance, Blood Glucose, Insulin Levels or Body Weight in db/db Mice

We nest sought to extend these observations from cellular models to *in vivo* models of insulin resistance, the HFD-induced insulin resistant mice and the leptin receptor-deficient db/db mice. To test whether administration of 5-PAHSA can improve glucose tolerance, an OGTT was performed in insulin-resistant HFD-fed mice and db/db mice. The results showed that 5-PAHSA treatment improved glucose tolerance with a reduced area under the glucose excursion curve in 5-PAHSA treated HFD-fed mice. However, low dose (50 mg/kg) and high dose (150 mg/kg) of 5-PAHSA treatment did not improve glucose tolerance in db/db mice (**Figure 3A**). Then we further test whether continuing 5-PAHSA treatment would affect glucose metabolism in db/db mice, blood glucose levels were tested after 5-PAHSA treatment for 10 and 30 days in db/db mice. There was still no significant differences in blood glucose levels as compared to before treatment (**Figures 3B,C**). To determine whether continuing administration of 5-PAHSA influenced insulin secretion, serum insulin levels were tested after 30 days of low dose and high dose of 5-PAHSA treatment. They had no effect on insulin secretion (**Figure 3D**). Further, 30 days of 5-PAHSA treatment did not significantly change body weight (**Figure 3E**) or food intake (data not shown) in db/db mice. Besides, 5-PAHSA treatment also had no effects on glucose metabolism in WT mice.

Chronic 5-PAHSA Administration Induced Liver Steatosis and Secretion of Inflammatory Factors in db/db Mice

Since we didn't observe hypoglycemic action of chronic 5-PAHSA treatment in db/db mice, we further investigated whether 5-PAHSA treatment could affect lipid metabolism in the livers of db/db mice. In low dose and high dose of 5-PAHSA treated db/db mice, more severe liver steatosis was

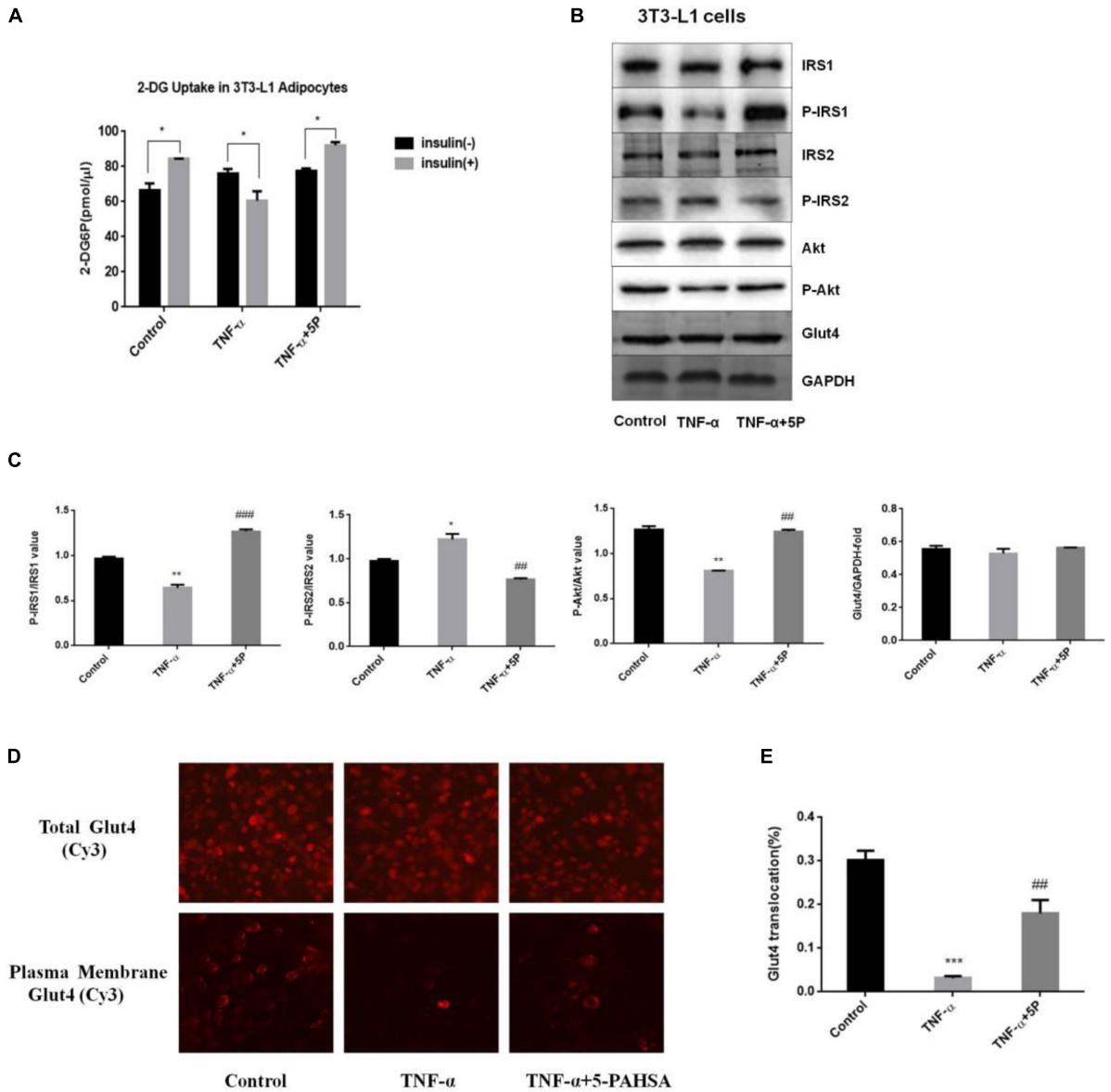

FIGURE 2 | Effects of 5-PAHSA treatment on glucose uptake and insulin signaling pathway in 3T3-L1 cells. **(A)** Rates of glucose transport in 3T3-L1 cells. Basal glucose transport (black) and insulin stimulated glucose transport (gray) are shown. Cells were untreated, treated with TNF-α alone or TNF-α plus 5-PAHSA. $^{*}p < 0.05$ versus basal rate (*t*-test). **(B)** Insulin signaling was examined by western blotting analysis in 3T3-L1 cells. Cells were untreated, treated with TNF-α alone or TNF-α plus 5-PAHSA. **(C)** Quantification of western blotting. $^{*}p < 0.05$, $^{**}p < 0.01$ versus control, $^{\#\#}p < 0.01$, $^{\#\#\#}p < 0.001$ versus TNF-α (one-way ANOVA). **(D)** Glut4 plasma membrane translocation in 3T3-L1 adipocytes treated with TNF-α alone or together with 5-PAHSA. **(E)** Quantification of Glut4 translocation in **(D)**. $^{***}p < 0.001$ versus control, $^{\#\#}p < 0.01$ versus TNF-α (one-way ANOVA). Data are representative of at least three different experiments. All data represent means ± standard error (SE).

observed, compared with vehicle control. And these effects of 5-PAHSA were not be depend on dosage (**Figure 4A**). In addition, the infiltration of inflammatory cells was also been seen in livers of low dose of 5-PAHSA-treated db/db mice (**Figure 4A**). In addition, no significant differences were observed in 5-PAHSA-treated WT mice and vehicle control.

We then tested the secretion of liver inflammatory factors, CRP and TNF-α. The protein levels of CRP and TNF-α were significantly increased in 5-PAHSA-treated db/db mice than vehicle control (**Figure 4B**). Similarly, serum levels of IL-1α, TNF-α, and CRP were significantly higher in 5-PAHSA-treated db/db mice than vehicle control (**Figure 4C**). However, the effects of 5-PAHSA were not dose-dependent. Likewise, 5-PAHSA had no effect on inflammatory factors in WT mice (**Figures 4B,C**). These results suggest that chronic 5-PAHSA administration may induce systemic inflammatory responses in db/db mice.

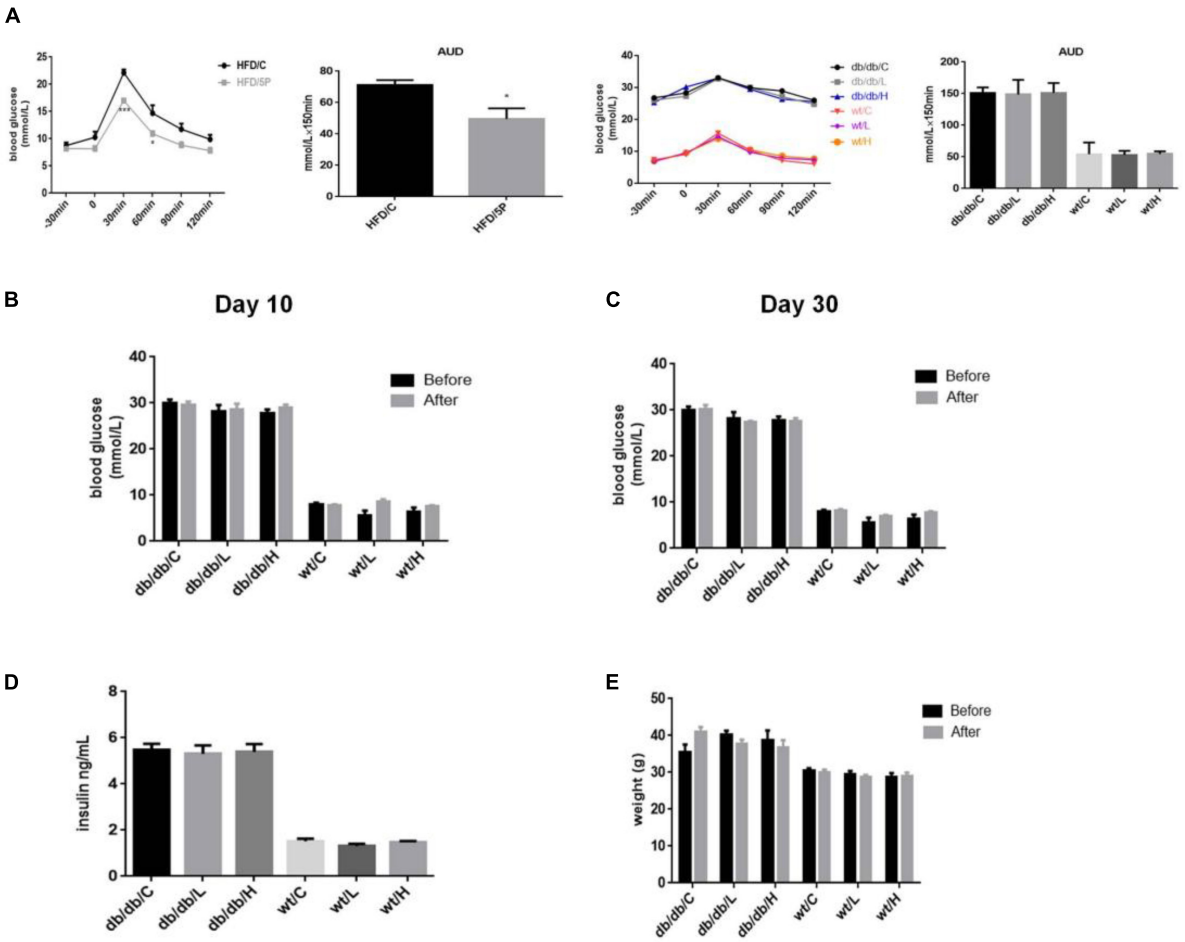

FIGURE 3 | 5-PAHSA treatment improved glucose tolerance in HFD-induced insulin-resistant mice, while had no effect on glucose tolerance, blood glucose, insulin levels or body weight in db/db mice. All mice were divided randomly as follows: control db/db group (db/db/C), db/db plus low-dose 9-PAHSA group (50 mg/kg per day; db/db/L), db/db plus high-dose 9-PAHSA group (150 mg/kg per day; db/db/H), control WT group (WT/C), WT plus low-dose 9-PAHSA group (50 mg/kg per day; WT/L), and WT plus high-dose 9-PAHSA group (150 mg/kg per day; WT/H); HFD control and HFD plus 50 mg/kg 5-PAHSA. **(A)** HFD-induced insulin-resistant mice, db/db mice and WT mice were gavaged with 5-PAHSA or a vehicle control 4.5 h after food removal. After 30 min, an oral glucose tolerance test (OGTT) was performed. Area under the curve (AUC) was calculated from –30 to 120 min. $^{*}p < 0.05$ (t test), $^{***}p < 0.001$ (two-way ANOVA) versus HDF/C. **(B,C)** Changes in blood glucose of db/db mice and WT mice after 10 and 30 days of 5-PAHSA treatment. **(D)** Serum insulin levels in db/db mice and WT mice after 30 days of 5-PAHSA treatment. **(E)** Body weight changes in db/db mice and WT mice after 30 days of 5-PAHSA treatment. $n = 5$ mice per group. All data represent means ± standard error (SE).

High Glucose Impaired the Effects of 5-PAHSA on Lipid Metabolism in HepG2 Cells

In HFD-induced insulin-resistant mice, 5-PAHSA improves glucose metabolism (Yore et al., 2014). In the study, we also found that 5-PAHSA treatment improved glucose tolerance and insulin sensitivity in HFD-fed mice, HepG2 cells and 3T3-L1 cell (**Figures 1**, **2**). However, 5-PAHSA treatment did not metabolically benefit db/db mice. Based on it, we hypothesized that hyperglycemia condition in db/db mice impaired 5-PAHSA effects on metabolism. To test this hypothesis, we exposed HepG2 cells to either a normal level of glucose or a high level of glucose. To determine whether the effects of 5-PAHSA on metabolic parameters are distinct from effects of ordinary free fatty acids, we performed similar studies with PA since 5-PAHSA is made up of palmitate and hydroxystearic acid. We found that 5-PAHSA treatment enhanced phosphorylation levels of key lipid metabolism enzymes in normal glucose conditions compared to control and PA treatment. As expected, 5-PAHSA treatment increased phosphorylation of AMPKα on Thr172 (**Figure 5A**). Consequently, phosphorylation of ACC on Ser79, an AMPKα target, also increased slightly (**Figure 5A**), indicating that 5-PAHSA treatment inactivated this rate-limiting enzyme of fatty acid synthesis. In high glucose conditions, 5-PAHSA treatment of HepG2 cells decreased phosphorylation levels of AMPKα, but had no significant influence on ACC phosphorylation (**Figure 5A**). PA treatment had similar effects (**Figure 5A**).

In normal glucose conditions, 5-PAHSA treatment upregulated mRNA and protein expression of CPT1,

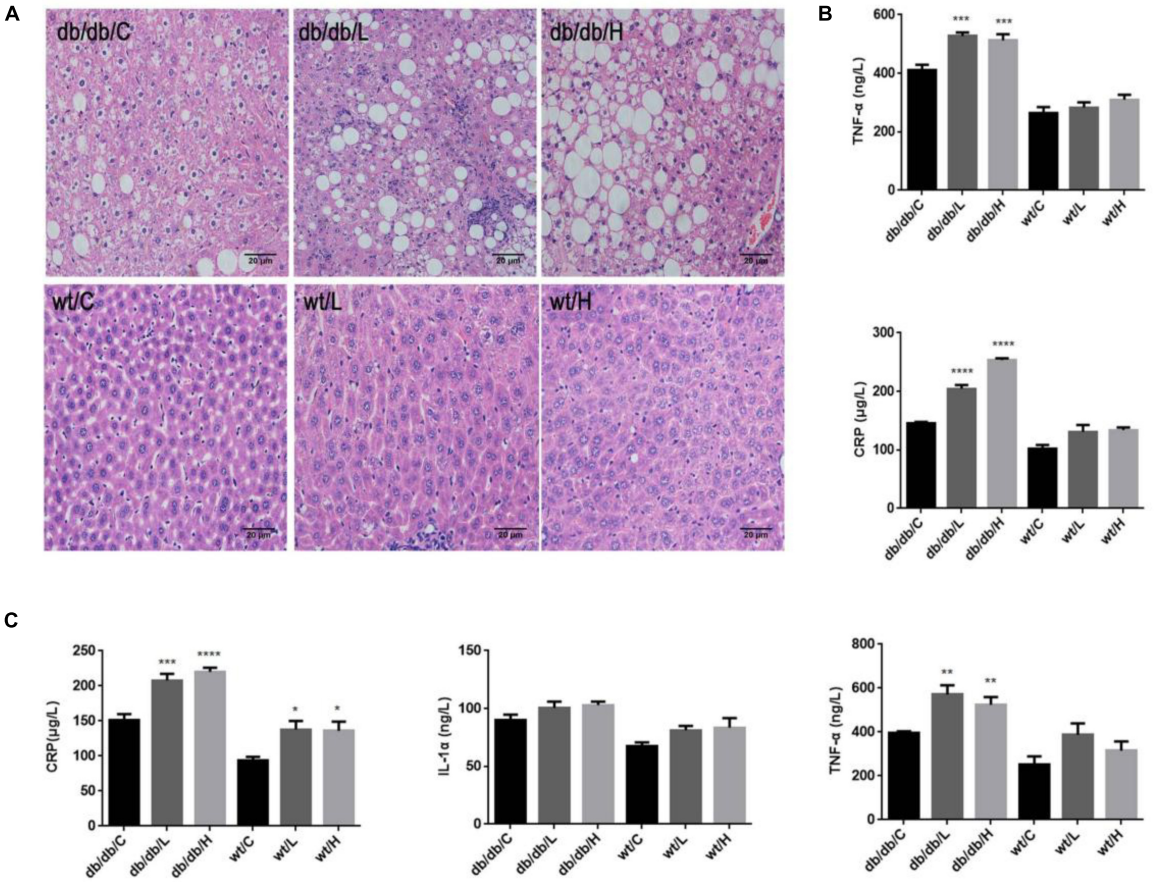

FIGURE 4 | Effects of repeated 5-PAHSA administration on hepatic lipid accumulation and inflammatory cytokines secretion in db/db mice and WT mice. **(A)** Hematoxylin and eosin staining of hepatic tissue sections after 30 days of 5-PAHSA treatment. Pictures were taken at 200× magnification and show: db/db/C, Mild steatosis; db/db/L, Severe steatosis and inflammatory cells infiltration; db/db/H, Severe steatosis; WT/C, None steatosis; WT/L, None steatosis; WT/H, None steatosis. **(B)** TNF-α and CRP levels in liver after 30 days of 5-PAHSA treatment. **(C)** Levels of serum inflammatory cytokines, including CRP, IL-1α and TNF-α after 30 days of 5-PAHSA treatment. $^{*}p < 0.05$, $^{**}p < 0.01$, $^{***}p < 0.001$, $^{****}p < 0.0001$ versus db/db/C or WT/C. $n = 5$ mice per group. Data represented means ± standard error (SE).

downregulated mRNA and protein expression of FAS or SREBP1c compared to control and PA treatment (**Figures 5B,C**). These effects of 5-PAHSA were lost when cells were subjected to high glucose conditions (**Figures 5B,C**).

As 5-PAHSA treatment in the presence of high glucose increased mRNA and protein levels of genes involved in lipid synthesis and reduced fatty acid oxidation, we further investigated whether this treatment promoted lipid accumulation in HepG2 cells. Oil Red O staining showed no signs of lipid accumulation among control group, 5-PAHSA group and PA group incubated with normal glucose. In contrast, in the high glucose conditions, 5-PAHSA and PA treatment showed significantly lipid accumulation compared with control group (**Figure 5D**). In addition, quantification of lipid content in HepG2 cells revealed that, in the normal glucose conditions, 5-PAHSA decreased intracellular levels of triglycerides and cholesterol in HepG2 cells, as compared to control and PA treatment (**Figure 5E**). In the high glucose conditions, 5-PAHSA treatment significantly increased intracellular levels of triglycerides and cholesterol, as effectively as PA treatment (**Figure 5E**).

High Glucose Impaired the Anti-inflammatory Effects of 5-PAHSA in HepG2 Cells

5-PAHSA treatment promoted the secretion of liver and serum inflammatory factors in db/db mice. To determine whether 5-PAHSA treatment increased inflammation induced by high glucose concentrations, HepG2 cells were incubated with either normal or high glucose concentrations in the absence or presence of 5-PAHSA. In the normal glucose conditions, 5-PAHSA treatment inhibited phosphorylation of IκBα and NF-κB, prevented IκBα degradation and then NF-κB activation, as compared to control and PA treatment (**Figure 6A**). Interestingly, all of these effects of 5-PAHSA were completely abrogated by high glucose concentrations (**Figure 6A**). Consistent with this, 5-PAHSA treatment decreased mRNA and protein levels of MCP1

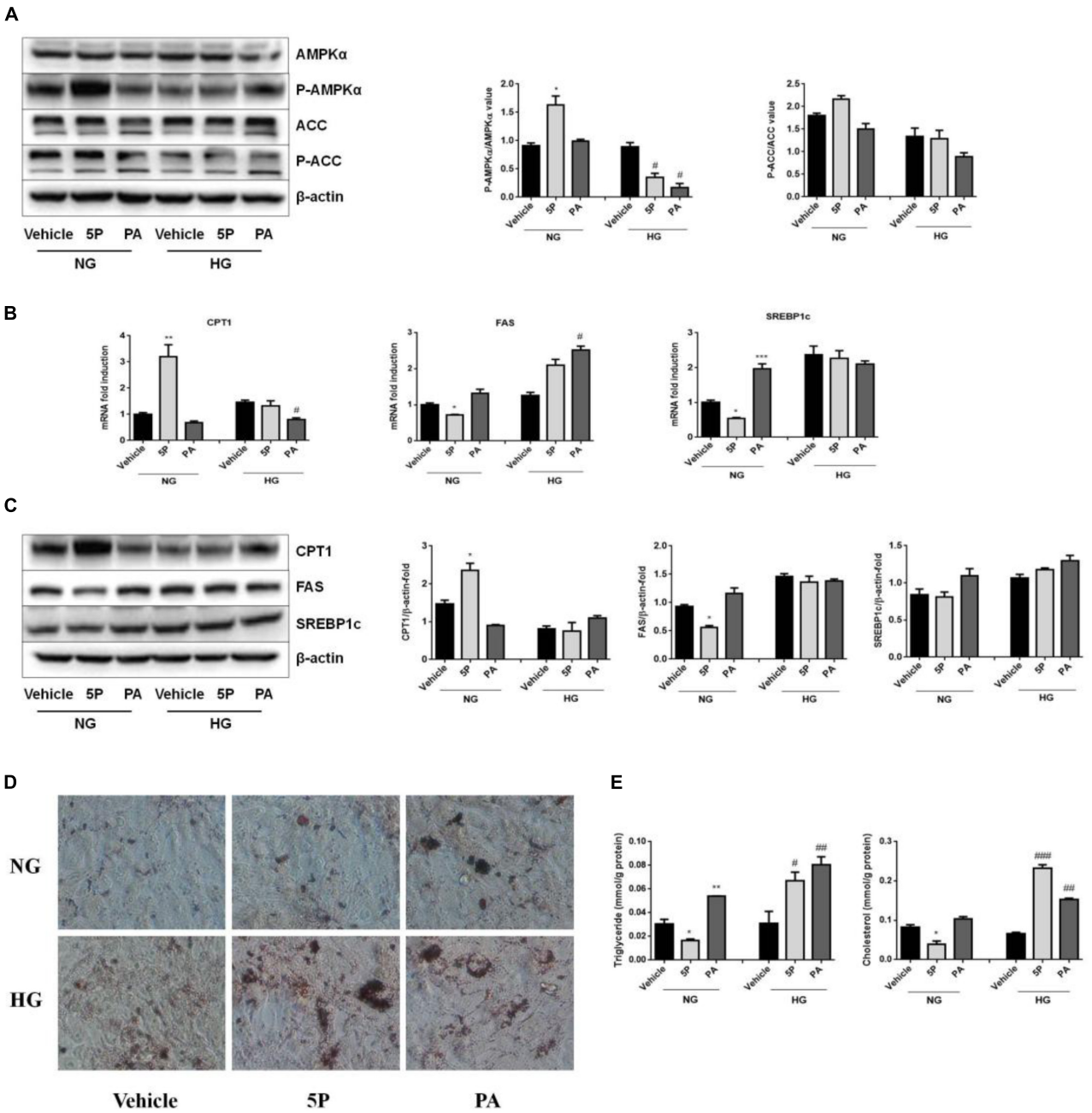

FIGURE 5 | Effects of 5-PAHSA treatment on lipid metabolism under normal and high glucose conditions in HepG2 cells. HepG2 cells were cultured with normal glucose (NG) or high glucose (HG) for 72 h. Cells were untreated (vehicle), treated with 5-PAHSA (5P) or palmitic acid (PA). **(A)** Western blotting analysis of protein expression, including total AMPKα and pThr172-AMPKα, total ACC and pSer79-ACC. **(B)** The mRNA expression of CPT1, FAS, and SREBP1c were evaluated by qPCR. **(C)** Western blotting analysis of protein expression, including CPT1, FAS, and SREBP1c. **(D)** Lipid accumulation was detected by Oil Red O staining (magnification, 200×). **(E)** The levels of intracellular triacylglycerols and cholesterol in HepG2 cells were tested by ELISA. $^{*}p < 0.5$, $^{**}p < 0.01$, $^{***}p < 0.001$ versus Vehicle under normal glucose condition; $^{\#}p < 0.5$, $^{\#\#}p < 0.01$, $^{\#\#\#}p < 0.001$ versus vehicle under high glucose condition (one-way ANOVA). Data are representative of at least three different experiments. Data represent means ± standard error (SE).

and IL-6 in normal glucose compared with control and PA treatment (**Figures 6B,C**). Similar to PA, 5-PAHSA increased mRNA and protein levels of MCP1 and IL-6 in high glucose conditions (**Figures 6B,C**). These results indicated that high glucose impaired the anti-inflammatory function of 5-PAHSA.

DISCUSSION

In the study, we found that the HFD-induced insulin-resistant mice exhibited improved glucose tolerance after 5-PAHSA treatment, evidenced by reduced area under the

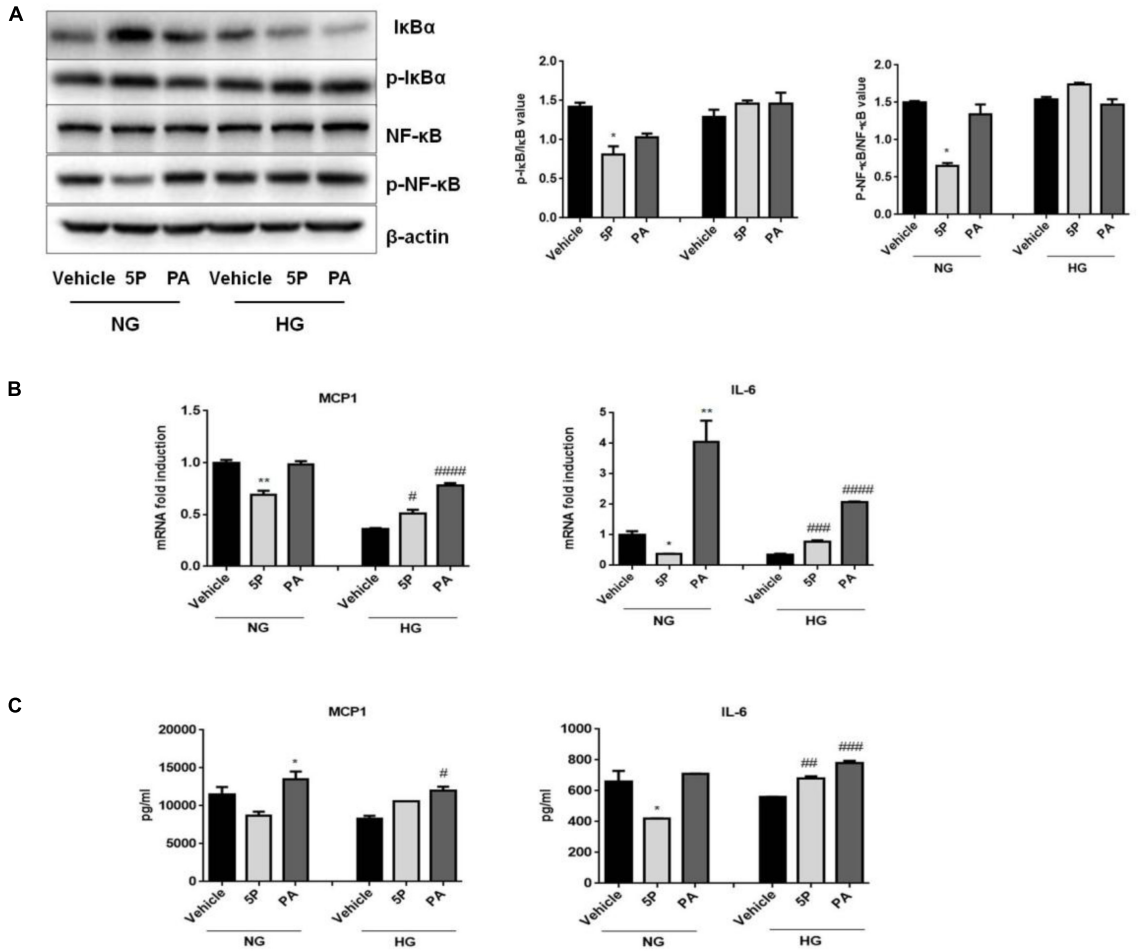

FIGURE 6 | Effects of 5-PAHSA treatment on the NF-κB-mediated signaling pathway under normal and high glucose conditions in HepG2 cells. **(A)** Western blotting analysis of expression of total IκBα and pSer36-IκBα, total NF-κB and pSer536-NF-κB. **(B)** The mRNA expression of MCP1 and IL-6 were evaluated by qPCR. **(C)** The protein levels of MCP1 and IL-6 were tested by ELISA. $^{*}p < 0.5$, $^{**}p < 0.01$ versus vehicle under normal glucose condition; $^{\#}p < 0.5$, $^{\#\#}p < 0.01$, $^{\#\#\#}p < 0.001$, $^{\#\#\#\#}p < 0.0001$ versus vehicle under high glucose condition (one-way ANOVA). Data are representative of at least three different experiments. Data represent means ± standard error (SE).

glucose excursion curve. Moreover, 5-PAHSA improved insulin sensitivity in 3T3-L1 cells and HepG2 cells. Specifically, 5-PAHSA treatment significantly increased insulin stimulated glucose uptake, thus improved insulin resistance induced by high insulin/TNF-α. Besides, 5-PAHSA treatment increased IRS1 phosphorylation at Thr896 and Akt phosphorylation at Ser473, two signaling proteins correlated with increases in glucose uptake. And 5-PAHSA treatment decreased IRS2 phosphorylation at Ser731, which related with insulin resistance. 5-PAHSA treatment also enhanced Glut4 translocation in 3T3-L1 cells, leading to increased uptake of glucose. Consistent with these findings, previous studies have reported acute oral administration of 5-PAHSA to insulin-resistant HFD-fed mice lowered basal glycemia and improved glucose tolerance (Yore et al., 2014). Chronic 5-PAHSA treatment also improved insulin sensitivity and glucose tolerance in chow- and HFD-fed mice (Syed et al., 2018). However, Pflimlin et al. (2018) challenge these findings that 5-PAHSA improves glucose control *in vivo*. They reported that acute and repeated treatment with 5-PAHSA in insulin-resistant diet-induced obese mice did not improve the metabolic status. Likewise, we found that repeated administration of 5-PAHSA for 1 month didn't metabolically benefit db/db mice.

The important methodological issues that may contribute to the different results among these researches. The db/db mouse is one of the most widely used animal models in T2DM research (Wang et al., 2014). However, unlike HFD-induced insulin-resistant mice, the diabetic characteristics of db/db mice derive from mutation of leptin receptor genes. In db/db mice at 10 weeks of age, fasting blood glucose levels can reach ∼600 mg/dl in comparison to ∼150 mg/dl in control mice (Han et al., 2008), indicating extreme hyperglycemia. High levels of glucose may impair 5-PAHSA signaling pathway in db/db mice. Our *in vitro* results also confirmed this hypothesis.

Here, we showed that 5-PAHSA treatment reduced lipogenesis and increased fatty acid oxidation in HepG2 cells in normal glucose conditions. In contrast, 5-PAHSA treatment under

high glucose conditions promoted fatty acid accumulation and reduced fatty acid oxidation in HepG2 cells. This promotion of lipogenesis was associated with upregulation of SREBP1c and its downstream target genes, FAS. Inhibition of fatty acid oxidation was associated with downregulation of phosphorylation of AMPKα and ACC, as well as downregulation of CPT1 expression. Consistent with *in vitro* results, hepatic pathology *in vivo* showed that continuous administration of 5-PAHSA for 1 month in db/db mice caused liver steatosis, suggesting that 5-PAHSA treatment may induce liver damage in db/db mice. As a primary metabolic organ in human body, the liver plays a key role in the regulation of lipid and glucose metabolism. Dysregulation of hepatic lipid metabolic pathways contributes to the development of insulin resistance (Farese et al., 2012; Quiroga et al., 2012). Liver steatosis induced by 5-PAHSA treatment may one of the reasons that result in failure of glucose control in db/db mice.

Metabolic inflammation in tissue can interfere with insulin action through inhibiting insulin signaling pathway (Nie et al., 2017). We observed that 1 month of 5-PAHSA administration in db/db mice induced inflammatory responses, which may indicate a possible cause for the observed negative effects on insulin resistance. Specifically, serum IL-1α, CPR, and TNF-α were significantly higher in 5-PAHSA treated db/db mice than in db/db control mice. Hepatic pathology showed that continuous 5-PAHSA treatment in db/db mice aggravated hepatic inflammation. In addition, the levels of CPR and TNF-α in liver were significantly higher in 5-PAHSA treated db/db mice. These results were contrary to the report by Yore et al. (2014), which showed that oral administration of 5-PAHSA in HFD mice for 3 days improved adipose tissue inflammation by reducing the levels of macrophages that were positive for the proinflammatory cytokines TNF-α and IL-1β. Moreover, chronic 5-PAHSA treatment in chow-fed and HFD-fed mice reduces adipose inflammation (Syed et al., 2018). Based on this, we hypothesized that discrepancies between findings may be due to different animal models, since db/db mice had higher hyperglycemia. And our *in vitro* results supported the hypothesis.

In an inactive form, NF-κB is composed of a p65-p50 heterodimer bound with IκBα in the cytoplasm. After cellular stimulation, IκBα is degraded after phosphorylation and NF-κB is released to become the bioactive form. Active NF-κB is then translocated into nucleus and adjusts transcriptional activity of target genes, such as MCP1 and IL-6 (Baldwin, 1996). In the normal glucose condition, 5-PAHSA treatment inhibited inflammation via downregulation of IκBα phosphorylation and NF-κB phosphorylation, prevented IκBα degradation, NF-κB activation and then decreased MCP1 and IL-6 secretion. However, hyperglycemia impaired the anti-inflammatory effects of 5-PAHSA via promoting IκBα degradation and activating NF-κB pathway. Furthermore, since 5-PAHSA treatment caused a systemic inflammatory response in db/db mice, and chronic low-grade inflammation contributes to obesity-related insulin resistance (Odegaard and Chawla, 2013; Castoldi et al., 2015), our findings may provide insight into the exacerbated insulin resistance in db/db mice.

CONCLUSION

We studied the effect of repeated 5-PAHSA treatment on glucose and lipid metabolism in db/db mice. Our results indicate that continuous 5-PAHSA treatment for 1 month might increase insulin resistance, promote lipid accumulation in the liver, and induce inflammatory responses. In mechanism, hyperglycemia impaired 5-PAHSA action by inhibiting the AMPKα signaling pathway and promoting NF-κB-mediated inflammation. In our future work, we plan to modify 5-PAHSA to further provide therapy for metabolic disease.

AUTHOR CONTRIBUTIONS

Y-MW and N-YF conceived the study. Y-MW and H-XL contributed to methodology. Y-MW investigated the study and wrote the manuscript. N-YF acquired funding, contributed to resources, and supervised the study.

FUNDING

This work was supported by grants from the National Natural Scientific Foundation, China (Grant Numbers 81370360 and 81170301). N-YF was the guarantor of this work and, as such, has full access to all the data in the study and takes responsibility for the integrity of the data and the accuracy of the data analysis.

SUPPLEMENTARY MATERIAL

The Supplementary Material for this article can be found online at: https://www.frontiersin.org/articles/10.3389/fphar.2018.01491/full#supplementary-material

REFERENCES

American Diabetes Association (2013). Economic costs of diabetes in the U.S. in 2012. *Diabetes Care* 36, 1033–1046. doi: 10.2337/dc12-2625

Baldwin, A. J. (1996). The NF-kappa B and I kappa B proteins: new discoveries and insights. *Annu. Rev. Immunol.* 14, 649–683. doi: 10.1146/annurev.immunol.14.1.649

Bao, X., Yang, C., Fang, K., Shi, M., Yu, G., and Hu, Y. (2017). Hospitalization costs and complications in hospitalized patients with type 2 diabetes mellitus in Beijing, China. *J. Diabetes* 9, 405–411. doi: 10.1111/1753-0407.12428

Castoldi, A., Naffah de Souza, C., Camara, N. O., and Moraes-Vieira, P. M. (2015). The macrophage switch in obesity development. *Front. Immunol.* 6:637. doi: 10.3389/fimmu.2015.00637

Devaraj, S., Torok, N., Dasu, M. R., Samols, D., and Jialal, I. (2008). Adiponectin decreases C-reactive protein synthesis and secretion from endothelial cells: evidence for an adipose tissue-vascular loop. *J. Arterioscler. Thromb. Vasc. Biol.* 28, 1368–1374. doi: 10.1161/ATVBAHA.108.163303

Farese, R. J., Zechner, R., Newgard, C. B., and Walther, T. C. (2012). The problem of establishing relationships between hepatic steatosis and hepatic insulin resistance. *Cell Metab.* 15, 570–573. doi: 10.1016/j.cmet.2012.03.004

Han, K. L., Choi, J. S., Lee, J. Y., Song, J., Joe, M. K., Jung, M. H., et al. (2008). Therapeutic potential of peroxisome proliferators–activated receptor-alpha/gamma dual agonist with alleviation of endoplasmic reticulum stress for the treatment of diabetes. *Diabetes Metab. Res. Rev.* 57, 737–745.

Le, C., Lin, L., Jun, D., Jianhui, H., Keying, Z., Wenlong, C., et al. (2013). The economic burden of type 2 diabetes mellitus in rural southwest China. *Int. J. Cardiol.* 165, 273–277. doi: 10.1016/j.ijcard.2011.08.039

Loomba, R., Abraham, M., Unalp, A., Wilson, L., Lavine, J., Doo, E., et al. (2012). Association between diabetes, family history of diabetes, and risk of nonalcoholic steatohepatitis and fibrosis. *Hepatology* 56, 943–951. doi: 10.1002/hep.25772

Nathan, D. M. (2015). Diabetes: advances in diagnosis and treatment. *JAMA* 314, 1052–1062. doi: 10.1001/jama.2015.9536

Nie, J., Chang, Y., Li, Y., Zhou, Y., Qin, J., Sun, Z., et al. (2017). Caffeic acid phenethyl ester (propolis extract) ameliorates insulin resistance by inhibiting JNK and NF-kappaB inflammatory pathways in diabetic mice and HepG2 cell models. *J. Agric. Food Chem.* 65, 9041–9053. doi: 10.1021/acs.jafc.7b02880

Odegaard, J. I., and Chawla, A. (2013). The immune system as a sensor of the metabolic state. *Immunity* 38, 644–654. doi: 10.1016/j.immuni.2013.04.001

Perry, R. J., Camporez, J. G., Kursawe, R., Titchenell, P. M., Zhang, D., Perry, C. J., et al. (2015). Hepatic acetyl CoA links adipose tissue inflammation to hepatic insulin resistance and type 2 diabetes. *J. Cell* 160, 745–758. doi: 10.1016/j.cell.2015.01.012

Pflimlin, E., Bielohuby, M., Korn, M., Breitschopf, K., Löhn, M., Wohlfart, P., et al. (2018). Acute and repeated treatment with 5-PAHSA or 9-PAHSA isomers does not improve glucose control in mice. *Cell Metab.* 28, 217–227. doi: 10.1016/j.cmet.2018.05.028

Quiroga, A. D., Li, L., Trötzmüller, M., Nelson, R., Proctor, S. D., Köfeler, H., et al. (2012). Deficiency of carboxylesterase 1/esterase-x results in obesity, hepatic steatosis, and hyperlipidemia. *Hepatology* 56, 2188–2198. doi: 10.1002/hep.25961

Reed, M. J., and Scribner, K. A. (1999). In-vivo and in-vitro models of type 2 diabetes in pharmaceutical drug discovery. *Diabetes Obes. Metab.* 1, 75–86. doi: 10.1046/j.1463-1326.1999.00014.x

Seuring, T., Archangelidi, O., and Suhrcke, M. (2015). The economic costs of Type 2 diabetes: a global systematic review. *Pharmacoeconomics* 33, 811–831. doi: 10.1007/s40273-015-0268-9

Stein, S. A., Lamos, E. M., and Davis, S. N. (2013). A review of the efficacy and safety of oral antidiabetic drugs. *Expert Opin. Drug Saf.* 12, 153–175. doi: 10.1517/14740338.2013.752813

Sun, Y., and Chen, X. (2010). Effect of adiponectin on apoptosis:proapoptosis or antiapoptosis? *J. Biofactors* 36, 179–186. doi: 10.1002/biof.83

Syed, I., Lee, J., Moraes-Vieira, P. M., Donaldson, C. J., Sontheimer, A., Aryal, P., et al. (2018). Palmitic acid hydroxystearic acids activate GPR40, which is involved in their beneficial effects on glucose homeostasis. *Cell Metab.* 27, 419.e4–427.e4. doi: 10.1016/j.cmet.2018.01.001

Wang, B., Chandrasekera, P. C., and Pippin, J. J. (2014). Leptin- and leptin receptor-deficient rodent models: relevance for human type 2 diabetes. *Curr. Diabetes Rev.* 10, 131–145. doi: 10.2174/1573399810666140508121012

Williams, C. D., Stengel, J., Asike, M. I., Torres, D. M., Shaw, J., Contreras, M., et al. (2011). Prevalence of nonalcoholic fatty liver disease and nonalcoholic steatohepatitis among a largely middle-aged population utilizing ultrasound and liver biopsy: a prospective study. *Gastroenterology* 140, 124–131. doi: 10.1053/j.gastro.2010.09.038

Yore, M. M., Syed, I., Moraes-Vieira, P. M., Zhang, T., Herman, M. A., Homan, E. A., et al. (2014). Discovery of a class of endogenous mammalian lipids with anti-diabetic and anti-inflammatory effects. *J. Cell* 159, 318–332. doi: 10.1016/j.cell.2014.09.035

Conflict of Interest Statement: The authors declare that the research was conducted in the absence of any commercial or financial relationships that could be construed as a potential conflict of interest.

frontiers in Pharmacology

ORIGINAL RESEARCH
published: 12 July 2019
doi: 10.3389/fphar.2019.00769

Synthesis of TPGS/Curcumin Nanoparticles by Thin-Film Hydration and Evaluation of Their Anti-Colon Cancer Efficacy *In Vitro* and *In Vivo*

Hong Li[2,3†], Liping Yan[2†], Edith K.Y. Tang[5], Zhen Zhang[6], Wei Chen[1], Guohao Liu[1,4] and Jingxin Mo[1*]*

[1] Clinical Research Center for Neurological Diseases of Guangxi Province, The Affiliated Hospital of Guilin Medical University, Guilin, China, [2] Department of Gastroenterology, The Second People's Hospital of Guilin, Guilin, China, [3] Department of Gastroenterology, The Affiliated Hospital of Guilin Medical University, Guilin, China, [4] Department of Radiology, The Affiliated Hospital of Jilin Medical University, Jilin, China, [5] School of Allied Health, Faculty of Health and Medical Sciences, University of Western Australia, Perth, WA, Australia, [6] Department of Ultrasound, the First Affiliated Hospital of China Medical University, Shenyang, China

OPEN ACCESS

Edited by:
Salvatore Salomone,
University of Catania, Italy

Reviewed by:
Biplob Koch,
Banaras Hindu University, India
Konstantinos Dimas,
University of Thessaly, Greece

***Correspondence:**
Jingxin Mo
Jingxin.mo@hotmail.com
Guohao Liu
lgh19810625@163.com

†These authors have contributed equally to this work.

Specialty section:
This article was submitted to Experimental Pharmacology and Drug Discovery, a section of the journal Frontiers in Pharmacology

Received: 09 January 2019
Accepted: 14 June 2019
Published: 12 July 2019

Citation:
Li H, Yan L, Tang EKY, Zhang Z, Chen W, Liu G and Mo J (2019) Synthesis of TPGS/Curcumin Nanoparticles by Thin-Film Hydration and Evaluation of Their Anti-Colon Cancer Efficacy In Vitro and In Vivo. Front. Pharmacol. 10:769. doi: 10.3389/fphar.2019.00769

Curcumin (CCM) has many potential uses in anticancer chemotherapy, but its low water solubility poses a major problem, preventing its translation into clinical use. TPGS is a water-soluble derivative of vitamin E that acts as a surfactant with the ability to form micellar nanoparticles in water. More importantly, TPGS acts as a potent antioxidant that can neutralize intracellular reactive oxygen species (ROS). In this study, we solubilized CCM with TPGS using thin-film rehydration to prepare aqueous formulations containing CCM at clinically relevant concentrations. We found that the minimal TPGS:CCM ratio for producing nanoparticles was 5:1 (w/w): at or above this ratio, stable nanoparticles formed with an average particle diameter of 12 nm. CCM was released from TPGS/CCM micelles in simulated colonic and gastric fluids. These TPGS/CCM nanoparticles were shown to decrease intracellular ROS levels and apoptosis and inhibited migration of HT-29 human colon cancer cells more potently than free CCM. Pharmacokinetic analysis showed TPGS/CCM to be more bioavailable than free CCM after oral administration to rats. Our results suggest that TPGS/CCM may increase therapeutic efficacy of CCM against colon cancer and merits further investigation in a clinical setting.

Keywords: curcumin, ROS, vitamin E TPGS, micellar nanoparticle, synergistic effects, colon cancer

INTRODUCTION

In recent years, there has been growing interest in the use of curcumin (CCM) for treating diseases. CCM is the active ingredient of the turmeric plant (*Curcuma longa*) and has demonstrated many chemopreventive and chemotherapeutic properties. (Scott et al., 2008; Yallapu et al., 2010) CCM has been reported to have antioxidant properties and inhibits pro-inflammatory proteins, cell proliferation, as well as tumor angiogenesis and metastasis (Nair et al., 2012). However, CCM has low water solubility, which limits oral bioavailability (Yen et al., 2010). As a result, CCM only has limited physiological effects unless very high doses are used.

One method to overcome poor aqueous solubility is to use nanoparticle techniques (Allam et al., 2015; Vecchione et al., 2016; Bagheri et al., 2018; Cheng et al., 2018). Encapsulation of CCM

in nano-sized micelles enables the drug to be formulated as an aqueous dispersion at therapeutically relevant concentrations that can be administered orally with increased bioavailability and cellular uptake.

Colorectal cancer is the third most common type of cancer in the world, comprising about 10% of all cancer cases. The incidence of colorectal cancer has steadily increased over the last 25 years due to factors such as obesity (Scott et al., 2008). In 2012 alone, 1.4 million new cases of colorectal cancer were diagnosed and 694,000 deaths occurred globally (Liang and Dominitz, 2019). Colorectal cancer manifests as adenomatous polyps and malignant cells in the colon (Yallapu et al., 2010) and is one of the most aggressive cancers (Dahlhaus et al., 2018). Current screening and detection methods for colorectal cancer are also inadequate, such that most diagnoses occur at the more advanced stages of the disease when treatments are no longer effective (Dolan et al., 2018; Shimada et al., 2018; Wrobel and Ahmed, 2018).

Nanotechnology is the development and application of nanoparticles, defined as particles ranging from 10 to 100 nm, for pharmaceutical purposes (Chen et al., 2017; Mo et al., 2017; Wang et al., 2018; Zambrano et al., 2018). Nanosuspensions, nanospheres, polymeric nanoparticles, liposomes, microemulsions, and microsomes have all been developed to enhance drug delivery by modifying the rate of drug release, circulation half-life, and targeting of the drug to specific cells or tissues (Chen et al., 2018; Ni et al., 2018). Nanoparticles have been synthesized from various materials. The small size of these micellar systems and their hydrophilic interface with blood plasma components allow them to evade uptake by the reticuloendothelial system (RES) and therefore remain longer in circulation (Sharma et al., 2017). While the hydrophobic core of these micelles provides a pocket in which poorly water-soluble drugs can be dissolved, the hydrophilic shell allows the micelles to remain stably dispersed in aqueous media. This acts as a physical barrier to reduce interaction between the drug cargo and blood components or non-target cells (Huang et al., 2017).

One technique used to produce polymeric nanoparticles is the thin-film rehydration method (Chen et al., 2017). This process uses amphiphilic surfactant molecules to stabilize the nanoparticles in aqueous media. One such surfactant is polyvinyl alcohol (PVA), which has been used extensively to produce polymer nanoparticles (Ghaffari et al., 2018). However, PVA is difficult to remove completely from the final nanoparticle product, and residual PVA may cause unwanted side effects when used in health care products. For these reasons, the preferred materials for biomedical nanoparticles are natural surfactants such as cholesterol, polysaccharides, phospholipids, and vitamins.

Our laboratory has previously synthesized stable phosphate calixarene-based micellar formulations of CCM using the thin-film rehydration method (Chen et al., 2017). In the present study, we build on these efforts to formulate nanoparticles with hydrophobic drugs by replacing Pluronic F127 with D-α-tocopheryl polyethylene glycol 1000 succinate (TPGS). TPGS is a water-soluble derivative of natural vitamin E that is produced by esterifying vitamin E succinate with polyethylene glycol 1000 (Zou and Gu, 2013; Gaonkar et al., 2017). The TPGS molecule is amphiphilic, with a lipophilic alkyl tail (tocopherol succinate moiety) and a hydrophilic polar head (polyethylene glycol chain). This allows TPGS to be used as a surfactant to encapsulate hydrophobic drugs into micellar structures. Given its ability to act simultaneously as a surfactant, emulsifier, solubilizer, absorption enhancer, and antioxidant (Zhang et al., 2015). TPGS has been studied extensively in recent years as an excipient for drug delivery systems.

We hypothesized that the combined use of CCM and TPGS in a nanoparticle may have synergistic effects in the treatment of colon cancer because both CCM and TPGS can reduce levels of reactive oxygen species (ROS). We also reasoned that loading TPGS micelles with CCM (TPGS/CCM) would protect CCM from degradation in the upper digestive tract, improving CCM pharmacokinetics. Therefore, in the present study, we used the thin-film rehydration method to synthesize TPGS/CCM nanoparticles, and we evaluated their characteristics using dynamic light scattering (DLS) and UV-visible (UV-Vis) spectrophotometry. We also evaluated *in vitro* release profiles of TPGS/CCM in simulated gastric and colonic fluids and tested whether loading CCM into nanoparticles improves its anti-migratory and pro-apoptotic effects on a human colon cancer cell line. Finally, we compared the pharmacokinetic profiles of free CCM and TPGS/CCM in rats to determine whether encapsulation of the drug improves its bioavailability.

MATERIALS AND METHODS

Materials

Curcumin (purity 95.0%, C110685), tween-80, was purchased from Aladdin Chemical Reagents, Shanghai, China; TPGS was obtained from Professional Compounding Centers of America, Houston, TX, USA. Chloroform [high performance liquid chromatography (HPLC) grade] was provided by Scharlau, Barcelona, Spain and 0.2-μm filter was purchased from SARSTEDT AG & Co. KG, Nümbrecht, Germany. Methanol (analytical grade) was obtained from Univar, New South Wales, Australia. Apoptosis kits based on staining with annexin V-FITC and propidium iodide (PI) were purchased from Lianke Technology (Hangzhou, China). Emodin, which was used as internal standard was obtained from National Institutes for Food and Drug Control, Beijing, China. 35-mm glass-bottom culture dishes were purchased from NEST Biotechnology Co., Ltd. Jiangsu, China. All other materials and solvents (analytical grade) were obtained from Sigma Aldrich, St Louis, MO, USA.

Cell Culture

HT-29 cells were obtained from Guilin UniK Biotechnology (Guilin, China) and cultured at 37.5°C in Dulbecco's modified Eagle medium (DMEM) supplemented with 10% fetal bovine serum (FBS) and 1 mM L-glutamine. All cell culture reagents were purchased from Thermo Fisher (Pittsburgh, PA) unless otherwise mentioned.

Animals

Male Wistar rats (200 ± 20 g) were provided by the Model Animal Research Center of Nanjing University (Nanjing, China).

All animal experiments were approved by the Ethics Committee of Guilin Medical University (ethics number YXLL-2017-085).

Preparation of TPGS/CCM Nanoparticles and Empty TPGS Micellar Particles

TPGS/CCM nanoparticles were prepared using the thin-film rehydration method developed in our laboratory. As CCM is highly hydrophobic and light-sensitive, it was handled only in glass vessels wrapped in aluminum foil. A stock solution of 10% (w/v) CCM was first prepared by dissolving 10 mg of CCM in 100 ml methanol. Solid TPGS was liquefied at 50°C, then dissolved in 50 ml HPLC-grade chloroform to produce a TPGS solution at concentrations of 0.01–1.00% (w/v) as required.

Nanoparticles were prepared at a TPGS:CCM weight ratio ranging from 50:1 to 1.5:1. For each batch of nanoparticles, relevant volumes of the CCM stock solution and the TPGS solution were mixed in a round-bottom flask, which was attached to a rotary evaporator (Eyela N1000, Japan). The solvents were evaporated at 50°C for at least 1 h or until a thin, dry film formed on the inner surface of the flask. The flask was then attached to a vacuum line for at least 12 h to dry. The dried film was rehydrated with double-deionized water that had been pre-heated to 37°C then vortexed (Vortex-Genie, New York, USA) until the thin dry film was no longer visible. We concentrated TPGS to ≥0.02% (w/v) in the final dispersion, based on the sum of masses of CCM and TPGS added at the outset. This was well above the critical micellar concentration of TPGS in water [0.02% (w/v)] (Mu and Feng, 2002). The sample was then centrifuged at 3,913 *g* for 10 min at 5°C in a refrigerated centrifuge (Sigma 2-16PK, Germany) and the supernatant was collected and filtered through a 0.2-μm filter to remove any unencapsulated CCM precipitate. The filtrate was considered a dispersion of TPGS/CCM nanoparticles, and it was lyophilized and stored in glass vials at −20°C. The nanoparticle dispersion was visually inspected for color, opacity, and presence of sediment at three stages: after rehydration of the dried film, after centrifugation, and again after filtration. TPGS/CCM samples were prepared in triplicates. Nanoparticles were resuspended in double-deionized water before use in experiments.

As blank/empty controls, TPGS micellar particles without CCM (MTPGS) were prepared using the same protocol as described above, except methanol was used instead of the CCM stock solution.

Nanoparticle Size Determination and Stability Testing in 0.9% Saline

Nanoparticle morphology was checked using DLS following centrifugation and filtration to ensure removal of precipitated particles. DLS was performed using the Zetasizer Nanoseries (Malvern Instruments, Worcestershire, UK), and each batch was checked in quadruplicate. The morphology of MTPGS and TPGS/CCM at 12.5:1 was investigated by transmission electron microscopy (JEM-1200EX, JEOL). MTPGS and TPGS/CCM at 12.5:1 were diluted with water and then placed over 400-mesh copper-coated grids. The grids were dried at room temperature (RT) before inspection with transmission electron microscope (TEM). The UV-Vis spectra of free and TPGS-encapsulated CCM were measured at 800–200 nm using a UV-Vis spectrophotometer (Cary 50 Bio UV-visible spectrophotometer, Varian, CA, USA). Nanoparticle samples were diluted with water to give absorbances within the measurable range. A control solution of free CCM was prepared by diluting the stock solution of CCM in methanol with water.

For *in vitro* stability tests, 1 mg of freshly produced TPGS/CCM at 5:1 and 12.5:1 were incubated in 10 ml 0.9% saline at 37°C for 9 days. At different time points, the particle size distribution profiles, polydispersity index (PDI), and zeta potential values of the corresponding samples were characterized by DLS.

In vitro Release Profiles of TPGS/CCM in Simulated Colonic and Gastric Fluids

In vitro CCM release profiles were measured using a dialysis sac in combination with a United States Pharmacopeia dissolution/release apparatus (7000/7010 Dissolution Apparatus, Agilent Technologies, Santa Clara, CA, USA). Nanoparticles were suspended in enzyme-free simulated gastric fluid (SGF) containing 0.2% tween-80 (pH 2.4) or simulated colonic fluid (SCF) containing 0.2% tween-80 and 0.13 U/ml β-galactosidase in phosphate buffer (pH 7.4). (Singh et al., 2004) The SGF was prepared by dissolving NaCl in Milli-Q (18Ω) water to a final concentration of 34.2 mM and then adjusted to pH 2.4 using 70 mM HCl (Axson et al., 2015).

TPGS/CCM sacs were dialyzed in 500 ml of either simulated fluid at 37 ± 0.5°C for 24 h with stirring at 100 cycles/min. At 0, 1, 2, 4, 8, 16, and 24 h, 0.5 ml of the release medium was sampled and the absorption at 425 nm was measured using a LAMBDA 950 UV-Vis Spectrophotometer (PerkinElmer, Wellesley, MA, USA). Each batch was analyzed in triplicates.

Intracellular ROS Detection

Intracellular ROS generation in HT-29 cells was measured using an ROS Assay Kit. HT-29 cells were seeded in a 35-mm glass-bottom culture dishes at a density of 1×10^6 cells/well and cultured overnight in 2 ml DMEM with 10% FBS at 37°C in a 5% CO_2 humidified atmosphere. On the next day, the medium was replaced with fresh DMEM+FBS, followed by the addition of 10 μM free CCM, TPGS/CCM, or 125 μM MTPGS. Control cultures were without treatment. After 24 h, the medium was removed, 2 ml of fresh DMEM medium was added, and the mixture was incubated for another 20 min. The cells were then washed three times with ice-cold phosphate-buffered saline (PBS) and imaged under a fluorescent confocal laser scanning microscope (Leica TCS SP5, Germany). The ROS-mediated decomposition of 2,7-Dichlorodihydrofluorescein diacetate (DCFH-DA) to dichlorofluorescein (DCF) was tracked based on DCF fluorescence at an excitation wavelength of 488 nm and emission wavelengths of 500–540 nm. The mean fluorescent intensity of HT-29 cells were quantified after counting 10,000 cells by flow cytometry (BD Biosciences, Franklin Lakes, NJ, USA).

In vitro Cytotoxicity

HT-29 cells were plated at a density of 1×10^5 cells/well in 96-well plates. After a 24-h incubation, the culture media was replaced

with 100 µl fresh media and then 100 µl formulation (TPGS/CCM, free CCM (dissolved in 0.1% DMSO), or MTPGS) was added to a final concentration of 10 or 125 µM. Control wells received 100 µl of water instead of any formulation. After incubation for 48 h, 20 µl MTT (5 mg/ml) was added to each well, the absorbance was measured at 570 nm using a UV-Vis spectrophotometer, and IC_{50} was calculated according to manufacturer protocols.

Annexin V/PI Apoptosis Detection

HT-29 cells were seeded at a density of 1×10^5 cells/well and incubated with 5 µM of MTPGS, TPGS/CCM, or free CCM for 48 h. Cells were then digested with trypsin and collected by centrifugation at 157 g for 5 min. The cells were rinsed twice with PBS, resuspended in 500 µl binding buffer, then mixed with 2.5 µl annexin V and 5 µl PI. The cells were incubated in the dark for 15 min and cell apoptosis was analyzed using flow cytometry.

Wound Healing Assay

To investigate the effects of TPGS/CCM on cell migration, we performed a wound healing assay. Cells were seeded into six-well plates at a density of 1×10^6 cells/well and cultured at 37°C in a 5% CO_2 incubator for 24 h until completely confluent. The cell monolayer was scratched with a 200-µl pipette tip, the well was washed twice with PBS to remove any floating cells, and then the medium was replaced with DMEM containing 0.5% FBS. Cells were treated with 60 µM MTPGS, 5 µM free CCM, 5 µM TPGS/CCM, or no treatment (control) for 48 h. Migrating cells were photographed at the leading edge of the wound using a light microscope. Cell migration was quantified by dividing the area of the wound at 48 h after scratching by the area at 0 h (immediately after scratching).

Pharmacokinetics

Male Wistar rats were fasted overnight and randomly divided into three groups (n = 6 per group). TPGS/CCM, MTPGS, or free CCM was then administered at a dose of 150 mg/kg by oral gavage. For the preparation of free CCM suspension, 2 ml of CCM solution (1.5 mg/ml in acetone) was added dropwise into 10 ml of 0.5% CMC-Na solution and sonicated for 0.5 h. Blood samples (0.5 ml) were collected from the suborbital vein into heparinized tubes at predetermined time points after administration. Plasma was collected by centrifugation at 10,000 g for 5 min and stored at –20°C.

For quantification, 200 µl plasma was mixed with 50 µl 1 mM emodin (internal standard) and then the mixture was extracted using 200 µl ethyl acetate. After vortexing for 3 min and centrifuging at 10,000 g for 5 min, the supernatant was transferred to a clean tube and the solvent was evaporated under nitrogen gas flow. The residue was redissolved in 200 µl mobile phase [acetonitrile: 0.5% phosphoric acid (56:44, v/v)], vortexed for 3 min and centrifuged at 10,000 g for 5 min. Finally, 20 µl of dissolved sample was analyzed by HPLC (Prominence, Shimadzu Corp., Japan), using a 150 × 4.6 mm Symmetry C18, 5-µm column (Kinetex, Phenomenex, CA, USA), and the mobile phase pumped at a flow rate of 1 ml/min. Pharmacokinetic parameters were calculated using the non-compartmental model in DAS 2.0 (Mathematical Pharmacology Professional Committee of China, Shanghai, China).

Statistical Analysis

All batches were produced in triplicates, otherwise mentioned. Each experiment was repeated twice. Experimental results are presented as mean ± SD and were analyzed using ANOVA and Student's t test. A p-value of <0.05 was considered statistically significant.

RESULTS

Characterization of TPGS/CCM Nanoparticles

Nanoparticle dispersions prepared with a TPGS:CCM weight ratio ≥5:1 consistently formed transparent yellow dispersions with no sediment visible (**Figure 1A**), indicating that the whole CCM load was successfully solubilized (i.e. 100% loading efficiency). These preparations remained stable based on visual inspection for at least 7 days, with stability increasing with higher TPGS:CCM ratio. In contrast, dispersions prepared with TPGS:CCM at ratios <5:1 formed a translucent orange liquid (**Figure 1B**) that yielded a sediment upon centrifugation, indicating the presence of unencapsulated, insoluble CCM.

Nanoparticle size and size distribution were examined using dynamic laser scattering. As shown in **Figures 1C** and **D**, loading TPGS micelles with CCM (at 12.5:1, w/w) did not visibly affect their sizes or size distribution. The average particle sizes of MTPGS and TPGS/CCM at 12.5:1 were 12.7 ± 0.1 nm (PDI = 0.18) and 12.3 ± 0.1 nm (PDI = 0.17), respectively (n = 3, $P > 0.05$), suggesting a narrow size distribution. Transmission electron micrographs revealed that MTPGS and TPGS/CCM (at 12.5:1) nanoparticles were spherical and their sizes are consistent with the results of dynamic light scattering (**Figures 1E** and **F**). The lack of change in particle size and size distribution observed due to drug loading is consistent with previous studies (Saxena and Hussain, 2012; Meng et al., 2017). One of the possible reasons for this phenomenon is that the relatively low concentration (7.58%, w/w) and low molecular weight (368.39 g/mol) of CCM has negligible impact on TPGS micelles formation.

Nanoparticle size as measured by DLS is summarized in **Table 1**. A scatterplot of particle size *versus* TPGS:CCM ratio revealed an inflexion point at a ratio of 5:1, suggesting that this was the threshold for effective nanoparticle formation (**Figure 2**). Nanoparticles formed at TPGS:CCM ratios ≥5:1 were smaller, with a mean size of 11.6–12.7 nm. These sizes were comparable to that of MTPGS (12.7 nm). In contrast, nanoparticles formed at TPGS:CCM ratios <5:1 were about 10-fold larger (117.6–179.9 nm).

Stability of Nanoparticles at Different TPGS:CCM Ratios in 0.9% Saline

As shown in **Figure 3A** and **B**, though there were no significant changes in the mean particle size upon incubation of the TPGS/CCM at weight ratio of 12.5:1 in 0.9% saline for up to 7 days

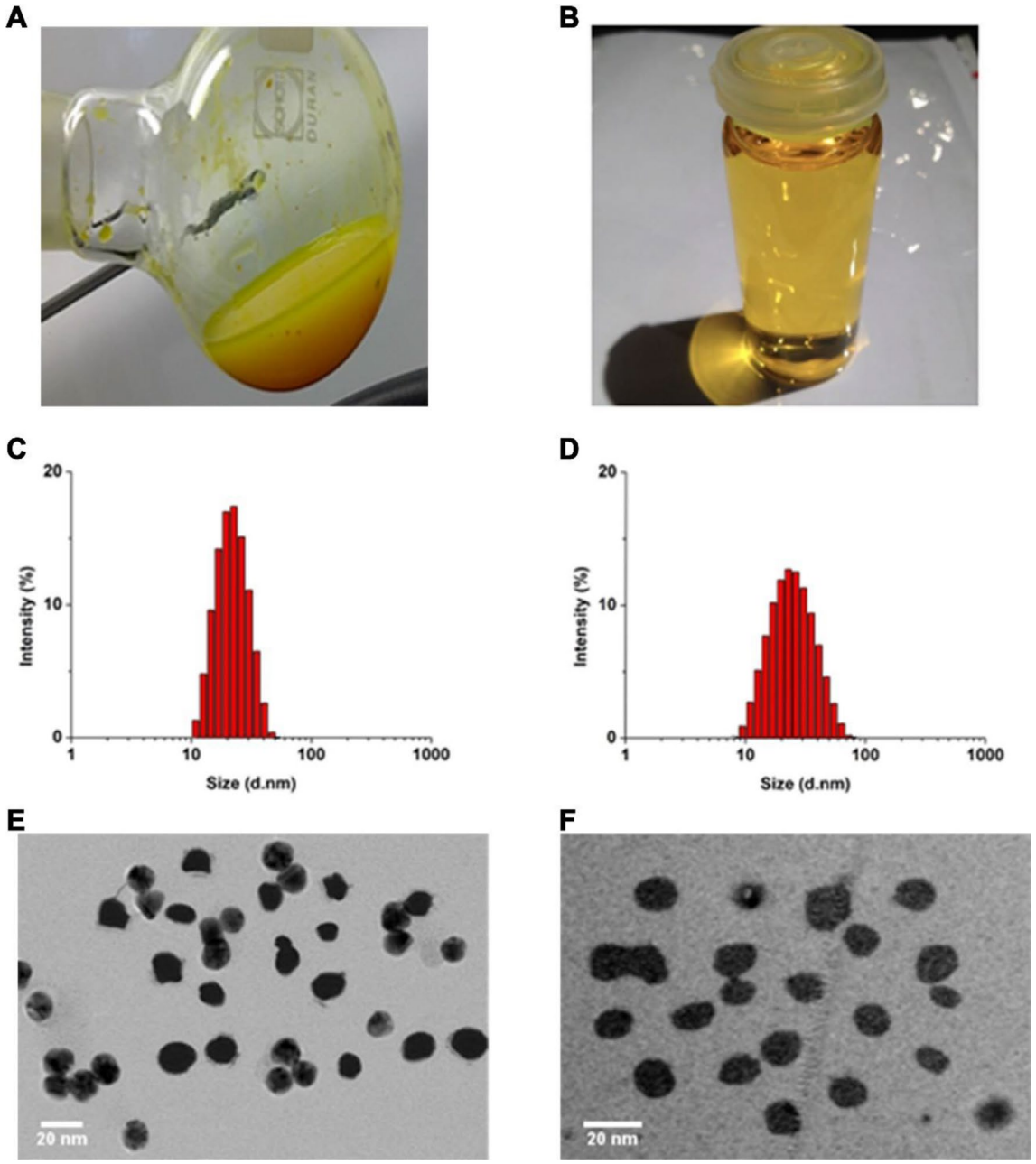

FIGURE 1 | Gross appearance of nanoparticle dispersions prepared using TPGS:CCM ratios of **(A)** 3.5:1 and **(B)** 12.5:1. Sample **(A)** was translucent orange with visible precipitation, while **(B)** was transparent yellow. Size distribution of **(C)** MTPGS micelles and **(D)** 12.5:1 of TPGS/CCM micelles, based on dynamic light scattering. Transmission electron micrographs of **(E)** MTPGS micelles and **(F)** 12.5:1 of TPGS/CCM micelles. Scale bar, 20 nm.

($p > 0.05$), the size distribution widened. Moreover, the PDI and zeta potential increased with extended incubation times (**Figures 3C**, **D**), indicating that the TPGS/CCM at 12.5:1 were not stable beyond 7 days and required preparation at the time of use or lyophilization for storage.

The hydrolytic stability of TPGS/CCM at weight ratio of 5:1 was shown to be poorer than that of TPGS/CCM at 12.5:1 (**Figure 3**). After 9 days of incubation in 0.9% saline, the TPGS/CCM at 5:1 aggregated into bigger particles and formed multiple peaks due to a sharp decrease in absolute value of zeta potential. In contrast, the size distribution of TPGS/CCM at 12.5:1 remained narrow, indicating higher hydrolytic stability under the same conditions. Thus, a TPGS:CCM ratio of 12.5:1 was chosen to be used in this study, because of the relatively higher stability of the resulting drug-loaded nanoparticles.

All nanoparticle dispersions showed an absorption peak at 425 nm, which corresponds to the absorption peak of free CCM (**Figure 4**). This suggests that the chemical structure of CCM

TABLE 1 | Nanoparticle morphology, size, and stability of nanoparticle dispersions at different TPGS:CCM ratios.

TPGS:CCM ratio (w/w)	Size, mean ± SD (nm, *n* = 8)	Polydispersity index	Color	Other observations
*1:0 (blank)	12.7 ± 0.1	0.18	Colorless	Transparent
50:1	12.3 ± 0.1	0.15	Yellow	Transparent
25:1	12.7 ± 0.1	0.18	Yellow	Transparent
20:1	12.5 ± 0.1	0.22	Yellow	Transparent
12.5:1	12.3 ± 0.1	0.17	Yellow	Transparent
5:1	11.6 ± 0.2	0.16	Yellow	Transparent
3.5:1	117.6 ± 17.2	0.28	Orange	Translucent; sediment upon centrifugation
3:1	129.0 ± 1.5	0.17	Orange	Translucent; sediment upon centrifugation
2.5:1	135.4 ± 1.6	0.12	Orange	Translucent; sediment upon centrifugation
1.5:1	179.9 ± 50.3	0.38	Orange	Translucent; sediment upon centrifugation

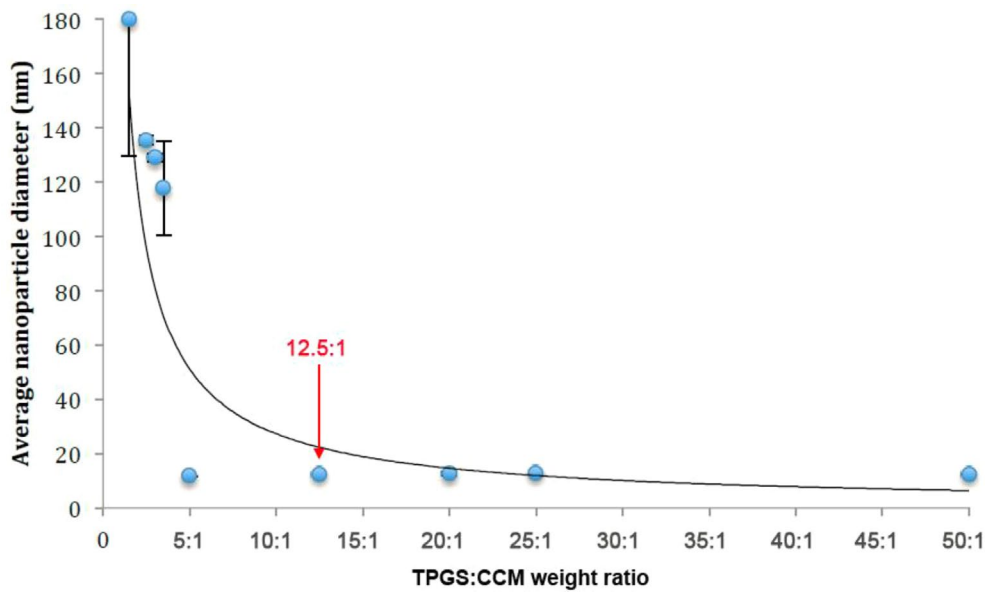

FIGURE 2 | Sizes of nanoparticle prepared at different TPGS:CCM ratios.

was retained regardless of the TPGS:CCM ratio used to prepare the samples, and that there was no chemical reaction between CCM and TPGS. This is consistent with our hypothesis that the hydrophobic CCM is physically trapped within the core of the TPGS micelles. Absorbance at this peak wavelength changed with CCM concentration in accordance with the Beer–Lambert Law.

TPGS/CCM Nanoparticles Release CCM More Effectively in Simulated Colonic Fluid Than Simulated Gastric Fluid

In vitro CCM release profiles of TPGS/CCM in each type of simulated fluid are shown in **Figure 5A** and **B**. The total amount of CCM released was lower in SGF than in SCF, with only about 25% of initial CCM released in gastric fluid after 24 h at 37°C. In contrast, more than 40% of initial CCM was released in colonic fluid within only 2 h and 95% was released by 24 h. We suggest that the greater release in colonic fluid may reflect oxidation of TPGS by β-galactosidase, which destabilizes the nanoparticles and thereby accelerates CCM release.

TPGS/CCM Nanoparticles Reduce the Intracellular Concentration of ROS in HT-29 Cells

Treatment of HT-29 cells with blank MTPGS or free CCM alone significantly decreased DCF fluorescence intensity compared to control cells, indicating a reduction in the level of intracellular ROS (**Figure 6**). Furthermore, DCF fluorescence was significantly lower in HT-29 cells treated with TPGS/CCM than in cells treated with free CCM or MTPGS.

Cytotoxicity of the TPGS/CCM Against HT-29 Cells

HT-29 cells treated with TPGS/CCM had a significantly lower IC_{50} (5.7 ± 0.5 μM) than those treated with free CCM (16.8 ± 1.4 μM),

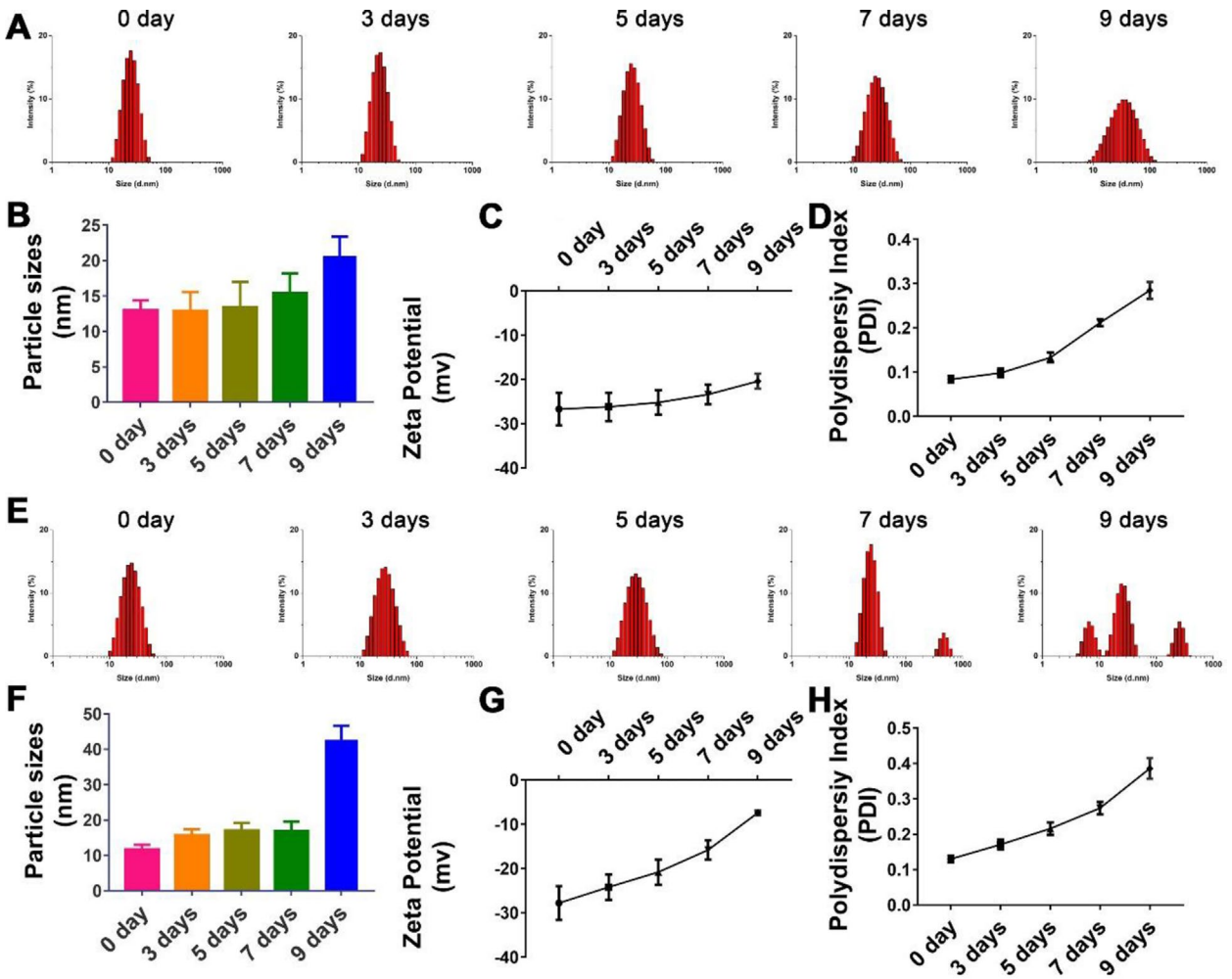

FIGURE 3 | Stability of nanoparticle with TPGS:CCM ratios at **(A–D)** 12.5:1 and **(E–H)** 5:1 in 0.9% saline solution after 9 days. Changes in size distribution profiles of **(A)** 12.5:1 and **(E)** 5:1, and mean diameter of **(B)** 12.5:1 and **(F)** 5:1; zeta potential of **(C)** 12.5:1 and **(G)** 5:1 and polydispersity index (PDI) of **(D)** 12.5:1 and **(H)** 5:1 nanoparticle dispersions in 0.9% saline for up to 9 days. Results are mean ± SD (n = 3).

which in turn had a significantly lower IC_{50} than cells treated with MTPGS (598.7 ± 27.4 μM) (**Figure 7A**). These results indicate that TPGS/CCM is more efficient at lower doses than free CCM alone.

Effects of CPM on BT-549 Apoptosis

The apoptosis results reflected by the flow cytometric analysis are shown in **Figure 7B**. Treatment of HT-29 cells with 5 μM free CCM resulted in 6.47 ± 1.4% annexin V-positive cells while cells treated with 5 μM TPGS/CCM resulted in 21.4 ± 3.0%. In other words, loading CCM into TPGS nanoparticles resulted in a 3.3-fold increase in HT-29 cell apoptosis. The collective data shown in **Figure 7C** suggests that CCM loaded in TPGS had evident superiority as compared with the free CCM or the carrier alone.

TPGS/CCM is More Effective Than Free CCM at Reducing Colon Cancer Cell Migration

After 48 h of incubation, the HT-29 cells in the control group had migrated to nearly completely cover the wound area, as had cells treated with MTPGS (**Figure 8A**). In contrast, migration was markedly reduced in the CCM-treated groups. Cells treated with free CCM had a wound area that was 23.2 ± 4.1% of the original size, while cells treated with TPGS/CCM showed a wound area that was 58.8 ± 4.3% of the original size (**Figure 8B**).

Pharmacokinetic Profiles of Orally Administered TPGS/CCM

The pharmacokinetic parameters of free CCM and TPGS/CCM are summarized in **Table 2** and the CCM blood concentration shown in **Figure 9**. For free CCM, the maximum drug concentration (C_{max}) achieved was 311.42 ± 15.51 ng/ml, which occurred immediately after administration (T_{max} = 0). In contrast, the C_{max} of TPGS/CCM was substantially higher at 794.97 ± 43.94 ng/ml, and occurred much later at 2 h after administration. The $AUC_{0\to24}$ of TPGS/CCM was 3,461.48 ± 102.47 ng/ml/h, nearly 6.5-fold higher than that of free CCM (529.49 ± 22.32 ng/ml/h). These results indicate that loading CCM into TPGS

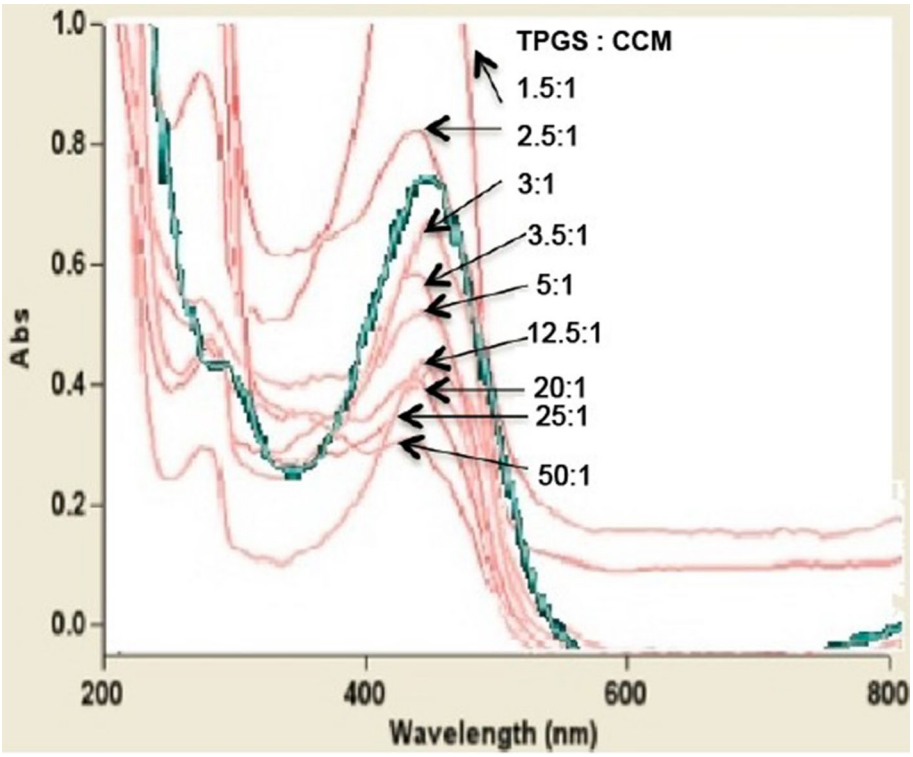

FIGURE 4 | UV-visible spectra for nanoparticle dispersions prepared at different TPGS:CCM ratios. The spectrum for free CCM is shown as a green line.

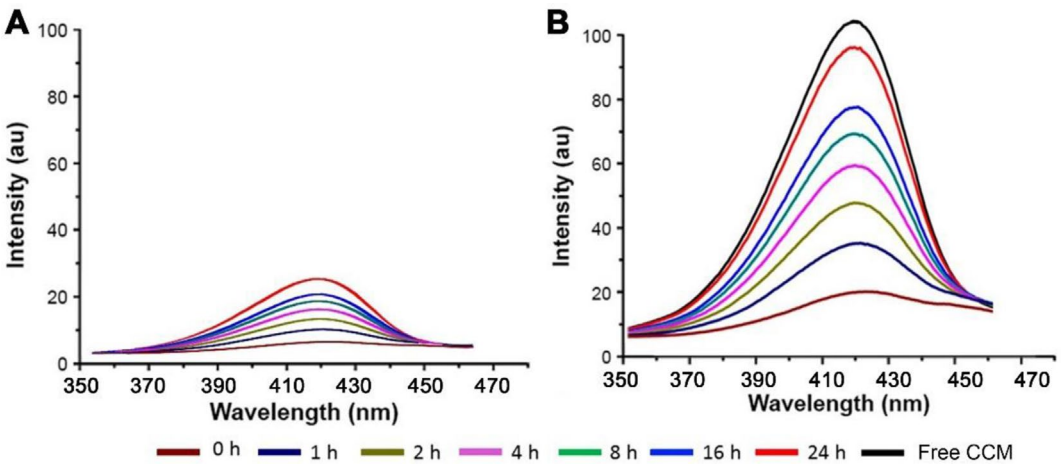

FIGURE 5 | Fluorescence spectra of CCM released from TPGS/CCM in **(A)** simulated gastric fluid and **(B)** simulated colonic fluid at different time points. The spectrum of free CCM is shown as a black line.

nanoparticles significantly enhances its systemic absorption, increasing its C_{max} and producing a more sustained release profile.

DISCUSSION

Loading lipophilic drugs into nanoparticles renders them dispersible in water (Bosselmann and Iii, 2012). CCM has great therapeutic potential but is poorly soluble in water (Nair et al., 2012). In this study, we demonstrate a method for loading CCM into nanoparticles using the surfactant, TPGS.

Optimizing the surfactant:drug ratio in nanoparticles is important for ensuring that their dispersions show low viscosity, high stability, and minimal particle aggregation (Tang et al., 2013). We found that the ratio of TPGS:CCM used was critical to the formulation of TPGS/CCM nanoparticles where stable

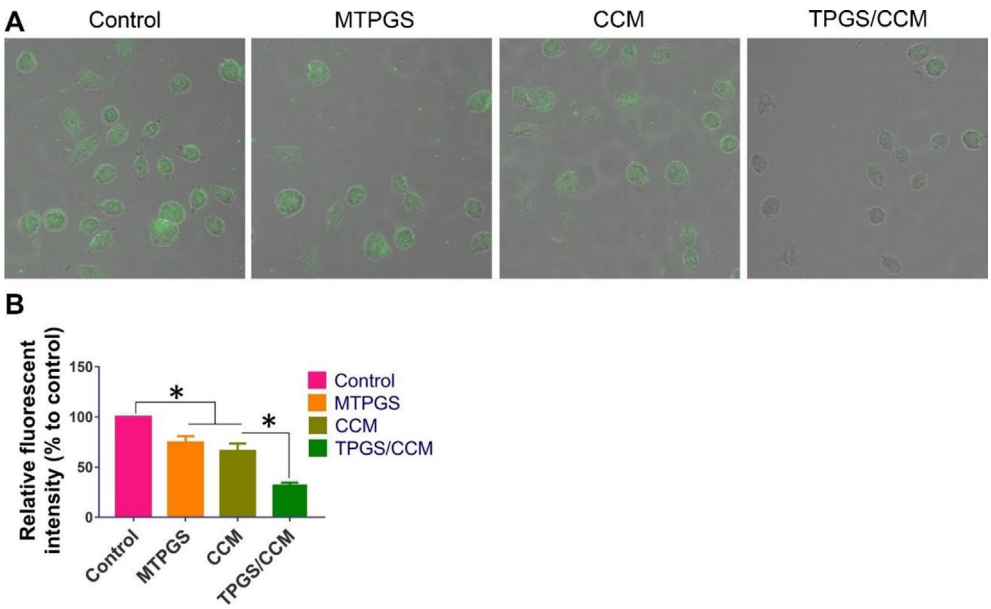

FIGURE 6 | DCF fluorescence in HT-29 cells treated with TPGS/CCM. **(A)** Representative images of cells treated with TPGS/CCM, MTPGS, free CCM, or no treatment (control). DCF fluorescence is shown in green overlaid on the bright-field image. Magnification, 500X. **(B)** Quantitation of DCF fluorescence in treated cells as a percentage of fluorescence in control cells. *$p < 0.05$.

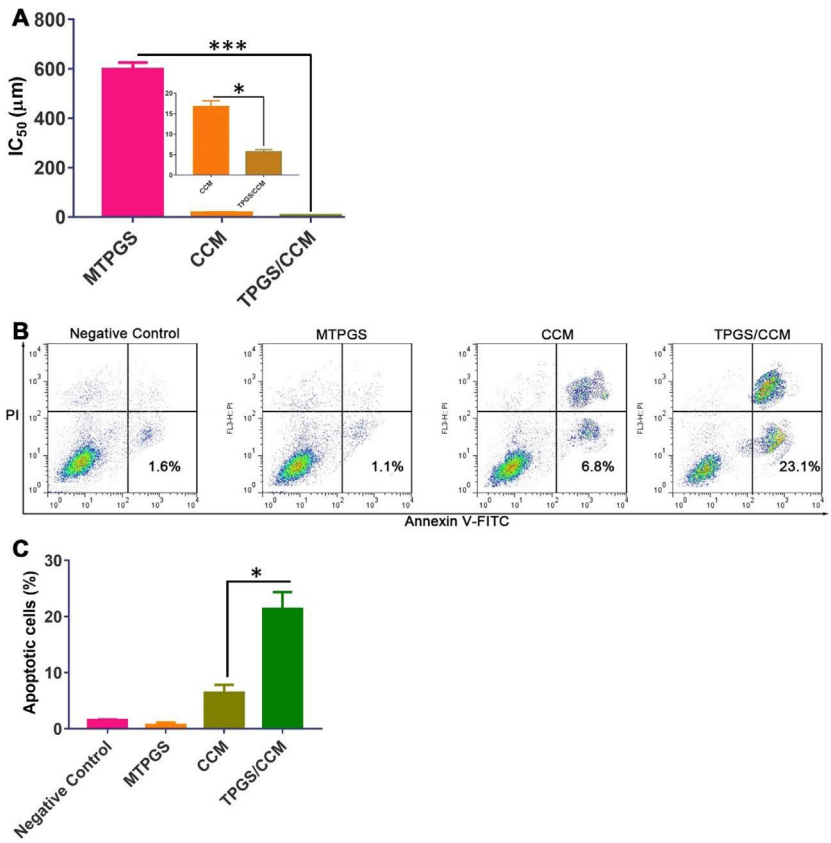

FIGURE 7 | HT-29 cell viability after treatment with TPGS/CCM, MTPGS, or free CCM. **(A)** Cytotoxicity was measured using the MTT assay. The inset in **(A)** shows a magnified view of the CCM and TPGS/CCM groups. **(B)** Flow cytometric analysis of HT-29 cells treated with different formulations. **(C)** Percentage of apoptotic cells in different treatment groups. *$p < 0.05$, ***$p < 0.001$.

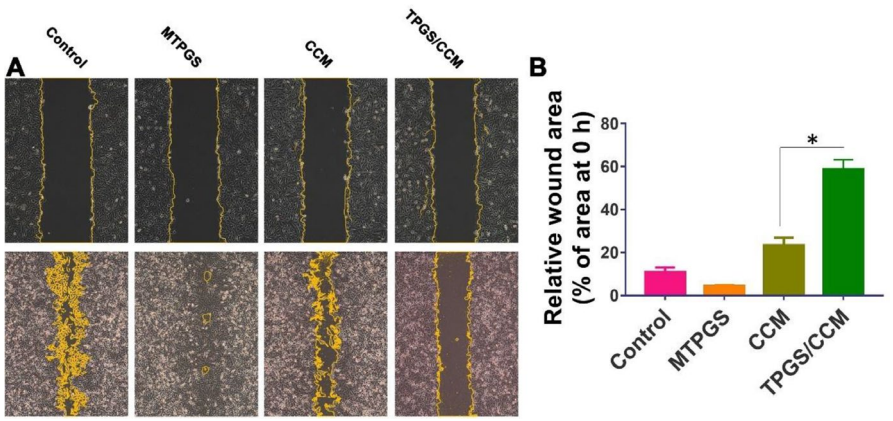

FIGURE 8 | Wound healing assay in HT-29 cells treated for 48 h with TPGS/CCM, MTPGS, free CCM, or no treatment (control). **(A)** Phase-contrast micrographs of the wound area at 0 h (upper row) and 48 h (lower row) later. Magnification, 100X. Cell edges along the scratch are falsely colored brown for visibility. **(B)** Quantitation of the wound area in each treatment group at 48 h, expressed as a percentage relative to the wound size at time 0. *$p < 0.05$.

TABLE 2 | Pharmacokinetic parameters of free curcumin (CCM) and TPGS/CCM.

Parameter	Free CCM	TPGS/CCM
C_{max} (ng/ml)	311.42 ± 15.51	794.97 ± 43.94
T_{max} (h)	0	2
$T_{1/2}$ (h)	0.35 ± 0.07	3.16 ± 0.78
Ke (h^{-1})	0.133	0.133
AUC_{0-24} (ng • h/ml)	529.49 ± 22.32	3,461.48 ± 102.47

dispersions were observed only for nanoparticles formulated at ratios >5:1. UV spectrophotometry analysis showed that the chemical structure of CCM was unchanged after encapsulation in TPGS/CCM nanoparticles. This suggests that CCM maintains its chemical properties and therefore its pharmacological activities within the TPGS micelles.

Two issues arose when dispersions were prepared using TPGS:CCM ratios below 5:1. First, precipitation was observed, even when the concentration of TPGS was well above its critical micellar concentration. This suggests that TPGS micellar volume could not accommodate the CCM load, leading to precipitation of excess CCM. Second, the nanoparticles formed were much larger than blank MTPGS micelles. We interpret this to mean that these dispersions did not contain TPGS micellar structures. The increase in particle size may also be indicative of decreasing nanoparticle stability, although the relatively low polydispersity indices for these dispersions suggests a narrow particle size range. These results, together with the observation that nanoparticles >100 nm are unable to enter cells by receptor-mediated processes (Montes-Burgos et al., 2010), leads us to recommend formulating TPGS/CCM nanoparticles at TPGS:CCM ratios >5:1.

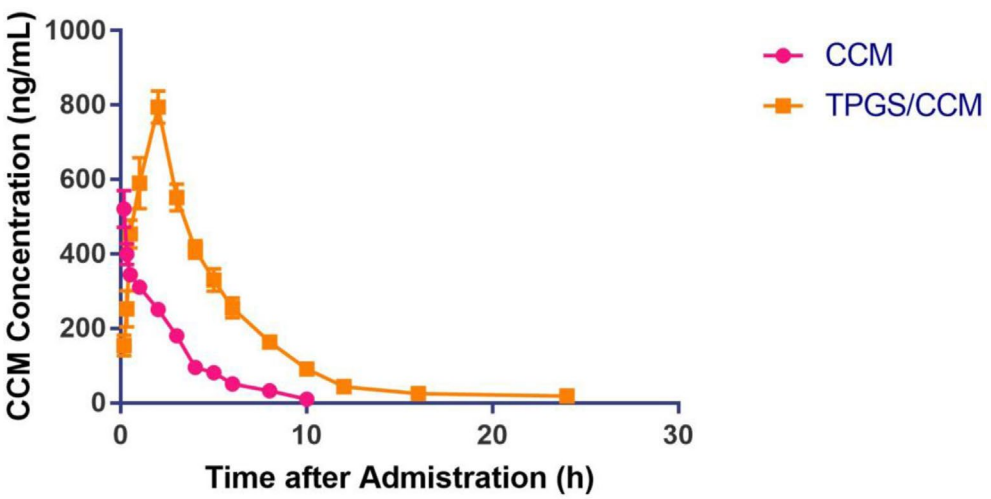

FIGURE 9 | Mean plasma CCM concentrations after oral administration of either free CCM or TPGS/CCM in rats ($n = 6$ per group).

We found that loading CCM into TPGS/CCM nanoparticles significantly improved the effects of the drug on HT-29 cells *in vitro*. ROS are known to be a key determinant of metabolic phenotype in cancer cells. Studies have shown that cancer cells have higher steady-state ROS levels than normal cells, and treating cancer cells with antioxidants can prevent their proliferation, invasion, migration, and metastasis (Nishikawa et al., 2009; Subramani et al., 2016). In our study, neither free CCM nor blank MTPGS affected intracellular ROS levels, whereas TPGS/CCM nanoparticles effectively reduced these levels. Both TPGS and CCM individually are known to have antioxidant properties at their rather high concentrations. One possible reason that only TPGS/CCM strongly reduced ROS levels is that TPGS and CCM simultaneously enter single cell and act synergistically to neutralize ROS.

TPGS/CCM was also more effective than free CCM at inducing apoptosis and inhibiting cell migration of HT-29 cells. One possibility is that loading into nanoparticles allows CCM to enter the cells more effectively by endocytosis and act synergistically with TPGS. Together, these results indicate that packaging CCM into TPGS nanoparticles increases drug potency.

Pharmacokinetic assessment of orally administered TPGS/CCM shows that the absorption modes of free CCM and TPGS/CCM are not the same, which is consistent with *in vitro* results. Loading CCM into TPGS/CCM nanoparticles provides greater drug bioavailability than free CCM when orally administered, which may mean that lower doses can be used. In other words, loading CCM into nanoparticles that are readily dispersible in aqueous media may allow administration of clinically relevant CCM doses by any route.

CONCLUSION

We showed that the thin-film rehydration method can be used to produce water-soluble CCM-loaded TPGS micellar nanoparticles. These nanoparticles efficiently release CCM in simulated colonic fluid and are significantly more effective than free CCM at reducing ROS concentration, increasing apoptosis, and inhibiting migration of HT-29 colon cancer cells *in vitro*. We also showed that CCM orally administered to rats is more bioavailable when formulated as TPGS/CCM than free CCM. These TPGS/CCM nanoparticles may therefore form the basis for the development of novel CCM formulations for treatment of colon cancer.

ETHICS STATEMENT

Male Wistar rats (200; 20 g) were provided by the Model Animal Research Center of Nanjing University (Nanjing, China). All animal experiments were approved by the Ethics Committee of Guilin Medical University (ethics number YXLL-2017-085).

AUTHOR CONTRIBUTIONS

HL carried out experiments; LY and ZZ carried out data analysis and drew figures; JM and WC wrote the paper; ET edited the paper; JM and GL led the research.

FUNDING

This work was supported by the National Natural Science Foundation of China (81860629, 81471809), Major Project of Guangxi Science and Technology Department (AA17292001) and the Open Funds of the Guangxi Key Laboratory of Tumor Immunology and Microenvironmental Regulation (2018KF003). Project of Guangxi Medical and Health Self-financing Plan (Z20180420).

REFERENCES

Allam, A. N., Komeil, I. A., Fouda, M. A., and Abdallah, O. Y. (2015). Preparation, characterization and in vivo evaluation of curcumin self-nano phospholipid dispersion as an approach to enhance oral bioavailability. *Int. J. Pharm.* 489, 117–123. doi: 10.1016/j.ijpharm.2015.04.067

Axson, J. L., Stark, D. I., Bondy, A. L., Capracotta, S. S., Maynard, A. D., Philbert, M. A., et al. (2015). Rapid kinetics of size and pH-dependent dissolution and aggregation of silver nanoparticles in simulated gastric fluid. *J. Phys. Chem. C. Nanomater. Interfaces* 119, 20632. doi: 10.1021/acs.jpcc.5b03634

Bagheri, R., Sanaat, Z., and Zarghami, N. (2018). Synergistic effect of free and nano-encapsulated chrysin-curcumin on Inhibition of hTERT gene expression in SW480 colorectal cancer cell line. *Drug Res.* 68, 335–343. doi: 10.1055/s-0043-121338

Bosselmann, S., and Williams, III, R. O. (2012). Has nanotechnology led to improved therapeutic outcomes? *Drug Dev. Ind. Pharm.* 38, 158. doi: 10.3109/03639045.2011.597764

Chen, R., Wulff, J. E., and Moffitt, M. G. (2018). Microfluidic Processing Approach to Controlling Drug Delivery Properties of Curcumin-Loaded Block Copolymer Nanoparticles. *Mol. Pharm.* 15, 4517–4528. doi: 10.1021/acs.molpharmaceut.8b00529

Chen, W., Li, L., Zhang, X., Liang, Y., Pu, Z., Wang, L., et al. (2017). Curcumin: a calixarene derivative micelle potentiates anti-breast cancer stem cells effects in xenografted, triple-negative breast cancer mouse models. *Drug Deliv.* 24, 1470–1481. doi: 10.1080/10717544.2017.1381198

Cheng, Y., Zhao, P., Wu, S., Yang, T., Chen, Y., Zhang, X., et al. (2018). Cisplatin and curcumin co-loaded nano-liposomes for the treatment of hepatocellular carcinoma. *Int. J. Pharm.* 545, 261–273. doi: 10.1016/j.ijpharm.2018.05.007

Dahlhaus, A., Siebenhofer, A., Guethlin, C., Taubenroth, M., Albay, Z., Schulz-Rothe, S., et al. (2018). Colorectal cancer stage at diagnosis in migrants and non-migrants: a crosssectional analysis of the KoMigra Study in Germany. *Z. Gastroenterol.* 56 (12), 1499–1506. doi: 10.1055/a-0655-2352

Dolan, R. D., Almasaudi, A. S., Dieu, L. B., Horgan, P. G., McSorley, S. T., and McMillan, D. C. (2018). The relationship between computed tomography-derived body composition, systemic inflammatory response, and survival in patients undergoing surgery for colorectal cancer. *J. Cachexia Sarcopenia Muscle* 10 (1), 111–122. doi: 10.1002/jcsm.12357

Gaonkar, R. H., Ganguly, S., Dewanjee, S., Sinha, S., Gupta, A., Ganguly, S., et al. (2017). Garcinol loaded vitamin E TPGS emulsified PLGA nanoparticles: preparation, physicochemical characterization, *in vitro* and *in vivo* studies. *Sci. Rep.* 7, 530. doi: 10.1038/s41598-017-00696-6

Ghaffari, S., Alihosseini, F., Rezayat Sorkhabadi, S. M., Arbabi Bidgoli, S., Mousavi, S. E., Haghighat, S., et al. (2018). Nanotechnology in wound healing; semisolid dosage forms containing curcumin-ampicillin solid lipid nanoparticles, *in-vitro*, *ex-vivo* and *in-vivo* characteristics. *Adv. Pharm. Bull.* 8, 395. doi: 10.15171/apb.2018.046

Huang, N., Lu, S., Liu, X. G., Zhu, J., Wang, Y. J., and Liu, R. T. (2017). *Oncotarget* 8, 81001. doi: 10.18632/oncotarget.20944

Liang, P. S., and Dominitz, J. A. (2019). Colorectal Cancer Screening: Is Colonoscopy the Best Option? *Med. Clin. North Am.* 103, 111–123. doi: 10.1016/j.mcna.2018.08.010

Meng, X., Liu, J., Yu, X., Li, J., Lu, X., and Shen, T. (2017). Pluronic F127 and D-α-tocopheryl polyethylene glycol succinate (TPGS) mixed micelles for targeting drug delivery across the blood brain barrier. *Sci. Rep.* 7, 2964. doi: 10.1038/s41598-017-03123-y

Mo, J., Wang, L., Huang, X., Lu, B., Zou, C., Wei, L., et al. (2017). Multifunctional nanoparticles for co-delivery of paclitaxel and carboplatin against ovarian cancer by inactivating the JMJD3-HER2 axis. *Nanoscale* 9, 13142–13152. doi: 10.1039/C7NR04473A

Montes-Burgos, I., Walczyk, D., Hole, P., Smith, J., Lynch, I., and Dawson, K. (2010). Characterisation of nanoparticle size and state prior to nanotoxicological studies. *J. Nanopart. Res.* 12, 47. doi: 10.1007/s11051-009-9774-z

Mu, L., and Feng, S. S. (2002). Vitamin E TPGS used as emulsifier in the solvent evaporation/extraction technique for fabrication of polymeric nanospheres for controlled release of paclitaxel (Taxol®). *J. Control. Release* 80, 129. doi: 10.1016/S0168-3659(02)00025-1

Nair, K. L., Thulasidasan, A. K. T., Deepa, G., Anto, R. J., and Kumar, G. S. V. (2012). Purely aqueous PLGA nanoparticulate formulations of curcumin exhibit enhanced anticancer activity with dependence on the combination of the carrier. *Int. J. Pharm.* 425, 44–52. doi: 10.1016/j.ijpharm.2012.01.003

Ni, W., Li, Z., Liu, Z., Ji, Y., Wu, L., Sun, S., et al. (2018). Dual-targeting nanoparticles: co-delivery of curcumin and 5- fluorouracil for synergistic treatment of hepatocarcinoma. *J. Pharm. Sci.* 108 (3), 1284–1295. doi: 10.1016/j.xphs.2018.10.042

Nishikawa, M., Hashida, M., and Takakura, Y. (2009). Catalase delivery for inhibiting ROS-mediated tissue injury and tumor metastasis. *Adv. Drug Deliv. Rev.* 61, 319. doi: 10.1016/j.addr.2009.01.001

Saxena, V., and Hussain, M. D. (2012). Poloxamer 407/TPGS mixed micelles for delivery of gambogic acid to breast and multidrug-resistant cancer. *Int. J. Nanomed.* 7, 713. doi: 10.2147/IJN.S28745

Scott, M., Jamie, S., Wallerstedt, D. B., Mary, R., and Mansky, P. J. (2008). Botanicals used in complementary and alternative medicine treatment of cancer: clinical science and future perspectives. *Expert Opin. Invest. Drugs* 17, 1353–1364.. doi: 10.1517/13543784.17.9.1353

Sharma, R. K., Cwiklinski, K., Aalinkeel, R., Reynolds, J. L., Sykes, D. E., Quaye, E., et al. (2017). Immunomodulatory activities of curcumin-stabilized silver nanoparticles: efficacy as an antiretroviral therapeutic. *Immunol. Invest.* 46, 833. doi: 10.1080/08820139.2017.1371908

Shimada, Y., Tajima, Y., Nagahashi, M., Ichikawa, H., Oyanagi, H., Okuda, S., et al. (2018). Clinical significance of BRAF Non-V600E mutations in colorectal cancer: a retrospective study of two institutions. *J. Surg. Res.* 232, 72–81. doi: 10.1016/j.jss.2018.06.020

Singh, B. N., Trombetta, L. D., and Kim, K. H. (2004). Biodegradation behavior of gellan gum in simulated colonic media. *Pharm. Dev. Technol.* 9, 399. doi: 10.1081/PDT-200035793

Subramani, R., Gonzalez, E., Arumugam, A., Nandy, S., Gonzalez, V., Medel, J., et al. (2016). Nimbolide inhibits pancreatic cancer growth and metastasis through ROS-mediated apoptosis and inhibition of epithelial-to-mesenchymal transition. *Sci. Rep.* 6, 19819. doi: 10.1038/srep19819

Tang, X., Cai, S., Zhang, R., Liu, P., Chen, H., Zheng, Y., et al. (2013). Paclitaxel-loaded nanoparticles of star-shaped cholic acid-core PLA-TPGS copolymer for breast cancer treatment. *Nanoscale Res. Lett.* 8, 420. doi: 10.1186/1556-276X-8-420

Vecchione, R., Quagliariello, V., Calabria, D., Calcagno, V., De Luca, E., Iaffaioli, R. V., et al. (2016). Curcumin bioavailability from oil in water nano-emulsions: In vitro and in vivo study on the dimensional, compositional and interactional dependence. *J. Control. Release* 233, 88–100. doi: 10.1016/j.jconrel.2016.05.004

Wang, J., Pan, W., Wang, Y., Lei, W., Feng, B., Du, C., et al. (2018). Enhanced efficacy of curcumin with phosphatidylserine-decorated nanoparticles in the treatment of hepatic fibrosis. *Drug Deliv.* 25, 1–11. doi: 10.1080/10717544.2017.1399301

Wrobel, P., and Ahmed, S. (2018). Current status of immunotherapy in metastatic colorectal cancer. *Int. J. Colorectal Dis.* 34 (1), 13–25. doi: 10.1007/s00384-018-3202-8

Yallapu, M. M., Maher, D. M., Sundram, V., Bell, M. C., Jaggi, M., and Chauhan, S. C. (2010). Curcumin induces chemo/radio-sensitization in ovarian cancer cells and curcumin nanoparticles inhibit ovarian cancer cell growth. *J. Ovarian Res.* 3, 11. doi: 10.1186/1757-2215-3-11

Yen, F. L., Wu, T. H., and Tzeng, C. W. (2010). Curcumin nanoparticles improve the physicochemical properties of curcumin and effectively enhance its antioxidant and antihepatoma activities. *J. Agric. Food. Chem.* 58, 7376–7382. doi: 10.1021/jf100135h

Zambrano, L. M. G., Brandao, D. A., Rocha, F. R. G., Marsiglio, R. P., Longo, I. B., Primo, F. L., et al. (2018). Local administration of curcumin-loaded nanoparticles effectively inhibits inflammation and bone resorption associated with experimental periodontal disease. *Sci. Rep.* 8, 6652. doi: 10.1038/s41598-018-24866-2

Zhang, J., Tao, W., Chen, Y., Chang, D., Wang, T., Zhang, X., et al. (2015). Doxorubicin-loaded star-shaped copolymer PLGA-vitamin E TPGS nanoparticles for lung cancer therapy. *J. Mater. Sci. Mater. Med.* 26, 165. doi: 10.1007/s10856-015-5498-z

Zou, T., and Gu, L. (2013). TPGS emulsified zein nanoparticles enhanced oral bioavailability of daidzin: *in vitro* characteristics and *in vivo* performance. *Mol. Pharm.* 10, 2062. doi: 10.1021/mp400086n

Conflict of Interest Statement: The authors declare that the research was conducted in the absence of any commercial or financial relationships that could be construed as a potential conflict of interest.

frontiers in Pharmacology

METHODS
published: 25 September 2019
doi: 10.3389/fphar.2019.01064

Modeling the Distribution of Diprotic Basic Drugs in Liposomal Systems: Perspectives on Malaria Nanotherapy

Ernest Moles[1,2,3]*, *Maria Kavallaris*[1,2,3] *and Xavier Fernàndez-Busquets*[4,5,6]*

[1] Children's Cancer Institute, Lowy Cancer Research Centre, UNSW Sydney, Randwick, NSW, Australia, [2] School of Women's and Children's Health, UNSW Sydney, Sydney, NSW, Australia, [3] ARC Centre of Excellence in Convergent Bio-Nano Science and Technology, Australian Centre for NanoMedicine, UNSW Sydney, Sydney, NSW, Australia, [4] Nanomalaria Group, Institute for Bioengineering of Catalonia (IBEC), The Barcelona Institute of Science and Technology, Barcelona, Spain, [5] Barcelona Institute for Global Health (ISGlobal, Hospital Clínic-Universitat de Barcelona), Barcelona, Spain, [6] Nanoscience and Nanotechnology Institute (IN2UB), University of Barcelona, Barcelona, Spain

OPEN ACCESS

Edited by:
Salvatore Salomone, University of Catania, Italy

Reviewed by:
Andrey A. Rosenkranz, Lomonosov Moscow State University, Russia
Sylvio May, North Dakota State University, United States

***Correspondence:**
Ernest Moles
emoles@ccia.org.au
Xavier Fernàndez-Busquets
xfernandez_busquets@ub.edu

Specialty section:
This article was submitted to Experimental Pharmacology and Drug Discovery, a section of the journal Frontiers in Pharmacology

Received: *08 March 2019*
Accepted: *20 August 2019*
Published: *25 September 2019*

Citation:
Moles E, Kavallaris M and Fernàndez-Busquets X (2019) Modeling the Distribution of Diprotic Basic Drugs in Liposomal Systems: Perspectives on Malaria Nanotherapy. Front. Pharmacol. 10:1064. doi: 10.3389/fphar.2019.01064

Understanding how polyprotic compounds distribute within liposome (LP) suspensions is of major importance to design effective drug delivery strategies. Advances in this research field led to the definition of LP-based active drug encapsulation methods driven by transmembrane pH gradients with evidenced efficacy in the management of cancer and infectious diseases. An accurate modeling of membrane-solution drug partitioning is also fundamental when designing drug delivery systems for poorly endocytic cells, such as red blood cells (RBCs), in which the delivered payloads rely mostly on the passive diffusion of drug molecules across the cell membrane. Several experimental models have been proposed so far to predict the partitioning of polyprotic basic/acid drugs in artificial membranes. Nevertheless, the definition of a model in which the membrane-solution partitioning of each individual drug microspecies is studied relative to each other is still a topic of ongoing research. We present here a novel experimental approach based on mathematical modeling of drug encapsulation efficiency (EE) data in liposomal systems by which microspecies-specific partition coefficients are reported as a function of pH and phospholipid compositions replicating the RBC membrane in a simple and highly translatable manner. This approach has been applied to the study of several diprotic basic antimalarials of major clinical importance (quinine, primaquine, tafenoquine, quinacrine, and chloroquine) describing their respective microspecies distribution in phosphatidylcholine-LP suspensions. Estimated EE data according to the model described here closely fitted experimental values with no significant differences obtained in 75% of all pH/lipid composition-dependent conditions assayed. Additional applications studied include modeling drug EE in LPs in response to transmembrane pH gradients and lipid bilayer asymmetric charge, conditions of potential interest reflected in our previously reported RBC-targeted antimalarial nanotherapeutics.

Keywords: partition coefficient, distribution coefficient, polyprotic drug, pH-controlled drug encapsulation, targeted drug delivery, liposomal systems, malaria therapy, nanomedicine

INTRODUCTION

A wide range of therapeutic nanoparticles in the form of nanocarrier-based delivery systems have been developed so far for the management of several medical conditions aiming to improve treatment outcomes while minimizing drug dosages (Anselmo and Mitragotri, 2016; Bobo et al., 2016). Among these, liposomes (LPs) have proven to be notably effective in the treatment of cancer, fungal infections, and age-related disorders, among other therapeutic purposes, as well as in analgesia and vaccine formulations (Allen and Cullis, 2013; Bulbake et al., 2017). Given their biphasic character analogous to biological membranes, LPs are capable of entrapping both lipophilic and hydrophilic compounds as well as buffer solutions (Torchilin, 2005; Pattni et al., 2015; Sercombe et al., 2015). Such particular features have been exploited for the generation of transmembrane pH and chemical gradients, which in turn drive the encapsulation of water-soluble, amphiphilic polyprotic drugs as a result of pH-driven variations in drug microspecies abundance (Madden et al., 1990; Cullis et al., 1991) and/or following the formation of drug precipitates in complexation with multivalent salts (Haran et al., 1993; Clerc and Barenholz, 1995; Wei et al., 2018).

Aforesaid encapsulation strategies rely on the selective partitioning and passive diffusion of unionized drug molecules, i.e., unionized microspecies, across the LP membrane. Such migratory process is triggered in response to drug concentration gradients between LP compartments (Gubernator, 2011; Sercombe et al., 2015) and persists until an equilibrium concentration is reached between the LP membrane (organic) and solvent (aqueous) fractions. Such ratio is indicative of drug lipophilicity and is generally expressed in the literature in the form of partition or distribution coefficients (*P* and *D*), depending on the respective absence or presence of ionized drug molecules, i.e., ionized microspecies, in solution (Leo et al., 1971; Scherrer and Howard, 1977; Hansch et al., 1995; Warhurst et al., 2003; Warhurst et al., 2007). An example of *P* and *D* calculation for a diprotic basic drug is illustrated in Equations 1–5. Furthermore, coefficient *D* is utilized to calculate LP encapsulated amounts for polyprotic drugs in the presence of predefined transmembrane pH gradients (Cullis et al., 1991), as exemplified in Equation 6. The resulting distribution model is referred here as D_P given the initial assumption of unionized drug molecules as sole microspecies able to diffuse into the lipid bilayer (Hansch et al., 1995; Warhurst et al., 2003; Tetko and Poda, 2004; Warhurst et al., 2007; Omodeo-Salè et al., 2009). This assumption has been theorized in a large number of works and is represented in **Figure 1** as an adaptation for liposomal systems.

(1) $$P = \frac{molDrug_{org}}{Vol_{org}} \Big/ \frac{molDrug_{aq}}{Vol_{aq}}$$

(2) $$D = \frac{molDrug_{org}}{Vol_{org}} \Big/ \frac{molDrug_{aq} + molDrug_{aq}^{H+} + molDrug_{aq}^{2H+}}{Vol_{aq}}$$

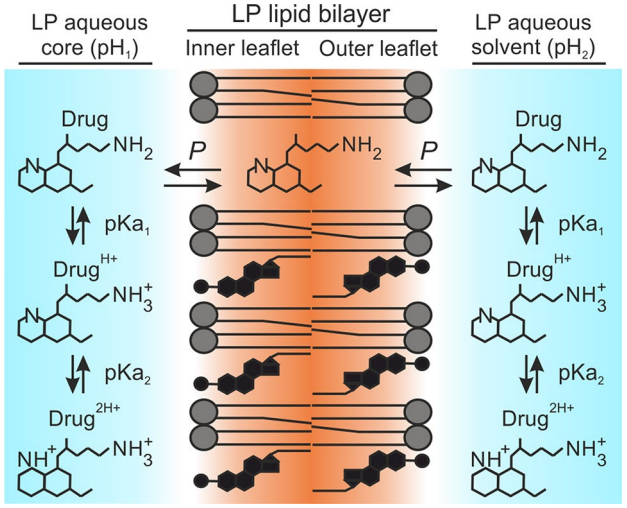

FIGURE 1 | D_P distribution model. Illustration adapted for amphiphilic diprotic basic drugs in liposomal systems. Primaquine is used as drug example.

(3) $$D = \left(\frac{molDrug_{org} \times Vol_{aq}}{Vol_{org} \times molDrug_{aq}}\right) \Big/ \left(1 + \frac{molDrug_{aq}^{H+}}{molDrug_{aq}} + \frac{molDrug_{aq}^{2H+}}{molDrug_{aq}}\right)$$

(4) $$pH = pKa_1 + \log\left(\frac{molDrug}{molDrug^{H+}}\right); \quad pH = pKa_2 + \log\left(\frac{molDrug^{H+}}{molDrug^{2H+}}\right)$$

(5) $$\log D = \log P - \log(1 + 10^{(\mathrm{pKa}_1 - pH)} + 10^{(pKa_1 + pKa_2 - 2\times pH)})$$

(6) $$\frac{[Drug_{aq} + Drug_{aq}^{H+} + Drug_{aq}^{2H+}]_{in}}{[Drug_{aq} + Drug_{aq}^{H+} + Drug_{aq}^{2H+}]_{out}} = \frac{1 + 10^{(pKa_1 - pH_{in})} + 10^{(pKa_1 + pKa_2 - 2\times pH_{in})}}{1 + 10^{(pKa_1 - pH_{out})} + 10^{(pKa_1 + pKa_2 - 2\times pH_{out})}}$$

However, amphiphilic polyprotic drugs, which indeed account for most of the therapeutic agents used in the clinic (Charifson and Walters, 2014), exhibit complex structural and physicochemical properties with multiple ionization states being present in physiological conditions, each one displaying a different degree of lipophilicity depending on (i) the overall number of ionized groups, as well as (ii) their position within the drug structure. In particular, some degree of interaction with biological membranes would be expected for drugs with size and 3D configuration similar to phospholipid molecules and, above all, those microspecies with the lowest ionization state and/or in which ionized moieties are excluded from the most lipophilic regions. Some examples of drugs fulfilling these requisites include quinoline derivatives, such as the 4-/8-aminoquinoline and naphtoquinoline compounds, aminoalcohols, acridine derivatives, and anthracyclines, among

many other drugs utilized for malaria and cancer therapy (Vennerstrom et al., 1999; Kaschula et al., 2002; Bawa et al., 2010; Shaul et al., 2013; Soares et al., 2015).

Variations in the interaction of polyprotic drugs with lipid bilayers have been reported as a function of pH and phospholipid charge, feature reflected by experimental changes in coefficient *D* (Ottiger and Wunderli-Allenspach, 1997; Krämer et al., 1998; Xia et al., 2005; Nair et al., 2012). Nevertheless, the separate contribution of each single microspecies to define the overall distribution of drugs in liposomal systems has never been studied. A detailed understanding of the partitioning behavior of all microspecies present in the system is essential to accurately model drug interactions with biological and synthetic membranes, and for the development of more effective drug delivery strategies.

Based on the above considerations and our experimentally collected data, we present here novel distribution models that accurately predict the distribution in LP suspensions of various diprotic basic antimalarials of major clinical significance. Using experimental encapsulation data in phosphatidylcholine-LPs, and the knowledge of *P* and pKa values for antimalarial drugs, microspecies-specific partition coefficients were estimated as a function of pH and phospholipid compositions that simulate the membrane properties of the red blood cell (RBC), the host cell for *Plasmodium falciparum* blood stages. With the aim to improve the design of our previously developed RBC-targeted LP models for severe malaria therapy (Moles et al., 2015; Moles et al., 2017), the distribution models described here were applied to estimate antimalarial drug encapsulation and release in response to transmembrane pH gradients along with their distribution within RBC compartments.

MATERIALS AND METHODS

Reagents and Chemicals

Except where otherwise indicated, reagents were purchased from Merck and Co., Inc. (Kenilworth, NJ, USA), and reactions were performed at room temperature (22 to 24°C). Anhydrous quinine (QN, ≥98% purity, 173–175°C mp), primaquine diphosphate salt (PQ, ≥98% purity, 205–206°C mp), tafenoquine succinate (TQ, ≥95% purity, 146–149°C mp), quinacrine dihydrochloride (QC, ≥90% purity, 248–250°C mp), and chloroquine diphosphate salt (CQ, ≥98% purity, 200°C mp) were purchased in solid form and used without further purification. The lipids 1,2-dioleoyl-*sn*-glycero-3-phosphocholine (PC), 1,2-dioleoyl-*sn*-glycero-3-phosphoethanolamine (PE), 1,2-distearoyl-sn-glycero-3-phosphoethanolamine-N-[methoxy(polyethylene glycol)-2000] (PE-PEG), and 1,2-dioleoyl-*sn*-glycero-3-phosphoethanolamine-N-[lissamine rhodamine B sulfonyl] (PE-Rho, used for LP tracking purposes) were purchased as solid material from Avanti Polar Lipids, Inc. (Alabaster, AL, USA). Phosphatidylserine (PS, average relative molar mass of 788) was obtained from bovine spinal cord, and was supplied in solid form by Lipid Products, Ltd. (South Nutfield, Redhill, UK). Purity for purchased lipids (≥95%), cholesterol (≥99%, 360°C bp), and drugs is reported by the respective suppliers according to HPLC analysis.

LP Phospholipid Compositions, LP Preparation, and Drug Partitioning Analysis

Phospholipid compositions (mole ratios) for the LP suspensions assayed in this work were: 1) PC-LPs (cholesterol:PE-Rho:PC, 20:0.5:77.5); 2) PC:PS-LPs (cholesterol:PE-Rho:PC:PS, 20:0.5:53.1:26.4); 3) PC:PS:PE-LPs (cholesterol:PE-Rho:PC:PS:PE, 40:0.5:13.9:19.8:25.8); and 4) PC:PS:PE:PEG-LPs (cholesterol:PE-Rho:PC:PS:PE:PE-PEG, 40:0.5:13.9:19.8:20.8:5).

LP suspensions were prepared by the lipid film hydration method in combination with particle extrusion through polycarbonate membranes (MacDonald et al., 1991). Briefly, stock lipids in chloroform were mixed and dissolved in chloroform:methanol (2:1 v/v) in a round-bottom flask, and the organic solvents were subsequently removed by rotary evaporation under reduced pressure at 37°C. The resulting dry lipid film was then hydrated in phosphate-buffered saline (PBS) (pH 7.4), or alternatively in citrate-/phosphate-/tris-buffered saline solutions at pH 4.0/6.5/9.0 when studying drug partitioning in non-physiological pH conditions. PBS was used as solvating buffer for drug partitioning analysis in the presence of negatively charged, PS-containing LPs. Unilamellar vesicles at 10 mM lipid, ca. 135 to 185 nm in diameter, were obtained upon lipid film hydration by four cycles of constant vortexing coupled to bath sonication (3 min each), followed by extrusion through 200-nm polycarbonate membranes in an extruder device (Avanti Polar Lipids, Inc.). Throughout the lipid film hydration and downsizing processes, samples were maintained above the lipids' transition temperature. Sterility of LP suspensions was preserved by rinsing all material in 70% ethanol and working in a laminar flow hood. For the characterization of LP surface charge and size by ζ-potential determination and dynamic light scattering, samples were diluted 1:30 in deionized water (Milli-Q® system; Millipore) and PBS, respectively, and analyzed in a Zetasizer NanoZS90 instrument (Malvern Ltd, Malvern, UK). Electrolyte concentration in diluted samples was sufficient for ζ-potential measurement.

When studying antimalarial partitioning in LP suspensions, 5 mM drug stocks were initially prepared in water and subsequently mixed with LPs at a 1:40 drug to lipid mole ratio (0.25 mM drug for 10 mM lipid), followed by 24-h incubation under orbital stirring. According to previous works, this incubation time led drugs to reach partition equilibrium upon their passive entrapment in LP organic and aqueous fractions, i.e., LP lipid bilayer plus aqueous core (Moles et al., 2015). As expected, given the drug:lipid ratio used, particle size and ζ-potential remained minimally affected after the addition of drugs with <10% percentual differences obtained (**Table S1**). Similar variations were also obtained at the different pH values studied here (data not shown).

To quantify entrapped drug amounts in LPs, these were pelleted by ultracentrifugation (150,000*g*, 4°C, 1 h) and treated with 1% sodium dodecyl sulphate coupled to 60°C bath sonication as previously reported (Moles et al., 2017). Drug extracts were analyzed by UV-visible spectroscopy using an Epoch™ spectrophotometer

(BioTek Instruments, Inc., Winooski, VT, USA) in 96-well plate mode. Drug standards for quantification were prepared in 1% sodium dodecyl sulphate, and the same solvent was used as blank control for absorbance subtraction. Standard curves were obtained by linear regression from at least three independent measurements (**Figure S1**). Unencapsulated drug amounts were determined by UV-visible spectroscopy from LP supernatants. Drug encapsulation efficiency (EE) was finally determined as the percentual amount of drug retained in LPs relative to the total amount present in the sample (LPs + external solution).

Antimalarial Drug Theoretical Distribution Modeling

The modeling of antimalarial drug distribution in liposomal systems was performed through the design of a sequential experimental method that comprises the following steps: i) an initial construction of a vesicular-like multicompartment system with aqueous/organic volumetric fractions corresponding to the experimental conditions used (e.g., lipid concentration, LP size, pH); ii) the subsequent theorization of a distribution model (D_P, $D_{P,PH+}$, and $D_{P,PH+,P2H+}$ defined here) which will delineate the abundance of drug microspecies present in aqueous solution along with their partitioning behavior, dependent on drug pKa and microspecies-specific partition coefficients (e.g., P, P^{H+}, and P^{2H+} for diprotic basic drugs); iii) estimation of hypothetical P^{H+}, P^{2H+} values ($\log_{10}$ units) and computing of theoretical EE values for the predefined vesicular system and distribution model; iv) isolation of P^{H+}, P^{2H+} values with least experimental versus theoretical EE variance; v) a final analysis of the goodness of the distribution model considered along with fitted P^{H+}, P^{2H+} values to describe experimental data. All calculations and graphical representations were performed using an algorithm created for Wolfram Mathematica 8.0 computing software (The Wolfram Centre, Oxford, UK). The complete set of algorithms used in this work are reported in **Supplementary Material**.

Construction of LP- and RBC-Like Vesicular Systems and Antimalarial Drug Distribution Modeling

For the pH- and lipid charge-dependent modeling of antimalarial drug distribution in our liposomal systems (LPs at 10 mM lipid in aqueous solution), we constructed a vesicular-like multicompartment system using the following parameters reported elsewhere (Lewis and Engelman, 1983; Petrache et al., 2000; Rawicz et al., 2000; Maurer et al., 2001; Leitmannova Liu, 2006): i) vesicles of 100 nm diameter; ii) lipid bilayer thickness of 5 nm, which includes phospholipid fatty acid chains (ca. 2.6–3.0 nm), glycerol (0.3 nm), and phosphocholine head group (0.7–1 nm); iii) vesicle internal aqueous versus membrane volume ratio of 2.7; iv) vesicle internal aqueous volume relative to total lipid molecules in the system of 2.4 µl solution/µmol lipid; and v) lipid molecule ratio between outer and inner lipid bilayer leaflets of 54/46. Resulting volumetric ratios for all organic/aqueous fractions present in the system at 10-mM lipid concentration are as follows: 2.40 (total LP aqueous cargo), 0.48 and 0.41 (outer and inner LP lipid bilayer leaflets), and 96.71 (solution external to LPs).

For the modeling of antimalarial distribution in RBC suspensions, a second vesicular multicompartment system was constructed replicating human RBC dimensions, physiological hematocrit and phospholipid charge asymmetry, i.e., i) total volume of the system occupied by vesicles of 40%; ii) vesicle volume and surface area of, respectively, 90 fl and 140 µm^2 (McLaren et al., 1987; Schrier, 2012; Parisio et al., 2013); iii) lipid bilayer thickness of 5 nm (Maurer et al., 2001; Leitmannova Liu, 2006), which makes an organic volume of 0.45 fl for each single vesicle; and iv) phosphate buffer at pH 7.4 as extravesicular solution. Resulting volumetric ratios for all organic/aqueous fractions present in the system at 40% hematocrit are as follows: 39.8 (total RBC aqueous cargo), 0.1/0.1 (outer and inner RBC plasma membrane leaflets), and 60.0 (extracellular solution).

Antimalarial distribution in aforesaid LP- and RBC-like vesicular systems was subsequently computed through the following sequential steps: i) determination of the molecular abundance of major drug microspecies present in aqueous fractions for the experimental pH range studied (pH 4.0–9.0), providing previous knowledge of drug pKas (Equation 4); ii) drug microspecies partitioning between aqueous solution and organic (LP and RBC lipid bilayer leaflets) fractions was thereafter determined as a function of the distribution model considered (D_P, $D_{P,PH+}$, or $D_{P,PH+,P2H+}$) and microspecies-respective partition coefficients (P, P^{H+} and P^{2H+}). The percentual amount of drug molecules retained within LP and RBC fractions (lipid bilayer leaflets and aqueous cargo) relative to their total amount present in the system (LP and RBC fractions plus extravesicular solution) was finally expressed as theoretical EE (EEt). More information about the volumetric fractions considered in our LP- and RBC-like vesicular systems, along with examples of drug microspecies distribution and resulting EEt in the abovementioned systems, can be found in **Supplementary Material** (**Figures S2–S4** and **Tables S3–S6**).

Statistical Methods

All reported experimental data are defined as mean ± standard deviation from at least three independent sample replicates. Significant differences (p values <0.05) in drug theoretical versus experimental EE were determined by Z-test estimation comparing theoretical EE values (single value for each condition studied) with the corresponding mean ± standard deviation of experimentally retrieved EE (population mean). The significance of variations among drug experimental EE for the conditions studied here, comparing mean ± standard deviation of pH- and lipid composition-dependent retention yields, was analyzed by t-test score; differences were considered significant for p values <0.05.

RESULTS AND DISCUSSION

Rationale Behind LP Formulation and Drug Partitioning Analysis

The initial aim of this work was to study the effect of differences in pH and RBC membrane-analogous phospholipid compositions

over the distribution of polyprotic antimalarials in LP suspensions. To do so and following previous works (Moles et al., 2015; Moles et al., 2016), a neutrally charged LP formulation based on phosphatidylcholine (PC):cholesterol at mole ratios 80:20 (PC-LPs), pH 7.4, was selected as standard physiological condition. Choline-containing phospholipids, mainly PC and phosphatidylethanolamine (PE), account for half of all lipids found in mammalian cell membranes, followed by 30% to 40% cholesterol (Chabanel et al., 1983; Virtanen et al., 1998; Arbustini, 2007; Leventis and Grinstein, 2010). Variations in solution pH and phospholipid composition were applied during LP preparation by, respectively, i) PC-LP lipid film hydration in different pH buffer solutions, and ii) the replacement of stock phospholipids in organic lipid mixtures followed by their subsequent hydration at pH 7.4 buffer.

Considering our ultimate goal to advance in the design of RBC-targeted, LP-based nanotherapeutics with improved prophylactic activity against *P. falciparum* intraerythrocytic stages, an alternative lipid composition consisting of 40% cholesterol and 60% phospholipid, mainly PC:phosphatidylserine (PS):PE at mole ratios 23:33:44 (PC:PS:PE-LPs), was studied reproducing the RBC inner membrane leaflet (Maguire et al., 1991; Virtanen et al., 1998; Ingólfsson et al., 2014). Similar to other works using RBCs as vascular supercarriers (Muzykantov, 2010; Villa et al., 2016), this strategy relies on the selective intracellular loading of therapeutic agents into non-infected RBCs, inhibiting parasite growth upon cell invasion (Moles and Fernàndez-Busquets, 2015; Moles et al., 2015; Moles et al., 2017).

Two additional LP formulations were considered to assess i) the influence on PC-based bilayers of PS (PC:PS-LPs) as major anionic phospholipid responsible for the asymmetric charge properties found in mammalian cell membranes (Fadeel and Xue, 2009; Marquardt et al., 2015), and ii) the effect of LP surface steric stabilization in RBC-like lipid bilayers by including 5% PEG-derivatized PE (PC:PS:PE:PEG-LPs).

Moreover, drug partitioning in LP suspensions was assessed in terms of Encapsulation Efficiency (EE), the percentual amount of drug retained within the LP fraction (LP internal aqueous core + lipid bilayer) relative to its total amount present in the system (LP fraction + external solvent). To prevent LP membrane saturation by supplemented antimalarials, these were assayed at 1:40 drug:lipid mole ratio, well below the maximum 1:20 reported for lipophilic compounds not disturbing the lipid bilayer structure (Fahr et al., 2005).

pH-Dependent Partitioning of Antimalarial Drugs in PC-LP Suspensions

The polyprotic antimalarials studied in this work were all diprotic weak bases and belong to the amino-alcohol (quinine, QN), 8-aminoquinoline (primaquine, PQ, and tafenoquine, TQ), 4-aminoquinoline (chloroquine, CQ), and 9-aminoacridine (quinacrine, QC) drug classes (**Figure 2**). These agents were selected considering: i) their clinical and translational significance (World Health Organization, 2012; World Health Organization, 2015); ii) applicability for LP-based nanotherapeutics relying on pH gradient and ammonium sulfate active encapsulation systems (Haran et al., 1993; Moles et al., 2017); iii) the presence of at least two ionizable groups at a pH range of 4.0 to 9.0, selected to avoid causing harmful effects on phospholipid stability while maintaining LP charge (Tsui et al., 1986; Moncelli et al., 1994), and iv) their lipophilic nature, reflected by drug *P* values >2 $\log_{10}$ units. All the antimalarials tested here exhibit sizes similar to phospholipid molecules, which can reach approximately 60 to 70 $Å^2$ average area for choline phospholipids (Petrache et al., 2000). This feature was prioritized to facilitate stable drug diffusion across lipid bilayers.

In accordance with antimalarial lipophilicity and basic nature, a positive correlation between experimental EE (EEe)

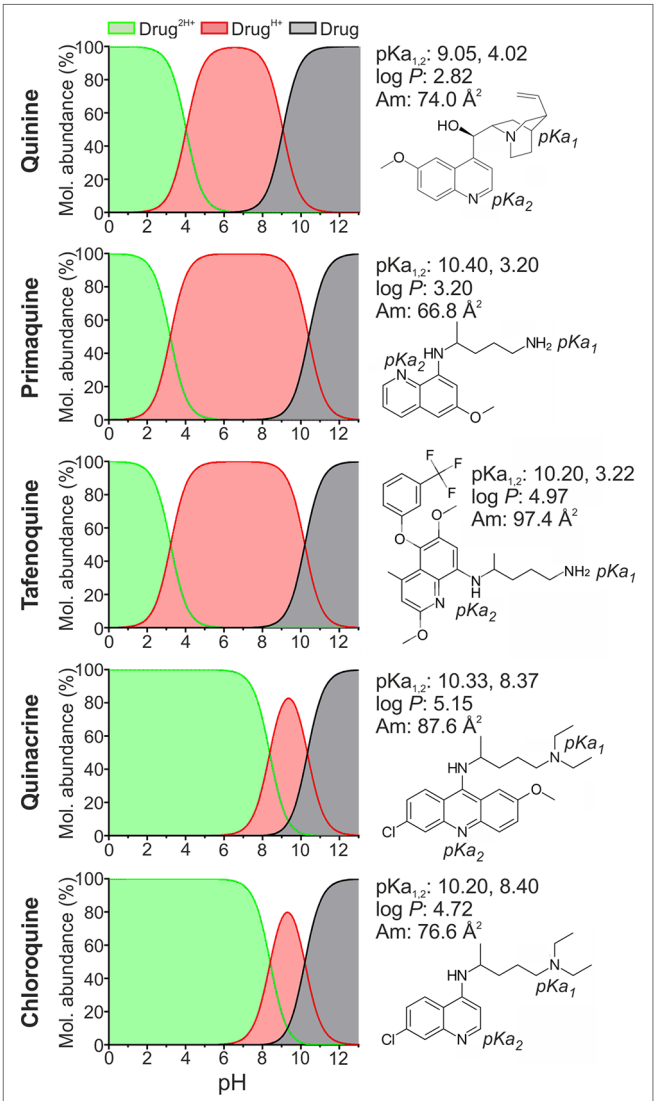

FIGURE 2 | Structure and physicochemical properties of the antimalarial drugs studied here. Molecular abundances in solution at pH 0 to 13 are illustrated for major drug microspecies: unionized (Drug), monoprotonated ($Drug^{H+}$) and diprotonated ($Drug^{2H+}$). pKa, molecular mean projection area (Am), and log *P* values were determined using the Chemicalize software developed by ChemAxon Ltd., except for CQ and PQ, whose pKa and log *P* have been experimentally determined elsewhere (Omodeo-Salè et al., 2009; Nair et al., 2012).

and pH was found for all drugs when incubated for 24 h in PC-LP suspensions (**Figure 3A**). EEe rates exceeding 40% were reached at pH ≥7.4, which highlights the increased capacity of antimalarials to accumulate in LPs in basic conditions. Analogously, lowest EEe values were obtained at the most acidic condition assayed, pH 4.0. Due to the noticeable differences in drug microspecies abundance at pH 4.0 to 9.0 (**Figure 2**), we classified the tested compounds into two main groups: monoprotonated (QN, PQ, TQ; $pKa_{1,2}$ ca. 10, 3.2–4.0) and diprotonated types (CQ, QC; $pKa_{1,2}$ ca. 10.2, 8.4) with the respective presence of $Drug^{H+}$ and $Drug^{2H+}$ as major microspecies for the pH range studied. Significantly larger pH-dependent variations in drug EE were likewise found to be associated with diprotonated-type antimalarials (**Table S2**), such differences reflecting the major role of pKa_2 8.4 in defining CQ and QC partitioning at pH ≥4.0.

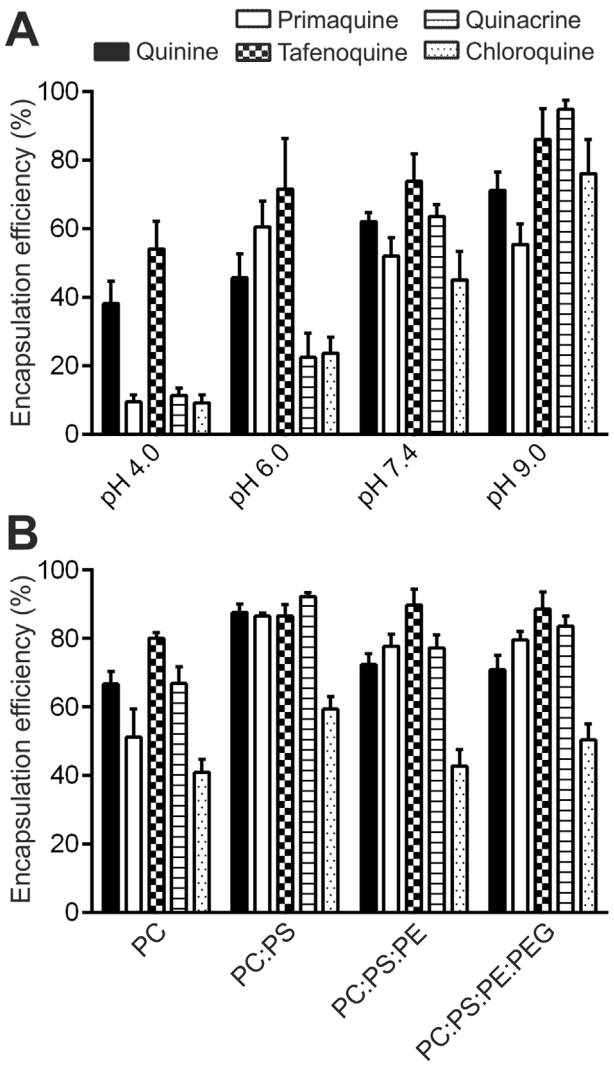

FIGURE 3 | Experimental EEs of antimalarials in LP suspensions. EE was determined as a function of **(A)** solution pH for PC-LP suspensions, and **(B)** phospholipid composition at pH 7.4.

Moreover, all five antimalarials exhibited EEe values far higher than the theoretical EE (EEt) that would be expected when considering D_p as preliminary distribution model, in which the drug unionized form is postulated as the sole microspecies capable of interacting with the lipid bilayer (**Figure 1**). EEt (D_p) data are reported in **Table 1** and were calculated as detailed in *Materials and Methods*. Variations in EEe versus EEt (D_p) were expressed as percentual difference, or ΔEE (Equation 7). In overall, median |ΔEE|, or $\overline{\Delta EE}$, ranging 55.7% to 85.9% were obtained for all antimalarials considering all four pH conditions studied (**Table 1**). Largest increases in EE were remarkably obtained for monoprotonated-type antimalarials at pH 6.0 (EEe >45% vs. EEt (D_p) ≤7.3%), condition in which $Drug^{H+}$ microspecies are dominant with abundances close to 100% (**Figure 2**). This observation evidenced the likely existence of ionized microspecies being stably incorporated in the LP membrane in mild acidic conditions.

$$\Delta EE\% = \left(\frac{EEt - EEe}{EEe} \right) \times 100 \quad (7)$$

By contrast, lower EEe values (<25%) were obtained for diprotonated-type antimalarials at pH 6.0 (**Figure 3A**), a condition in which $Drug^{2H+}$ is the dominant microspecies reaching molecular abundances >95% (**Figure 2**). A higher ionization state and consequent decrease in lipophilicity for $Drug^{2H+}$ in comparison with $Drug^{H+}$ microspecies would explain such variations in EEe. Increases in QC and CQ EEe in the pH range 6.0 to 9.0 further highlighted the role of $Drug^{2H+}$ to $Drug^{H+}$ conversion in modulating their interaction with LPs (**Figure 3A**). Similarly, the observation of ca. fourfold higher EEe values than those theoretically expected at pH 4.0 hinted at the existence of additional partitioning events involving the effective incorporation of diprotonated microspecies into the LP membrane.

Antimalarial Drug Partitioning in LPs Simulating RBC-Like Phospholipid Compositions

Significant EEe increases of >30% (**Figure 3B** and **Table S2**) were obtained at pH 7.4 for all antimalarials (except TQ, 8%), in the presence of PS (PC:PS-LPs, −61 ± 1.2 mV, **Table S1**) when compared to neutrally charged lipid bilayers (PC-LPs, −6.49 ± 4.7 mV, **Table S1**). As previously observed for PC-LPs comparing distinct pH values, significantly higher experimental EE values than those theoretically expected according to D_p were obtained for all antimalarials when assayed in all three PS-containing lipid formulations: PC:PS-LPs, PC:PS:PE-LPs, and PC:PS:PE:PEG-LPs (**Table 2**). These results additionally revealed the interaction and possible internalization of cationic microspecies into LP bilayers and, particularly, the role of PS negative charge in stabilizing such interactions.

The remarkable drug EEe obtained in LPs simulating the RBC membrane inner leaflet (PC:PS:PE-LPs), which ranged from 60% (CQ) to >86% (rest of drugs), further highlighted the potential role of RBCs as drug carriers for malaria therapy and validated their capacity to stably encapsulate weakly basic

TABLE 1 | Experimental vs. theoretical EEs for PC-LP suspensions as a function of pH and D_P, $D_{P,PH+}$, $D_{P,PH+,P2H+}$ drug distribution models.

Drug	pH	%EEe	%EEt (D_P)	*ΔEE* (%)/*p* value	%EEt ($D_{P,PH+}$)	*ΔEE* (%)/*p* value	%EEt ($D_{P,PH+,P2H+}$)	*ΔEE* (%)/*p* value
Quinine	4.0	38.2 ± 6.6	2.4	–93.7/**<10^{-5}**	37.1	–2.9/**0.87**	–	–
	6.0	45.7 ± 7.0	2.9	–93.7/**<10^{-5}**	54.0	+18.2/**0.23**	–	–
	7.4	62.0 ± 2.7	13.6	–78.1/**<10^{-5}**	56.3	–9.2/**0.03**	–	–
	9.0	71.2 ± 5.2	74.3	+4.4/**0.55**	77.8	+9.3/**0.21**	–	–
$\Sigma\lvert\Delta EE\rvert/\widetilde{\Delta EE}$			–	269.9/85.9	–	39.6/9.3	–	
Primaquine	4.0	9.5 ± 2.0	2.4	–74.7/**4.0×10^{-4}**	39.6	+316.8/<**1×10^{-5}**	–	–
	6.0	60.5 ± 7.6	2.5	–95.9/**<10^{-5}**	43.0	–28.9/**0.02**	–	–
	7.4	52.0 ± 5.3	3.8	–92.7/**<10^{-5}**	43.5	–16.3/**0.11**	–	–
	9.0	55.4 ± 5.9	36.8	–33.6/**1.5×10^{-3}**	56.2	+1.4/**0.89**	–	–
$\Sigma\lvert\Delta EE\rvert/\widetilde{\Delta EE}$			–	296.9/83.7	–	363.4/22.6	–	
Tafenoquine	4.0	54.0 ± 8.1	2.5	–95.4/**<10^{-5}**	61.5	+13.9/**0.35**	–	–
	6.0	71.6 ± 14.8	7.3	–89.8/**1.4×10^{-5}**	65.6	–8.4/**0.69**	–	–
	7.4	73.9 ± 8.0	58.0	–21.5/**0.04**	76.3	+3.2/**0.76**	–	–
	9.0	86.1 ± 8.9	98.1	+13.9/**0.18**	98.1	+13.9/**0.18**	–	–
$\Sigma\lvert\Delta EE\rvert/\widetilde{\Delta EE}$			–	220.6/55.7	–	39.4/11.2	–	
Quinacrine	4.0	11.3 ± 2.1	2.4	–78.8/**1.7×10^{-5}**	2.5	–77.9/**2.1×10^{-5}**	14.6	+29.2/**0.12**
	6.0	22.5 ± 6.9	2.4	–89.3/**3.9×10^{-3}**	8.0	–64.4/**0.04**	18.8	–16.4/**0.60**
	7.4	63.5 ± 3.5	14.7	–76.9/**<10^{-5}**	61.3	–3.5/**0.52**	63.1	–0.6/**0.90**
	9.0	94.8 ± 2.7	97.9	+3.3/**0.25**	98.3	–3.7/**0.20**	98.3	+3.7/**0.20**
$\Sigma\lvert\Delta EE\rvert/\widetilde{\Delta EE}$			–	248.3/77.9	–	149.5/34.1	–	49.9/10.1
Chloroquine	4.0	9.2 ± 2.3	2.4	–73.9/**2.9×10^{-3}**	2.4	–73.9/**2.9×10^{-3}**	14.6	+58.7/**0.02**
	6.0	23.7 ± 4.6	2.4	–89.9/**<10^{-5}**	5.1	–78.5/**6.3×10^{-5}**	16.6	–30.0/**0.13**
	7.4	45.1 ± 8.3	8.6	–80.9/**1.1×10^{-5}**	43.1	–4.4/**0.81**	47.1	+4.4/**0.80**
	9.0	76.1 ± 10.0	95.9	+26.0/**0.04**	96.6	+26.9/**0.04**	96.6	+26.9/**0.04**
$\Sigma\lvert\Delta EE\rvert/\widetilde{\Delta EE}$			–	270.7/77.4	–	183.7/50.4	–	120/28.5

Variations in EE (ΔEE, %) and Z-test p values were obtained when comparing experimental (reference condition) vs. theoretical EE values.

TABLE 2 | Experimental vs. theoretical EEs for LP suspensions at pH 7.4 as a function of phospholipid composition and D_P, $D_{P,PH+}$ drug distribution models.

Drugs	LP formulation	EEe (%)	%EEt (D_P)	*ΔEE* (%)/*p* value	%EEt ($D_{P,PH+}$)	*ΔEE* (%)/*p* value
Quinine	PC	66.7 ± 3.7	13.6	–79.6/**<10^{-5}**	66.1	–0.9/**0.86**
	PC:PS	87.6 ± 2.4	13.6	–84.5/**<10^{-5}**	87.9	+0.3/**0.91**
	PC:PS:PE	72.4 ± 3.1	13.6	–81.2/**<10^{-5}**	70.7	–2.3/**0.59**
	PC:PS:PE:PEG	70.9 ± 4.2	13.6	–80.8/**<10^{-5}**	70.7	–0.3/**0.97**
Primaquine	PC	51.2 ± 8.2	3.8	–92.6/**<10^{-4}**	48.9	–4.5/**0.78**
	PC:PS	86.5 ± 0.9	3.8	–95.6/**<10^{-5}**	85.4	–1.3/**0.20**
	PC:PS:PE	77.8 ± 3.4	3.8	–95.1/**<10^{-5}**	78.7	+1.2/**0.79**
	PC:PS:PE:PEG	79.6 ± 2.4	3.8	–95.2/**<10^{-5}**	78.7	–1.1/**0.70**
Tafenoquine	PC	80.1 ± 1.7	58.0	–27.6/**<10^{-5}**	74.6	–6.9/**<10^{-5}**
	PC:PS	86.6 ± 3.3	58.0	–33.0/**<10^{-5}**	82.3	–5.0/**0.18**
	PC:PS:PE	89.8 ± 4.6	58.0	–35.4/**<10^{-5}**	88.0	–2.0/**0.70**
	PC:PS:PE:PEG	88.6 ± 4.9	58.0	–34.5/**<10^{-5}**	85.4	–3.6/**0.52**
Quinacrine	PC	66.9 ± 4.8	14.7	–78.0/**<10^{-5}**	66.1	–1.2/**0.86**
	PC:PS	92.3 ± 1.1	14.7	–84.1/**<10^{-5}**	91.9	–0.4/**0.70**
	PC:PS:PE	77.3 ± 3.8	14.7	–81.0/**<10^{-5}**	78.8	+1.9/**0.70**
	PC:PS:PE:PEG	83.6 ± 3.0	14.7	–82.4/**<10^{-5}**	82.2	–1.7/**0.64**
Chloroquine	PC	40.9 ± 3.8	8.6	–79.0/**<10^{-5}**	43.1	+5.4/**0.57**
	PC:PS	59.4 ± 3.6	8.6	–85.5/**<10^{-5}**	58.7	–1.2/**0.84**
	PC:PS:PE	42.8 ± 4.8	8.6	–79.9/**<10^{-5}**	43.1	+0.7/**0.94**
	PC:PS:PE:PEG	50.4 ± 4.7	8.6	–82.9/**<10^{-5}**	51.8	+2.8/**0.76**

Variations in EE (ΔEE, %) and Z-test p values were obtained when comparing experimental (reference condition) vs. theoretical EE values.

antimalarials (**Figure 3B**). Finally, non-significant differences in antimalarial EEes were detected in RBC-like LPs upon surface steric stabilization (PC:PS:PE-LPs versus PC:PS:PE:PEG-LPs, **Figure 3B** and **Table S2**). This observation likely suggested the stable internalization into the LP membrane of ionized drug microspecies, which account for ca. 100% of all microspecies found at pH 7.4 (**Figure 2**), rather than the existence of transitory ionic interactions at the LP surface.

Determination of Partition Coefficients for Ionized Drug Microspecies in PC-LP Suspensions

The discrepancies observed between EEe and EEt (D_P) for PC-LPs (pH 4.0–9.0, **Table 1**) called for the definition of a revised distribution model that envisages the existence of partitioning events for antimalarial drug ionized microspecies in the LP bilayer. As an initial approximation, we first studied the simultaneous participation of P (Equation 1) together with a second partition coefficient defined here as P^{H+} and relative to monoprotonated drug microspecies. The resulting $D_{P,PH+}$ distribution model is represented in **Figure 4**.

Given this second distribution model, hypothetical log P^{H+} values were considered in the range of 1.0 to 6.0 units (0.1 interval) a range comprising 90% of marketed drugs (Mandić, 2014), and the resulting EEt data were calculated as detailed in *Materials and Methods*. Variances in estimated EEt versus EEe were then determined for all pH conditions assayed (**Figure 5A**) and added up for each given P^{H+} value (**Figure 5B** and Equation 8). Finally, the P^{H+} value exhibiting least cumulative variance was independently retrieved for each antimalarial (**Table 3** and Equation 9).

$$(8)\qquad VAR(P^{H+}) = \Sigma_{pH[i];\,i=1}^{pH[i];\,i=4}\left(EEe_{pH[i]} - EEt_{pH[i]}(D_{p,p^{H+}})\right)^2;\quad pH = \langle 4.0, 6.0, 7.4, 9.0\rangle$$

$$(9)\qquad P^{H+}(Drug) = \min_{4.0\le P^{H+}\le 9.0} VAR(P^{H+})$$

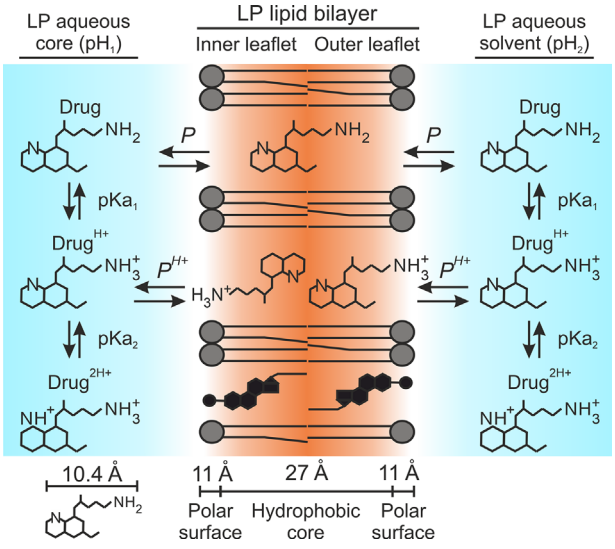

FIGURE 4 | $D_{P,PH+}$ distribution model. Illustration adapted for amphiphilic diprotic basic drugs in liposomal systems. Primaquine is used as drug example. Dimensions of the bilayer hydrophobic core and associated headgroup polar surface considering 18-carbon PC have been retrieved from previous publications (Petrache et al., 2000; Maurer et al., 2001). Primaquine molecular dimensions were determined using the Chemicalize software developed by ChemAxon Ltd.

Calculated log P^{H+} values for all antimalarials ranged between 1.9 and 3.2 units and resulted to be remarkably smaller than their log P counterpart, with an average of 1.7 ± 0.7 units lower (**Table 3**). The ionized amino group present in monoprotonated microspecies would be responsible in this case for their reduced lipophilicity and consequent decreased internalization into the LP lipid bilayer. Ionized moieties are nevertheless located away from the hydrophobic regions of aromatic rings and hydrocarbon chains (**Figure 2**) thereby enabling these regions to stably internalize into LP membrane leaflets. Such lipophilic character would be reflected by the modest log P^{H+} values obtained.

The estimated theoretical drug EE values based on the $D_{P,PH+}$ distribution model, EEt ($D_{P,PH+}$), and retrieved P^{H+} are summarized in **Table 1**, and an example of drug microspecies overall abundance for all fractions present in the system is illustrated in **Table S3**. EEt values better fitting EEe data were obtained for all drugs in comparison to the D_P model (**Table 1**), i.e., $\Delta\widetilde{EE}$ (D_P) = 55.7–85.9 versus $\Delta\widetilde{EE}$ ($D_{P,PH+}$) = 9.3–50.4, and especially at pH values ≤7.4, where ionized microspecies are predominantly found, i.e., $\Delta\widetilde{EE}$ (D_P) = 78.8–93.7 vs. $\Delta\widetilde{EE}$ ($D_{P,PH+}$) = 8.4–30. The best fitting to experimental data with ΔEE <30%, along with an overall ca. 6-fold reduction in $\Delta\widetilde{EE}$ in comparison to D_P, was obtained for monoprotonated-type antimalarials (QN, PQ, TQ), which illustrates the capacity of $D_{P,PH+}$ to accurately model their distribution in PC-LP suspensions at pH 4.0 to 9.0.

Moreover, given the large variations in EEe versus EEt ($D_{P,PH+}$) of >64% obtained for diprotonated-type antimalarials (CQ, QC) at pH 4.0 and 6.0 (**Table 1**), an additional partition coefficient, defined here as P^{2H+}, was contemplated describing the partitioning of diprotonated drug microspecies. The resulting $D_{P,PH+,P2H+}$ distribution model is represented in **Figure 6**.

Similarly to P^{H+} determination, $\log_{10}$ values ranging from 0.5 to 4.0 (0.1 interval) were considered for P^{2H+} and the resulting EEt data were calculated as detailed in *Materials and Methods*. Predefined P^{H+} values were maintained constant for EEt calculation. EEe versus EEt variances were determined for all pH conditions assayed (**Figure 7A**), subsequently added up for each given P^{2H+} value (**Figure 7B** and Equation 10), and the P^{2H+} value exhibiting least cumulative variance was individually retrieved for CQ and QC (**Table 3** and Equation 11). Calculated P^{2H+} values (1.2 $\log_{10}$ units) were considerably lower than their associated P and P^{H+} coefficients, a result that suggests the likely impaired solubility of diprotonated microspecies in the LP membrane due to their doubly ionized state and the consequent reduction in drug nonpolar surface area.

$$(10)\qquad VAR(P^{2H+}) = \Sigma_{pH[i];\,i=1}^{pH[i];\,i=4}\left(EEe_{pH[i]} - EEt_{pH[i]}(D_{p,p^{H+},p^{2H+}})\right)^2;\quad pH = \langle 4.0, 6.0, 7.4, 9.0\rangle$$

$$(11)\qquad P^{2H+}(Drug) = \min_{0.5\le P^{2H+}\le 4.0} VAR(P^{2H+})$$

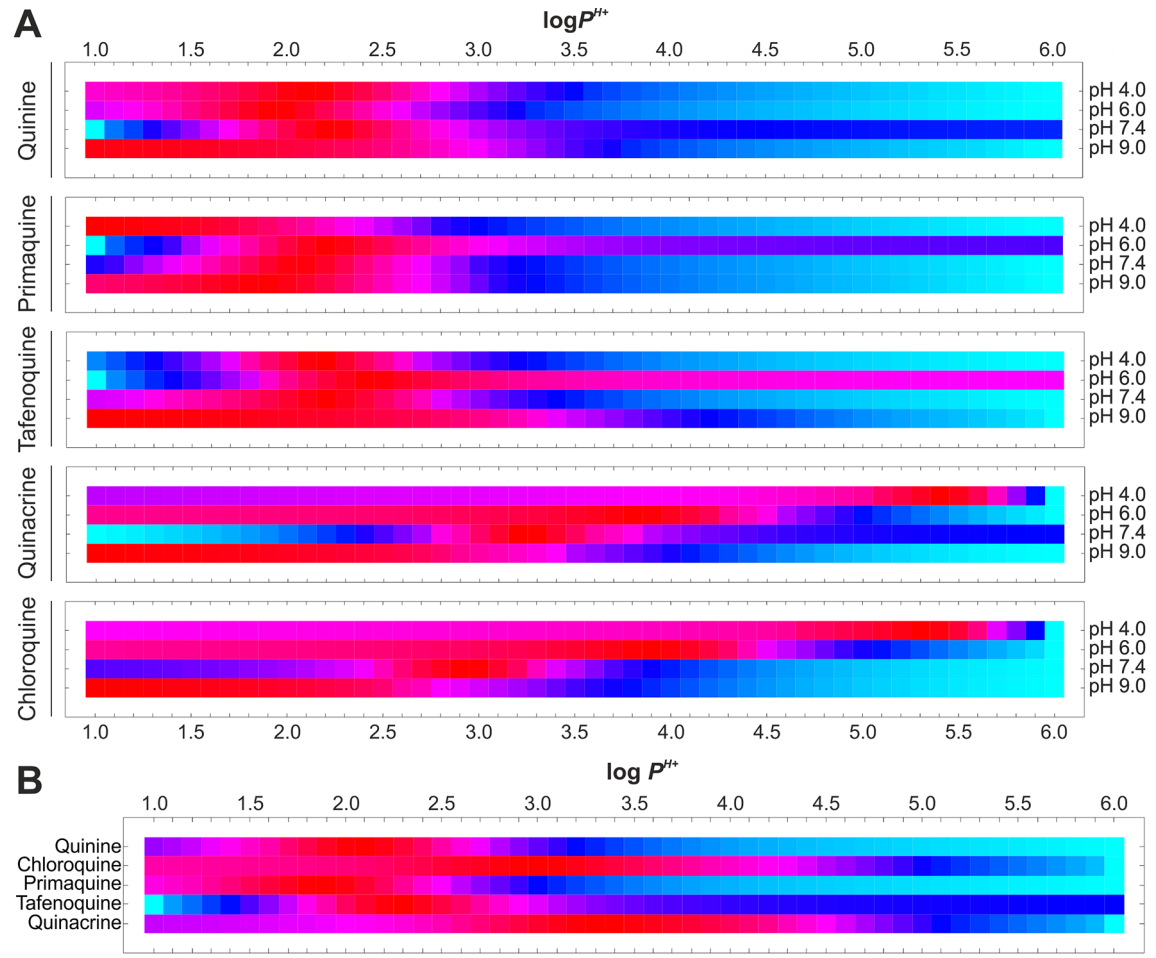

FIGURE 5 | Estimation of antimalarial P^{H+} coefficient values for PC-based LPs. **(A)** P^{H+}-dependent drug EEt vs. EEe variances for all experimental pH values studied in accordance with the $D_{P,PH+}$ distribution model. **(B)** Isolation of P^{H+} coefficient exhibiting least cumulative variances. Normalized variances are individually illustrated for each drug and pH value using the Hue color function (light blue and dark red as maximum and minimum variance levels, respectively).

TABLE 3 | Summary of antimalarial partitioning coefficients estimated in LP suspensions.

		pH-dependent distribution (PC-LPs)		Phospholipid composition-dependent distribution (log P^{H+}, pH 7.4)			
Drug	**log *P***	**log P^{H+}**	**log P^{2H+}**	**PC**	**PC:PS**	**PC:PS:PE**	**PC:PS:PE:PEG**
Quinine	2.82	2.1	–	2.3	2.9	2.4	2.4
Primaquine	3.20	1.9	–	2.0	2.8	2.6	2.6
Tafenoquine	4.97	2.3	–	2.5	2.7	2.9	2.8
Quinacrine	5.15	3.2	1.2	3.3	4.1	3.6	3.7
Chloroquine	4.72	2.9	1.2	2.9	3.2	2.9	3.0
							RBC-like LPs

Log P values were determined using the Chemicalize software developed by ChemAxon Ltd., except for CQ and PQ, whose log P has been experimentally determined elsewhere (Omodeo-Salè et al., 2009; Nair et al., 2012).

Theoretical EE data for diprotonated-type antimalarials obtained according to the $D_{P,PH+,P2H+}$ distribution model, EEt ($D_{P,PH+,P2H+}$), are summarized in **Table 1**. **Table S4** illustrates an example of CQ microspecies overall partitioning in our LP system. Using this model, an improved fitting to EEe data was obtained with respective ca. threefold and fivefold reductions in $\widetilde{\Delta EE}$ when compared to the $D_{P,PH+}$ and D_P distribution models (**Table 1**). Furthermore, the $D_{P,PH+,P2H+}$ model resulted in a better approximation to EEe data at pH $\leq$6.0 when compared to previous distribution models, i.e., $\widetilde{\Delta EE}$ (D_P) = 81.9–84.1 versus $\widetilde{\Delta EE}$ ($D_{P,PH+}$) = 71.1–76.2 versus $\widetilde{\Delta EE}$ ($D_{P,PH+,P2H+}$) = 22.8–44.3. The largest ΔEE of 58.7% was found

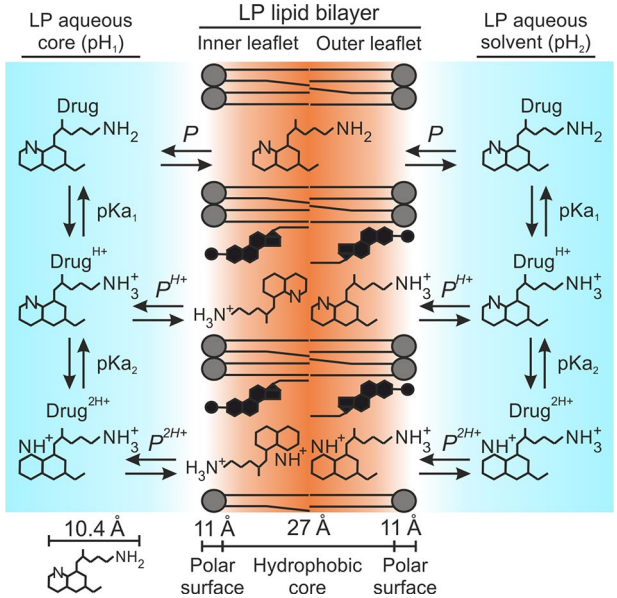

FIGURE 6 | $D_{P,PH+,P2H+}$ distribution model. Illustration adapted for amphiphilic diprotic basic drugs in liposomal systems. Primaquine is used as drug example. Dimensions of the bilayer hydrophobic core and associated headgroup polar surface considering 18-carbon PC have been retrieved from previous publications (Petrache et al., 2000; Maurer et al., 2001). Primaquine molecular dimensions were determined using the Chemicalize software developed by ChemAxon Ltd.

for CQ at pH 4.0. Such improved fitting to EEe data provided by $D_{P,PH+,P2H+}$ evidences the important and combined role of both P^{H+} and P^{2H+} coefficients to more accurately model the distribution of diprotic basic antimalarials in LP suspensions.

Determination of Partition Coefficients for Ionized Drug Microspecies in RBC-Like LPs

Additional partition coefficients were determined aiming to better describe the interaction of antimalarial drug ionized microspecies in physiological conditions with LP suspensions that contain RBC-like phospholipid compositions. To do so, $D_{P,PH+}$ was considered as simplest distribution model of reference given its previously demonstrated capacity to model EEe data for all studied antimalarials at pH 7.4 (ΔEE = 3.5–16.3, **Table 1**). Analogously to P^{H+} estimation related to pH changes, we considered log P^{H+} values in the range of 1.0 to 6.0 units (0.1 interval), followed by EEt calculation as explained in *Materials and Methods*. EEt versus EEe variances were subsequently calculated for all lipid compositions studied (**Figure 8**) and the single least variant P^{H+} value was finally extracted for each antimalarial (**Table 3** and Equations 12–13).

(12)
$$Lipid\ composition = \langle PC, PC/PS, PC/PS/PE, PC/PS/PE/PEG \rangle$$

(13)
$$P^{2H+}(Lipid\ composition[\![i]\!]) = \min_{1.0 \le p^{H+} \le 6.00} (EEe_{Lipid\ composition[\![i]\!]} - EEt(D_{p,p^{H+}}))^2$$

In an analogous manner to EEe data, a positive correlation between P^{H+} and the presence of PS was observed for all antimalarials, with mean log P^{H+} of 2.88 to 3.14 and 2.60 for all PS-containing LPs and PC-LPs, respectively (**Table 3**). These results are in accordance with the suggested role of PS in increasing the accumulation of cationic drug molecules in lipid bilayers. Overall decreases in ca. 1.4- and 1.6-fold $\log_{10}$ units were furthermore noticed for P^{H+} in,

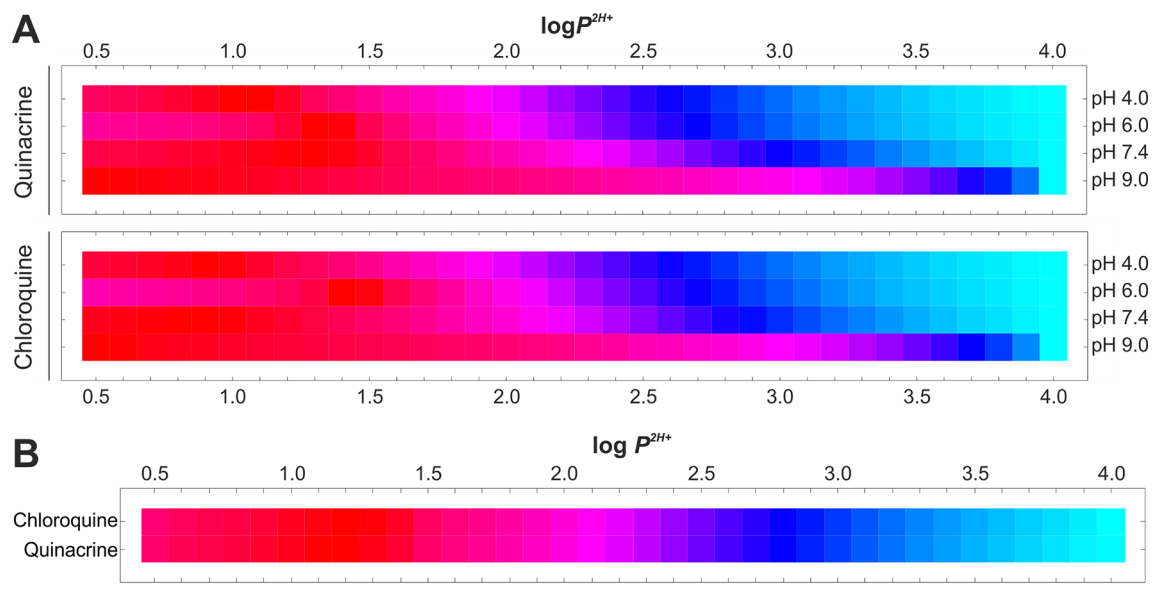

FIGURE 7 | Estimation of P^{2H+} coefficient values for diprotonated-type drugs in PC-based LPs. **(A)** P^{2H+}-dependent drug EEt vs. EEe variances for all experimental pH values studied in accordance with $D_{P,PH+,P2H+}$ distribution model. **(B)** Isolation of P^{2H+} coefficient exhibiting least cumulative variances. Normalized variances are individually illustrated for each drug and pH value using the Hue color function (light blue and dark red as maximum and minimum variance levels, respectively).

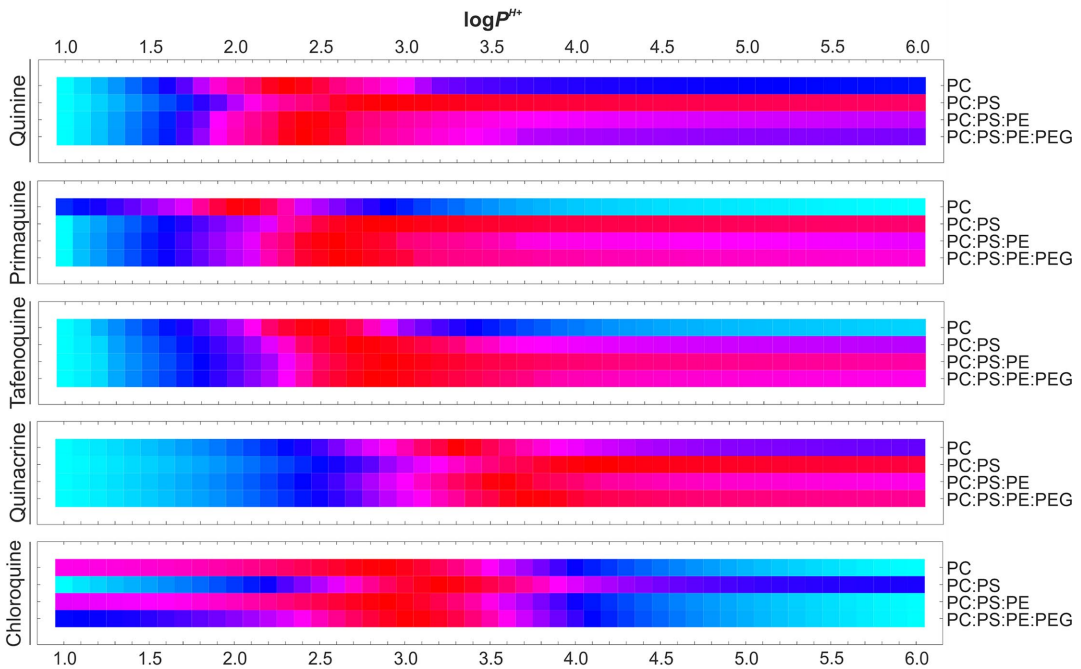

FIGURE 8 | Estimation of antimalarial P^{H+} coefficient values for RBC-like LPs. P^{H+}-dependent drug EEt vs. EEe variances are illustrated for all the experimental phospholipid compositions studied in accordance with $D_{P,PH+}$ distribution model. Normalized variances are individually illustrated for each drug and lipid composition using the Hue color function (light blue and dark red as maximum and minimum variance levels, respectively).

respectively, all PS-containing LPs and PC-LPs when compared to drug-associated *P* values, which reflects again the function of PS in regulating antimalarial partitioning along with the effect of drug ionized groups on diminishing their stable internalization into LPs. Moreover, P^{H+} small variations of <0.5 $\log_{10}$ units were obtained between PS-LPs and RBC-like LPs (**Table 3**), which could be caused by the increased cholesterol amounts present in the latter formulations along with the consequent reduced number of total phospholipid molecules. Undetectable differences in log P^{H+}(<0.1 units) were obtained after LP steric stabilization (PC:PS:PE:PEG-LPs versus PC:PS:PE-LPs).

In summary, the definition of $D_{P,PH+}$, together with the estimation of P^{H+} coefficients relative to phospholipid composition allowed for the calculation of EEt values properly fitting experimental data (**Table 2**). Non-significant differences (*p* value <0.05) in EEe versus EEt ($D_{P,PH+}$) were obtained in this regard for all antimalarials, with ΔEE ≤7% in all conditions assayed. All together, these results importantly stress the role of lipid composition and phospholipid charge in modulating the partitioning of polyprotic drugs in liposomal systems, as well as the potential role of RBCs as supercarriers for weakly basic antimalarials, which might potentially accumulate within the cell membrane inner leaflet as ion pair in association with PS.

Determination of Antimalarial Drug Distribution Coefficient Based on $D_{P,PH+}$ and $D_{P,PH+,P2H+}$

The new distribution models reported here enabled the reformulation of the initially considered *D* coefficient (Equations 2–5) to properly represent our experimental EE data. Modified *D* coefficients in accordance with $D_{P,PH+}$ and $D_{P,PH+,PH+}$ models, i.e., $D(P,P^{H+})$ and $D(P,P^{H+},P^{2H+})$, Equations 14–17, were calculated for the pH range 4.0 to 9.0, using the previously estimated P^{H+} and P^{2H+} values relative to PC-LP suspensions (**Figure 9**). As expected, a sustained reduction in *D* was obtained when lowering pH, as a reflection of the increased drug ionization state and consequently reduced lipophilic character. In more detail, a drastic fall in *D* reaching negative $\log_{10}$ values below pH 7.0 (PQ, CQ, QC), pH 6.0 (QN), and pH 5.0 (TQ), was calculated for D_P, whereas the application of $D_{P,PH+}$ and $D_{P,PH+,P2H+}$ alternative models provided positive log *D* values still maintained below pH 4.0. Such differences in antimalarial lipophilicity in acidic conditions would be expected as a result of the predicted capacity of drug ionized microspecies in $D_{P,PH+}$ and $D_{P,PH+,P2H+}$ models to stably internalize into the LP lipid bilayer.

(14)

$$D(P,P^{H+}) = \left(\frac{mol\,Drug_{org}\times Vol_{aq}}{Vol_{org}\times mol\,Drug_{aq}} + \frac{mol\,Drug_{org}^{H+}\times Vol_{aq}}{Vol_{org}\times mol\,Drug_{aq}}\right) \Big/ \left(1 + \frac{mol\,Drug_{aq}^{H+}}{mol\,Drug_{aq}} + \frac{mol\,Drug_{org}^{2H+}}{mol\,Drug_{aq}}\right)$$

(15)

$$\log D(P,P^{H+}) = \log\left(P + \left(P^{H+}\times 10^{(pKa_1-pH)}\right)\right) - \log(1+10^{(pKa_1-pH)} + 10^{(pKa_1+pKa_2-2\times pH)})$$

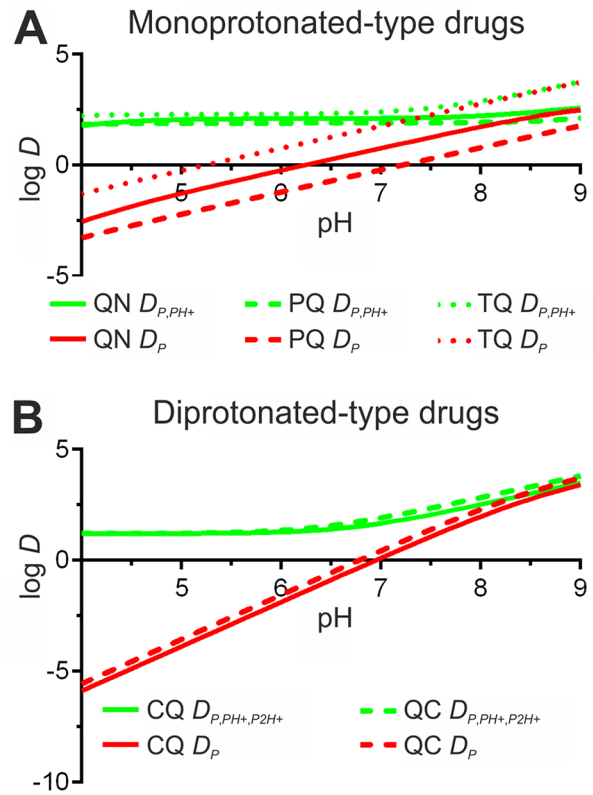

FIGURE 9 | Reformulation of antimalarial *D* coefficient for PC-LPs according to the new drug distribution models reported here. The original D_P model is included for comparison. **(A)** Monoprotonated-type drugs quinine (QN), primaquine (PQ), and tafenoquine (TQ). **(B)** Diprotonated-type antimalarials chloroquine (CQ) and quinacrine (QC).

(16)

$$D(P,P^{H+},P^{2H+})= \left(\frac{molDrug_{org}\times Vol_{aq}}{Vol_{org}\times molDrug_{aq}}+\frac{molDrug_{org}^{H+}\times Vol_{aq}}{Vol_{org}\times molDrug_{aq}}+\frac{molDrug_{org}^{2H+}\times Vol_{aq}}{Vol_{org}\times molDrug_{aq}}\right)\Bigg/ \left(1+\frac{molDrug_{aq}^{H+}}{molDrug_{aq}}+\frac{molDrug_{aq}^{2H+}}{molDrug_{aq}}\right)$$

(17)

$$\log D(P,P^{H+},P^{2H+})=\log\left(P+(P^{H+}\times 10^{(pKa_1-pH)})+(P^{2H+}\times 10^{(pKa_1+pKa_2-2\times pH)})\right)-\log(1+10^{(pka_1-pH)}+10^{(pKa_1+pKa_2-2\times pH)})$$

Modeling Antimalarial Drug EE in Response to Transmembrane pH Gradients

Considering our previously reported use of a transmembrane pH 4.0_{in} to 7.4_{out} gradient for the active encapsulation of diprotic antimalarials into RBC-targeted PC-based LPs (Moles et al., 2015; Moles et al., 2017), we evaluated a possible application of the novel $D_{P,PH+}$ and $D_{P,PH+,P2H+}$ distribution models in estimating drug EE and intravesicular distribution in LPs as a function of their internal pH (pH_{in} range, 4.0–7.4). Modeled EE (**Figure 10A**) along with drug microspecies molecular abundance within LP fractions (lipid bilayer leaflets and aqueous core, **Figure 10B**), were calculated considering 10 mM PC-LP suspensions at pH 7.4 together with estimated drug P^{H+} and P^{2H+} values (**Table 3**). An exemplification of microspecies overall abundance for all fractions present in the system is illustrated in **Table S5**.

Given the lipophilic character evidenced here for antimalarial ionized microspecies, larger EEs were predicted for $D_{P,PH+}$ and

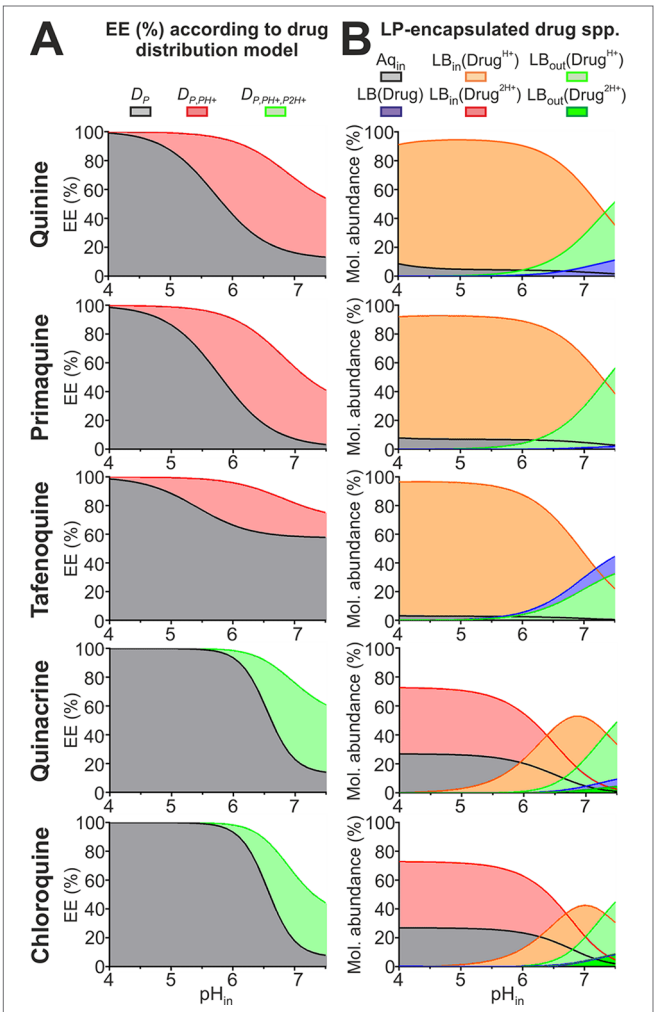

FIGURE 10 | Modeling antimalarial EEs and intravesicular distribution for PC-LP suspensions in response to pH gradients. **(A)** EEs calculated considering all distribution models studied in this work for 10 mM lipid particles containing internal pH 4.0 to 7.4 values and suspended in aqueous solution at pH 7.4. **(B)** Molecular abundances for all monoprotonated- and diprotonated-type antimalarial encapsulated microspecies (spp.) according to, respectively, $D_{P,PH+}$ and $D_{P,PH+,P2H+}$ distribution models. Drug spp. and intravesicular fractions comprise: (i) all spp. located inside the LP aqueous core (Aq_{in}), (ii) monoprotonated ($Drug^{H+}$) and diprotonated ($Drug^{2H+}$) ionized spp. incorporated into outer and inner lipid bilayer leaflets (LB_{out}, LB_{in}), and (iii) membrane-solubilized unionized spp., LB(Drug).

$D_{P,PH+,P2H+}$ models when compared to D_P (**Figure 10A**). Such differences were more pronounced for pH_{in} >4.0, and particularly in the range of pH 5.0 to 7.4, where monoprotonated microspecies abound (**Figure 2**). Drug EE ≥90% was estimated to be maintained up to pH_{in} 6.4 when following $D_{P,PH+}$ and $D_{P,PH+,P2H+}$, with >70% drug molecules being predicted to localize at the LP bilayer (**Figure 10B**). Ionized microspecies, in particular monoprotonated molecules, were estimated to be the dominant form in the LP bilayer at pH_{in} ≤7.4 with abundances reaching >50%.

The new distribution models further led to the hypothesis that whereas only minor amounts (<10%) of ionized microspecies are exposed at the LP surface at pH_{in} ≤6.0, a slight pH_{in} increase to 7.4 triggers their massive exposure to the extraliposomal environment reaching abundances of >50%. Such increase in LP internal pH could be triggered during *in vivo* conditions by the sustained leakage of the encapsulated buffering agent and/or as result of membrane destabilization by plasma components, as already demonstrated in the literature (Allen and Cleland, 1980; Silvander et al., 1998; Russell et al., 2018) and evidenced in our previous publications (Moles et al., 2015; Moles et al., 2017). Exposed antimalarial molecules would then become rapidly exchanged with other lipid bilayers found in solution (Moles et al., 2016; Moles et al., 2017), which represents an attractive operating mechanism for delivering drugs to cells lacking endocytic mechanisms and intracellular vesicle trafficking such as RBCs (Ji et al., 2011).

Modeling Antimalarial Drug EE and Distribution in RBC-Like Vesicular Systems

In view of our dual purpose of using RBCs as nanotherapeutic target and ultimate vascular drug carrier against blood-borne pathogens (Anselmo et al., 2013; Moles et al., 2015; Moles et al., 2017), we envisaged the application of $D_{P,PH+}$ and $D_{P,PH+,P2H+}$ to model antimalarial drug encapsulation and distribution within RBC fractions (plasma membrane and cytoplasm) at physiological pH 7.4. For this purpose, we considered a RBC-like vesicular system simulating the human RBC dimensions, its asymmetric lipid composition (100% PC and 67:33 PC:PS as phospholipid composition for outer and inner membrane leaflets, respectively), and a typical human blood hematocrit, as detailed in *Materials and Methods*. A similar vesicular system but entirely composed of PC, and therefore displaying an absence of lipid charge asymmetry, was considered for comparison. These vesicular systems are referred here as PC/PS and PC, and an example reproducing CQ distribution in PC/PS is reported in **Table S6**.

EEs exceeding 50% were predicted for all antimalarials in both PC and PC/PS systems (**Table 4**), which encourages once more the utilization of RBCs as effective drug carrier for polyprotic basic drugs (Muzykantov, 2010; Villa et al., 2016). Larger EEs were estimated in the presence of lipid charge asymmetry, with 4% to 6% increases for TQ and CQ and up to 20% to 30% for QN, PQ and QC, a result in good correlation with the previously noticed superior P^{H+} values in PS-containing lipid mixtures (**Table 3**).

Moreover, when looking at the distribution of antimalarials within RBC fractions, a clear shift in QN, PQ, and QC molecular abundance was determined for PC versus PC/PS vesicular systems, with drugs preferentially accumulating in the RBC cytoplasm (49–66% of all drug molecules) and the plasma membrane leaflets (65–78% of all drug molecules), respectively (**Table 4**). By contrast, TQ was found to be concentrated mostly within membrane leaflets in ≥70% and CQ exhibited a cytoplasmic preference (>63% molecules) regardless of the vesicular system considered. Additionally, the presence of lipid charge asymmetry in PC/PS resulted in two major compelling changes when compared to PC that encourage the use of RBCs as drug carriers: a remarkable boost in drug abundance within the plasma membrane inner leaflet (increases of 133–238% for QN, PQ and QC, and of 40–76% for TQ and CQ) and a mild decrease in the number of drug molecules exposed at the RBC

TABLE 4 | Modeling antimalarial EEs and distribution in RBC-like PC/PS versus PC vesicular systems.

			% Drug molecule abundance within RBC fractions			
Antimalarial	**Vesicular system**	**EE (%)**	**Drug (LB)**	**Drug$^+$ (LB_{out})**	**Drug$^+$ (LB_{in})**	**Total molecules Aq_{in}**
Quinine	PC	57.5	3.5	23.8	23.8	49.0
	PC/PS	69.8	2.0	13.9	55.4	28.7
	Δ (%)	+21.4	–42.3	–41.7	+132.7	–41.6
Primaquine	PC	50.0	0.6	16.4	16.4	66.4
	PC/PS	65.2	0.3	8.7	55.5	35.4
	Δ (%)	+30.4	–48.9	–46.7	+238.6	–46.6
Tafenoquine	PC	68.7	22.3	23.7	23.7	30.3
	PC/PS	71.4	19.5	20.9	33.1	26.6
	Δ (%)	+3.9	–12.6	–12.0	+39.3	–12.1
Quinacrine	PC	57.5	4.0	23.5	23.5	49.0
	PC/PS	75.3	1.7	10.5	66.0	21.8
	Δ (%)	+31.0	–56.8	–55.3	+181.1	–55.6
Chloroquine	PC	48.1	2.7	12.9	12.9	71.5
	PC/PS	51.1	2.3	11.4	22.7	63.4
	Δ (%)	+6.2	–13.1	–11.9	+76.1	–11.3

EE was calculated considering a 40% v/v suspension of vesicles simulating RBC dimensions in pH 7.4 solution. Antimalarial microspecies (spp.) and fractions studied included *ionized (Drug$^+$) molecules internalized into lipid bilayer inner (LB_{in}) and outer (LB_{out}) leaflets, unionized molecules (Drug) distributed throughout both bilayer leaflets (LB), and all antimalarial molecules retained inside the RBC aqueous core/cytoplasm (Aq_{in}). The percentual increase (+) or decrease (–) in drug EE and spp. molecular abundance between PC (reference condition) and PC/PS* vesicular systems is indicated as Δ (%).

surface (reductions of 41–55% for QN, PQ and QC, and of 12% for TQ and CQ).

Based on the distribution data obtained for the RBC-like PC/PS vesicular model and considering a clinical scenario, all diprotic basic antimalarials studied in this work are predicted to largely accumulate in circulating RBCs upon their intravenous administration (>50% EEs, **Table 4**). A preferential distribution would then be expected to take place within either the cell aqueous core (CQ), and/or the internal side of the RBC membrane (QN, PQ, QC, and to a lesser extent, TQ), whereas minor amounts of drugs would remain exposed at the cell surface. This particular subcellular distribution is attractive because it would contribute to preventing the easy exchange of drug molecules with circulating structures (e.g., other cells and high-/low-density lipoproteins) (Fahr et al., 2005; Hefesha et al., 2011; Loew et al., 2011), as well as a potential loss of drug function due to its degradation in both extracellular (blood plasma and body tissues) and cytoplasmic aqueous environments (Waterman et al., 2002). Our models omit the participation of other circulating organic bodies and particles that are known to affect drug distribution *in vivo*, such as plasma lipoproteins and albumin aggregates (Yamasaki et al., 2013; Sobansky and Hage, 2014), though point out at the remarkable potential of RBCs as vascular carriers and prompt the utilization of *ex vivo* RBC loading techniques for drug delivery-based therapeutics (Zhou et al., 2010; Biagiotti et al., 2011; Villa et al., 2016).

CONCLUSION

Based on pH- and lipid composition-dependent experimental encapsulation data acquired using liposomal systems, we have theorized here novel distribution models ($D_{P,PH+}$ and $D_{P,PH+,P2H+}$) that precisely describe the partitioning behavior of diprotic basic drugs in PC-based and RBC-analogous LP suspensions. Partition coefficients relative to monoprotonated (P^{H+}) and diprotonated (P^{2H+}) microspecies have been estimated in a simple and highly translatable manner for several diprotic antimalarials of clinical significance, for which theoretical EEs have been retrieved *in silico* closely fitting experimental data (non-significant differences were obtained in >75% of all pH/lipid composition conditions studied).

It is important to note that the distribution models, methods, and resulting partition coefficients have been determined for and are therefore applicable to diprotic drugs with differences in pK_{a1} versus pK_{a2} of >2 log_{10} units and to LP suspensions at a maximum of 1:40 drug:lipid ratio and within a pH range of 4.0 to 9.0 units. It is expected that higher drug:lipid ratios can lead to a saturation and consequent disturbance of the lipid bilayer structure by the supplemented drug with ultimate effects on altering LP morphology, membrane charge, size, and overall drug partition behavior. pH values below/above 4.0/9.0 units can additionally alter the lipid bilayer structure and overall particle charge due to phospholipid ionization at such strongly acidic/basic conditions. However, the reported approach has the potential to be adapted to study the distribution of both polyprotic acids and bases in any type of lipid-based vesicular system, and can be furthermore extended to polyprotic drugs with more than two acid dissociation constants.

Our data importantly stress the role of lipid composition and phospholipid charge in modulating the interaction of water-soluble polyprotic drugs with lipid bilayers as well as the remarkable potential of RBCs as vascular drug carriers against blood diseases. The results and models presented here further hint at the stable internalization of ionized drug microspecies into neutrally charged and anionic lipid bilayer leaflets as suggested in other works (de Souza Santos et al., 2014; Barroso et al., 2015), and likely in the latter in the form of ion pairs in association with anionic lipids.

Potential therapeutic applications for the distribution models and partition coefficients reported here include the accurate design of LP-based controlled drug delivery strategies relying on pH gradients, the study of RBCs as clinically safe long-circulating carrier for polyprotic drugs, and the optimization of antimalarial therapies using RBC-targeted liposomal drug formulations (Moles and Fernàndez-Busquets, 2015; Moles et al., 2015, Moles et al., 2017). The approach and methods reported here have demonstrated to accurately fit experimental encapsulation data and aim at serving as an experimental tool for researchers from different scientific disciplines. Our models can be nevertheless improved to better describe the distribution of ionized drugs and variations in local pH at the lipid–water interface, particularly in the case of ionized bilayers, by means of incorporating concepts from the classic Gouy–Chapman model and novel theories (Shapovalov and Brezesinski, 2006). A further optimization of the vesicular model presented here is required for a more accurate representation of a clinical scenario. Plasma components are known to interact with circulating drugs (Yamasaki et al., 2013; Sobansky and Hage, 2014), and these additionally present large biodistribution volumes broadly diffusing across animal tissues.

DATA AVAILABILITY

All datasets generated for this study are included in the manuscript and the **Supplementary files**.

AUTHOR CONTRIBUTIONS

EM conceived the study, designed the methodology, and wrote the manuscript. XF-B acquired funding, contributed to resources, and supervised the study. MK contributed to resources and supervised the study.

FUNDING

This work was supported by (i) *Ministerio de Ciencia, Innovación y Universidades*, Spain, grant numbers RTI2018-094579-B-I00 and PCIN-2017-100, which included FEDER funds, (ii) ERA-NET Cofund EURONANOMED, grant number 2017-178 (NANOpheles), and (iii) Generalitat de Catalunya, Spain, grant number 2017-SGR-908.

ACKNOWLEDGMENTS

ISGlobal and IBEC are members of the CERCA Programme, *Generalitat de Catalunya*. This research is part of ISGlobal's Program on the Molecular Mechanisms of Malaria, which is partially supported by the *Fundación Ramón Areces*.

SUPPLEMENTARY MATERIAL

The Supplementary Material for this article can be found online at: https://www.frontiersin.org/articles/10.3389/fphar.2019.01064/full#supplementary-material

Additional figures (**Figures S1-S4**; reporting UV-visible absorption spectra used for drug quantification, along with illustrations summarizing the calculations and schemes used to determine EEt and drug microspecies abundance in liposomal fractions), tables (**Tables S1-S6**; including LP ζ-potential data, variations in experimental versus theoretical EE data, along with detailed drug distribution examples), and an Appendix section including the mathematical algorithms used in this work, all providing supporting information to the results presented in this manuscript, have been supplied into a single PDF file as **Supplementary Material**.

REFERENCES

Allen, T. M., and Cleland, L. G. (1980). Serum-induced leakage of liposome contents. *BBA—Biomembr.* 597 (2), 418–426. doi: 10.1016/0005-2736(80)90118-2

Allen, T. M., and Cullis, P. R. (2013). Liposomal drug delivery systems: from concept to clinical applications. *Adv. Drug Deliv. Rev.* 65, 36–48. doi: 10.1016/j.addr.2012.09.037

Anselmo, A. C., Gupta, V., Zern, B. J., Pan, D., Zakrewsky, M., Muzykantov, V., et al. (2013). Delivering nanoparticles to lungs while avoiding liver and spleen through adsorption on red blood cells. *ACS Nano* 7 (12), 11129–11137. doi: 10.1021/nn404853z

Anselmo, A. C., and Mitragotri, S. (2016). Nanoparticles in the clinic. *Bioeng. Transl. Med.* 1 (1), 10–29. doi: 10.1002/btm2.10003

Arbustini, E. (2007). Total erythrocyte membrane cholesterol: an innocent new marker or an active player in acute coronary syndromes? *J. Am. Coll. Cardiol.* 49 (21), 2090–2092. doi: 10.1016/j.jacc.2007.03.014

Barroso, R. P., Basso, L. G. M., and Costa-Filho, A. J. (2015). Interactions of the antimalarial amodiaquine with lipid model membranes. *Chem. Phys. Lipids* 186, 68–78. doi: 10.1016/j.chemphyslip.2014.12.003

Bawa, S., Kumar, S., Drabu, S., and Kumar, R. (2010). Structural modifications of quinoline-based antimalarial agents: recent developments. *J. Pharm. Bioallied Sci.* 2 (2), 64–71. doi: 10.4103/0975-7406.67002

Biagiotti, S., Paoletti, M. F., Fraternale, A., Rossi, L., and Magnani, M. (2011). Drug delivery by red blood cells. *IUBMB Life* 63 (8), 621–631. doi: 10.1002/iub.478

Bobo, D., Robinson, K. J., Islam, J., Thurecht, K. J., and Corrie, S. R. (2016). Nanoparticle-based medicines: a review of FDA-approved materials and clinical trials to date. *Pharm. Res.* 33 (10), 2373–2387. doi: 10.1007/s11095-016-1958-5

Bulbake, U., Doppalapudi, S., Kommineni, N., and Khan, W. (2017). Liposomal formulations in clinical use: an updated review. *Pharmaceutics* 9 (2), 12. doi: 10.3390/pharmaceutics9020012

Chabanel, A., Flamm, M., and Sung, K. L. P. (1983). Influence of cholesterol content on red cell membrane viscoelasticity and fluidity. *Biophys. J.* 44 (2), 171–176. doi: 10.1016/S0006-3495(83)84288-X

Charifson, P. S., and Walters, W. P. (2014). Acidic and basic drugs in medicinal chemistry: a perspective. *J. Med. Chem.* 57 (23), 9701–9717. doi: 10.1021/jm501000a

Clerc, S., and Barenholz, Y. (1995). Loading of amphipathic weak acids into liposomes in response to transmembrane calcium acetate gradients. *Biochim. Biophys. Acta* 1240 (2), 257–265. doi: 10.1016/0005-2736(95)00214-6

Cullis, P. R., Bally, M. B., Madden, T. D., Mayer, L. D., and Hope, M. J. (1991). pH gradients and membrane transport in liposomal systems. *Trends Biotechnol.* 9 (1), 268–272. doi: 10.1016/0167-7799(91)90088-Y

de Souza Santos, M., de Morais del Lama, M. P. F., Siuiti Ito, A., and Zumstein Georgetto Naal, R. M. (2014). Binding of chloroquine to ionic micelles: effect of pH and micellar surface charge. *J. Lumin.* 147, 49–58. doi: 10.1016/j.jlumin.2013.10.037

Fadeel, B., and Xue, D. (2009). The ins and outs of phospholipid asymmetry in the plasma membrane: roles in health and disease. *Crit. Rev. Biochem. Mol. Biol.* 44 (5), 264–277. doi: 10.1080/10409230903193307

Fahr, A., van Hoogevest, P., May, S., Bergstrand, N., and Leigh, M. L. S. (2005). Transfer of lipophilic drugs between liposomal membranes and biological interfaces: consequences for drug delivery. *Eur. J. Pharm. Sci.* 26 (3-4), 251–265. doi: 10.1016/j.ejps.2005.05.012

Gubernator, J. (2011). Active methods of drug loading into liposomes: recent strategies for stable drug entrapment and increased in vivo activity. *Expert Opin. Drug Deliv.* 8 (5), 565–580. doi: 10.1517/17425247.2011.566552

Hansch, C., Leo, A., and Hoekman, D. (1995). *Exploring QSAR: Fundamentals and applications in chemistry and biology*. University of Michigan: American Chemical Society.

Haran, G., Cohen, R., Bar, L. K., and Barenholz, Y. (1993). Transmembrane ammonium sulfate gradients in liposomes produce efficient and stable entrapment of amphipathic weak bases. *BBA—Biomembr.* 1151 (2), 201–215. doi: 10.1016/0005-2736(93)90105-9

Hefesha, H., Loew, S., Liu, X., May, S., and Fahr, A. (2011). Transfer mechanism of temoporfin between liposomal membranes. *J. Control. Release* 150 (3), 279–286. doi: 10.1016/j.jconrel.2010.09.021

Ingólfsson, H. I., Melo, M. N., van Eerden, F. J., Arnarez, C., Lopez, C. A., Wassenaar, T. A., et al. (2014). Lipid organization of the plasma membrane. *J. Am. Chem. Soc.* 136 (41), 14554–14559. doi: 10.1021/ja507832e

Ji, P., Murata-Hori, M., and Lodish, H. F. (2011). Formation of mammalian erythrocytes: chromatin condensation and enucleation. *Trends Cell Biol.* 21 (7), 409–415. doi: 10.1016/j.tcb.2011.04.003

Kaschula, C. H., Egan, T. J., Hunter, R., Basilico, N., Parapini, S., Taramelli, D., et al. (2002). Structure–activity relationships in 4-aminoquinoline antiplasmodials. The role of the group at the 7-position. *J. Med. Chem.* 45 (16), 3531–3539. doi: 10.1021/jm020858u

Krämer, S. D., Braun, A., Jakits-Deiser, C., and Wunderli-Allenspach, H. (1998). Towards the predictability of drug–lipid membrane interactions: the pH-dependent affinity of propranolol to phosphatidylinositol containing liposomes. *Pharm. Res.* 15 (5), 739–744. doi: 10.1023/A:1011923103938

Leitmannova Liu, A. (2006). *Advances in planar lipid bilayers and liposomes,* 1st Edition Vol. 3. (Cambridge, Massachusetts, USA: Academic Press)

Leo, A., Hansch, C., and Elkins, D. (1971). Partition coefficients and their uses. *Chem. Rev.* 71 (6), 525–616. doi: 10.1021/cr60274a001

Leventis, P. A., and Grinstein, S. (2010). The distribution and function of phosphatidylserine in cellular membranes. *Annu. Rev. Biophys.* 39, 407–427. doi: 10.1146/annurev.biophys.093008.131234

Lewis, B. A., and Engelman, D. M. (1983). Lipid bilayer thickness varies linearly with acyl chain length in fluid phosphatidylcholine vesicles. *J. Mol. Biol.* 166 (2), 211–217. doi: 10.1016/S0022-2836(83)80007-2

Loew, S., Fahr, A., and May, S. (2011). Modeling the release kinetics of poorly water-soluble drug molecules from liposomal nanocarriers. *J. Drug Deliv.* 2011, 1–10. doi: 10.1155/2011/376548

MacDonald, R. C., MacDonald, R. I., Menco, B. P. M., Takeshita, K., Subbarao, N. K., and Hu, L. R. (1991). Small-volume extrusion apparatus for preparation of large, unilamellar vesicles. *Biochim. Biophys. Acta - Biomembr.* 1061 (2), 297–303. doi: 10.1016/0005-2736(91)90295-J

Madden, T. D., Harrigan, P. R., Tai, L. C., Bally, M. B., Mayer, L. D., Redelmeier, T.E., et al. (1990). The accumulation of drugs within large unilamellar vesicles exhibiting a proton gradient: a survey. *Chem. Phys. Lipids* 53 (1), 37–46. doi: 10.1016/0009-3084(90)90131-A

Maguire, P. A., Prudhomme, J., and Sherman, I. W. (1991). Alterations in erythrocyte membrane phospholipid organization due to the intracellular growth of the human malaria parasite, *Plasmodium falciparum*. *Parasitology* 102 Pt 2, 179–186. doi: 10.1017/S0031182000062466

Mandić, Z. (2014). *Physico-chemical methods in drug discovery and development*. Zagreb: IAPC Publishing. doi: 10.5599/obp.7.0

Marquardt, D., Geier, B., and Pabst, G. (2015). Asymmetric lipid membranes: towards more realistic model systems. *Membranes (Basel)* 5 (2), 180–196. doi: 10.3390/membranes5020180

Maurer, N., Fenske, D. B., and Cullis, P. R. (2001). Developments in liposomal drug delivery systems. *Expert Opin. Biol. Ther.* 1 (6), 923–947. doi: 10.1517/14712598.1.6.923

McLaren, C. E., Brittenham, G. M., and Hasselblad, V. (1987). Statistical and graphical evaluation of erythrocyte volume distributions. *Am. J. Physiol.* 252 (4 Pt 2), H857–H866. doi: 10.1152/ajpheart.1987.252.4.H857

Moles, E., and Fernàndez-Busquets, X. (2015). Loading antimalarial drugs into noninfected red blood cells: an undesirable roommate for *Plasmodium*. *Futur. Med. Chem.* 7 (7), 837–840. doi: 10.4155/fmc.15.35

Moles, E., Galiano, S., Gomes, A., Quiliano, M., Teixeira, C., Aldana, I., et al. (2017). ImmunoPEGliposomes for the targeted delivery of novel lipophilic drugs to red blood cells in a falciparum malaria murine model. *Biomaterials* 145, 178–191. doi: 10.1016/j.biomaterials.2017.08.020

Moles, E., Moll, K., Ch'ng, J. H., Parini, P., Wahlgren, M., and Fernàndez-Busquets, X. (2016). Development of drug-loaded immunoliposomes for the selective targeting and elimination of rosetting *Plasmodium falciparum*-infected red blood cells. *J. Control. Release* 241, 57–67. doi: 10.1016/j.jconrel.2016.09.006

Moles, E., Urbán, P., Jiménez-Díaz, M. B., Viera-Morilla, S., Angulo-Barturen, I., Busquets, M. A., et al. (2015). Immunoliposome-mediated drug delivery to *Plasmodium*-infected and non-infected red blood cells as a dual therapeutic/prophylactic antimalarial strategy. *J. Control. Release* 210, 217–229. doi: 10.1016/j.jconrel.2015.05.284

Moncelli, M. R., Becucci, L., and Guidelli, R. (1994). The intrinsic pKa values for phosphatidylcholine, phosphatidylethanolamine, and phosphatidylserine in monolayers deposited on mercury electrodes. *Biophys. J.* 66 (6), 1969–1080. doi: 10.1016/S0006-3495(94)80990-7

Muzykantov, V. R. (2010). Drug delivery by red blood cells: vascular carriers designed by Mother Nature. *Expert Opin. Drug Deliv.* 7 (4), 403–427. doi: 10.1517/17425241003610633

Nair, A., Abrahamsson, B., Barends, D. M., Groot, D. W., Kopp, S., Polli, J. E., et al. (2012). Biowaiver monographs for immediate-release solid oral dosage forms: primaquine phosphate. *J. Pharm. Sci.* 101 (3), 936–945. doi: 10.1002/jps.23006

Omodeo-Salè, F., Cortelezzi, L., Basilico, N., Casagrande, M., Sparatore, A., and Taramelli, D. (2009). Novel antimalarial aminoquinolines: heme binding and effects on normal or *Plasmodium falciparum*-parasitized human erythrocytes. *Antimicrob. Agents Chemother.* 53 (10), 4339–4344. doi: 10.1128/AAC.00536-09

Ottiger, C., and Wunderli-Allenspach, H. (1997). Partition behaviour of acids and bases in a phosphatidylcholine liposome-buffer equilibrium dialysis system. *Eur. J. Pharm. Sci.* 5 (4), 223–231. doi: 10.1016/S0928-0987(97)00278-9

Parisio, G., Stocchero, M., and Ferrarini, A. (2013). Passive membrane permeability: beyond the standard solubility-diffusion model. *J. Chem. Theory Comput.* 9 (12), 5236–5246. doi: 10.1021/ct400690t

Pattni, B. S., Chupin, V. V., and Torchilin, V. P. (2015). New developments in liposomal drug delivery. *Chem. Rev.* 115 (19), 10938–10966. doi: 10.1021/acs.chemrev.5b00046

Petrache, H. I., Dodd, S. W., and Brown, M. F. (2000). Area per lipid and acyl length distributions in fluid phosphatidylcholines determined by 2H NMR spectroscopy. *Biophys. J.* 79 (6), 3172–3192. doi: 10.1016/S0006-3495(00)76551-9

Rawicz, W., Olbrich, K. C., McIntosh, T., Needham, D., and Evans, E. A. (2000). Effect of chain length and unsaturation on elasticity of lipid bilayers. *Biophys. J.* 79 (1), 328–339. doi: 10.1016/S0006-3495(00)76295-3

Russell, L. M., Hultz, M., and Searson, P. C. (2018). Leakage kinetics of the liposomal chemotherapeutic agent Doxil: the role of dissolution, protonation, and passive transport, and implications for mechanism of action. *J. Control. Release* 269, 171–176. doi: 10.1016/j.jconrel.2017.11.007

Scherrer, R. A., and Howard, S. M. (1977). Use of distribution coefficients in quantitative structure-activity relationships. *J. Med. Chem.* 20 (1), 53–58. doi: 10.1021/jm00211a010

Schrier, S. L. (2012). What does the spleen see? *Blood* 120, 242–243. doi: 10.1182/blood-2012-05-425991

Sercombe, L., Veerati, T., Moheimani, F., Wu, S. Y., Sood, A. K., and Hua, S. (2015). Advances and challenges of liposome assisted drug delivery. *Front. Pharmacol.* 6, 286. doi: 10.3389/fphar.2015.00286

Shapovalov, V. L., and Brezesinski, G. (2006). Breakdown of the Gouy-Chapman model for highly charged Langmuir monolayers: counterion size effect. *J. Phys. Chem. B.* 110 (20), 10032–10040. doi: 10.1021/jp056801b

Shaul, P., Frenkel, M., Goldstein, E. B., Mittelman, L., Grunwald, A., Ebenstein, Y., et al. (2013). The structure of anthracycline derivatives determines their subcellular localization and cytotoxic activity. *ACS Med. Chem. Lett.* 4 (3), 323–328. doi: 10.1021/ml3002852

Silvander, M., Johnsson, M., and Edwards, K. (1998). Effects of PEG-lipids on permeability of phosphatidylcholine/cholesterol liposomes in buffer and in human serum. *Chem. Phys. Lipids* 97 (1), 15–26. doi: 10.1016/S0009-3084(98)00088-7

Soares, R. R., da Silva, J. M. F., Carlos, B. C., da Fonseca, C. C., de Souza, L. S. A., Lopes, F. V., et al. (2015). New quinoline derivatives demonstrate a promising antimalarial activity against *Plasmodium falciparum* in vitro and *Plasmodium berghei* in vivo. *Bioorg. Med. Chem. Lett.* 25 (11), 2308–2313. doi: 10.1016/j.bmcl.2015.04.014

Sobansky, M. R., and Hage, D. S. (2014). Analysis of drug interactions with very low density lipoprotein by high-performance affinity chromatography. *Anal. Bioanal. Chem.* 406 (25), 6203–6211. doi: 10.1007/s00216-014-8081-4

Tetko, I. V., and Poda, G. I. (2004). Application of ALOGPS 2.1 to predict log D distribution coefficient for Pfizer propietary compounds. *J. Med. Chem.* 24 (23), 5601–5604. doi: 10.1021/jm049509l

Torchilin, V. P. (2005). Recent advances with liposomes as pharmaceutical carriers. *Nat. Rev. Drug Discov.* 4 (2), 145–160. doi: 10.1038/nrd1632

Tsui, F. C., Ojcius, D. M., and Hubbell, W. L. (1986). The intrinsic pKa values for phosphatidylserine and phosphatidylethanolamine in phosphatidylcholine host bilayers. *Biophys. J.* 49 (2), 459–468. doi: 10.1016/S0006-3495(86)83655-4

Vennerstrom, J. L., Nuzum, E. O., Miller, R. E., Dorn, A., Gerena, L., Dande, P. A., et al. (1999). 8-Aminoquinolines active against blood stage *Plasmodium falciparum* in vitro inhibit hematin polymerization. *Antimicrob. Agents Chemother.* 43 (3), 598–602. doi: 10.1128/AAC.43.3.598

Villa, C. H., Anselmo, A. C., Mitragotri, S., and Muzykantov, V. (2016). Red blood cells: supercarriers for drugs, biologicals, and nanoparticles and inspiration for advanced delivery systems. *Adv. Drug Deliv. Rev.* 106 (Pt A), 88–103. doi: 10.1016/j.addr.2016.02.007

Virtanen, J. A., Cheng, K. H., and Somerharju, P. (1998). Phospholipid composition of the mammalian red cell membrane can be rationalized by a superlattice model. *Proc. Natl. Acad. Sci. U. S. A.* 95 (9), 4964–4969. doi: 10.1073/pnas.95.9.4964

Warhurst, D. C., Craig, J. C., Adagu, I. S., Guy, R. K., Madrid, P. B., and Fivelman, Q. L. (2007). Activity of piperaquine and other 4-aminoquinoline antiplasmodial drugs against chloroquine-sensitive and resistant blood-stages of *Plasmodium falciparum.* Role of beta-haematin inhibition and drug concentration in vacuolar water- and lipid-phases. *Biochem. Pharmacol.* 73 (12), 1910–1926. doi: 10.1016/j.bcp.2007.03.011

Warhurst, D. C., Craig, J. C., Adagu, I. S., Meyer, D. J., and Lee, S. Y. (2003). The relationship of physico-chemical properties and structure to the differential antiplasmodial activity of the cinchona alkaloids. *Malar. J.* 2, 26. doi: 10.1186/1475-2875-2-26

Waterman, K. C., Adami, R. C., Alsante, K. M., Antipas, A. S., Arenson, D. R., Carrier, R., et al. (2002). Hydrolysis in pharmaceutical formulations. *Pharm. Dev. Technol.* 7 (2), 113–146. doi: 10.1081/PDT-120003494

Wei, X., Shamrakov, D., Nudelman, S., Peretz-Damari, S., Nativ-Roth, E., Regev, O., et al. (2018). Cardinal role of intraliposome doxorubicin-sulfate nanorod crystal in Doxil properties and performance. *ACS Omega* 3 (3), 2508–2517. doi: 10.1021/acsomega.7b01235

World Health Organization (2012). *Management of severe malaria—A practical handbook*. 3rd edition. Geneva, Switzerland: World Health Organization. doi: 10.2217/thy.09.81

World Health Organization (2015). *Guidelines for the treatment of malaria*. 3rd edition. Geneva, Switzerland: World Health Organization.

Xia, X. R., Baynes, R. E., Monteiro-Riviere, N. A., and Riviere, J. E. (2005). Determination of the partition coefficients and absorption kinetic parameters of chemicals in a lipophilic membrane/water system by using a membrane-coated fiber technique. *Eur. J. Pharm. Sci.* 24 (1), 15–23. doi: 10.1016/j.ejps.2004.09.004

Yamasaki, K., Chuang, V. T. G., Maruyama, T., and Otagiri, M. (2013). Albumin–drug interaction and its clinical implication. *Biochim. Biophys. Acta - Gen. Subj.* 1830 (12), 5435–1543. doi: 10.1016/j.bbagen.2013.05.005

Zhou, X., Yuan, J., Liu, J., and Liu, B. (2010). Loading trehalose into red blood cells by electroporation and its application in freeze-drying. *Cryo-Letters* 31 (2), 147–156. doi: 10.1089/cpt.2008.0001

Conflict of Interest Statement: The authors declare that the research was conducted in the absence of any commercial or financial relationships that could be construed as a potential conflict of interest.

frontiers in Pharmacology

REVIEW
published: 16 October 2019
doi: 10.3389/fphar.2019.01196

Physiological and Pharmaceutical Considerations for Rectal Drug Formulations

Susan Hua[1,2]*

[1] Therapeutic Targeting Research Group, School of Biomedical Sciences and Pharmacy, University of Newcastle, Callaghan, NSW, Australia, [2] Hunter Medical Research Institute, New Lambton Heights, NSW, Australia

Although the oral route is the most convenient route for drug administration, there are a number of circumstances where this is not possible from either a clinical or pharmaceutical perspective. In these cases, the rectal route may represent a practical alternative and can be used to administer drugs for both local and systemic actions. The environment in the rectum is considered relatively constant and stable and has low enzymatic activity in comparison to other sections of the gastrointestinal tract. In addition, drugs can partially bypass the liver following systemic absorption, which reduces the hepatic first-pass effect. Therefore, rectal drug delivery can provide significant local and systemic levels for various drugs, despite the relatively small surface area of the rectal mucosa. Further development and optimization of rectal drug formulations have led to improvements in drug bioavailability, formulation retention, and drug release kinetics. However, despite the pharmaceutical advances in rectal drug delivery, very few of them have translated to the clinical phase. This review will address the physiological and pharmaceutical considerations influencing rectal drug delivery as well as the conventional and novel drug delivery approaches. The translational challenges and development aspects of novel formulations will also be discussed.

Keywords: rectal, rectum, drug delivery, dosage form, nanoparticles, drug formulation, physiological considerations, translation

OPEN ACCESS

Edited by:
Biswajit Mukherjee, Jadavpur University, India

Reviewed by:
Nadeem Irfan Bukhari, University of the Punjab, Pakistan
Pio Maria Furneri, University of Catania, Italy

***Correspondence:**
Susan Hua
Susan.Hua@newcastle.edu.au

Specialty section:
This article was submitted to Experimental Pharmacology and Drug Discovery, a section of the journal Frontiers in Pharmacology

Received: *06 August 2019*
Accepted: *17 September 2019*
Published: *16 October 2019*

Citation:
Hua S (2019) Physiological and Pharmaceutical Considerations for Rectal Drug Formulations. Front. Pharmacol. 10:1196. doi: 10.3389/fphar.2019.01196

INTRODUCTION

The oral route is the most convenient route for drug administration. However, there are circumstances where this is not possible from either a clinical or pharmaceutical perspective (de Boer et al., 1982; De Boer et al., 1984). In these cases, the rectal route may represent a practical alternative and can be used to administer drugs for both local and systemic actions. The rectal route is already used clinically to deliver a variety of therapies to treat both local (**Table 1**) and systemic conditions (**Table 2**). This includes the local treatment of constipation, hemorrhoids, anal fissures, inflammation, and hyperkalemia. Rectal formulations for systemic drug delivery are used clinically for the treatment of pain, fever, nausea and vomiting, migraines, allergies, and sedation. These rectal formulations are based on conventional dosage forms, such as suppositories and enemas, and are typically used for short-term therapy.

Rectal dosage forms are generally inexpensive to manufacture and can also be self-administered by patients without the need for a medically trained person in comparison to parenteral dosage forms (e.g., intramuscular and intravenous injections) (Turner et al., 2012; Jannin et al., 2014). This is

TABLE 1 | Examples of rectal formulations clinically approved for local absorption.

Drug	Brand name	Indication	Dosage form
Bisacodyl	*Dulcolax*	Constipation	Suppository
	Bisalax		Enema
Glycerol	*Glycerol*	Constipation	Suppository
Saline laxatives	*Micolette*	Constipation	Enema
	Microlax	Bowel preparation	
Mesalazine	*Pentasa*	Inflammatory bowel	Suppository
	Salofalk	disease	Enema
			Rectal foam
Budesonide	*Budenofalk*	Anti-inflammatory	Rectal foam
Prednisolone	*Colifoam*	Anti-inflammatory	Rectal foam
Hydrocortisone	*Predsol*	Anti-inflammatory	Suppository
	Colocort		Enema
Polystyrene sulfonate resins	*Resonium A*	Hyperkalemia	Enema
Glyceryl trinitrate	*Rectogesic*	Anal fissure, hemorrhoids	Ointment

TABLE 2 | Examples of rectal formulations clinically approved for systemic absorption.

Drug	Brand name	Indication	Dosage form
Acetaminophen	*Panadol*	Pain, fever	Suppository
	Acephen		
	Feverall		
Oxycodone	*Proladone*	Pain	Suppository
Ondansetron	*Zofran*	Nausea and vomiting	Suppository
Caffeine + ergotamine	*Migergot*	Migraine	Suppository
Prochlorperazine	*Compro*	Nausea and vomiting	Suppository
Promethazine	*Phenergan*	Antihistamine	Suppository
Ibuprofen	*Nurofen*	Pain, fever	Suppository
Diclofenac	*Voltaren*	Pain, fever	Suppository
Indomethacin	*Indocin*	Pain	Suppository
Diazepam	*Diazepam rectal solution*	Seizures, sedation	Enema
	Diastat AcuDial		Gel

particularly advantageous for rural communities and developing countries for specific drugs that cannot be delivered by other convenient routes (Abolhassani et al., 2000; Turner et al., 2012; Jannin et al., 2014). However, the rectal route of administration is generally not preferred by patients due to cultural issues and/or potential for discomfort and leakage (de Boer et al., 1982; De Boer et al., 1984; Jannin et al., 2014; Nunes et al., 2014). These factors have contributed to (i) a lack of drugs that are clinically available in rectal dosage forms, (ii) a lack of clinical conditions that are treated with rectal drug formulation, and (iii) a lack of comprehensive bioavailability studies in humans (Jannin et al., 2014).

Further development and optimization of rectal drug formulations have led to improvements in drug availability (i.e., locally and systemically), formulation retention, and drug release kinetics (e.g., rapid or controlled release). However, despite the pharmaceutical advances in rectal drug delivery, very few of them have translated to the clinical phase. This review will address the physiological and pharmaceutical considerations influencing rectal drug delivery as well as the conventional and novel drug delivery approaches. The translational challenges and development aspects of novel formulations will also be discussed.

FUNCTIONAL ANATOMY

The rectum is the final portion of the large intestine that starts from the end of the sigmoid colon to the anal canal. It primarily acts as a transportation (conduit) or temporary storage site in the defecation process, with only minimal involvement in the absorption of water and electrolytes from the gastrointestinal contents (Shafik et al., 2006; Leppik and Patel, 2015). Fecal matter is stored by the rectum if it is small in volume until it reaches a degree of rectal distension sufficient to initiate the defecation reflex (Shafik et al., 2006). The main anatomical difference between the rectum of adults and children is based on size. The length of the rectum is ~15–20 cm in adults, with a surface area of around 200–400 cm^2 (de Boer et al., 1982; van Hoogdalem et al., 1991; Nunes et al., 2014). In children, further size differences are evident due to the developing gastrointestinal tract. For example, the rectum is ~3 cm in length and has a surface area of ~18 cm^2 at 1 month of age compared to ~12 cm in length and ~230 cm^2 at 10 years of age (Woody et al., 1989; Jannin et al., 2014). Although the rectum is formed at birth, it is only functional when the baby starts to feed orally (Jannin et al., 2014).

In general, the environment in the rectum is relatively constant and static in comparison to other parts of the gastrointestinal tract (Jannin et al., 2014). The rectum has an average fluid volume of 1–3 ml and a neutral pH of 7–8, with minimal buffering capacity (Evans et al., 1988; Jannin et al., 2014; Nunes et al., 2014; Purohit et al., 2018). There have been conflicting reports regarding the rectal pH in children. Jantzen et al. (1989) measured the rectal pH in 100 healthy pediatric patients (25 infants and 75 children). Mean rectal pH was reported as 9.6; however, there was a wide range in rectal pH values (pH 7.2–12.1). Conversely, Turner et al. (2012) reported an average rectal pH of 6.75 from 100 well and 45 unwell infants, with no significant difference between the two groups. Interestingly, the mean rectal pH of well neonates (pH 6.47) was significantly lower than that of older infants (> 28 days of age, pH 6.90). The reason for the discrepancy in results may be due to physiological or technical differences in the studies; however, they should still be considered when developing or evaluating rectal dosage forms for pediatric patients, as this may affect drug partitioning and absorption. In addition, although the colon contains the majority of the gastrointestinal microbiome, it has been suggested that some residual bacterial enzymes are found in the rectum (Sartor, 2008; Macfarlane and Macfarlane, 2011). However, presystemic loss of drug by intraluminal degradation by microorganisms or metabolism within the mucosal cells in the rectum is generally not considered to be significant (de Boer et al., 1982; De Boer et al., 1984; Jannin et al., 2014).

In terms of histology, the rectal mucosa forms the innermost layer of the rectum that is in contact with fecal matter. The rectum does not have villi or microvilli on the luminal surface, hence the relatively small surface area for absorption in comparison to the small intestine (van Hoogdalem et al., 1991; Nunes et al., 2014; Reinus and Simon, 2014). The mucosal surface of the rectum is structured with a single layer of columnar cells to form the epithelium (Reinus and Simon, 2014). The epithelium also consists of numerous goblet cells that are interspersed among the absorptive cells (Reinus and Simon, 2014). Goblet cells are important for secreting mucus, which protects the rectal epithelia and helps to lubricate fecal matter as they pass through the rectum. At the anorectal junction, the mucosa transitions to non-keratinized stratified squamous epithelium and eventually to keratinized stratified squamous epithelium at the external anal sphincter (Nunes et al., 2014; Reinus and Simon, 2014).

The rectal region is drained by rectal (hemorrhoidal) veins and lymphatic vessels (de Boer et al., 1982; De Boer et al., 1984; van Hoogdalem et al., 1991; Dujovny et al., 2004; Nunes et al., 2014; Purohit et al., 2018). The superior rectal vein drains the upper part of the rectum, and the inferior and middle rectal veins drain the lower part of the rectum. More specifically, the superior rectal vein drains into the portal vein, which passes the blood through the liver prior to reaching the systemic circulation. In contrast, the inferior and middle rectal veins drain into the inferior vena cava and, therefore, directly into the systemic circulation. Between these three rectal veins exist extensive anastomoses, which connect all three veins throughout the rectum. The rectum is also extensively drained by the lymphatic system that originates in the mucosa and submucosa. The influence of the lymphatic vessels on the absorption of drugs is not well established; however, it may contribute to the systemic absorption of highly lipophilic drugs (Jannin et al., 2014; Nunes et al., 2014; Purohit et al., 2018). Lymphatic drainage also avoids the hepatic first-pass effect (de Boer et al., 1982; van Hoogdalem et al., 1991).

COMPARISON OF THE RECTAL ROUTE OF ADMINISTRATION TO OTHER SECTIONS OF THE GASTROINTESTINAL TRACT

For a balanced view of rectal drug delivery in the clinical setting, it is important to compare this route of drug administration to other sections of the gastrointestinal tract. In general, the oral route is the most preferred by patients, due to its advantages such as ease of use, non-invasiveness, and convenience for self-administration (Homayun et al., 2019; Shreya et al., 2018). The major site of drug absorption following oral administration is the small intestine, which has a much larger surface area compared to the rectum (Marieb and Hoehn, 2010; Reinus and Simon, 2014). Although the small intestine has been estimated to have a surface area of 200 m^2 in an adult, recent reports have suggested this to be more closer to approximately 32 m^2 for the interior of the gastrointestinal tract, with approximately 2 m^2 representing the large intestine (Helander and Fandriks, 2014). However, drugs administered orally can be unpleasant in taste, cause gastric irritation, and suffer from high first-pass drug elimination processes in the intestine and/or liver (Martinez and Amidon, 2002; Homayun et al., 2019). The physiological environment in the gastrointestinal tract can also affect the stability, solubility, and permeability of drugs, including the acidic gastric pH, gastrointestinal transit time, gastrointestinal mucus, and metabolism through enzymatic or microbial degradation (Martinez and Amidon, 2002; Homayun et al., 2019; Shreya et al., 2018). In addition, oral drug delivery can be challenging as the physiology of the human gastrointestinal tract can display both intra-individual and inter-individual variability (Martinez and Amidon, 2002). Therefore, the oral route of administration is less attractive for drugs that are significantly affected by these conditions.

The rectal route for drug delivery can be useful for drugs that have poor stability, solubility, or permeability following oral administration. It can also be used when oral ingestion is precluded—for example, in patients experiencing nausea and vomiting, when the patient is unconscious, or for patients that have swallowing difficulties (e.g., pediatric and geriatric patients). Although the surface area of the rectum is considerably smaller than that of the small intestine, the environment in the empty rectum is considered relatively constant and stable (Jannin et al., 2014). This favors a reproducible absorption process and has low enzymatic activity as compared to other sections of the gastrointestinal tract. In addition, drugs can partially bypass the liver following systemic absorption, which reduces the hepatic first-pass effect. Therefore, rectal drug formulations can be useful for drugs that: (i) undergo high hepatic first-pass metabolism, (ii) have limited absorption in the upper gastrointestinal tract, (iii) are readily degradable or

unstable in the gastrointestinal tract, (iv) cause irritation to the gastric mucosa, (v) cannot be easily formulated for other routes of administration, and (vi) have localized actions in the rectum or distal colon (de Boer et al., 1982; De Boer et al., 1984; Jannin et al., 2014; Nunes et al., 2014).

BIOPHARMACEUTICAL CONSIDERATIONS INFLUENCING RECTAL DRUG ABSORPTION

Drug absorption following rectal administration is determined by a combination of formulation-related factors, drug-related factors, and physiology-related factors. The latter has been covered in other sections of the review (refer to *"Functional anatomy"* and *"Physiological factors influencing rectal drug delivery"*). For absorption to occur, drugs must first be released from the formulation and then be solubilized in the low volume of rectal fluid before crossing the mucus layer and epithelium (van Hoogdalem et al., 1991). This is highly dependent on the formulation, with liquid dosage forms that contain drugs in solution (e.g., enemas) having faster absorption rates in comparison to solid dosage forms (e.g., suppositories and tablets) that require disintegration, liquefaction, and/or dissolution of the formulation to release the drug. Suspended drug particles will then need to dissolve in the luminal fluid before absorption can occur. It should be noted that the drug release rate from the formulation will depend on the partition coefficient of the drug between the vehicle and the aqueous rectal fluid (Nunes et al., 2014). For example, drugs with a high partition coefficient will be more lipophilic. This may lead to slow release of the drug from formulations that have fatty bases in comparison to more hydrophilic bases, which may produce a more sustained release effect. Therefore, the rate limiting step for drug absorption differs based on the formulation and the physical state of the drug in the formulation.

The physicochemical characteristics of the drug will also affect its ability to be absorbed *via* the rectal route. This includes solubility, degree of ionization, partition coefficient, and particle size. Following release from the formulation, the solubility of the drug in the rectal fluid will determine the maximum concentration available for absorption and will also establish a concentration-dependent gradient to drive absorption. In general, higher drug solubility is associated with faster dissolution rates and more rapid absorption. Drug molecules are predominantly transported passively *via* paracellular diffusion (between cells) or transcellular diffusion (through the cell), depending on its physicochemical characteristics. Paracellular transport is preferred for more hydrophilic molecules, ionized molecules, and high molecular weight compounds (Muranishi, 1984; Hayashi et al., 1997; Nunes et al., 2014); however, it can be restricted by the narrow tight junction space (Madara, 1998; Reinus and Simon, 2014). Therefore, the transcellular route is the main mechanism for drug absorption in the rectum (Muranishi, 1984; Hayashi et al., 1997; Nunes et al., 2014). Transcellular diffusion is affected by many factors, but it is usually proportional to the lipid solubility of the drug. Drug molecules in the non-ionized form are much more lipophilic than the ionized form (Allen et al., 2011; Jannin et al., 2014; Nunes et al., 2014; Purohit et al., 2018). At the relatively neutral pH of the rectum, basic drugs with an acid dissociation constant (pKa) near or above the physiologic range tend to be more readily absorbed, as they will predominantly be in their non-ionized form.

Having the optimal balance between hydrophilicity and lipophilicity is important for effective rectal drug delivery. Ideally, drugs should have adequate hydrophilic properties to be soluble in the rectal fluid and be lipophilic enough to cross the epithelium. As many drugs, including more than 40% of new chemical entities, have significant solubility issues in water, various techniques have been investigated to enhance their solubility. This includes particle size reduction, salt formation, use of surfactants, and encapsulation into nanoparticulate formulations (Savjani et al., 2012). In particular, the particle size distribution of active ingredients and excipients is an important physical characteristic of a formulation that has a strong impact on the rate of drug dissolution and absorption (Savjani et al., 2012; Sandri et al., 2014). Smaller particles tend to have higher dissolution rates due to the larger surface area to volume ratio and, therefore, a better chance for faster absorption. The larger surface area allows greater interaction with the solvent, thereby increasing its solubility. It should be noted that particle size has little effect on drugs that are readily water-soluble. However, particles in the size range of 50–100 μm are considered ideal, as they minimize both agglomeration and sedimentation (Sandri et al., 2014).

PHYSIOLOGICAL FACTORS INFLUENCING RECTAL DRUG DELIVERY

Rectal drug delivery can provide significant local and systemic levels for various drugs, despite the relatively small surface area of the rectal mucosa. However, the rectal route of administration can be affected by a number of physiological factors that will be discussed in this section. These factors should be considered in rectal formulation design, as they can affect drug bioavailability, efficacy, and safety.

Anatomical Considerations

When developing rectal dosage forms for different age groups, it is important to consider the anatomical size difference between the rectum of adults and children (Jannin et al., 2014; Linakis et al., 2016). Any new formulations should be evaluated for bioavailability, efficacy, and safety in the target population. However, there are a few patient groups in which rectal dosage forms should be avoided or used with caution. In general, drugs are not commonly administered rectally in neonates (term or preterm), as it is associated with erratic absorption as well as a risk of damage to the delicate rectal lining that could lead to infection (Jannin et al., 2014). Similarly, the risk of trauma and subsequent infection with rectal dosage forms is also high for immunocompromized patients (Berlin et al., 1997).

In addition, it is anatomically easier for rectally administered drugs to reach the distal colon than the proximal colon. Drugs given by this route are typically formulated in solid dosage forms (e.g., suppositories) or in liquid/semi-liquid dosage forms (e.g., enemas and foams). In general, foams and suppositories are retained mainly in the rectum and sigmoid colon, while enema solutions have a greater spreading capacity (van Hoogdalem et al., 1991; Brown et al., 1997; Loew and Siegel, 2012). Enemas are able to spread over an area situated between the rectum and the splenic flexure, which is the sharp bend between the transverse colon and the descending colon (van Hoogdalem et al., 1991; Brown et al., 1997). Therefore, rectal administration of drugs for local action may be more suitable for conditions that affect the distal part of the large intestine, such as proctitis (inflammation of the lining of the rectum), hemorrhoids, and distal colitis.

Site of Drug Absorption

The site of drug delivery in the rectum can affect the amount of the drug that reaches the systemic circulation. In general, drug absorption in the upper part of the rectum is transported to the liver *via* the portal system and thus undergoes first-pass metabolism, whereas drug absorption in the lower rectum is transported directly to the systemic circulation (de Boer et al., 1982; De Boer et al., 1984; Dujovny et al., 2004; Nunes et al., 2014; Purohit et al., 2018). This is of particular significance for drugs that have high hepatic clearance. However, it can be difficult to differentiate between the upper and lower regions when drugs are administered rectally. Anatomical differences in the venous drainage of the rectum between individuals can also significantly affect the amount of drug absorbed in the systemic circulation (de Boer et al., 1982; De Boer et al., 1984; van Hoogdalem et al., 1991). In addition, although systemic absorption cannot be completely avoided *via* rectal administration, limiting the amount of drug that is systemically absorbed is ideal for the treatment of local pathologies. Although a broad approximation, it has been reported that ~50% of a drug that is absorbed from the rectum will bypass the liver, thus reducing the hepatic first-pass effect (De Boer et al., 1984; Brunton et al., 2018). However, wide variations of bioavailability can occur due to the aforementioned issues.

Retention of the Formulation

For local or systemic drug absorption to occur, the formulation needs to be retained in the rectum for an adequate period of time. However, rectal formulations, particularly conventional dosage forms, can have problems with leakage, retention, and bloating (Allen et al., 2011). The contact time of the drug with the rectal mucosa is also important for absorption, as this will influence its bioavailability and efficacy. For absorption to occur, drugs need to be able to penetrate the mucus layer in order to reach the epithelial cells lining the rectum. Rectal mucus is mainly composed of water and mucins to form a fluid layer of ~150 μm in thickness (range 75–250 μm) (Pullan et al., 1994; Johansson et al., 2013), with an estimated turnover time of 3–4 h (MacDermott et al., 1974; Nunes et al., 2014). This layer can act as a barrier for drug absorption.

Fluid Volume and pH

The small fluid volume in the rectum and distal colon can affect rectal drug delivery. Compared to the small intestine, the volume of liquid in this region is significantly less, which may produce problems with the dissolution of some drugs (Jannin et al., 2014; Nunes et al., 2014; Purohit et al., 2018). As mentioned earlier, the pH in the rectum is typically considered neutral, which favors the absorption of drugs with pKa values near or above the physiologic range (Allen et al., 2011; Jannin et al., 2014; Nunes et al., 2014; Purohit et al., 2018). Changes in rectal pH can affect drug uptake by altering the ionization state of drugs. The rectal fluid has low buffering capacity, which means that administration of external products can significantly alter the pH in the rectum (Evans et al., 1988; Jannin et al., 2014; Nunes et al., 2014; Purohit et al., 2018). Variations in pH can impact on the absorption of drugs as well as lead to irritation or damage to the rectal mucosa (Allen et al., 2011; Nunes et al., 2014). These factors should be taken into account during formulation design to ensure efficient rectal drug delivery.

Viscosity of Rectal Contents and Bowel Movements

The presence of stool in the rectum affects the viscosity of the rectal contents, which can subsequently affect drug dissolution, drug stability as well as contact of the drug with the mucosal wall for absorption (de Boer et al., 1982; van Hoogdalem et al., 1991; Nunes et al., 2014). These factors can lead to irregular drug absorption and non-specific interaction of drugs with fecal matter and mucus. Early expulsion of the drug, including following defecation, will also affect the concentration available to undergo passive absorption. Hence, it is important to consider the time of dosing with respect to an individual's bowel movements (Sathyan et al., 2000). Frequency of bowel movements can be highly variable. For example, colonic transit times can vary significantly within and between individuals, with ranges from 6 to 70 h reported (Coupe et al., 1991; Rao et al., 2004). In addition, increased colonic motility in diarrhea can lead to reduced retention of rectal dosage forms and incomplete drug release (de Boer et al., 1982; van Hoogdalem et al., 1991; Nunes et al., 2014).

Pathophysiological Factors Influencing Rectal Drug Delivery

Pathological conditions can influence the effectiveness of rectally administered drugs. This includes colorectal diseases such as inflammatory bowel disease (IBD), irritable bowel syndrome (IBS), hemorrhoids, anal fissures, bowel incontinence, and acute gastrointestinal infections. Variations in the amount of drug absorbed can occur with changes in tissue integrity, mucosal inflammation, and bowel motility. Conditions that affect the integrity and the barrier qualities of the rectal mucosa (e.g., local trauma, anal fissures, and ruptured hemorrhoids) can lead to increased drug absorption that can be difficult to predict as well as being painful to administer (Reinus and Simon, 2014).

Likewise, mucosal inflammation can enhance epithelial permeability and, therefore, increase the amount of drug absorbed across the colorectal mucosa. For example, mucosal inflammation in IBD causes pathophysiological changes, including a disrupted intestinal barrier due to the presence of mucosal surface alterations, ulcers, and crypt distortions, as well as infiltration of immune cells (e.g., macrophages, lymphocytes, neutrophils, and dendritic cells) that promote inflammation (Li and Thompson, 2003; Antoni et al., 2014). Inflammation of the lining of the rectum (proctitis) can also occur in infections (e.g., sexually transmitted infections and gastrointestinal infections) and anal trauma (Hoque et al., 2012; Hatton et al., 2018).

Diseases that alter the motility of the gastrointestinal tract can also impact the effectiveness of rectally administered drugs by influencing retention, mucosal interaction, and the time available for disintegration, dissolution, and/or drug absorption. For example, diarrhea can occur in many acute gastrointestinal infections (Grover et al., 2008; Albenberg and Wu, 2014), in bowel incontinence (e.g., from muscle or nerve damage), and in chronic conditions such as IBD (Hua et al., 2015). Conversely, constipation is common in IBS and systemic pathologies that affect the endocrine system (e.g., hypothyroidism and diabetes) or central nervous system (e.g., multiple sclerosis and Parkinson's disease) (Konturek et al., 2011; Hatton et al., 2019). Similarly, drugs that alter gastrointestinal motility can also affect rectal drug delivery (Watts et al., 1992; Brunton et al., 2018). This includes drugs that can cause constipation (e.g., opioids, anticholinergic agents, antidiarrheal agents, antacids containing aluminium or calcium, iron/calcium supplements, diuretics, verapamil, and clonidine) and drugs that can cause diarrhea (e.g., laxatives, antibiotics, colchicine, cytotoxic agents, digoxin, magnesium, NSAIDs, orlistat, acarbose, and metformin). Therefore, understanding the effect of disease comorbidities and co-administered drugs on gastrointestinal physiology is important when considering rectal drug formulations.

CONVENTIONAL RECTAL DRUG DELIVERY APPROACHES

Conventional rectal dosage forms can be categorized into three groups—liquid dosage forms (e.g., enemas), solid dosage forms (e.g., suppositories, capsules, and tablets), and semi-solid dosage forms (e.g., gels, foams, and creams). Rectal formulations have been developed to deliver drugs either locally or systematically and have been investigated to release the drug immediately or over a prolonged period of time (Purohit et al., 2018). The physicochemical properties of the drug (e.g., molecular weight, solubility, pKa, stability) and the required speed of absorption are important factors to determining which formulation to use (Jannin et al., 2014). For solid dosage forms, disintegration, liquefaction, and dissolution are required before drug absorption into the mucosa can occur. Therefore, absorption is generally slower from solid dosage forms compared to liquid dosage forms (Jannin et al., 2014; Purohit et al., 2018). This section will discuss the main conventional rectal dosage forms and the developments to improve their effectiveness for rectal drug delivery.

Liquid Dosage Forms

Enemas are the main liquid dosage form for rectal drug delivery. They contain drugs in solution, suspension, or emulsion that are typically administered from disposable plastic squeeze bottles with an extended tip for rectal insertion. The solubility characteristics of the drug and additional solutes should be considered during pharmaceutical formulation, especially for solutions (Allen et al., 2011). Suspensions generally contain finely divided drug particles distributed throughout a vehicle in which the drug has minimal solubility. This formulation is particularly useful for drugs that are chemically unstable in solution (Allen et al., 2011). Emulsions are liquid preparations that have a dispersed phase composed of small globules of a liquid distributed throughout a vehicle in which it is immiscible. Emulsification enables the preparation of relatively stable and homogenous mixtures of two immiscible liquids (Allen et al., 2011). Enemas are mainly used to deliver drugs for the acute treatment of seizures, IBD, constipation, and as a bowel preparation for gastrointestinal diagnostic or surgical procedures (**Tables 1**, **2**).

There have been limited advances in the formulation of conventional enemas. Self-emulsifying drug delivery systems (SEDDS) were developed as a means to improve the bioavailability of poorly soluble drugs (Cherniakov et al., 2015). In general, SEDDS are composed of an oily base and a surfactant, with or without a hydrophilic co-solvent or cosurfactant. This creates a liquid dosage form that transitions to an oil-in-water emulsion once in contact with the aqueous phase at the site of administration. SEDDS are thought to improve bioavailability by enhancing drug solubility and improving membrane permeability (Cherniakov et al., 2015). Although more commonly studied for the oral route of administration (Gupta et al., 2013; Cherniakov et al., 2015; Karamanidou et al., 2016), the advantages of SEDDS have shown promise for rectal drug delivery (Kim and Ku, 2000; Kauss et al., 2018). For example, Kauss et al. (2018) evaluated the use of SEDDS to improve the systemic bioavailability of ceftriaxone for potential use as a rectal antibiotic therapy in neonates. *In vivo* results in rabbits showed rapid absorption of ceftriaxone in the SEDDS formulation following rectal administration, achieving 128% bioavailability compared to rectally delivered ceftriaxone capsule (powder control formulation).

The properties of the enema itself can influence rectal drug delivery. Maisel et al. (2015) demonstrated that the composition of the enema can determine whether drugs are delivered locally or systemically. In particular, strongly hypotonic (absorption-inducing) and hypertonic (secretion-inducing) enemas caused rapid systemic drug uptake, whereas moderately hypotonic enemas (with ion compositions similar to feces) resulted in high local tissue levels with minimal systemic drug absorption. Interestingly, hypertonic enemas caused extensive epithelial tissue damage in the colorectal region, which promoted systemic drug absorption. Hypotonic enemas, however, caused no detectable epithelial damage. Strongly hypotonic enemas were

suggested to transport drug through the epithelium by both transcellular and paracellular fluid absorption to the systemic circulation. Moderately hypotonic enemas were able to flow through the mucus layer and increase local drug bioavailability in the colorectal tissues, but they were mild enough to minimize systemic absorption.

Further study is required to determine the safety of various enema ion compositions in humans and for repetitive use (Maisel et al., 2015). In addition, the interaction of specific drugs in liquid dosage forms with the colorectal mucosa can also impact on the efficiency of drug absorption, and therefore, should be comprehensively evaluated. The use of liquid dosage forms generally allow faster absorption since drug release and dissolution issues are usually circumvented (Allen et al., 2011). However, the volume administered can affect drug retention in the rectum. For example, smaller volumes have been shown to have greater retention, while volumes higher than 80 ml can stimulate defecation (van Hoogdalem et al., 1991; Nunes et al., 2014). All conventional liquid dosage forms can suffer from various degrees of leakage, which can lead to irregular drug absorption.

Solid Dosage Forms

Suppositories are the most common rectally administered dosage form used clinically. They are solid dosage forms containing drugs that are either dispersed or dissolved in a suitable base (Allen et al., 2011). Drugs are typically mixed with the suppository excipients during manufacturing to form a homogenous system. Suppositories are generally composed of either a lipophilic base (e.g., cocoa butter, coconut oil, hydrogenated vegetable oils, and hard fats) or hydrophilic base (e.g., glycerinated gelatin and polyethylene glycols) (Allen et al., 2011; Jannin et al., 2014; Ham and Buckheit, 2017). Lipophilic bases are immiscible with body fluids and readily melt at body temperature to release the drug on the mucosal surface, whereas hydrophilic bases need to dissolve in the physiological fluids for drug release (Allen et al., 2011; Jannin et al., 2014; Ham and Buckheit, 2017).

Suppositories can be designed to have different rates and degrees of drug release for absorption. In particular, the composition of the suppository base, including the use of surfactants or other additives, and the physicochemical properties of the drug (e.g., solubility and particle size) can confer different drug release profiles (Nunes et al., 2014; Leppik and Patel, 2015). For drugs that are dissolved (soluble) in the suppository base, drug release occurs as the suppository dissolves or melts onto the mucosal surface where the drug molecules then diffuse out. For drugs that are dispersed (insoluble) in the suppository base, the opposing solubility properties encourage the drug to leave the dosage form and then begin solubilizing in the physiological fluid (Jannin et al., 2014; Ham and Buckheit, 2017). Therefore, hydrophilic drugs tend to show better release in lipophilic bases, and lipophilic drugs have better release in hydrophilic bases. In this case, particle size of the drug will also influence the rate of absorption and bioavailability (Leppik and Patel, 2015).

Despite the advantages of conventional suppositories for rectal drug delivery, they are associated with issues such as irregular drug absorption, leakage, and discomfort. Several advances have been made to improve on bioavailability, formulation retention, and patient acceptability of these solid dosage forms. This includes the addition of surfactants (e.g., polysorbate 80, Tween 20, and Span 60) to either the hydrophilic or lipophilic phase of the formulation to create solid emulsion-type suppositories (Abd el-Gawad et al., 1988; Gugulothu et al., 2010; Abou el Ela Ael et al., 2016). Emulsion bases were reported to have higher rates of drug release compared to lipophilic and hydrophilic suppository bases (Abd el-Gawad et al., 1988; Jannin et al., 2014; Abou el Ela Ael et al., 2016). The presence of surfactants in the formulation improved the wettability of the suppository base matrix, thereby enhancing the release and dissolution of the embedded drug particles (Abd el-Gawad et al., 1988; Jannin et al., 2014; Abou el Ela Ael et al., 2016).

Hollow-type suppositories have been developed and modified to enhance the absorption of various drugs (Watanabe et al., 1986; Watanabe et al., 1986; Matsumoto et al., 1989; Uekama et al., 1995; Watanabe et al., 1998; Kowari et al., 2002; Kaewnopparat et al., 2004; Shiohira et al., 2009). This type of suppository essentially contains a hollow space in the center that is filled with the drug in solid, liquid, or semi-solid form. The solid outer shell of the suppository can be composed of hydrophilic or lipophilic base materials and can incorporate other constituents to confer additional release properties, such as mucoadhesion and sustained release. This design has the benefits of controlling the dose of the drug, allowing convenient interchangeability of the drug, and preventing any interactions between the drug and the base material.

Furthermore, dimple-type suppositories were developed by Matsumoto et al. (2017) to improve the rectal delivery of poorly absorbable drugs such as peptides and oligonucleotides. These suppositories have one or more dimples on the surface where drugs are embedded. It was proposed that concentrating the drug to a limited area on the surface of the suppository would lead to a higher rate of drug release and absorption when administered into the rectum. In addition, limiting the drug concentration toward the surface of the suppository increases its contact with the rectal mucosal surface and creates a concentration gradient for passive absorption of the drug across the mucosa. Interestingly, *in vitro* release studies showed that the time to 50% drug release was dependent on the melting point of the lipid used for sealing the dimples and not on the number of dimples (Matsumoto et al., 2017).

Additional studies are required to comprehensively evaluate the pharmacokinetics, efficacy, and safety of drugs formulated in the different suppository dosage forms in humans for both local and systemic absorption. Evaluations should also be compared between single dose and multiple dose therapies to ensure reproducibility of the results. This data will determine the clinical translatability of the formulations.

Semi-Solid Dosage Forms

Gels and foams are the most common semi-solid dosage forms used for rectal drug delivery. These formulations generally require the use of an applicator that has to be filled with the

drug formulation prior to dose administration (Allen et al., 2011). Rectal gels are a semi-solid formulations that contain a solvent trapped within a polymer network to create a viscous consistency. Viscosity of the gel can be modified by the addition of co-solvents (e.g., glycerin and propylene glycol) and electrolytes (Allen et al., 2011; Nunes et al., 2014). They are easy and inexpensive to manufacture, however can suffer from stability issues, leakage, and messiness upon administration. The spreading features of rectal gel formulations are highly dependent on properties such as mucoadhesion and viscosity (Allen et al., 2011; Nunes et al., 2014). These properties can also affect the site of drug delivery and the fraction that undergoes hepatic first-pass metabolism.

One of the main advancements in conventional rectal dosage forms is the development of liquid suppositories, which more closely resemble semi-solid dosage forms rather than solid dosage forms. This includes the development of liquid suppositories containing thermosensitive polymers (Miyazaki et al., 1998; Fakhar Ud and Khan, 2019), mucoadhesive polymers (Koffi et al., 2008; Ye et al., 2016; Xu et al., 2017; Shi et al., 2019), or a combination of thermosensitive and mucoadhesive polymers (Choi et al., 1998; Yun et al., 1999; Ryu et al., 1999; Koffi et al., 2008; Barakat, 2009; Lo et al., 2013; Liu et al., 2018; Akl et al., 2019). Poloxamers are the most commonly used thermosensitive polymers in pharmaceutical formulation. They are nontoxic amphiphilic molecules that exhibit reverse thermal gelation. This allows them to remain in a liquid state at room temperature and convert into a gel consistency at body temperature, thereby allowing ease of administration into the body, reduced leakage, restricted spreading in the rectal cavity, and improved contact with the rectal mucosal surface (Yong et al., 2001; Barakat, 2009; Akl et al., 2019). Poloxamer molecules form small micellar units at room temperature and large micellar cross-linked network at body temperature (Akl et al., 2019). However, poloxamer gels on their own can have inadequate mucoadhesion, weak mechanical strength, and high permeability to water (Yong et al., 2001; Barakat, 2009; Akl et al., 2019).

Mucoadhesive polymers (e.g., carbopol, sodium alginate, polycarbophil, hydroxypropyl methylcellulose, hydroxyethyl cellulose, and methylcellulose) have been used in combination with thermosensitive polymers to improve gel strength and mucoadhesion. For example, the carboxyl groups in the mucoadhesive polymers can bind strongly with the cross-linked poloxamer gel, thereby positioning its molecules in between the gel to enhance overall strength (Barakat, 2009; Akl et al., 2019; Fakhar Ud and Khan, 2019). In addition, mucoadhesion is enhanced by hydrogen bonding of the polymers with the oligosaccharide chains of the rectal mucosal layer through hydroxyl and carboxyl groups (Lehr et al., 1990; Qi et al., 2006; Barakat, 2009; Akl et al., 2019). The enhanced mucosal retention of these hydrogels promotes improved drug release and absorption. It should be noted that cellulose ether polymers (e.g., hydroxypropyl methylcellulose, hydroxyethyl cellulose, and methylcellulose) also possess controlled release characteristics. These hydrogels are able to swell over time, which would also allow the encapsulated drug to be released at a continuous rate (Vueba et al., 2006; Barakat, 2009; Shi et al., 2019).

Foams are generally considered a colloidal dosage form, with a hydrophilic liquid continuous phase containing a foaming agent and a gaseous dispersion phase distributed throughout (Allen et al., 2011). Following rectal administration, they transition from a foam state to a liquid or semi-solid state on the mucosal surface. The structure of the foam is affected by parameters such as concentration and nature of the foaming agent, pH and temperature of the system, and viscosity of the liquid phase (Arzhavitina and Steckel, 2010). Foaming agents are amphiphilic substances that are important for foam generation and stabilization. The molecules contain hydrophilic components that are soluble in the aqueous phase and hydrophobic components that form micelles to minimize contact with the aqueous phase (Arzhavitina and Steckel, 2010). Rectal foams are mostly aerosol foams that are formulated to treat anorectal inflammation (e.g., hemorrhoids and anal fissures) and distal proctocolitis (e.g., distal ulcerative colitis) (Campieri et al., 1992; Lee et al., 1996; Arzhavitina and Steckel, 2010; Loew and Siegel, 2012; Sandborn et al., 2015). The advantages of foams for rectal drug delivery include convenient administration with minimal discomfort and leakage. Despite these advantages, there are not many rectal foam formulations that are commercially available. This is partly due to the issues with foam stabilization, accuracy of the dose administered, and irregular drug absorption (Arzhavitina and Steckel, 2010). Developments in this area have included the addition of mucoadhesive polymers to improve the retention of the formulation with the rectal mucosa for drug absorption (Arzhavitina and Steckel, 2010; Petkova et al., 2012; Politova et al., 2012).

NANOPARTICULATE RECTAL DRUG DELIVERY APPROACHES

Incorporation of nanoparticulate systems into rectal dosage forms has been investigated to improve the therapeutic effectiveness of drugs for both local and systemic therapy. Nanoparticulate rectal dosage forms differ from conventional rectal dosage forms by encapsulating or loading the drug into nanoparticles prior to dispersion in a formulation base (e.g., gel, suppository, and enema). From a pharmaceutical perspective, nanoencapsulation allows the ability to improve the solubility of hydrophobic compounds, modify drug release kinetics (e.g., controlled release or sustained release), and protect compounds that are sensitive to degradation (Shajari et al., 2017; Hua et al., 2018; Mesquita et al., 2019). From a biological perspective, nanoparticulate systems confer the following advantages: (i) improve cellular uptake into mucosal tissues and cells, (ii) promote accumulation to the site of mucosal disease (e.g., inflamed tissues), (iii) prolong residence time of encapsulated compounds (even when colonic motility is increased in diarrhea), and (iv) enable easier transport in the gastrointestinal tract to provide more uniform distribution and drug release within the colorectal region (Hua et al., 2015; Zhang et al., 2017; Hua et al., 2018; Mesquita et al., 2019).

For nanoparticulate dosage forms to be effective for rectal drug delivery, two main factors should be considered. First are the physicochemical properties of the nanoparticles (e.g., size, charge,

composition, and surface properties) for optimal interaction with the rectal or colorectal mucosa. These properties can promote better contact with the mucosal surface for improved mucosal penetration, cellular uptake, and drug release (Hua et al., 2015; Zhang et al., 2017). Second is the interaction of the nanoparticles with the formulation base. The nanoparticles should be stable when incorporated into the pharmaceutical base, especially during manufacturing and storage. In addition, the formulation base should increase the retention of the formulation in the rectum, without impeding the transport and interaction of the nanoparticles with the mucosal tissue. Adhesion to the mucosa is a requirement for effective rectal drug delivery, as it reduces the clearance of nanoformulations by mucus, leakage, or rapid transit time (e.g., diarrhea) (Mesquita et al., 2019). A number of different nanoparticulate systems have been evaluated for rectal drug delivery. This section will discuss the effectiveness of each of the systems in terms of the formulation base.

Nanoparticulate Liquid Dosage Forms

Liquid dosage forms are typically used in initial studies to evaluate the potential of nanoparticulate systems for rectal drug delivery. This is likely due to convenience, as the nanoparticles are usually manufactured in aqueous liquid such as water and buffered solutions (Mesquita et al., 2019). In addition, it is common for proof-of-concept studies to be evaluated in aqueous liquid to minimize the interference of the formulation base with the nanoparticles. This is evident in a large portion of studies focused on colon-targeted drug delivery, whereby nanoparticles are administered rectally to determine efficacy and safety early on in animal models (Lamprecht, 2010; Hua et al., 2015; Maisel et al., 2015; Zhang et al., 2017) and humans (Schmidt et al., 2013), prior to the added complexities of formulation design for clinical translation. For example, Maisel et al. (2015) evaluated the effect of surface chemistry on nanoparticle interaction and distribution in the gastrointestinal tract following oral and rectal administration in healthy mice and in a mouse model of ulcerative colitis. Various nanoparticle sizes (40, 100, 200, and 500 nm) were also assessed. The study showed that nanoparticles coated with polyethylene glycol (PEG) of all sizes were able to be efficiently distributed over more of the colorectal tissue surface in both healthy mice and mice with TNBS-induced colitis, which is likely to provide improved drug delivery for both local and systemic applications. Surface PEGylation of nanoparticles creates a hydrophilic surface chemistry that reduces interaction of the nanoparticles with the gastrointestinal environment and confers mucus-penetrating properties (Cu and Saltzman, 2008; Lai et al., 2009; Tang et al., 2009; Hua et al., 2015).

There are fewer studies focused on nanoparticulate drug delivery in a liquid dosage form to specifically the rectal mucosa for local and/or systemic action (das Neves et al., 2013; Kamel et al., 2013; Schmidt et al., 2013; Maisel et al., 2015; Nunes et al., 2018). Of these studies, Schmidt et al. (2013) were the first to investigate the potential of conventional nanoparticle (mean particle size of 250 nm) and microparticle (mean particle size of 3 μm) uptake into the rectal mucosa of humans with and without IBD. Both poly(lactic-co-glycolic acid) (PLGA) nanoparticles and microparticles were dispersed in saline solution containing 10% human albumin. The addition of the protein in the dispersion medium sterically stabilized the particles and reduced their surface charge by adsorption to the particle surface. The results showed accumulation of microparticles in ulcerous lesions of patients with both rectal Crohn's disease and ulcerative colitis. There was a clear size-dependent difference regarding the accumulation of particles in IBD patients, with nanoparticles only detectable in traces in the mucosa of these patients. The study demonstrated that microparticles exhibited accumulation and bioadhesion to the inflamed mucosal wall; however, no absorption across the epithelial barrier was detected. Conversely, nanoparticles were translocated to the serosal compartment of IBD patients, possibly leading to systemic absorption. In healthy control patients with the rectal mucosal surface intact, nearly no nanoparticles or microparticles were visible. The study suggested that nanoparticles might not be required for local drug delivery to intestinal lesions in humans. However, the reason for the discrepancy of particle size between animal and human studies is unclear. It should be noted that, while particle accumulation in ulcerated areas was statistically significant, the total fraction of particles penetrating into the rectal mucosa was relatively low in the study.

Liquid bases at physiological pH and osmolality are commonly used for rectal drug delivery. However, Maisel et al. (2015) showed that the composition of enemas can be optimized for the local and/or systemic delivery of nanoparticles. Hypotonic sodium-based enemas were shown to be an ideal liquid formulation base to enhance the distribution of PEGylated polystyrene nanoparticles (mean particle size of 60 and 230 nm) on the colorectal epithelial surface in comparison to isotonic and hypertonic enemas and potassium-based enemas. In particular, hypotonic sodium-based enemas induced fluid absorption that promoted uniform nanoparticle distribution over the epithelial surface, whereas hypertonic sodium-based enemas caused fluid secretion and bowel distension that prevented nanoparticles from being in close contact with the mucosal surface. Although when used as a pretreatment, strongly hypertonic enemas were able to damage the colorectal epithelium, which allowed penetration of the hypotonically delivered nanoparticles into the tissue.

Overall, nanoparticulate liquid dosage forms would still have the same issues as conventional liquid dosage forms that were mentioned earlier. Although liquid dosage forms have greater spreading capacity in the rectum, they can suffer from low retention and leakage—both of which can lead to irregular drug absorption. Their use will be highly dependent on the clinical application and frequency of dosage. Importantly, the initial results from liquid dosage forms support the potential of nanoparticles (and microparticles) for improving rectal drug delivery.

Nanoparticulate Solid Dosage Forms

There are only a few studies which have incorporated nanoparticles into solid dosage forms for rectal drug delivery. Abdelbary et al. (Abdelbary and Fahmy, 2009) developed solid lipid nanoparticles (SLN) containing the water-insoluble drug, diazepam, to confer both rapid onset of action and

prolonged drug release for the potential acute management of severe seizures. Results showed that varying the concentration or type of lipid matrix or surfactant affected the particle size, entrapment efficiencies, and release profiles of the nanoparticles. Transmission electron microscopy and laser diffractometry studies revealed that 60% of the formulations had particle sizes less than 500 nm. The nanoparticles were effectively incorporated into suppositories composed of hard fats (Witepsol W35 and Witepsol S58). *In vitro* studies showed significantly prolonged drug release from the SLN-containing suppositories in comparison to suppositories containing free drug (control). However, drug release from the control formulation was significantly faster than the SLN-containing suppository formulations. Further investigation is necessary to determine the efficacy of the rectal formulations *in vivo*. The release profile of the diazepam-loaded SLNs in a primarily hydrophilic base would also be of interest, as this may allow a faster release of drug into the physiological fluid that would be beneficial in emergency clinical applications.

This concept of having opposing solubility properties of the drug-loaded nanoparticles and suppository base was investigated by Mohamed et al. (2013). This study incorporated the hydrophilic drug, metoclopramide, into SLNs (particle size range of 24.99–396.8 nm) that were then formulated into suppositories with a lipophilic base. Suppositories containing a cocoa butter base demonstrated the highest release of metoclopramide from SLNs, which was likely due to it having a lower melting point and its lack of hydrophilicity. The formulation also demonstrated sustained release of the drug due to coating with lipids in the nanoparticles. In particular, metoclopramide-loaded SLN suppositories produced the same gastric emptying percentage as the marketed metoclopramide suppository (Primperan) with additional sustained release characteristics *in vivo*, thereby avoiding the need for multiple dosing.

Similarly, Siczek et al. (2018) used cocoa butter suppositories to validate the possibility of effectively releasing silver from silver-coated glass beads for local anti-inflammatory action in conditions such as IBD. It should be noted that the borosilicate glass beads had an initial diameter of 1,000 μm before coating with silver. *In vitro* drug release assays of the silver-coated glass beads showed rapid release of silver, with nearly half of the amount of the deposited metal being released in the first 30 min of incubation. After 24 h, approximately 30% of the silver remained on the glass beads. Further studies are still needed to evaluate the rate of silver release from silver-coated glass beads from the suppository as well as the effectiveness of the formulation *in vivo*. Analysis of the prepared suppositories containing silver-coated glass beads using X-ray CT demonstrated an effective method to attain homogenous distribution of the beads in the entire volume of the suppository with minimal sinking or agglomeration.

Despite there being only a few studies to date that have incorporated nanoparticles into solid dosage forms for rectal drug delivery, the basis for further investigation is warranted. In particular, the *in vitro* data and initial *in vivo* data show potential of the formulation strategy in terms of drug release profiles. Proof-of-concept studies are still required to demonstrate the bioavailability, efficacy, and safety of these nanoparticulate formulations.

Nanoparticulate Semi-Solid Dosage Forms

Gels are the most likely of the formulation bases to have translational potential for the delivery of nanoparticles rectally. The viscous consistency of gels promotes improved retention of formulations in the rectum and enhances contact with the rectal mucosa for drug absorption. As mentioned previously for conventional semi-solid dosage forms, a number of advances have been made for rectal drug delivery with the use of mucoadhesive polymers and/or thermosensitive polymers in the formulation base. The choice of gel base and its composition are dependent on the physicochemical properties of the nanoparticles and ideally should not interfere with drug release from the nanoparticles or the interaction of nanoparticles with the rectal mucosa.

Mucoadhesive bases alone have not been evaluated for nanoparticle delivery into the rectum. Instead, the use of thermosensitive polymers in the formulation base has been more common for the rectal delivery of nanoparticles (Seo et al., 2013; Din et al., 2015; Din et al., 2017; Melo et al., 2019). These polymers create an initial liquid dosage form at room temperature that allows ease of administration and mucosal spreading, before transitioning to a gel phase at body temperature. Melo et al. (Melo et al., 2019) investigated the colorectal distribution and retention of PLGA nanoparticles (mean particle size of 170–180 nm) incorporated into a thermosensitive base (poloxamer 407). *In vitro* drug release assays of dapivirine loaded into this nanoparticle formulation showed faster and overall higher drug release over 8 h in comparison to free drug in thermosensitive base and dapivirine-loaded nanoparticles in PBS. In addition, *in vivo* studies in mice indicated that the thermosensitive base exhibited slower but wider distribution of the nanoparticles in the colorectal region. Enhanced retention of the nanoparticles was also evident in the colorectum.

Similarly, Din et al. (2017) developed a novel rectal formulation of irinotecan for the local treatment of rectal cancer. This nanoparticulate dosage form consisted of thermosensitive irinotecan-encapsulated SLNs (mean particle size of 190 nm) dispersed in a thermosensitive poloxamer solution to create a double-reverse thermosensitive nanocarrier system (DRTN). Therefore, the formulation base transitions from a liquid to a gel state after rectal administration, whereas the SLNs are composed of lipids that are solid at 25°C and melt at body temperature. The DRTN dosage form showed sustained drug release with minimal burst effect and a relatively constant plasma concentration of irinotecan at 1–3 h in healthy rats. Interestingly, *in vivo* evaluation in tumor xenograft athymic nude mice showed significant decreases in tumor volume with both DRTN and the control hydrogel (irinotecan in thermosensitive base) in comparison to intravenous irinotecan solution. Histopathological analysis suggested that DRTN had significantly improved anti-tumor activity compared to both controls due to its sustained plasma concentrations.

The combination of thermosensitive and mucoadhesive polymers in the formulation base for the rectal delivery of nanoparticles has not been extensively examined. Moawad et al. (2017) developed nanotransfersomes (mean particle size of 150 nm) that were incorporated into a formulation base containing poloxamer 407 (thermosensitive polymer) and hydroxypropyl methylcellulose (mucoadhesive polymer) to improve the bioavailability of tizanidine (myotonolytic drug). *In vivo* pharmacokinetic studies in rabbits showed enhanced drug bioavailability by approximately 2.2-fold and 1.4-fold for nanotransfersome gel and free drug in gel, respectively, in comparison to oral drug solution. This enhancement in bioavailability was likely to be due to the partial avoidance of hepatic first-pass metabolism by the rectal route. Higher bioavailability of the nanotransfersome gel was also attributed to the permeation enhancing effect of the nanoparticles. In addition, both rectal formulations significantly increased the half-life of tizanidine (10.13 h for nanotransferome gel and 7.21 h for free drug gel) compared to oral drug solution (3.41 h). The results suggest that the use of the thermosensitive-mucoadhesive gel base as well as nanoparticulate encapsulation of the drug both delayed the release of tizanidine to produce a sustained release effect.

The limited studies to date support the use of semi-solid dosage forms for the rectal delivery of nanoparticles. Further studies are needed to determine the interaction of the semi-solid dosage forms on the nanoparticulate systems, including: (i) distribution following rectal administration, (ii) retention of the formulation in the rectum, (iii) adhesion and/or uptake of nanoparticles in the rectal mucosa, (iv) movement of nanoparticles in the semi-solid dosage form, (v) drug release from nanoparticles entrapped in the semi-solid dosage form, and (v) stability of the formulation during manufacturing and storage.

TABLE 3 | Rectal formulations in clinical trials *(Ref: clinicaltrials.gov).*

Drug	Dosage form	Indication	Status
Ceftriaxone	Suppository	Healthy	Phase I
Quetiapine	Suppository	Dementia, delirium	Phase I completed
Ibuprofen	Suppository	Healthy	Phase I completed
NRL001	Suppository (slow release)	Incontinence	Phase I completed
Hydrocortisone	Suppository, enema	Healthy	Phase I completed
Nifedipine	Suppository	Chronic anal fissure	Phase I/II completed
Hydrocortisone	Suppository	Internal hemorrhoids	Phase II completed
Diclofenac	Suppository	Carcinoma prostate	Phase II completed
Meloxicam	Suppository	Ankylosing spondylitis	Phase III completed
Balsalazide	Suppository, enema	Ulcerative colitis	Phase III completed
Belladonna + opium	Suppository	Nephrolithiasis	Phase IV completed
Belladonna + opium	Suppository	Post-partum pain	Phase IV completed
Belladonna + opium	Suppository	Post-operative pain	Completed
Fluocortolone + lidocaine	Suppository, cream	Acute hemorrhoids	Not stated
Nil	Suppository, enema and rectal insert	HIV prevention	Not stated
Tenofovir	Enema	HIV prevention	Phase I
Fecal microbiota	Enema	Infection due to resistant organism	Phase I
Fecal microbiota	Enema	Crohn's Disease	Phase I
Fecal microbiota	Enema	Acute pancreatitis	Phase I
Mesalamine	Enema	Healthy	Phase I completed
ALTH12	Enema	Ulcerative colitis	Phase I completed
TF037	Enema	Colonoscopy	Phase I completed
SB012	Enema	Ulcerative colitis	Phase I/II completed
Fecal microbiota	Enema	Severe acute malnutrition	Phase I/II
Fecal microbiota	Enema	Clostridium difficile infection	Phase II
Fecal microbiota	Enema	Ulcerative colitis	Phase II completed
PUR0110	Enema	Left-sided ulcerative colitis	Phase II completed
Manuka honey	Enema	Pouchitis	Phase II completed
Promelaxin	Enema	Chronic functional constipation	Phase IV
Chloral hydrate	Enema	Congenital cataract	Completed
NER1008	Enema	Colorectal cancer	Completed
IQP-0528	Rectal gel	HIV prevention	Phase I
Lidocaine	Rectal gel	Hemorrhoids	Phase I
Nil	Rectal gel (thermosensitive)	Ulcerative colitis	Phase I completed
Tenofovir	Rectal gel (mucoadhesive)	HIV prevention	Phase I completed
Tenofovir	Rectal gel (mucoadhesive)	HIV infection	Phase I completed
Dapivirine	Rectal gel	HIV infection	Phase I completed
PC-1005	Rectal gel	HIV infections	Phase I completed
Maraviroc	Rectal gel	HIV/AIDS	Phase I completed
PP110	Rectal gel	Bleeding hemorrhoids	Phase II/III completed
Lidocaine + diclofenac	Rectal gel	Anal fissure	Phase IV completed
Nil	Rectal gel (thermosensitive)	Healthy	Completed

RECTAL FORMULATIONS APPROVED AND IN CLINICAL TRIALS

A number of rectal formulations are on the market with more in clinical development. **Tables 1** and **2** show examples of the rectal formulations that are clinically approved for local absorption and systemic absorption, respectively. These formulations generally contain drugs that have a wide therapeutic window between the concentration that causes therapeutic effects and the concentration that causes toxicity. This allows a safe margin that accounts for the variability in rectal drug absorption. Approved rectal formulations are typically indicated for conditions that require short-term therapy. Exceptions include a few locally acting formulations, such as mesalazine or corticosteroids that are used for a longer duration to induce remission in patients with ulcerative proctitis or ulcerative proctosigmoiditis that occurs in IBD. Clinical studies have demonstrated budesonide rectal foam and enema to be efficacious in these conditions, while reducing the risk of systemic steroid-related adverse effects (Gross et al., 2006; Sandborn et al., 2015).

The majority of the rectal formulations in clinical trials (**Table 3**) incorporate already approved drugs or novel compounds into conventional rectal dosage forms—in particular, suppositories, enemas, and rectal gels. Many of these formulations are still in the early clinical phases of investigation and are indicated for local pathologies, including hemorrhoids, constipation, bowel preparation, anal fissure, IBD, fecal microbiota transplant, and infections (e.g., HIV prevention). The very few that are focused on systemic drug absorption with rectal formulations are for the treatment of pain. Similar to the approved rectal formulations, those in clinical trials are predominantly used for short-term therapy. Furthermore, innovative rectal dosage forms, such as nanoparticulate systems, have yet to reach the clinical development phase. Thermosensitive rectal gels are likely the most innovative platform in clinical trials. They have been evaluated for parameters such as safety, preference, distribution, and retention in healthy patients as well as in patients with ulcerative colitis. With further advances in rectal drug formulation and comprehensive preclinical evaluation, we should expect to see more progressing to clinical studies.

CONSIDERATIONS FOR TRANSLATIONAL DEVELOPMENT

The rectal route of administration has significant advantages for both the local and systemic delivery of drugs. However, there has been a general lack of research in this important area of drug formulation when compared to other routes for gastrointestinal drug delivery. In particular, there is a need for comprehensive studies on the biological interactions of rectal drug delivery in both adults and children, as well as continued innovations in rectal drug formulations.

From a biological perspective, there should be comprehensive analysis of the *in vivo* fate and interactions of drugs delivered in existing and new rectal dosage forms with the blood, tissue, cellular, and intracellular compartments in both healthy and diseased states (Nehoff et al., 2014; Sercombe et al., 2015; Hare et al., 2017; Hua et al., 2018). This includes pharmacokinetics, stability, permeability, efficacy, and safety of the formulation. Attention should also be given to the performance of these dosage forms in the heterogeneous nature of the human gastrointestinal environment (Hua et al., 2015; Zhang et al., 2017). As discussed earlier, rectal drug delivery can be affected by a number of physiological factors, which can lead to wide variations in the amount of drug absorbed. This is particularly problematic for drugs with a narrow therapeutic index or serious conditions that require predictable drug levels. Therefore, use of the rectal route of administration is unlikely to be clinically feasible in these situations.

In addition, there are an increasing number of studies investigating the potential of rectal drug delivery for the treatment of more chronic conditions, including diabetes (Matsumoto et al., 2017; Shi et al., 2019), infections (das Neves et al., 2013; Ham and Buckheit, 2017; Nunes et al., 2018), hypertension (Abou el Ela Ael et al., 2016), asthma (Shiohira et al., 2009), chronic anal fissure (Ivanova et al., 2019), and cancer (Lo et al., 2013; Seo et al., 2013; Ye et al., 2016; Din et al., 2017). Although encouraging results were reported in these studies, with many designed for sustained release activity, they generally did not evaluate the formulations over a long study period. Further studies are required to assess the reproducibility and variation in the pharmacokinetics, efficacy, and safety of these formulations for long-term dosing. Dosing frequency of rectal formulations will also be a major factor for clinical translation, with once daily dosing providing better patient compliance.

For innovative platforms, such as nanoparticles, safety of the different carriers following uptake needs to be explored further, including both acute and chronic toxicity (Nystrom and Fadeel, 2012; Accomasso et al., 2018). Studies focused on the toxicology of these delivery systems in the human gastrointestinal tract have been limited and is likely to vary according to the particle size and composition (Bergin and Witzmann, 2013; Talkar et al., 2018; Vita et al., 2019). The pace for the clinical translation of nanoparticulate dosage forms has been relatively slow as the development trajectory is very costly, complex, and time-consuming (Hua et al., 2018). There has to be a clear positive benefit-to-risk ratio that will accompany the use of nanoparticles for rectal drug delivery, especially when compared to an approved counterpart or existing therapies (Hua et al., 2018). Therefore, *in vivo* evaluation of innovative platforms should be compared with appropriate control formulations to provide meaningful data on the influence of the drug, carrier, and/or formulation base for effective rectal drug delivery (Hua et al., 2018).

Furthermore, the evaluation of many of the rectal dosage formulations has been limited to *in vitro* (e.g., drug release and cellular uptake) and/or *ex vivo* (e.g., mucoadhesion) studies. Therefore, caution should be taken when interpreting the data, as the same effect in animals or humans cannot be guaranteed. Use of rodents for *in vivo* studies can also have its limitations for examining rectal drug delivery for clinical use. For example, the anatomy and physiology of rodents can affect the distribution of the dosage form as well as the amount of the formulation that can be administered rectally (Melo et al., 2019). In comparison

to humans, rodents tend to defecate more frequently, have more intense bowel movements, and have faster turnover of mucus in the rectum (Mule et al., 2010; Ermund et al., 2013; Padmanabhan et al., 2013; Melo et al., 2019). These factors should be taken into account when designing *in vivo* studies. Although assessment in larger animal models with similar gastrointestinal transit times to humans (e.g., pigs and dogs) would be more applicable for clinical translation (Kararli, 1995; Maisel et al., 2015), this is generally not feasible and is associated with its own ethical considerations. Therefore, previous studies have suggested an alternate time scale to evaluate colorectal retention of drug formulations administered rectally in rodents, with 15 min, 2 h, and 6 h corresponding to short, medium, and long retention times, respectively (Maisel et al., 2015; Nunes et al., 2018; Melo et al., 2019).

From a commercial development point of view, the complexity in the design and development of rectal dosage forms also needs to be minimized as much as possible, to create dosage forms that are able to be reproducibly prepared and characterized (Hua et al., 2018). The pharmaceutical characterization of different rectal dosage forms has been comprehensively addressed in other reviews (Jannin et al., 2014; Nunes et al., 2014; Purohit et al., 2018) and is an important consideration for translational development. This includes the availability of appropriate testing methods and standardized protocols for quality control that meet regulatory requirements. For example, rectal formulations should be physically and chemically stable after the manufacturing process, during long-term storage, and upon clinical administration to ensure reproducible release kinetics. In addition, rectal dosage forms should be tailored for use in adults and children, with the latter also having further anatomical size differences and dose requirements that should be taken into consideration (Jannin et al., 2014; Linakis et al., 2016). Ideally, they should deliver single doses to provide reproducible bioavailability, efficacy, and safety. Other considerations include potential for scale-up for large-scale manufacturing, availability of materials and industrial equipment, and overall cost of dosage form development (Hua et al., 2018; Purohit et al., 2018). As mentioned for nanoparticulate formulations, there also needs to be a clear benefit of efficacy and/or safety with any new drug formulation compared to clinically available dosage forms for clinical translation to be justified (Hua et al., 2018).

CONCLUSION

The rectal route for drug delivery is still relatively underutilized despite its advantages. Although the oral route is the most convenient and preferred route for drug administration, there are a number of circumstances that have been discussed where this is not possible from either a clinical or pharmaceutical perspective. In these cases, the rectal route may represent a practical alternative and can be used to administer drugs for both local and systemic action. Continued innovations in rectal drug formulation and comprehensive studies on the biological interactions of rectal drug delivery are required to fully exploit the potential of this route to treat systemic and local diseases.

AUTHOR CONTRIBUTIONS

SH was involved in conception of the idea for the review, drafted the manuscript, and approved the final version of the manuscript.

ACKNOWLEDGMENTS

The author wishes to thank the University of Newcastle, Pharmacy Research Trust of New South Wales, Rebecca L. Cooper Medical Research Foundation, Gladys M Brawn Fellowship, and ausEE Research Foundation for providing financial support for this work.

REFERENCES

Berlin, C., May-McCarver, D. G., Notterman, D. A., Ward, R. M., Weismann, D. N., Wilson, G. S., Wilson, J. T. et al. (1997). Alternative routes of drug administration—advantages and disadvantages (subject review). *Am. Acad. Pediatr.* 100, 143–152. doi: 10.1542/peds.100.1.143

Abd el-Gawad, A. H., el-Din, E. Z., and Abd el-Alim, H. A. (1988). Effect of surfactant incorporation techniques on sulphamethoxazole suppository formulations. *Pharmazie* 43 (9), 624–627.

Abdelbary, G., and Fahmy, R. H. (2009). Diazepam-loaded solid lipid nanoparticles: design and characterization. *AAPS PharmSciTech.* 10 (1), 211–219. doi: 10.1208/s12249-009-9197-2

Abolhassani, M., Lagranderie, M., Chavarot, P., Balazuc, A. M., and Marchal, G. (2000). Mycobacterium bovis BCG induces similar immune responses and protection by rectal and parenteral immunization routes. *Infect. Immun.* 68 (10), 5657–5662. doi: 10.1128/IAI.68.10.5657-5662.2000

Abou el Ela Ael, S., Allam, A. A., and Ibrahim, E. H. (2016). Pharmacokinetics and anti-hypertensive effect of metoprolol tartrate rectal delivery system. *Drug Deliv.* 23 (1), 69–78. doi: 10.3109/10717544.2014.904021

Accomasso, L., Cristallini, C., and Giachino, C. (2018). Risk assessment and risk minimization in nanomedicine: a need for predictive, alternative, and 3Rs strategies. *Front. Pharmacol.* 9, 228. doi: 10.3389/fphar.2018.00228

Akl, M. A., Ismael, H. R., Abd Allah, F. I., Kassem, A. A., and Samy, A. M. (2019). Tolmetin sodium-loaded thermosensitive mucoadhesive liquid suppositories for rectal delivery; strategy to overcome oral delivery drawbacks. *Drug Dev. Ind. Pharm.* 45 (2), 252–264. doi: 10.1080/03639045.2018.1534858

Albenberg, L. G., and Wu, G. D. (2014). Diet and the intestinal microbiome: associations, functions, and implications for health and disease. *Gastroenterology* 146 (6), 1564–1572. doi: 10.1053/j.gastro.2014.01.058

Allen, L. V., Popovich, N. G., and Ansel, H. C. (2011). *Ansel's pharmaceutical dosage forms and drug delivery systems*. 9th edn. Philadelphia: Lippincott Williams & Wilkins.

Antoni, L., Nuding, S., Wehkamp, J., and Stange, E. F. (2014). Intestinal barrier in inflammatory bowel disease. *World J. Gastroenterol.* 20 (5), 1165–1179. doi: 10.3748/wjg.v20.i5.1165

Arzhavitina, A., and Steckel, H. (2010). Foams for pharmaceutical and cosmetic application. *Int. J. Pharm.* 394 (1–2), 1–17. doi: 10.1016/j.ijpharm.2010.04.028

Barakat, N. S. (2009). In vitro and in vivo characteristics of a thermogelling rectal delivery system of etodolac. *AAPS PharmSci.Tech.* 10 (3), 724–731. doi: 10.1208/s12249-009-9261-y

Bergin, I. L., and Witzmann, F. A. (2013). Nanoparticle toxicity by the gastrointestinal route: evidence and knowledge gaps. *Int. J. Biomed. Nanosci. Nanotechnol.* 3, 1–44. doi: 10.1504/IJBNN.2013.054515

Brown, J., Haines, S., and Wilding, I. R. (1997). Colonic spread of three rectally administered mesalazine (Pentasa) dosage forms in healthy volunteers as assessed by gamma scintigraphy. *Aliment. Pharmacol. Therapeut.* 11 (4), 685–691. doi: 10.1046/j.1365-2036.1997.00193.x

Brunton, L. L., Knollmann, B. C., and Hilal-Dandan, R. (2018). *Goodman & Gilman's: the pharmacological basis of therapeutics*. 13th edn. New York: McGraw-Hill Education.

Campieri, M., Corbelli, C., Gionchetti, P., Brignola, C., Belluzzi, A., Di Febo, G., et al. (1992). Spread and distribution of 5-ASA colonic foam and 5-ASA enema in patients with ulcerative colitis. *Dig. Dis. Sci.* 37 (12), 1890–1897. doi: 10.1007/BF01308084

Cherniakov, I., Domb, A. J., and Hoffman, A. (2015). Self-nano-emulsifying drug delivery systems: an update of the biopharmaceutical aspects. *Expert Opin. Drug Deliv.* 12 (7), 1121–1133. doi: 10.1517/17425247.2015.999038

Choi, H. G., Oh, Y. K., and Kim, C. K. (1998). In situ gelling and mucoadhesive liquid suppository containing acetaminophen: enhanced bioavailability. *Int. J. Pharm.* 165, 23–32. doi: 10.1016/S0378-5173(97)00385-2

Coupe, A. J., Davis, S. S., and Wilding, I. R. (1991). Variation in gastrointestinal transit of pharmaceutical dosage forms in healthy subjects. *Pharmaceut. Res.* 8 (3), 360–364. doi: 10.1023/A:1015849700421

Cu, Y., and Saltzman, W. M. (2008). Controlled surface modification with poly(ethylene) glycol enhances diffusion of PLGA nanoparticles in human cervical mucus. *Mol. Pharmaceut.* 6, 173–181. doi: 10.1021/mp8001254

das Neves, J., Araujo, F., Andrade, F., Michiels, J., Arien, K. K., Vanham, G., et al. (2013). In vitro and ex vivo evaluation of polymeric nanoparticles for vaginal and rectal delivery of the anti-HIV drug dapivirine. *Mol. Pharm.* 10 (7), 2793–2807. doi: 10.1021/mp4002365

de Boer, A. G., Moolenaar, F., de Leede, L. G., and Breimer, D. D. (1982). Rectal drug administration: clinical pharmacokinetic considerations. *Clin. Pharmacokinet.* 7 (4), 285–311. doi: 10.2165/00003088-198207040-00002

De Boer, A. G., De Leede, L. G., and Breimer, D. D. (1984). Drug absorption by sublingual and rectal routes. *Br. J. Anaesth.* 56 (1), 69–82. doi: 10.1093/bja/56.1.69

Din, F. U., Mustapha, O., Kim, D. W., Rashid, R., Park, J. H., Choi, J. Y., et al. (2015). Novel dual-reverse thermosensitive solid lipid nanoparticle-loaded hydrogel for rectal administration of flurbiprofen with improved bioavailability and reduced initial burst effect. *Eur. J. Pharm. Biopharm.* 94, 64–72. doi: 10.1016/j.ejpb.2015.04.019

Din, F. U., Choi, J. Y., Kim, D. W., Mustapha, O., Kim, D. S., Thapa, R. K., et al. (2017). Irinotecan-encapsulated double-reverse thermosensitive nanocarrier system for rectal administration. *Drug Deliv.* 24 (1), 502–510. doi: 10.1080/10717544.2016.1272651

Dujovny, N., Quiros, R. M., and Saclarides, T. J. (2004). Anorectal anatomy and embryology. *Surg. Oncol. Clin. North Am.* 13 (2), 277–293. doi: 10.1016/j.soc.2004.01.002

Ermund, A., Schutte, A., Johansson, M. E., Gustafsson, J. K., and Hansson, G. C. (2013). Studies of mucus in mouse stomach, small intestine, and colon. I. Gastrointestinal mucus layers have different properties depending on location as well as over the Peyer's patches. *Am. J. Physiol. Gastrointest. Liver Physiol.* 305 (5), G341–G347. doi: 10.1152/ajpgi.00046.2013

Evans, D. F., Pye, G., Bramley, R., Clark, A. G., Dyson, T. J., and Hardcastle, J. D. (1988). Measurement of gastrointestinal pH profiles in normal ambulant human subjects. *Gut* 29 (8), 1035–1041. doi: 10.1136/gut.29.8.1035

Fakhar Ud, D., and Khan, G. M. (2019). Development and characterisation of levosulpiride-loaded suppositories with improved bioavailability in vivo. *Pharm. Dev. Technol.* 24 (1), 63–69. doi: 10.1080/10837450.2017.1419256

Gross, V., Bar-Meir, S., Lavy, A., Mickisch, O., Tulassay, Z., Pronai, L., et al. (2006). Budesonide foam versus budesonide enema in active ulcerative proctitis and proctosigmoiditis. *Aliment. Pharmacol. Therapeut.* 1523 (2), 303–312. doi: 10.1111/j.1365-2036.2006.02743.x

Grover, M., Kanazawa, M., Palsson, O. S., Chitkara, D. K., Gangarosa, L. M., Drossman, D. A., et al. (2008). Small intestinal bacterial overgrowth in irritable bowel syndrome: association with colon motility, bowel symptoms, and psychological distress. *Neurogastroenterol. Motil.* 20 (9), 998–1008. doi: 10.1111/j.1365-2982.2008.01142.x

Gugulothu, D., Pathak, S., Suryavanshi, S., Sharma, S., and Patravale, V. (2010). Self-microemulsifiyng suppository formulation of beta-artemether. *AAPS PharmSciTech.* 11 (3), 1179–1184. doi: 10.1208/s12249-010-9478-9

Gupta, S., Kesarla, R., and Omri, A. (2013). Formulation strategies to improve the bioavailability of poorly absorbed drugs with special emphasis on self-emulsifying systems. *ISRN Pharmaceut.* 2013, 848043. doi: 10.1155/2013/848043

Ham, A. S., and Buckheit, R. W., Jr. (2017). Designing and developing suppository formulations for anti-HIV drug delivery. *Ther. Deliv.* 8 (9), 805–817. doi: 10.4155/tde-2017-0056

Hare, J. I., Lammers, T., Ashford, M. B., Puri, S., Storm, G., and Barry, S. T. (2017). Challenges and strategies in anti-cancer nanomedicine development: an industry perspective. *Adv. Drug Deliv. Rev.* 108, 25–38. doi: 10.1016/j.addr.2016.04.025

Hatton, G. B., Madla, C. M., Rabbie, S. C., and Basit, A. W. (2018). All disease begins in the gut: influence of gastrointestinal disorders and surgery on oral drug performance. *Int. J. Pharm.* 548 (1), 408–422. doi: 10.1016/j.ijpharm.2018.06.054

Hatton, G. B., Madla, C. M., Rabbie, S. C., and Basit, A. W. (2019). Gut reaction: impact of systemic diseases on gastrointestinal physiology and drug absorption. *Drug Discov. Today* 24 (2), 417–427. doi: 10.1016/j.drudis.2018.11.009

Hayashi, M., Tomita, M., and Awazu, S. (1997). Transcellular and paracellular contribution to transport processes in the colorectal route. *Adv. Drug Deliv. Rev.* 28, 191–204. doi: 10.1016/S0169-409X(97)00072-0

Helander, H. F., and Fandriks, L. (2014). Surface area of the digestive tract—revisited. *Scand. J. Gastroenterol.* 49 (6), 681–689. doi: 10.3109/00365521.2014.898326

Homayun, B., Lin, X., and Choi, H. J. (2019). Challenges and recent progress in oral drug delivery systems for biopharmaceuticals. *Pharmaceutics* 11 (3), 129. doi: 10.3390/pharmaceutics11030129

Hoque, K. M., Chakraborty, S., Sheikh, I. A., and Woodward, O. M. (2012). New advances in the pathophysiology of intestinal ion transport and barrier function in diarrhea and the impact on therapy. *Expert. Rev. Anti-infect. Ther.* 10 (6), 687–699. doi: 10.1586/eri.12.47

Hua, S., Marks, E., Schneider, J. J., and Keely, S. (2015). Advances in oral nano-delivery systems for colon targeted drug delivery in inflammatory bowel disease: selective targeting to diseased versus healthy tissue. *Nanomedicine* 11 (5), 1117–1132. doi: 10.1016/j.nano.2015.02.018

Hua, S., de Matos, M. B. C., Metselaar, J. M., and Storm, G. (2018). Current trends and challenges in the clinical translation of nanoparticulate nanomedicines: pathways for translational development and commercialization. *Front. Pharmacol.* 9, 790. doi: 10.3389/fphar.2018.00790

Ivanova, N. A., Trapani, A., Franco, C. D., Mandracchia, D., Trapani, G., Franchini, C., et al. (2019). In vitro and ex vivo studies on diltiazem hydrochloride-loaded microsponges in rectal gels for chronic anal fissures treatment. *Int. J. Pharm.* 25557, 53–65. doi: 10.1016/j.ijpharm.2018.12.039

Jannin, V., Lemagnen, G., Gueroult, P., Larrouture, D., and Tuleu, C. (2014). Rectal route in the 21st Century to treat children. *Adv. Drug Deliv. Rev.* 73, 34–49. doi: 10.1016/j.addr.2014.05.012

Jantzen, J. P., Tzanova, I., Witton, P. K., and Klein, A. M. (1989). Rectal pH in children. *Can. J. Anaesth.* 36 (6), 665–667. doi: 10.1007/BF03005418

Johansson, M. E., Sjovall, H., and Hansson, G. C. (2013). The gastrointestinal mucus system in health and disease. *Nat. Rev. Gastroenterol. Hepatol.* 10 (6), 352–361. doi: 10.1038/nrgastro.2013.35

Kaewnopparat, N., Kaewnopparat, S., Rojanarat, W., and Ingkatawornwong, S. (2004). Enhanced release of diazepam from hollow-type suppositories. *Int. J. Pharm. Compd.* 8 (4), 310–312.

Kamel, R., Basha, M., and Abd El-Alim, S. H. (2013). Development of a novel vesicular system using a binary mixture of sorbitan monostearate and polyethylene glycol fatty acid esters for rectal delivery of rutin. *J. Liposome Res.* 23 (1), 28–36. doi: 10.3109/08982104.2012.727422

Karamanidou, T., Bourganis, V., Kammona, O., and Kiparissides, C. (2016). Lipid-based nanocarriers for the oral administration of biopharmaceutics. *Nanomedic. (Lond).* 11 (22), 3009–3032. doi: 10.2217/nnm-2016-0265

Kararli, T. T. (1995). Comparison of the gastrointestinal anatomy, physiology, and biochemistry of humans and commonly used laboratory animals. *Biopharm. Drug Dispos.* 16 (5), 351–380. doi: 10.1002/bdd.2510160502

Kauss, T., Gaubert, A., Tabaran, L., Tonelli, G., Phoeung, T., Langlois, M. H., et al. (2018). Development of rectal self-emulsifying suspension of a moisture-labile water-soluble drug. *Int. J. Pharm.* 536 (1), 283–291. doi: 10.1016/j.ijpharm.2017.11.067

Kim, J. Y., and Ku, Y. S. (2000). Enhanced absorption of indomethacin after oral or rectal administration of a self-emulsifying system containing indomethacin to rats. *Int. J. Pharm.* 194 (1), 81–89. doi: 10.1016/S0378-5173(99)00367-1

Koffi, A. A., Agnely, F., Besnard, M., Kablan Brou, J., Grossiord, J. L., and Ponchel, G. (2008). In vitro and in vivo characteristics of a thermogelling and bioadhesive delivery system intended for rectal administration of quinine in children. *Eur. J. Pharm. Biopharm.* 69 (1), 167–175. doi: 10.1016/j.ejpb.2007.09.017

Konturek, P. C., Brzozowski, T., and Konturek, S. J. (2011). Stress and the gut: pathophysiology, clinical consequences, diagnostic approach and treatment options. *J. Physiol. Pharmacol.* 62 (6), 591–599.

Kowari, K., Hirosawa, I., Kurai, H., Utoguchi, N., Fujii, M., and Watanabe, Y. (2002). Pharmacokinetics and pharmacodynamics of human chorionic gonadotropin (hCG) after rectal administration of hollow-type suppositories containing hCG. *Biol. Pharm. Bull.* 25 (5), 678–681. doi: 10.1248/bpb.25.678

Lai, S. K., Wang, Y. Y., and Hanes, J. (2009). Mucus-penetrating nanoparticles for drug and gene delivery to mucosal tissues. *Adv. Drug Deliv. Rev.* 61 (2), 158–171. doi: 10.1016/j.addr.2008.11.002

Lamprecht, A. (2010). IBD: selective nanoparticle adhesion can enhance colitis therapy. *Nat. Rev. Gastroenterol. Hepatol.* 7 (6), 311–312. doi: 10.1038/nrgastro.2010.66

Lee, F. I., Jewell, D. P., Mani, V., Keighley, M. R., Kingston, R. D., Record, C. O., et al. (1996). A randomised trial comparing mesalazine and prednisolone foam enemas in patients with acute distal ulcerative colitis. *Gut* 38 (2), 229–233. doi: 10.1136/gut.38.2.229

Lehr, C. M., Bouwstra, J. A., Tukker, J. J., and Junginger, H. E. (1990). Intestinal transit of bioadhesive microspheres in an in situ loop in the rat: a comparative study with copolymers and blends based on poly(acrylic acid). *J. Control Release* 13, 51–62. doi: 10.1016/0168-3659(90)90074-4

Leppik, I. E., and Patel, S. I. (2015). Intramuscular and rectal therapies of acute seizures. *Epilepsy Behav.* 49, 307–312. doi: 10.1016/j.yebeh.2015.05.001

Li, A. C., and Thompson, R. P. (2003). Basement membrane components. *J. Clin. Pathol.* 56 (12), 885–887. doi: 10.1136/jcp.56.12.885

Linakis, M. W., Roberts, J. K., Lala, A. C., Spigarelli, M. G., Medlicott, N. J., Reith, D. M., et al. (2016). Challenges associated with route of administration in neonatal drug delivery. *Clin. Pharmacokinet.* 55 (2), 185–196. doi: 10.1007/s40262-015-0313-z

Liu, Y., Wang, X., Liu, Y., and Di, X. (2018). Thermosensitive in situ gel based on solid dispersion for rectal delivery of ibuprofen. *AAPS PharmSciTech.* 19 (1), 338–347. doi: 10.1208/s12249-017-0839-5

Lo, Y. L., Lin, Y., and Lin, H. R. (2013). Evaluation of epirubicin in thermogelling and bioadhesive liquid and solid suppository formulations for rectal administration. *Int. J. Mol. Sci.* 15 (1), 342–360. doi: 10.3390/ijms15010342

Loew, B. J., and Siegel, C. A. (2012). Foam preparations for the treatment of ulcerative colitis. *Curr. Drug Deliv.* 9 (4), 338–344. doi: 10.2174/156720112801323062

MacDermott, R. P., Donaldson, R. M., Jr., and Trier, J. S. (1974). Glycoprotein synthesis and secretion by mucosal biopsies of rabbit colon and human rectum. *J. Clin. Invest.* 54, 545–554. doi: 10.1172/JCI107791

Macfarlane, G. T., and Macfarlane, S. (2011). Fermentation in the human large intestine: its physiologic consequences and the potential contribution of prebiotics. *J. Clin. Gastroenterol.* 45 Suppl, S120–S127. doi: 10.1097/MCG.0b013e31822fecfe

Madara, J. L. (1998). Regulation of the movement of solutes across tight junctions. *Annu. Rev. Physiol.* 60, 143–159. doi: 10.1146/annurev.physiol.60.1.143

Maisel, K., Chattopadhyay, S., Moench, T., Hendrix, C., Cone, R., Ensign, L. M., et al. (2015). Enema ion compositions for enhancing colorectal drug delivery. *J. Control Release* 209, 280–287. doi: 10.1016/j.jconrel.2015.04.040

Maisel, K., Ensign, L., Reddy, M., Cone, R., and Hanes, J. (2015). Effect of surface chemistry on nanoparticle interaction with gastrointestinal mucus and distribution in the gastrointestinal tract following oral and rectal administration in the mouse. *J. Control Release* 197, 48–57. doi: 10.1016/j.jconrel.2014.10.026

Marieb, E. N., and Hoehn, K. (2010). *Human anatomy and physiology*. 8th edn. USA: Pearson Benjamin Cummings.

Martinez, M. N., and Amidon, G. L. (2002). A mechanistic approach to understanding the factors affecting drug absorption: a review of fundamentals. *J. Clin. Pharmacol.* 42 (6), 620–643. doi: 10.1177/00970002042006005

Matsumoto, Y., Watanabe, Y., Tojima, T., Murakoshi, R., Murakami, C., and Matsumoto, M. (1989). Rectal absorption enhancement of gentamicin in rabbits from hollow type suppositories by sodium salicylate or sodium caprylate. *Drug Des. Deliv.* 4 (3), 247–256.

Matsumoto, A., Murakami, K., Watanabe, C., and Murakami, M. (2017). Improved systemic delivery of insulin by condensed drug loading in a dimpled suppository. *Drug Discov. Therapeut.* 11 (6), 293–299. doi: 10.5582/ddt.2017.01072

Melo, M., Nunes, R., Sarmento, B., and das Neves, J. (2019). Colorectal distribution and retention of polymeric nanoparticles following incorporation into a thermosensitive enema. *Biomater. Sci.* 7, 3801–3811. doi: 10.1039/C9BM00759H

Mesquita, L., Galante, J., Nunes, R., Sarmento, B., and das Neves, J. (2019). Pharmaceutical vehicles for vaginal and rectal administration of anti-HIV microbicide nanosystems. *Pharmaceutics* 11 (3), 145. doi: 10.3390/pharmaceutics11030145

Miyazaki, S., Suisha, F., Kawasaki, N., Shirakawa, M., Yamatoya, K., and Attwood, D. (1998). Thermally reversible xyloglucan gels as vehicles for rectal drug delivery. *J. Control Release* 56 (1–3), 75–83. doi: 10.1016/S0168-3659(98)00079-0

Moawad, F. A., Ali, A. A., and Salem, H. F. (2017). Nanotransfersomes-loaded thermosensitive in situ gel as a rectal delivery system of tizanidine HCl: preparation, in vitro and in vivo performance. *Drug Deliv.* 24 (1), 252–260. doi: 10.1080/10717544.2016.1245369

Mohamed, R. A., Abass, H. A., Attia, M. A., and Heikal, O. A. (2013). Formulation and evaluation of metoclopramide solid lipid nanoparticles for rectal suppository. *J. Pharm. Pharmacol.* 65 (11), 1607–1621. doi: 10.1111/jphp.12136

Mule, F., Amato, A., and Serio, R. (2010). Gastric emptying, small intestinal transit and fecal output in dystrophic (mdx) mice. *J. Physiol. Sci.* 60 (1), 75–79. doi: 10.1007/s12576-009-0060-8

Muranishi, S. (1984). Characteristics of drug absorption via the rectal route. *Methods Find. Exp. Clin. Pharmacol.* 6 (12), 763–772.

Nehoff, H., Parayath, N. N., Domanovitch, L., Taurin, S., and Greish, K. (2014). Nanomedicine for drug targeting: strategies beyond the enhanced permeability and retention effect. *Int. J. Nanomed.* 9, 2539–2555. doi: 10.2147/IJN.S47129

Nunes, R., Sarmento, B., and das Neves, J. (2014). Formulation and delivery of anti-HIV rectal microbicides: advances and challenges. *J. Control Release* 28194, 278–294. doi: 10.1016/j.jconrel.2014.09.013

Nunes, R., Araujo, F., Barreiros, L., Bartolo, I., Segundo, M. A., Taveira, N., et al. (2018). Noncovalent PEG coating of nanoparticle drug carriers improves the local pharmacokinetics of rectal anti-HIV microbicides. *ACS Appl. Mater. Interface* 10 (41), 34942–34953. doi: 10.1021/acsami.8b12214

Nystrom, A. M., and Fadeel, B. (2012). Safety assessment of nanomaterials: implications for nanomedicine. *J. Control Release* 161 (2), 403–408. doi: 10.1016/j.jconrel.2012.01.027

Padmanabhan, P., Grosse, J., Asad, A. B., Radda, G. K., and Golay, X. (2013). Gastrointestinal transit measurements in mice with 99mTc-DTPA-labeled activated charcoal using NanoSPECT-CT. *EJNMMI Res.* 3 (1), 60. doi: 10.1186/2191-219X-3-60

Petkova, R., Tcholakova, S., and Denkov, N. D. (2012). Foaming and foam stability for mixed polymer-surfactant solutions: effects of surfactant type and polymer charge. *Langmuir* 28 (11), 4996–5009. doi: 10.1021/la3003096

Politova, N., Tcholakova, S., Golemanov, K., Denkov, N. D., Vethamuthu, M., and Ananthapadmanabhan, K. P. (2012). Effect of cationic polymers on foam rheological properties. *Langmuir* 28 (2), 1115–1126. doi: 10.1021/la2035517

Pullan, R. D., Thomas, G. A., Rhodes, M., Newcombe, R. G., Williams, G. T., Allen, A., et al. (1994). Thickness of adherent mucus gel on colonic mucosa in humans and its relevance to colitis. *Gut* 35 (3), 353–359. doi: 10.1136/gut.35.3.353

Purohit, T. J., Hanning, S. M., and Wu, Z. (2018). Advances in rectal drug delivery systems. *Pharm. Dev. Technol.* 23 (10), 942–952. doi: 10.1080/10837450.2018.1484766

Qi, H., Li, L., Huang, C., Li, W., and Wu, C. (2006). Optimization and physicochemical characterization of thermosensitive poloxamer gel containing puerarin for ophthalmic use. *Chem. Pharm. Bull. (Tokyo).* 54 (11), 1500–1507. doi: 10.1248/cpb.54.1500

Rao, K. A., Yazaki, E., Evans, D. F., and Carbon, R. (2004). Objective evaluation of small bowel and colonic transit time using pH telemetry in athletes with gastrointestinal symptoms. *Br. J. Sports Med.* 38 (4), 482–487. doi: 10.1136/bjsm.2003.006825

Reinus, J. F., and Simon, D. (2014). *Gastrointestinal anatomy and physiology: the essentials*. (West Sussex, UK: John Wiley & Sons) doi: 10.1002/9781118833001

Ryu, J. M., Chung, S. J., Lee, M. H., and Kim, C. K. (1999). ShimCk. Increased bioavailability of propranolol in rats by retaining thermally gelling liquid suppositories in the rectum. *J. Control Release* 59 (2), 163–172. doi: 10.1016/S0168-3659(98)00189-8

Sandborn, W. J., Bosworth, B., Zakko, S., Gordon, G. L., Clemmons, D. R., Golden, P. L., et al. (2015). Budesonide foam induces remission in patients with mild to moderate ulcerative proctitis and ulcerative proctosigmoiditis. *Gastroenterology* 148 (4), 740–50 e2. doi: 10.1053/j.gastro.2015.01.037

Sandri, G., Bonferoni, M. C., Ferrari, F., Rossi, S., and Caramella, C. M. (2014). *The role of particle size in drug release and absorption*. Merkus H, Meesters G, editors. (Switzerland: Springer) doi: 10.1007/978-3-319-00714-4_11

Sartor, R. B. (2008). Microbial influences in inflammatory bowel diseases. *Gastroenterology* 134 (2), 577–594. doi: 10.1053/j.gastro.2007.11.059

Sathyan, G., Hwang, S., and Gupta, S. K. (2000). Effect of dosing time on the total intestinal transit time of non-disintegrating systems. *Int. J. Pharm.* 204 (1–2), 47–51. doi: 10.1016/S0378-5173(00)00472-5

Savjani, K. T., Gajjar, A. K., and Savjani, J. K. (2012). Drug solubility: importance and enhancement techniques. *ISRN Pharmaceut.* 2012, 195727. doi: 10.5402/2012/195727

Schmidt, C., Lautenschlaeger, C., Collnot, E. M., Schumann, M., Bojarski, C., Schulzke, J. D., et al. (2013). Nano- and microscaled particles for drug targeting to inflamed intestinal mucosa: a first in vivo study in human patients. *J. Control Release* 28165 (2), 139–145. doi: 10.1016/j.jconrel.2012.10.019

Seo, Y. G., Kim, D. W., Yeo, W. H., Ramasamy, T., Oh, Y. K., Park, Y. J., et al. (2013). Docetaxel-loaded thermosensitive and bioadhesive nanomicelles as a rectal drug delivery system for enhanced chemotherapeutic effect. *Pharmaceut. Res.* 30 (7), 1860–1870. doi: 10.1007/s11095-013-1029-0

Sercombe, L., Veerati, T., Moheimani, F., Wu, S. Y., Sood, A. K., and Hua, S. (2015). Advances and challenges of liposome assisted drug delivery. *Front. Pharmacol.* 6, 286. doi: 10.3389/fphar.2015.00286

Shafik, A., Mostafa, R. M., Shafik, I., Ei-Sibai, O., and Shafik, A. A. (2006). Functional activity of the rectum: a conduit organ or a storage organ or both? *World J. Gastroenterol.* 12 (28), 4549–4552. doi: 10.3748/wjg.v12.i28.4549

Shajari, N., Mansoori, B., Davudian, S., Mohammadi, A., and Baradaran, B. (2017). Overcoming the challenges of siRNA delivery: nanoparticle strategies. *Curr. Drug Deliv.* 14 (1), 36–46. doi: 10.2174/1567201813666160816105408

Shi, Y., Xue, J., Sang, Y., Xu, X., and Shang, Q. (2019). Insulin-loaded hydroxypropyl methyl cellulose-co-polyacrylamide-co-methacrylic acid hydrogels used as rectal suppositories to regulate the blood glucose of diabetic rats. *Int. J. Biol. Macromol.* 121, 1346–1353. doi: 10.1016/j.ijbiomac.2018.09.044

Shiohira, H., Fujii, M., Koizumi, N., Kondoh, M., and Watanabe, Y. (2009). Novel chronotherapeutic rectal aminophylline delivery system for therapy of asthma. *Int. J. Pharm.* 379 (1), 119–124. doi: 10.1016/j.ijpharm.2009.06.017

Shreya, A. B., Raut, S. Y., Managuli, R. S., Udupa, N., and Mutalik, S. (2018). Active targeting of drugs and bioactive molecules via oral administration by ligand-conjugated lipidic nanocarriers: recent advances. *AAPS PharmSciTech.* 20 (1), 15. doi: 10.1208/s12249-018-1262-2

Siczek, K., Fichna, J., Zatorski, H., Karolewicz, B., Klimek, L., and Owczarek, A. (2018). Development of the rectal dosage form with silver-coated glass beads for local-action applications in lower sections of the gastrointestinal tract. *Pharm. Dev. Technol.* 23 (3), 295–300. doi: 10.1080/10837450.2017.1359843

Talkar, S., Dhoble, S., Majumdar, A., and Patravale, V. (2018). Transmucosal nanoparticles: toxicological overview. *Adv. Exp. Med. Biol.* 1048, 37–57. doi: 10.1007/978-3-319-72041-8_3

Tang, B. C., Dawson, M., Lai, S. K., Wang, Y. Y., Suk, J. S., Yang, M., et al. (2009). Biodegradable polymer nanoparticles that rapidly penetrate the human mucus barrier. *Proc. Natl. Acad. Sci. U. S. A.* 106 (46), 19268–19273. doi: 10.1073/pnas.0905998106

Turner, C., Aye Mya Thein, N., Turner, P., Nosten, F., and White, N. J. (2012). Rectal pH in well and unwell infants. *J. Trop. Pediatr.* 58 (4), 311–313. doi: 10.1093/tropej/fmr088

Uekama, K., Kondo, T., Nakamura, K., Irie, T., Arakawa, K., Shibuya, M., et al. (1995). Modification of rectal absorption of morphine from hollow-type suppositories with a combination of alpha-cyclodextrin and viscosity-enhancing polysaccharide. *J. Pharm. Sci.* 84 (1), 15–20. doi: 10.1002/jps.2600840106

van Hoogdalem, E., de Boer, A. G., and Breimer, D. D. (1991). Pharmacokinetics of rectal drug administration, part I. General considerations and clinical applications of centrally acting drugs. *Clin. Pharmacokinet.* 21 (1), 11–26. doi: 10.2165/00003088-199121010-00002

Vita, A. A., Royse, E. A., and Pullen, N. A. (2019). Nanoparticles and danger signals: oral delivery vehicles as potential disruptors of intestinal barrier homeostasis. *J. Leukocyte Biol.* 106 (1), 95–103. doi: 10.1002/JLB.3MIR1118-414RR

Vueba, M. L., Batista de Carvalho, L. A., Veiga, F., Sousa, J. J., and Pina, M. E. (2006). Influence of cellulose ether mixtures on ibuprofen release: MC25, HPC and HPMC K100M. *Pharm. Dev. Technol.* 11 (2), 213–228. doi: 10.1080/10837450600561349

Watanabe, Y., Matsumoto, Y., Baba, K., and Matsumoto, M. (1986). Pharmaceutical evaluation of hollow type suppositories. IV. Improvement of bioavailability of propranolol in rabbits after rectal administration. *J. Pharmacobiodyn.* 9 (6), 526–531. doi: 10.1248/bpb1978.9.526

Watanabe, Y., Tone, Y., Nishihara, S., and Matsumoto, M. (1986). Pharmaceutical evaluation of hollow type suppositories. V. Preparation of valproic acid suppository and rectal absorption of valproic acid in rabbits. *J. Pharmacobiodyn.* 9 (12), 953–961. doi: 10.1248/bpb1978.9.953

Watanabe, Y., Mizufune, Y., Kubomura, A., Kiriyama, M., Utoguchi, N., and Matsumoto, M. (1998). Studies of drug delivery systems for a therapeutic agent used in osteoporosis. I. Pharmacodynamics (hypocalcemic effect) of elcatonin in rabbits following rectal administration of hollow-type suppositories containing elcatonin. *Biol. Pharm. Bull.* 21 (11), 1187–1190. doi: 10.1248/bpb.21.1187

Watts, P. J., Barrow, L., Steed, K. P., Wilson, C. G., Spiller, R. C., Melia, C. D., et al. (1992). The transit rate of different-sized model dosage forms through the human colon and the effects of a lactulose-induced catharsis. *Int. J. Pharm.* 87, 215–221. doi: 10.1016/0378-5173(92)90245-W

Woody, R. C., Golladay, E. S., and Fiedorek, S. C. (1989). Rectal anticonvulsants in seizure patients undergoing gastrointestinal surgery. *J. Pediatr. Surg.* 24 (5), 474–477. doi: 10.1016/S0022-3468(89)80405-1

Xu, J., Tam, M., Samaei, S., Lerouge, S., Barralet, J., Stevenson, M. M., et al. (2017). Mucoadhesive chitosan hydrogels as rectal drug delivery vessels to treat ulcerative colitis. *Acta Biomater.* 48, 247–257. doi: 10.1016/j.actbio.2016.10.026

Ye, X., Yin, H., Lu, Y., Zhang, H., and Wang, H. (2016). Evaluation of hydrogel suppositories for delivery of 5-aminolevulinic acid and hematoporphyrin monomethyl ether to rectal tumors. *Molecules* 21 (10), 1347. doi: 10.3390/molecules21101347

Yong, C. S., Choi, J. S., Quan, Q. Z., Rhee, J. D., Kim, C. K., Lim, S. J., et al. (2001). Effect of sodium chloride on the gelation temperature, gel strength and bioadhesive force of poloxamer gels containing diclofenac sodium. *Int. J. Pharm.* 226 (1–2), 195–205. doi: 10.1016/S0378-5173(01)00809-2

Yun, M. O., Choi, H. G., Jung, J. H., and Kim, C. K. (1999). Development of a thermo-reversible insulin liquid suppository with bioavailability enhancement. *Int. J. Pharm.* 189, 137–145. doi: 10.1016/S0378-5173(99)00227-6

Zhang, S., Langer, R., and Traverso, G. (2017). Nanoparticulate drug delivery systems targeting inflammation for treatment of inflammatory bowel disease. *Nano Today.* 16, 82–96. doi: 10.1016/j.nantod.2017.08.006

Conflict of Interest: The author declares that the research was conducted in the absence of any commercial or financial relationships that could be construed as a potential conflict of interest.

frontiers in Pharmacology

MINI REVIEW
published: 05 November 2019
doi: 10.3389/fphar.2019.01328

Advances in Nanoparticulate Drug Delivery Approaches for Sublingual and Buccal Administration

Susan Hua[1,2]*

[1] Therapeutic Targeting Research Group, School of Biomedical Sciences and Pharmacy, University of Newcastle, Callaghan, NSW, Australia, [2] Hunter Medical Research Institute, New Lambton Heights, NSW, Australia

The sublingual and buccal routes of administration have significant advantages for both local and systemic drug delivery. They have shown to be an effective alternative to the traditional oral route, especially when fast onset of action is required. Drugs can be rapidly and directly absorbed into the systemic circulation *via* venous drainage to the superior vena cava. Therefore, they are useful for drugs that undergo high hepatic clearance or degradation in the gastrointestinal tract, and for patients that have swallowing difficulties. Drugs administered *via* the sublingual and buccal routes are traditionally formulated as solid dosage forms (e.g., tablets, wafers, films, and patches), liquid dosage forms (e.g., sprays and drops), and semi-solid dosage forms (e.g., gels). Conventional dosage forms are commonly affected by physiological factors, which can reduce the contact of the formulation with the mucosa and lead to unpredictable drug absorption. There have been a number of advances in formulation development to improve the retention and absorption of drugs in the buccal and sublingual regions. This review will focus on the physiological aspects that influence buccal and sublingual drug delivery and the advances in nanoparticulate drug delivery approaches for sublingual and buccal administration. The clinical development pipeline with formulations approved and in clinical trials will also be addressed.

Keywords: buccal, sublingual, drug delivery, mucosal, formulation, nanoparticles, physiological factors, translation

OPEN ACCESS

Edited by:
Paul Chi-Lui Ho, National University of Singapore, Singapore

Reviewed by:
Joshua Boateng, University of Greenwich, United Kingdom
Nadeem Irfan Bukhari, University of the Punjab, Pakistan

***Correspondence:**
Susan Hua
Susan.Hua@newcastle.edu.au

Specialty section:
This article was submitted to Experimental Pharmacology and Drug Discovery, a section of the journal Frontiers in Pharmacology

Received: *14 August 2019*
Accepted: *15 October 2019*
Published: *05 November 2019*

Citation:
Hua S (2019) Advances in Nanoparticulate Drug Delivery Approaches for Sublingual and Buccal Administration. Front. Pharmacol. 10:1328. doi: 10.3389/fphar.2019.01328

INTRODUCTION

Drugs are generally administered in the oral cavity to either treat local conditions (e.g., infections and ulcers) or for the systemic absorption of drugs. In particular, the sublingual and buccal mucosal regions are highly vascularized and, therefore, are useful for systemic drug delivery. Sublingual administration involves placing a drug under the tongue and buccal administration involves placing a drug between the gums and cheek. The sublingual and buccal routes are considered promising alternatives to the traditional oral route for drug delivery.

Figure 1 shows a schematic diagram of the sublingual and buccal regions in the oral cavity. The oral cavity has a relatively neutral pH of approximately 6.2–7.4 and has limited enzymatic activity. The surface area of the oral mucosa is relatively small (100–200 cm^2), with the sublingual and buccal regions having an estimated surface area of 26.5 ± 4.2 cm^2 and 50.2 ± 2.9 cm^2, respectively (Czerkinsky and Holmgren, 2012; Kraan et al., 2014). These regions in the oral cavity are lined by non-keratinized, stratified squamous epithelium that is 100–200 μm and 8–12 cells thick in the sublingual region, and 500–800 μm and 40–50 cells thick in the buccal region (Czerkinsky and Holmgren, 2012; Kraan et al., 2014). Components from the saliva also binds to the surface of the buccal and sublingual epithelium

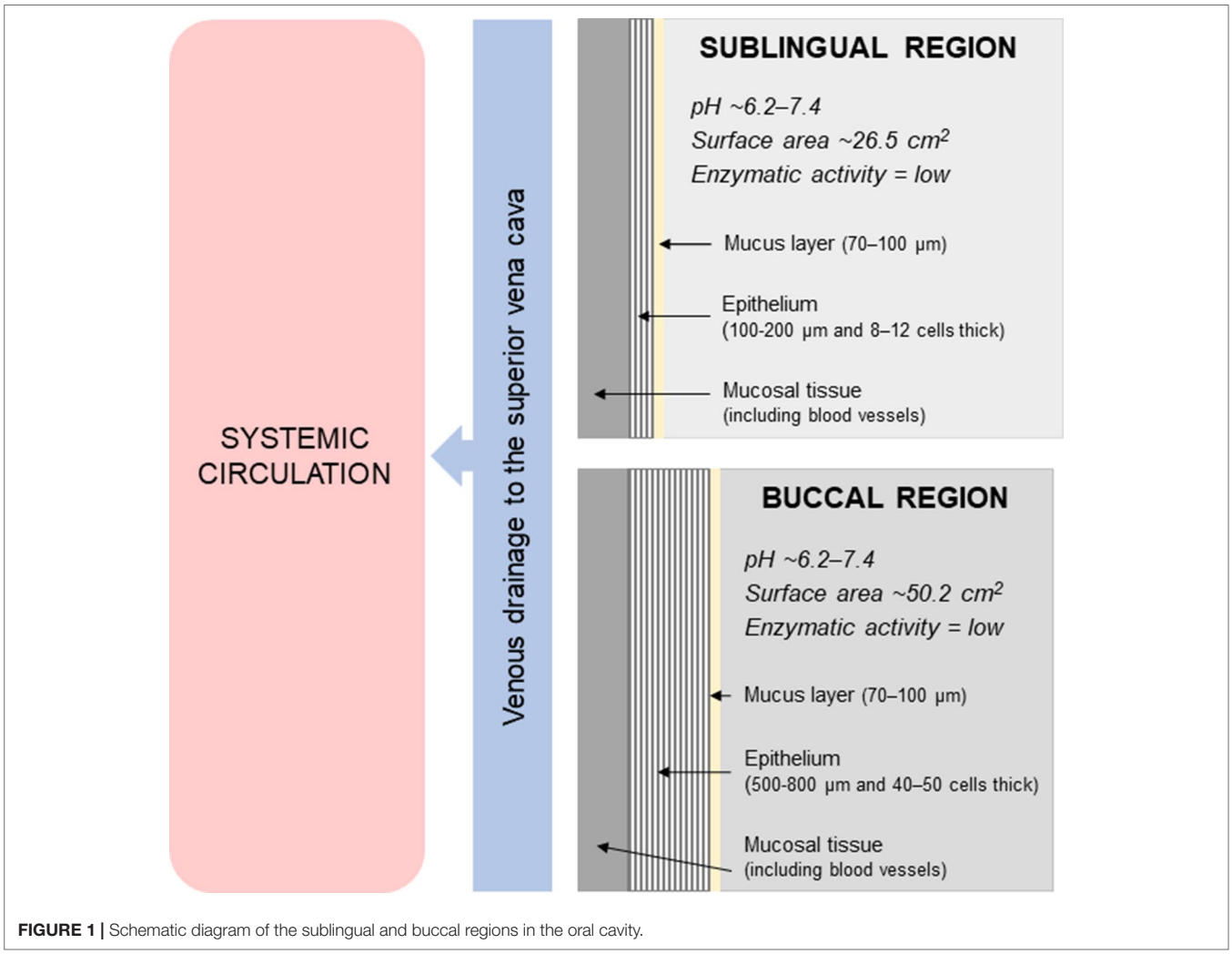

FIGURE 1 | Schematic diagram of the sublingual and buccal regions in the oral cavity.

to create a mucus layer with an average thickness of 70–100 μm (Teubl et al., 2013). Underneath the epithelium is the lamina propria and submucosa that consists of connective tissue with a network of blood vessels, lymphatic vessels and smooth muscles. Drugs can be rapidly and directly absorbed into the systemic circulation *via* venous drainage to the superior vena cava.

A number of advances in drug formulation have been made in the area of sublingual and buccal drug delivery. This review will focus on the physiological aspects that influence buccal and sublingual drug delivery and the advances in nanoparticulate drug delivery approaches for sublingual and buccal administration. The clinical development pipeline with formulations approved and in clinical trials will also be addressed.

ADVANTAGES AND DISADVANTAGES OF THE SUBLINGUAL AND BUCCAL ROUTES FOR DRUG DELIVERY

The sublingual and buccal routes of administration have a number of advantages (De Boer et al., 1984; Allen et al., 2011; Teubl et al., 2013), especially for systemic drug delivery. In general, they produce faster onset of action compared to orally ingested drug formulations. Drug absorption is relatively faster across the sublingual mucosa compared to the buccal mucosa due to the thinner epithelium. In addition to rapid absorption, the portion of drug that is absorbed through the blood vessels directly enters the systemic circulation and bypasses hepatic first-pass metabolic processes. Therefore, this route is particularly useful for highly soluble drugs that undergo high hepatic clearance or decomposition in the gastrointestinal tract. The non-adherent saliva in the buccal and sublingual regions also contains less mucin and limited enzymes (e.g., salivary amylase). Drugs may also be more stable owing to the pH in the mouth being relatively neutral compared to other parts of the gastrointestinal tract. Patients can easily self-administer doses and in most cases the effect of the drug can be quickly terminated, for example, by spitting out or swallowing the tablet. It is also beneficial for patients who suffer from swallowing difficulties.

In terms of disadvantages (De Boer et al., 1984; Allen et al., 2011; Teubl et al., 2013), the sublingual and buccal routes can be inconvenient for patients as it can involve some technical

procedures to maintain the drug in the sublingual or buccal area for absorption without swallowing the drug. Not all drugs can be delivered *via* this route and generally only small doses can be administered. Drugs may also be unpalatable, bitter, or cause irritation to the oral mucosa, which may lead to voluntary expulsion or swallowing. Although the risk is low, there is a chance of accidental aspiration of the medication. Therefore, patients are recommended to be in an upright position when administering a dose. For similar reasons, sublingual or buccal medication should be avoided when a patient is unconscious or uncooperative. Furthermore, the buccal and sublingual routes are generally not suited or preferred for sustained drug release or for prolonged administration due to discomfort or inconvenience, especially when eating or drinking.

PHYSIOLOGICAL FACTORS INFLUENCING SUBLINGUAL AND BUCCAL DRUG DELIVERY

For effective drug delivery *via* the sublingual or buccal route of administration, several physiological factors should be considered in drug formulation design and development. These factors may influence drug bioavailability, stability, efficacy, and safety.

- *Residence time of the formulation:* Absorption is highly dependent on the residence time of the drug in the sublingual and buccal area. This may vary considerably depending on the formulation and the patient. Sublingual and buccal drugs are generally formulated as tablets, films, wafers, or sprays. The formulations differ in terms of need for disintegration and dissolution prior to drug absorption. In addition, patients should avoid eating, drinking, chewing, or swallowing until the medication has been absorbed (De Boer et al., 1984; Allen et al., 2011). Swallowing the medication will decrease the drug's effectiveness. This can be particularly difficult for some patients, such as younger children.
- *Drug absorption:* For effective absorption to occur, the drug needs to have a balance between hydrophilic and lipophilic properties (De Boer et al., 1984; Allen et al., 2011; Brunton et al., 2018). That is, the drug needs to be soluble in aqueous buccal fluids and should also have high lipid solubility to be able to cross the epithelial membrane in these regions, which is usually by passive diffusion. This route is also more suitable for low to medium molecular weight drugs (De Boer et al., 1984; Allen et al., 2011; Brunton et al., 2018)— refer to examples in **Table 1**. In addition, drug absorption can be affected if the gums or mucosal membranes have open sores or areas of inflammation. This may lead to enhanced or irregular drug absorption and, therefore, should be avoided or used with caution. Conversely, smoking can decrease the sublingual or buccal absorption of medications due to vasoconstriction of the blood vessels.
- *pH of the saliva:* The pH of the saliva can affect drug absorption by affecting the ionization state of drugs. Drug molecules predominantly undergo passive absorption pathways *via* transcellular diffusion (through the cell) or paracellular diffusion (between cells), depending on their physicochemical characteristics (De Boer et al., 1984; Allen et al., 2011; Brunton et al., 2018). Transcellular diffusion is the most common mechanism and is usually proportional to the lipid solubility of the drug. Therefore, absorption is favored when the drug molecule is in the non-ionized form, which is much more lipophilic than the ionized form. For sublingual and buccal administration, this means that drugs with a high pKa value are preferred due to the relatively neutral pH of the saliva. Conversely, the paracellular pathway is favored for more hydrophilic or ionized molecules. It should be noted that the pH of the saliva can be temporarily altered by environmental (e.g., foods and drinks) or personal factors [e.g., oral disease (Baliga et al., 2013)], which can affect the sublingual and buccal absorption of drugs.
- *Flow of saliva:* Saliva flow can influence buccal and sublingual drug delivery by altering the rate of disintegration of the formulation and dissolution of the drug. For example, if the mouth is dry, this can negatively affect drug absorption. Conversely, if saliva flow is considerable, this can lead to the drug being swallowed before absorption. Saliva flow can be affected by age, medications (e.g., anticholinergic drugs), and medical conditions (e.g., Sjögren's syndrome, cheilosis, glossodynia, dehydration, dysphagia, and problems with mastication) (Dawes, 1987; von Bultzingslowen et al., 2007).

NANOPARTICULATE DRUG DELIVERY APPROACHES

Nanoparticulate systems have previously been shown to improve the accumulation, uptake, and absorption of drugs across a variety of biological barriers, including the skin (Hua, 2015) and gastrointestinal tract (Hua et al., 2015). Therefore, it was inevitable for nanoparticles to be investigated for sublingual and buccally drug delivery. Nanoparticulate dosage forms differ from conventional dosage forms by loading the drug or active compound into nanoparticles prior to dispersion in a formulation base. They have been incorporated into various dosage forms for sublingual and buccal drug delivery, including gels (Marques et al., 2017), sprays (Baltzley et al., 2018), tablets (Gavin et al., 2015; El-Nahas et al., 2017), films (Giovino et al., 2013; Mortazavian et al., 2014; Al-Dhubiab et al., 2016; Masek et al., 2017; Castro et al., 2018a; Mahdizadeh Barzoki et al., 2018; Al-Nemrawi et al., 2019), and patches (Mahdizadeh Barzoki et al., 2016). These nanoparticulate formulations have been shown to: (i) improve drug permeability across the epithelium; (ii) modify drug release kinetics (e.g., controlled release or sustained release); (iii) provide solubilization (i.e., to deliver compounds which have physicochemical properties that strongly limit their aqueous solubility); and/or (iv) protect compounds that are sensitive to degradation (e.g., peptides) (Morales and Brayden, 2017; Hua et al., 2018). These factors all aim to promote higher sublingual or buccal bioavailability of drugs for subsequent systemic absorption.

TABLE 1 | Sublingual and buccal formulations marketed and in clinical trials

Drug	Dosage form	Indication	Status
Lorazepam	Tablet	Sedation	Marketed *(Ativan)*
Zolpidem	Tablet	Insomnia	Marketed *(Edluar)*
Melatonin	Tablet	Insomnia	Marketed *(Melatonin Sublingual)*
Allergen extract	Tablet	Allergic rhinitis	Marketed *(Grastek, Oralair, Odactra, Ragwitek)*
Polyvalent mechanical bacterial lysate (biological)	Tablet	Chronic obstructive pulmonary disease	Marketed *(Ismigen)*
Isosorbide dinitrate	Tablet	Angina	Marketed *(Isordil)*
Sufentanil	Tablet	Pain	Marketed *(Dsuvia, Zalviso)*
Glyceryl trinitrate (nitroglycerin)	Tablet, spray	Angina	Marketed *(Anginine, Lycinate, Nitrolingual Pump Spray)*
Fentanyl	Tablet, spray, film, lozenge	Pain	Marketed *(Abstral, Actiq, Subsys, Fentora, Onsolis)*
Buprenorphine	Tablet, film	Pain	Marketed *(Temgesic, Belbuca)*
Nicotine	Tablet, film, gum, lozenge, spray	Smoking cessation	Marketed *(Nicabate, Nicotinell, Nicorette, QuitX, Nicaway, Nicabate Oral Strips, Nicorette QuickMist)*
Vitamin B12	Tablet, spray, oral liquid	Vitamin deficiency	Marketed *(Sublingual Vitamin B12)*
Desmopressin	Tablet, wafer	Nocturia	Marketed *(Minirin Melt, Nocdurna)*
Buprenorphine + naloxone	Film	Opioid dependence	Marketed *(Suboxone)*
Asenapine	Wafer	Schizophrenia	Marketed *(Saphris)*
Midazolam	Oral liquid (prefilled oral syringes)	Epilepsy	Marketed *(Buccolam, Epistatus)*
Nystatin	Oral liquid	Oral candidiasis	Marketed *(Nilstat, Mycostatin)*
Miconazole	Gel	Oral candidiasis	Marketed *(Daktarin, Decozol)*
Triamcinolone	Paste	Oral ulceration	Marketed *(Kenalog in Orabase)*
Zolmitriptan	Tablet	Cluster headache	Phase IV
Misoprostol	Tablet	Induction of labor, blood loss in myomectomy, abortion	Phase III/IV
Y-2 (adaravone and borneol)	Tablet	Healthy	Phase I
Alprazolam	Tablet	Anxiety disorder, sedation for endoscopy	Phase I/II/III completed
Riluzole	Tablet	Social anxiety disorder, amyotrophic lateral sclerosis	Phase I/II/III
Lobeline	Tablet	Methamphetamine dependence, Attention deficit disorder	Phase I/II
Cyclobenzaprine	Tablet	PTSD, fibromyalgia	Phase III
Olanzapine	Tablet	Schizophrenia	Phase IV completed
Agomelatine	Tablet	Major depressive disorder	Phase III completed
ALKS 5461	Tablet	Major depressive disorder	Phase III completed
Sildenafil	Tablet, wafer	Erectile dysfunction	Phase III completed
Cannabidiol	Tablet, oral liquid	Diabetic neuropathies, chronic pain, anxiety, inflammatory bowel disease	Phase I/II
Allergen extract (mite, artemisia annua, apple, birch pollen, grass pollen, blatella germanica, milk, peanuts, ragweed)	Oral liquid	Atopic dermatitis, allergic rhinitis, allergic conjunctivitis, food hypersensitivity	Phase I/II/III/IV
Influenza vaccine	Oral liquid	Healthy	Phase I completed
Naloxone	Oral liquid	Chronic pruritus	Phase I/II completed
Ketorolac	Oral liquid	Postoperative pain	Phase IV
Oral enterotoxigenic Escherichia coli vaccine (biological)	Oral liquid	Gastroenteritis Escherichia coli	Phase I
Cholera toxin B subunit (biological)	Oral liquid	Healthy	Phase I completed
UISH001	Oral liquid	Urinary incontinence	Phase I/II completed
Methadone	Oral liquid	Cancer Pain	Phase I completed
Cyclobenzaprine	Oral liquid	Healthy	Phase I completed
Tacrolimus	Oral liquid, powder	Bone marrow transplant, organ transplant, chronic renal failure	Phase IV
Ticagrelor	Powder, tablet	Acute coronary syndrome, percutaneous coronary intervention	Phase IV
Tizanidine	Powder	Muscle spasticity	Phase I/II completed
Polyoxidonium	Spray	Acute respiratory infection	Phase III
Flumazenil	Spray	Healthy	Phase I/II completed
Artemether	Spray	Plasmodium falciparum malaria	Phase III completed
Insulin	Film, spray	Healthy, type 1 diabetes, Type 2 diabetes	Phase I/III

(*Continued*)

TABLE 1 | Continued

Drug	Dosage form	Indication	Status
Ketamine	Film, wafer	Healthy, pain	Phase I/II completed
Dexmedetomidine	Film	Schizophrenia	Phase I
Apomorphine	Film	Parkinson's disease	Phase II/III
Montelukast	Film	Alzheimer disease	Phase II
Diazepam	Film	Epilepsy	Phase III
NTG1523 (nitroglycerin)	Rapid absorbable capsule	Angina pectoris	Phase IV
Ropivacaine	Liposomal gel	Topical anesthesia	Phase I completed

(Ref: clinicaltrials.gov; ema.europa.eu; fda.gov; tga.gov.au; drugs.com).

For nanoparticulate dosage forms to be effective for sublingual or buccal drug delivery, two main factors should be considered. Firstly, the physicochemical properties of the nanoparticles themselves (e.g., size, charge, composition, and surface properties) for optimal interaction with the sublingual or buccal mucosa. A number of different nanoparticulate systems have been evaluated for sublingual and buccal drug delivery, with polymer-based and lipid-based compositions being the most common (He et al., 2009; Roblegg et al., 2012; Teubl et al., 2013; Teubl et al., 2015; Mouftah et al., 2016; Patil and Devarajan, 2016; Chaves et al., 2017; Xu et al., 2018). The composition and structure of nanoparticles can be designed to confer a number of different properties, including mucoadhesion, bioadhesion, mucus-penetration, controlled release, and deformability (Hua et al., 2015). For example, inclusion of a hydrophilic polyethylene glycol (PEG) coating to the surface of nanoparticles has been shown to reduce its interaction with the mucus constituents, increase particle translocation through the mucus and mucosa, and enhance its delivery into lymph nodes (Wang et al., 2008; Hua et al., 2015; Masek et al., 2017).

In terms of optimal nanoparticle size for sublingual or buccal administration, most of the studies in this area have used nanoparticles between approximately 100 to 300 nm in size. Very few studies have comprehensively evaluated a range of particle sizes for optimal interaction with the buccal or sublingual mucosa. For example, Teubl et al. (2013) demonstrated in *ex vivo* studies using porcine buccal mucosa that neutral polystyrene nanoparticles (25, 50, and 200 nm) dispersed in an aqueous base were able to penetrate into the mucosal tissue intact, with the 200-nm sized nanoparticles penetrating more rapidly and into deeper regions of the mucosa. It was suggested that the smaller nanoparticles were readily entrapped and immobilized in the mucus network. This is also supported by Holpuch et al. (Holpuch et al., 2010) which showed that 200-nm nanoparticles (FluoSpheres® polystyrene nanoparticles) were able to penetrate through the epithelium and basement membrane into the underlying connective tissue of intact normal human oral mucosal tissues that were obtained from patients undergoing surgical procedures. It should be noted that both studies used polystyrene nanoparticles, which are unable to be metabolized and can interfere with cell metabolism pathways (Holpuch et al., 2010). Therefore, further studies would be useful to evaluate the effect of more clinically translatable nanoparticulate compositions over a range of particle sizes for mucosal permeability and drug absorption for sublingual and buccal drug delivery.

There are conflicting results regarding the influence of surface charge on nanoparticle interaction with the oral mucosa. Roblegg et al. (2012) showed that 20 nm anionic (negatively charged) and 200 nm cationic (positively charged) nanoparticles were both able to permeate the mucus layer of porcine buccal mucosa. The cationic nanoparticles (200 nm) penetrated deeper into the buccal mucosal tissue compared to the 20 nm anionic nanoparticles, which remained in the top third region of the epithelium. The study reported that 200 nm anionic nanoparticles were entrapped within the mucus, formed agglomerates, and were unable to penetrate the epithelium. Similar differences in the interaction of the mucosa with nanoparticles of opposite charges were observed by Chaves et al. (2017). However, other studies have reported that cationic nanoparticles interacted more with the mucus and exhibited lower mucosal permeability in comparison to anionic nanoparticles (Chen et al., 2010; Yuan et al., 2011; Mouftah et al., 2016; Patil and Devarajan, 2016; Xu et al., 2018). This is also supported by studies in the lower gastrointestinal tract, whereby electrostatic interaction between cationic nanoparticles and the negatively charged mucins impeded the transport of the nanoparticles through the mucus layer (Hua et al., 2015). Anionic nanoparticles were able to interdiffuse among the mucus network due to less electrostatic interaction with the mucus (Hua et al., 2015).

The second main factor that should be considered for effective sublingual or buccal drug delivery is the interaction of the nanoparticles with the formulation base. The nanoparticles should be stable when incorporated into the pharmaceutical base, especially during manufacturing and storage. In addition, the formulation base should increase the residence time of the formulation in the sublingual or buccal region to optimize drug permeability and systemic absorption. There are inconsistent results as to the actual interaction of the nanoparticle-embedded formulations with the mucosal tissue. The majority of the studies have demonstrated sustained drug release from the nanoparticles embedded in the dosage form, with the drug then being diffused into the formulation base and absorbed into the adhered mucosa. These include nanoparticles incorporated into gels (Marques et al., 2017), sprays (Baltzley et al., 2018), tablets (Gavin et al., 2015; El-Nahas et al., 2017), films (Giovino et al., 2013; Mazzarino et al., 2014; Mortazavian et al., 2014; Al-Dhubiab et al., 2016; Masek et al., 2017; Castro et al., 2018a; Mahdizadeh Barzoki et al., 2018; Al-Nemrawi et al., 2019), and

patches (Mahdizadeh Barzoki et al., 2016). Very few studies have demonstrated release of nanoparticles from the formulation base and mucosal penetration of intact nanoparticles for drug delivery (Mortazavian et al., 2014; Masek et al., 2017). For example, Masek et al. (2017) developed nanofiber-based mucoadhesive films consisting of an electrospun nanofibrous reservoir layer (with nanoparticles reversibly adsorbed to the surface of the nanofibers or deposited in the pores between the nanofibers), a mucoadhesive film layer, and a protective backing layer. The results from both *ex vivo* and *in vivo* studies in pigs demonstrated that the nanofibrous mucoadhesive films were able to avoid rapid clearance of nanoparticles from the site of application, maintain a long-term concentration gradient of nanoparticles at the mucosal surface, and ensure unidirectional diffusion of nanoparticles towards mucosal surfaces. Histological samples excised 2 h after *in vivo* administration showed penetration of intact nanoparticles into the mucosa as well as regional lymph nodes.

The reasons for the discrepancy in the mechanism of action of nanoparticles when administered in a liquid base (e.g., water or buffered solution) or embedded into a formulation base (e.g., films, gels, and tablets) for sublingual or buccal drug delivery are still incompletely understood. Further studies are needed to determine whether it is more beneficial for nanoparticles to be used as a scaffold to promote stability and control drug release kinetics from within the formulation base or following mucosal penetration as intact particles. The former mechanism would place more importance on the retention of the formulation base to the mucosa and the stability of the nanoparticles in the formulation base for drug release, whereas the latter mechanism would place more importance on the physicochemical characteristics of the nanoparticles themselves for mucosal penetration. Most of the studies have only been conducted in *in vitro* and/or *ex vivo* models, with very limited *in vivo* studies available. *In vivo* studies provide better insights into the real-time performance of the formulation, as drug absorption is affected by a number of physiological factors as discussed earlier. In addition, there are significant anatomical differences in the sublingual and buccal mucosa among species. Porcine mucosa is the most similar to human mucosa and is widely used in *ex vivo* studies, however it is more common to use rodents in *in vivo* studies which have keratinized mucosa (Masek et al., 2017). Keratinization of the mucosa acts as an additional barrier for the penetration of drugs and nanoparticles, which should be taken into account when evaluating the results. Although the results to date support the use of nanoparticulate drug delivery approaches for sublingual and buccal administration, further comprehensive mechanistic and preclinical studies are required to ensure reproducibility of efficacy and safety outcomes.

SUBLINGUAL AND BUCCAL FORMULATIONS APPROVED AND IN CLINICAL TRIALS

A number of sublingual and buccal formulations are on the market with more in clinical development. **Table 1** shows examples of the sublingual and buccal formulations that are approved or in clinical trials. Those approved for clinical use have varied indications that also benefit from faster onset of action, including sedation, insomnia, angina, pain, and smoking cessation. The drugs incorporated vary in their therapeutic index as well as their duration of use, which indicate the prospect of using drugs with a narrow therapeutic index and for long-term therapy. Biologics have also made its way into the market with the delivery of allergen extracts and polyvalent mechanical bacterial lysate for use in allergic rhinitis and chronic obstructive pulmonary disease (COPD), respectively. Sublingual and buccal formulations approved for clinical use generally incorporate drugs in conventional dosage forms such as solid dosage forms (e.g., tablets, wafers, lozenges, and films), liquid dosage forms (e.g., sprays and oral liquid drops), and semi-solid dosage forms (e.g., gels and paste) (Allen et al., 2011). Solid dosage forms are typically manufactured to disintegrate or dissolve rapidly in a small quantity of saliva to allow fast drug absorption through the mucosa, without the need for water. In contrast, liquid dosage forms for sublingual and buccal use contain the drug dissolved (solution) or dispersed (suspension) in a vehicle. This is then administered as oral liquid drops or sprays, with the latter typically having a metered valve to control the dose of the drug delivered.

The majority of the formulations in clinical trials (**Table 1**) incorporate already approved drugs or novel compounds into conventional sublingual and buccal dosage forms—in particular, tablets, films, and oral liquids. It should be noted that drugs evaluated in the early phases of clinical investigation are commonly administered as a powder or oral liquid. Powders are typically formulated by opening clinically available capsules or crushing tablets, whereas oral liquids are attained by dispersing the powder into a liquid base or using the parenteral formulations of the drug. These studies are mainly focused on evaluating the pharmacokinetics and efficacy of the drug following sublingual or buccal administration, rather than assessing the performance of novel formulations.

Very few innovative dosage forms for sublingual and buccal drug delivery have reached the clinical development phase. The main strategies have been the incorporation of permeation enhancers or mucoadhesive constituents to conventional dosage forms. Conventional dosage forms are commonly affected by physiological factors (e.g., saliva and swallowing), which can reduce the contact of the formulation with the mucosa and lead to unpredictable drug absorption. In addition, the multicellular thickness and stratified nature of the sublingual and buccal epithelium can contribute to reduced drug absorption across these regions. These strategies have been shown to improve mucosal retention and/or permeability of conventional dosage forms. For example, permeation enhancers (e.g., surfactants, bile salts, fatty acids, cyclodextrins, and chelators) have been shown to improve the mucosal permeability and absorption of various compounds (Tsutsumi et al., 1998; Shojaei et al., 1999; Bird et al., 2001; Burgalassi et al., 2006; Sohi et al., 2010; Tian et al., 2012; Prasanth et al., 2014; Patil and Devarajan, 2014; Ojewole et al., 2014; Marxen et al., 2018) by: (i) changing mucus rheology; (ii) increasing the fluidity of the lipid bilayer membrane; (iii) acting

on the components at tight junctions; (iv) inhibiting mucosal enzymes; and (v) increasing the thermodynamic activity of drugs (Chinna Reddy and Chaitanya, 2011). In addition, the incorporation of mucoadhesive constituents has been demonstrated to enhance formulation retention time with the sublingual or buccal mucosa (Das and Das, 2004; Razafindratsita et al., 2007; Perioli and Pagano, 2013; Ikram et al., 2015; Yildiz Pekoz et al., 2016; El-Nabarawi et al., 2016; Ammar et al., 2017; Parodi et al., 2017; Celik, 2017; Salehi and Boddohi, 2017; Vasseur et al., 2017; Khan and Boateng, 2018; Razzaq et al., 2018; Sharma et al., 2018). This has been done primarily for solid dosage forms and semi-solid dosage forms. In particular, mucoadhesive polymers are commonly used in these formulations, including synthetic polymers (e.g., cellulose derivatives and poly(acrylic acid)-based polymers) and those from natural sources (e.g., chitosan, hyaluronic acid, agarose, and various gums). An impermeable backing layer may be incorporated in solid dosage forms (e.g., films, patches, and tablets) to allow unidirectional drug delivery (Guo and Cooklock, 1996; Benes et al., 1997; Shojaei et al., 1998; El-Nabarawi et al., 2016).

It is expected that more innovative dosage forms will eventually reach clinical trials following comprehensive preclinical assessment and optimization. This includes nanoparticulate formulations, especially for the systemic delivery of drugs. Ropivacaine liposomal gel is the only nanoparticulate formulation that has reached clinical studies for sublingual and buccal drug delivery. It has been evaluated for local drug delivery as a topical anesthetic in Phase I clinical studies. Furthermore, slow-disintegrating and non-disintegrating dosage forms, particularly for buccal drug delivery, have been extensively investigated in the literature to extend or control the release of active substances over a prolonged period (Scholz et al., 2008; Bahri-Najafi et al., 2014; Kaur et al., 2014; Jaipal et al., 2016; Celik, 2017; Lindert and Breitkreutz, 2017; Celik et al., 2017; Farag et al., 2018; Castro et al., 2018b). For example, multilayered films have been developed for controlled drug delivery and are generally designed to remain in their form and slowly release drug over a specified time (Lindert and Breitkreutz, 2017). It should be noted that formulations that have prolonged contact with the mucosa may cause irritation and/or discomfort for the patient, especially with concurrent eating or drinking. There is also a possibility for the dosage form to detach from the mucosa and be swallowed, which can lead to subsequent adherence to other parts of the gastrointestinal tract (e.g., esophagus). The results from clinical studies will determine the feasible of these dosage forms in clinical practice.

CONCLUSION

The sublingual and buccal routes of administration have significant advantages for systemic drug delivery. They have shown to be an effective alternative to the traditional oral route, especially when fast onset of action is required. In addition, they are useful for drugs that undergo high hepatic clearance or degradation in the gastrointestinal tract, and for patients that have swallowing difficulties. Although significant advances in drug formulation have been reported in the literature, particularly to improve retention and absorption in the buccal and sublingual regions, very few of them have translated to the clinical phase. For clinical translation to be justified, there needs to be a clear benefit of efficacy and/or safety with any new drug formulation compared to clinically available dosage forms (Hua et al., 2018). In addition, comprehensive evaluations of the pharmacokinetics, stability, efficacy, and safety of the formulations are required in appropriate animal models as well as in clinical studies, based on regulatory standards and protocols. For innovative platforms, such as nanoparticles, mechanism of action and safety of the different carriers following mucosal interaction and/or uptake need to be explored further (Bergin and Witzmann, 2013; Talkar et al., 2018; Vita et al., 2019). Complexity in drug formulation is also a key factor that can be a barrier to clinical translation, irrespective of its therapeutic efficacy (Hua et al., 2018). Therefore, simplification in formulation design is required to allow efficient and reproducible large-scale manufacturing. The availability of standardized testing methods can also be a limitation to reliably assess the quality of more complex or innovative formulations for regulatory standards.

AUTHOR CONTRIBUTIONS

SH was involved in conception of the idea for the review, drafted the manuscript, and approved the final version of the manuscript.

ACKNOWLEDGMENTS

The author wishes to thank the University of Newcastle, Pharmacy Research Trust of New South Wales, Rebecca L. Cooper Medical Research Foundation, Gladys M Brawn Fellowship, and AusEE Research Foundation for providing financial support for this work.

REFERENCES

Al-Dhubiab, B. E., Nair, A. B., Kumria, R., Attimarad, M., and Harsha, S. (2016). Development and evaluation of buccal films impregnated with selegiline-loaded nanospheres. *Drug Deliv.* 23 (7), 2154–2162. doi: 10.3109/10717544.2014.948644

Allen, L. V., Popovich, N. G., and Ansel, H. C. (2011). *Ansel's pharmaceutical dosage forms and drug delivery systems.* Philadelphia: Lippincott Williams & Wilkins;.

Al-Nemrawi, N. K., Alsharif, S. S. M., Alzoubi, K. H., and Alkhatib, R. Q. (2019). Preparation and characterization of insulin chitosan-nanoparticles loaded in buccal films. *Pharm. Dev. Technol.* 24 (8), 967–974. doi: 10.1080/10837450.2019.1619183

Ammar, H. O., Ghorab, M. M., Mahmoud, A. A., and Shahin, H. I. (2017). Design and *in vitro*/*in vivo* evaluation of ultra-thin mucoadhesive buccal film containing fluticasone propionate. *AAPS PharmSciTech* 18 (1), 93–103. doi: 10.1208/s12249-016-0496-0

Bahri-Najafi, R., Tavakoli, N., Senemar, M., and Peikanpour, M. (2014). Preparation and pharmaceutical evaluation of glibenclamide slow release mucoadhesive buccal film. *Res. Pharmaceut. Sci.* 9 (3), 213–223.

Baliga, S., Muglikar, S., and Kale, R. (2013). Salivary pH: a diagnostic biomarker. *J. Indian Soc. Periodontol.* 17 (4), 461–465. doi: 10.4103/0972-124X.118317

Baltzley, S., Malkawi, A. A., Alsmadi, M., and Al-Ghananeem, A. M. (2018). Sublingual spray drug delivery of ketorolac-loaded chitosan

nanoparticles. *Drug Dev. Ind. Pharm.* 44 (9), 1467–1472. doi: 10.1080/03639045.2018.1460378

Benes, L., Claustrat, B., Horriere, F., Geoffriau, M., Konsil, J., Parrott, K. A., et al. (1997). Transmucosal, oral controlled-release, and transdermal drug administration in human subjects: A crossover study with melatonin. *J. Pharm. Sci-Us.* 86 (10), 1115–1119. doi: 10.1021/js970011z

Bergin, I. L., and Witzmann, F. A. (2013). Nanoparticle toxicity by the gastrointestinal route: evidence and knowledge gaps. *Int. J. BioMed. Nanosci. Nanotechnol* 3 (1–2), 1–44. doi: 10.1504/IJBNN.2013.054515.

Bird, A. P., Faltinek, J. R., and Shojaei, A. H. (2001). Transbuccal peptide delivery: stability and in vitro permeation studies on endomorphin-1. *J. Control Release* 73 (1), 31–36. doi: 10.1016/S0168-3659(01)00246-2

Brunton, L. L., Knollmann, B. C., and Hilal-Dandan, R., (2018). *Goodman & Gilman's: The Pharmacological Basis of Therapeutics 13th edition*. New York: McGraw-Hill Education;.

Burgalassi, S., Chetoni, P., Dini, L., Najarro, M., Monti, D., Morelli, P., et al. (2006). Effect of permeation enhancers on buccal absorption. *Arzneimittel-Forschung* 56 (7), 561–567. doi: 10.1055/s-0031-1296752

Castro, P. M., Baptista, P., Madureira, A. R., Sarmento, B., and Pintado, M. E. (2018a). Combination of PLGA nanoparticles with mucoadhesive guar-gum films for buccal delivery of antihypertensive peptide. *Int. J. Pharm.* 547 (1-2), 593–601. doi: 10.1016/j.ijpharm.2018.05.051

Castro, P. M., Sousa, F., Magalhaes, R., Ruiz-Henestrosa, V. M. P., Pilosof, A. M. R., Madureira, A. R., et al. (2018b). Incorporation of beads into oral films for buccal and oral delivery of bioactive molecules. *Carbohydr. Polymers* 194, 411–421. doi: 10.1016/j.carbpol.2018.04.032

Celik, B. (2017). Risperidone mucoadhesive buccal tablets: formulation design, optimization and evaluation. *Drug Des. Devel. Ther.* 11, 3355–3365. doi: 10.2147/DDDT.S150774

Celik, B., Ozdemir, S., Barla Demirkoz, A., and Uner, M. (2017). Optimization of piribedil mucoadhesive tablets for efficient therapy of Parkinson's disease: physical characterization and ex vivo drug permeation through buccal mucosa. *Drug Dev. Ind. Pharm.* 43 (11), 1836–1845. doi: 10.1080/03639045.2017.1349785

Chaves, P. D., Ourique, A. F., Frank, L. A., Pohlmann, A. R., Guterres, S. S., and Beck, R. C. (2017). Carvedilol-loaded nanocapsules: Mucoadhesive properties and permeability across the sublingual mucosa. *Eur. J. Pharm. Biopharm.* 114, 88–95. doi: 10.1016/j.ejpb.2017.01.007

Chen, E. Y., Wang, Y. C., Chen, C. S., and Chin, W. C. (2010). Functionalized positive nanoparticles reduce mucin swelling and dispersion. *PloS One* 5 (11), e15434. doi: 10.1371/journal.pone.0015434

Chinna Reddy, P., Chaitanya, K. S., and Madhusudan Rao, Y. (2011). A review on bioadhesive buccal drug delivery systems: current status of formulation and evaluation methods. *Daru* 19 (6), 385–403.

Czerkinsky, C., and Holmgren, J. (2012). Mucosal delivery routes for optimal immunization: targeting immunity to the right tissues. *Curr. Topics Microbiol. Immunol.* 354, 1–18. doi: 10.1007/82_2010_112

Das, N. G., and Das, S. K. (2004). Development of mucoadhesive dosage forms of buprenorphine for sublingual drug delivery. *Drug Deliv.* 11 (2), 89–95. doi: 10.1080/10717540490280688

Dawes, C. (1987). Physiological factors affecting salivary flow rate, oral sugar clearance, and the sensation of dry mouth in man. *J. Dental Res.* 66, 648–653. doi: 10.1177/00220345870660S107

De Boer, A. G., De Leede, L. G., and Breimer, D. D. (1984). Drug absorption by sublingual and rectal routes. *Br. J. Anaesthesia* 56 (1), 69–82. doi: 10.1093/bja/56.1.69

El-Nabarawi, M. A., Ali, A. A., Aboud, H. M., Hassan, A. H., and Godah, A. H. (2016). Transbuccal delivery of betahistine dihydrochloride from mucoadhesive tablets with a unidirectional drug flow: *in vitro*, *ex vivo* and *in vivo* evaluation. *Drug Des. Devel. Ther.* 10, 4031–4045. doi: 10.2147/DDDT.S120613

El-Nahas, A. E., Allam, A. N., and El-Kamel, A. H. (2017). Mucoadhesive buccal tablets containing silymarin Eudragit-loaded nanoparticles: formulation, characterisation and ex vivo permeation. *J. Microencapsul.* 34 (5), 463–474. doi: 10.1080/02652048.2017.1345996

Farag, M. M., Abd El Malak, N. S., and Yehia, S. A. (2018). Zaleplon loaded bi-layered chronopatch: a novel buccal chronodelivery approach to overcome circadian rhythm related sleep disorder. *Int. J. Pharm.* 542 (1-2), 117–124. doi: 10.1016/j.ijpharm.2018.03.014

Gavin, A., Pham, J. T., Wang, D., Brownlow, B., and Elbayoumi, T. A. (2015). Layered nanoemulsions as mucoadhesive buccal systems for controlled delivery of oral cancer therapeutics. *Int. J. Nanomed.* 10, 1569–1584. doi: 10.2147/IJN.S75474

Giovino, C., Ayensu, I., Tetteh, J., and Boateng, J. S. (2013). An integrated buccal delivery system combining chitosan films impregnated with peptide loaded PEG-b-PLA nanoparticles. *Colloids Surf B Biointerfaces* 112, 9–15. doi: 10.1016/j.colsurfb.2013.07.019

Guo, J. H., and Cooklock, K. M. (1996). The effects of backing materials and multilayered systems on the characteristics of bioadhesive buccal patches. *J. Pharm. Pharmacol.* 48 (3), 255–257. doi: 10.1111/j.2042-7158.1996.tb05912.x

He, C., Cui, F., Yin, L., Qian, F., Tang, C., and Yin, C. (2009). A polymeric composite carrier for oral delivery of peptide drugs: Bilaminated hydrogel film loaded with nanoparticles. *Eur. Polym. J.* 45, 368–376. doi: 10.1016/j.eurpolymj.2008.11.004

Holpuch, A. S., Hummel, G. J., Tong, M., Seghi, G. A., Pei, P., Ma, P., et al. (2010). Nanoparticles for local drug delivery to the oral mucosa: proof of principle studies. *Pharmaceut. Res.* 27 (7), 1224–1236. doi: 10.1007/s11095-010-0121-y

Hua, S. (2015). Lipid-based nano-delivery systems for skin delivery of drugs and bioactives. *Front. Pharmacol.* 6, 219. doi: 10.3389/fphar.2015.00219

Hua, S., Marks, E., Schneider, J. J., and Keely, S. (2015). Advances in oral nano-delivery systems for colon targeted drug delivery in inflammatory bowel disease: selective targeting to diseased versus healthy tissue. *Nanomedicine.* 11 (5), 1117–1132. doi: 10.1016/j.nano.2015.02.018

Hua, S., de Matos, M. B. C., Metselaar, J. M., and Storm, G. (2018). Current Trends and Challenges in the Clinical Translation of Nanoparticulate Nanomedicines: Pathways for Translational Development and Commercialization. *Front. Pharmacol.* 9, 790. doi: 10.3389/fphar.2018.00790

Ikram, M., Gilhotra, N., and Gilhotra, R. M. (2015). Formulation and optimization of mucoadhesive buccal patches of losartan potassium by using response surface methodology. *Advanced Biomed. Res.* 4, 239. doi: 10.4103/2277-9175.168606

Jaipal, A., Pandey, M. M., Charde, S. Y., Sadhu, N., Srinivas, A., and Prasad, R. G. (2016). Controlled release effervescent buccal discs of buspirone hydrochloride: in vitro and in vivo evaluation studies. *Drug Deliv.* 23 (2), 452–458. doi: 10.3109/10717544.2014.917388

Kaur, G., Singh, D., and Brar, V. (2014). Bioadhesive okra polymer based buccal patches as platform for controlled drug delivery. *Int. J. Biol. Macromol.* 70, 408–419. doi: 10.1016/j.ijbiomac.2014.07.015

Khan, S., and Boateng, J. (2018). Effects of cyclodextrins (beta and gamma) and l-Arginine on stability and functional properties of mucoadhesive buccal films loaded with omeprazole for pediatric patients. *Polymers* 10 (2), 157. doi: 10.3390/polym10020157.

Kraan, H., Vrieling, H., Czerkinsky, C., Jiskoot, W., Kersten, G., and Amorij, J. P. (2014). Buccal and sublingual vaccine delivery. *J. Control Release* 190, 580–592. doi: 10.1016/j.jconrel.2014.05.060

Lindert, S., and Breitkreutz, J. (2017). Oromucosal multilayer films for tailor-made, controlled drug delivery. *Expert Opin. Drug Deliv.* 14 (11), 1265–1279. doi: 10.1080/17425247.2017.1276899

Mahdizadeh Barzoki, Z., Emam-Djomeh, Z., Mortazavian, E., Akbar Moosavi-Movahedi, A., and Rafiee Tehrani, M. (2016). Formulation, *in vitro* evaluation and kinetic analysis of chitosan-gelatin bilayer muco-adhesive buccal patches of insulin nanoparticles. *J. Microencapsul.* 33 (7), 613–624. doi: 10.1080/02652048.2016.1234513

Mahdizadeh Barzoki, Z., Emam-Djomeh, Z., Mortazavian, E., Rafiee-Tehrani, N., Behmadi, H., Rafiee-Tehrani, M., et al. (2018). Determination of diffusion coefficient for released nanoparticles from developed gelatin/chitosan bilayered buccal films. *Int. J. Biol. Macromol.* 112, 1005–1013. doi: 10.1016/j.ijbiomac.2018.01.215

Marques, A. C., Rocha, A. I., Leal, P., Estanqueiro, M., and Lobo, J. M. S. (2017). Development and characterization of mucoadhesive buccal gels containing lipid nanoparticles of ibuprofen. *Int. J. Pharm.* 533 (2), 455–462. doi: 10.1016/j.ijpharm.2017.04.025

Marxen, E., Jin, L., Jacobsen, J., Janfelt, C., Hyrup, B., and Nicolazzo, J. A. (2018). Effect of permeation enhancers on the Buccal permeability of nicotine: ex vivo transport studies complemented by MALDI MS Imaging. *Pharmaceut. Res.* 35 (3), 70. doi: 10.1007/s11095-017-2332-y

Masek, J., Lubasova, D., Lukac, R., Turanek-Knotigova, P., Kulich, P., Plockova, J., et al. (2017). Multi-layered nanofibrous mucoadhesive films for buccal and

sublingual administration of drug-delivery and vaccination nanoparticles - important step towards effective mucosal vaccines. *J. Control Release* 249, 183–195. doi: 10.1016/j.jconrel.2016.07.036

Mazzarino, L., Borsali, R., and Lemos-Senna, E. (2014). Mucoadhesive films containing chitosan-coated nanoparticles: a new strategy for buccal curcumin release. *J. Pharm. Sci.* 103 (11), 3764–3771. doi: 10.1002/jps.24142

Morales, J. O., and Brayden, D. J. (2017). Buccal delivery of small molecules and biologics: of mucoadhesive polymers, films, and nanoparticles. *Curr. Opin. Pharmacol.* 36, 22–28. doi: 10.1016/j.coph.2017.07.011

Mortazavian, E., Dorkoosh, F. A., and Rafiee-Tehrani, M. (2014). Design, characterization and ex vivo evaluation of chitosan film integrating of insulin nanoparticles composed of thiolated chitosan derivative for buccal delivery of insulin. *Drug Dev. Ind. Pharm.* 40 (5), 691–698. doi: 10.3109/03639045.2014.886590

Mouftah, S., Abdel-Mottaleb, M. M. A., and Lamprecht, A. (2016). Buccal delivery of low molecular weight heparin by cationic polymethacrylate nanoparticles. *Int. J. Pharm.* 515 (1-2), 565–574. doi: 10.1016/j.ijpharm.2016.10.039

Ojewole, E., Kalhapure, R., Akamanchi, K., and Govender, T. (2014). Novel oleic acid derivatives enhance buccal permeation of didanosine. *Drug Dev. Ind. Pharm.* 40 (5), 657–668. doi: 10.3109/03639045.2014.892958

Parodi, B., Russo, E., Baldassari, S., Zuccari, G., Pastorino, S., Yan, M., et al. (2017). Development and characterization of a mucoadhesive sublingual formulation for pain control: extemporaneous oxycodone films in personalized therapy. *Drug Dev. Ind. Pharm.* 43 (6), 917–924. doi: 10.1080/03639045.2017.1281290

Patil, N. H., and Devarajan, P. V. (2014). Enhanced insulin absorption from sublingual microemulsions: effect of permeation enhancers. *Drug Deliv. Trans. Res.* 4 (5-6), 429–438. doi: 10.1007/s13346-014-0205-z

Patil, N. H., and Devarajan, P. V. (2016). Insulin-loaded alginic acid nanoparticles for sublingual delivery. *Drug Deliv.* 23 (2), 429–436. doi: 10.3109/10717544.2014.916769

Perioli, L., and Pagano, C. (2013). Preformulation studies of mucoadhesive tablets for carbamazepine sublingual administration. *Colloids Surf B Biointerfaces* 102, 915–922. doi: 10.1016/j.colsurfb.2012.10.001

Prasanth, V. V., Puratchikody, A., Mathew, S. T., and Ashok, K. B. (2014). Effect of permeation enhancers in the mucoadhesive buccal patches of salbutamol sulphate for unidirectional buccal drug delivery. *Res. Pharmaceut. Sci.* 9 (4), 259–268.

Razafindratsita, A., Saint-Lu, N., Mascarell, L., Berjont, N., Bardon, T., Betbeder, D., et al (2007). Improvement of sublingual immunotherapy efficacy with a mucoadhesive allergen formulation. *J. Allergy Clin. Immunol.* 120 (2), 278–285. doi: 10.1016/j.jaci.2007.04.009

Razzaq, S., Hanif, S., Syed, M. A., Iqbal, J., Hassan, S. S., Raza, S. A., et al (2018). Development and evaluation of mucoadhesive buccal tablet containing metronidazole for the treatment of periodontitis and gingivitis. *Pakistan J. Pharmaceut. Sci.* 31 (5), 1903–1910.

Roblegg, E., Frohlich, E., Meindl, C., Teubl, B., Zaversky, M., and Zimmer, A. (2012). Evaluation of a physiological *in vitro* system to study the transport of nanoparticles through the buccal mucosa. *Nanotoxicology.* 6 (4), 399–413. doi: 10.3109/17435390.2011.580863

Salehi, S., and Boddohi, S. (2017). New formulation and approach for mucoadhesive buccal film of rizatriptan benzoate. *Prog. Biomater.* 6 (4), 175–187. doi: 10.1007/s40204-017-0077-7

Scholz, O. A., Wolff, A., Schumacher, A., Giannola, L. I., Campisi, G., Ciach, T., et al. (2008). Drug delivery from the oral cavity: focus on a novel mechatronic delivery device. *Drug Discovery Today* 13 (5-6), 247–253. doi: 10.1016/j.drudis.2007.10.018

Sharma, D., Sharma, A., and Garg, R. (2018). Design, development and *in vitro*/*ex vivo* evaluation of mucoadhesive buccal film of benzydamine hydrochloride for the effective treatment of aphthous stomatitis. *Recent Pat. Drug Delivery Formul.* 12 (4), 277–294. doi: 10.2174/1872211313666190128151038

Shojaei, A. H., Zhuo, S. L., and Li, X. (1998). Transbuccal delivery of acyclovir (II): feasibility, system design, and *in vitro* permeation studies. *J. Pharm. Pharm. Sci.* 1 (2), 66–73.

Shojaei, A. H., Khan, M., Lim, G., and Khosravan, R. (1999). Transbuccal permeation of a nucleoside analog, dideoxycytidine: effects of menthol as a permeation enhancer. *Int. J. Pharm.* 192 (2), 139–146. doi: 10.1016/S0378-5173(99)00301-4

Sohi, H., Ahuja, A., Ahmad, F. J., and Khar, R. K. (2010). Critical evaluation of permeation enhancers for oral mucosal drug delivery. *Drug Dev. Ind. Pharm.* 36 (3), 254–282. doi: 10.3109/03639040903117348

Talkar, S., Dhoble, S., Majumdar, A., and Patravale, V. (2018). Transmucosal Nanoparticles: Toxicological Overview. *Adv. Exp. Med. Biol.* 1048, 37–57. doi: 10.1007/978-3-319-72041-8_3

Teubl, B. J., Meindl, C., Eitzlmayr, A., Zimmer, A., Frohlich, E., and Roblegg, E. (2013). *In-vitro* permeability of neutral polystyrene particles via buccal mucosa. *Small.* 9 (3), 457–466. doi: 10.1002/smll.201201789

Teubl, B. J., Leitinger, G., Schneider, M., Lehr, C. M., Frohlich, E., Zimmer, A., et al. (2015). The buccal mucosa as a route for TiO2 nanoparticle uptake. *Nanotoxicology.* 9 (2), 253–261. doi: 10.3109/17435390.2014.921343

Tian, W., Hu, Q., Xu, Y., and Xu, Y. (2012). Effect of soybean-lecithin as an enhancer of buccal mucosa absorption of insulin. *Biomed. Materials Eng.* 22 (1-3), 171–178. doi: 10.3233/BME-2012-0704

Tsutsumi, K., Obata, Y., Takayama, K., Loftsson, T., and Nagai, T. (1998). Effect of cod-liver oil extract on the buccal permeation of ergotamine tartrate. *Drug Dev. Ind. Pharm.* 24 (8), 757–762. doi: 10.3109/03639049809082723

Vasseur, B., Dufour, A., Houdas, L., Goodwin, H., Harries, K., Emul, N. Y., et al. (2017). Comparison of the systemic and local pharmacokinetics of clonidine mucoadhesive buccal tablets with reference clonidine oral tablets in healthy volunteers: an open-label randomised cross-over trial. *Adv. Ther.* 34 (8), 2022–2032. doi: 10.1007/s12325-017-0585-9

Vita, A. A., Royse, E. A., and Pullen, N. A. (2019). Nanoparticles and danger signals: oral delivery vehicles as potential disruptors of intestinal barrier homeostasis. *J. Leukocyte Biol.* 106 (1), 95–103. doi: 10.1002/JLB.3MIR1118-414RR

von Bultzingslowen, I., Sollecito, T. P., Fox, P. C., Daniels, T., Jonsson, R., Lockhart, P. B., et al. (2007). Salivary dysfunction associated with systemic diseases: systematic review and clinical management recommendations. *Surg. Med. Pathol. Radiol. Endodontics* 103 Suppl, S57 e1–S57 15. doi: 10.1016/j.tripleo.2006.11.010

Wang, Y. Y., Lai, S. K., Suk, J. S., Pace, A., Cone, R., and Hanes, J. (2008). Addressing the PEG mucoadhesivity paradox to engineer nanoparticles that "slip" through the human mucus barrier. *Angew Chem. Int. Ed. Engl.* 47 (50), 9726–9729. doi: 10.1002/anie.200803526

Xu, Y., Zhang, X., Zhang, Y., Ye, J., Wang, H. L., Xia, X., et al. (2018). Mechanisms of deformable nanovesicles based on insulin-phospholipid complex for enhancing buccal delivery of insulin. *Int. J. Nanomed.* 13, 7319–7331. doi: 10.2147/IJN.S175425

Yildiz Pekoz, A., Sedef Erdal, M., Okyar, A., Ocak, M., Tekeli, F., Kaptan, E., et al. (2016). Preparation and *in-vivo* evaluation of dimenhydrinate buccal mucoadhesive films with enhanced bioavailability. *Drug Dev. Ind. Pharm.* 42 (6), 916–925. doi: 10.3109/03639045.2015.1091470

Yuan, Q., Fu, Y., Kao, W. J., Janigro, D., and Yang, H. (2011). Transbuccal delivery of CNS therapeutic nanoparticles: synthesis, characterization, and *in vitro* permeation studies. *ACS Chem. Neurosci.* 2 (11), 676–683. doi: 10.1021/cn200078m

Conflict of Interest: The author declares that the research was conducted in the absence of any commercial or financial relationships that could be construed as a potential conflict of interest.

frontiers in Pharmacology

ORIGINAL RESEARCH
published: 03 February 2020
doi: 10.3389/fphar.2019.01692

Physiologically Based Pharmacokinetic Modeling to Understand the Absorption of Risperidone Orodispersible Film

Fang Chen[1†], Hongrui Liu[1†], Bing Wang[1], Liuliu Yang[1], Weimin Cai[2], Zheng Jiao[3], Zhou Yang[4], Yusheng Chen[4], Yingjun Quan[4], Xiaoqiang Xiang[2] and Hao Wang[1*]*

[1] National Pharmaceutical Engineering Research Center, China State Institute of Pharmaceutical Industry, Shanghai, China, [2] Department of Clinical Pharmacy, School of Pharmacy, Fudan University, Shanghai, China, [3] Shanghai Chest Hospital, Shanghai Jiao Tong University, Shanghai, China, [4] Department of General Surgery, Shanghai Pudong Hospital, Fudan University Pudong Medical Center, Shanghai, China

OPEN ACCESS

Edited by:
Paul Chi-Lui Ho,
National University of Singapore,
Singapore

Reviewed by:
Xin Liu,
University of Queensland, Australia
Hui Xie,
Guangzhou Medical University, China

***Correspondence:**
Xiaoqiang Xiang
xiangxq@fudan.edu.cn
Hao Wang
wanghao10@sinopharm.com

[†]These authors have contributed equally to this work

Specialty section:
This article was submitted to Experimental Pharmacology and Drug Discovery, a section of the journal Frontiers in Pharmacology

Received: 05 September 2019
Accepted: 26 December 2019
Published: 03 February 2020

Citation:
Chen F, Liu H, Wang B, Yang L, Cai W, Jiao Z, Yang Z, Chen Y, Quan Y, Xiang X and Wang H (2020) Physiologically Based Pharmacokinetic Modeling to Understand the Absorption of Risperidone Orodispersible Film. Front. Pharmacol. 10:1692. doi: 10.3389/fphar.2019.01692

Objective: The aim of the present study was to investigate the absorption routes as well as the potential application of the oral transmucosal delivery of risperidone orodispersible film (ODF) using physiologically based pharmacokinetic modeling.

Methods: The pharmacokinetic study after intragastric (i.g.), supralingual, and sublingual administration of risperidone ODF was conducted in Beagle dogs. Then a mechanic absorption model which combined Oral Cavity Compartment Absorption and Transit (OCCAT) model with Advanced Compartment Absorption and Transit (ACAT) model for predicting the absorption routes of risperidone ODF *in vivo* was constructed using GastroPlus™. A sensitivity analysis was performed to investigate the impact of oral residence time on the *in vivo* absorption of risperidone ODF. Based on the fraction of intraoral absorption, the potential of the oral transmucosal delivery of risperidone were predicted.

Results: There were no statistical differences in the AUC_{0-t} (P = 0.4327), $AUC_{0-\infty}$ (P = 0.3278), C_{max} (P = 0.0531), and T_{max} (P = 0.2775) values among i.g., supralingual, and sublingual administration of risperidone ODF in Beagle dogs. The predicted absorption percentage *via* oral mucosa at oral residence time of 2 min, 5 min, and 10 min was 7.0%, 11.4%, and 19.5%, respectively. No obvious difference was observed for the bioavailability of risperidone ODF within 10 min of oral residence time. The PBPK absorption model for risperidone could be simplified to include ACAT model solely.

Conclusion: The main absorption route for risperidone ODF was the gastrointestine. The absorption percentage *via* oral mucosa was almost negligible due to the physicochemical properties of risperidone although ODF dissolved completely in the oral cavity of Beagle dogs within 2 min.

Keywords: risperidone orodispersible film, oral cavity compartment absorption and transit model, advanced compartment absorption and transit model, GastroPlus™, oral residence time, oral transmucosal delivery

INTRODUCTION

Orodispersible films (ODFs) are single or multilayer sheets of water-soluble polymer materials (Madhav et al., 2009; Hoffmann et al., 2011; Lam et al., 2014; Krampe et al., 2016; Foo et al., 2018). Due to the instant disintegration and release of the drug into the saliva once the film is put into the oral cavity, there is no need of water for the ingestion and it is more convenient than conventional tablets (Poston and Waters, 2007; Hoffmann et al., 2011; Lam et al., 2014). Owing to the characteristic of fast wetting, ODFs may adhere to the oral mucosa site and dissolve rapidly, so they cannot be spat out easily. Therefore, they are very suitable for special patients such as pediatric, geriatric, and psychiatric patients. They can effectively improve the clinical compliance (Poston and Waters, 2007; Krampe et al., 2016).

Risperidone, a benzisoxazole derivative, is a second-generation antipsychotics which has a high affinity for multiple receptors including 5-HT_{2A} serotonin, D_2 dopamine, α_1, α_2 adrenergic, and histamine receptors (Huang et al., 1993; Megens et al., 1994; Meuldermans et al., 1994; Gong et al., 2015). Risperidone has been widely used for acute and chronic schizophrenia (Huang et al., 1993; Mannens et al., 1993; Gong et al., 2015; Narayan et al., 2016). It can also alleviate the symptoms of schizophrenia and improve the social and personal performance (Huang et al., 1993; de Leon et al., 2010). It is available as tablets, oral solutions, capsules, dispersible tablets, orally disintegrating tablets (ODTs), and ODFs in the dose strengths ranging from 0.5 to 4 mg (Khames, 2017). Taken orally, risperidone is completely and rapidly absorbed. The oral bioavailability of risperidone is about 70% and the pre-systemic metabolism yields the active metabolite of 9-hydroxy (9-OH) risperidone *via* cytochrome P450 2D6, 3A4, and 3A5 (Huang et al., 1993; de Leon et al., 2010; Shimizu et al., 2017).

Heemstra et al. employed a modified Ussing chamber to investigate the permeability of risperidone through porcine buccal mucosa at various concentrations (Heemstra et al., 2010). The results showed that risperidone could permeate through the buccal mucosa in the way of passive diffusion, indicating the potential application of the intraoral delivery for risperidone mucoadhesive gel. ODFs stick to the oral mucosa and dissolve in the oral cavity within minutes, and a portion of the drug may be absorbed directly into the bloodstream *via* oral mucosa, avoiding pre-systemic metabolism. Thus, it is necessary to understand the absorption routes that are crucial for the development of risperidone ODF.

Physiologically based pharmacokinetic (PBPK) modeling combines the system dependent physiological, anatomical, and biochemical properties, specific properties of compounds as well as the formulation parameters, providing an approach to predict the plasma concentration–time profiles from *in vitro* data (Upton et al., 2016; Lin and Wong, 2017; Hens et al., 2018). Therefore, it has gained high popularity to support decision making throughout the drug research and development.

In the present study, we aimed to investigate the application potential of the oral transmucosal delivery of risperidone ODF using PBPK model. The pharmacokinetic study was conducted in Beagle dogs to identify the difference among intragastric (i.g.), supralingual, and sublingual administration of risperidone ODF. Then a mechanic PBPK model for understanding how risperidone ODF was absorbed was constructed. To build a model, intravenous (i.v.) data were generated to obtain risperidone disposition parameter (e.g. CL and V), i.g. data were generated to understand the gastrointestinal absorption, and *in vitro* dissolution was performed to provide information to predict *in vivo* dissolution. A schematic diagram of the adopted methodology was shown in **Figure 1**. Based on the fraction of intraoral absorption, the application potential of the oral transmucosal delivery of risperidone was evaluated.

MATERIALS AND METHODS

Preparation of Risperidone ODF

The formulation design, optimization and evaluation have been described in our previous study (Zhang et al., 2017). Briefly, risperidone ODF was prepared by solvent casting method (Foo et al., 2018).Weighted amount of risperidone was dispersed in purified water at ambient temperature under constant stirring. Subsequently, the required amount of citric acid, PEG 4000, HPMC E3, HPMC E15, aspartame, titanium dioxide, and peppermint essence were added separately under continuous grinding to obtain a homogeneous mixture. The uniform dispersion was processed in the vacuum deaeration pot to remove the air bubbles and then casted onto the backing by using a homemade coating machine with a drying temperature of 80–90 °C. The prepared films were cut into the sizes of 3 cm^2 (2.2 cm×1.4 cm) containing 1 mg of risperidone and stored at ambient temperature for further analysis.

In Vitro Dissolution Study

The *in vitro* dissolution of risperidone ODF was conducted using USP paddle at a rotation speed of 50 rpm in 500 ml of four different media, in 0.1 M HCl (pH 1.0), in acetate buffer of pH 4.0, in phosphate buffer of pH 6.8 and in water. Temperature was maintained at 37 ± 0.5 °C. Samples were collected at predetermined time intervals and filtered through a membrane filter of 0.22 μm.

The amount of risperidone was determined by a reported high-performance liquid chromatography (HPLC, Shimadzu Co. Ltd, Kyoto, Japan) method in our previous study (Zhang et al., 2017). Mobile phases consisted of acetonitrile and 5 mg/ml ammonium acetate in water (11:39, v/v) at a flow rate of 1.5 ml/min. Ten μl of the aliquot was injected into a Waters Atlantis®T3 C_{18} column (4.6 mm×100 mm, 3 μm, Waters Co. Ltd, Ireland) at a column oven of 40 °C. The quantity of risperidone was measured at ultraviolet wavelength of 275 nm.

Pharmacokinetic Study

The study included a four period, 1 week wash-out, crossover, single dose by i.v., i.g., supralingual, and sublingual administration. For i.v. administration, a 0.2 mg/ml of risperidone solution was prepared by dissolving 5 mg

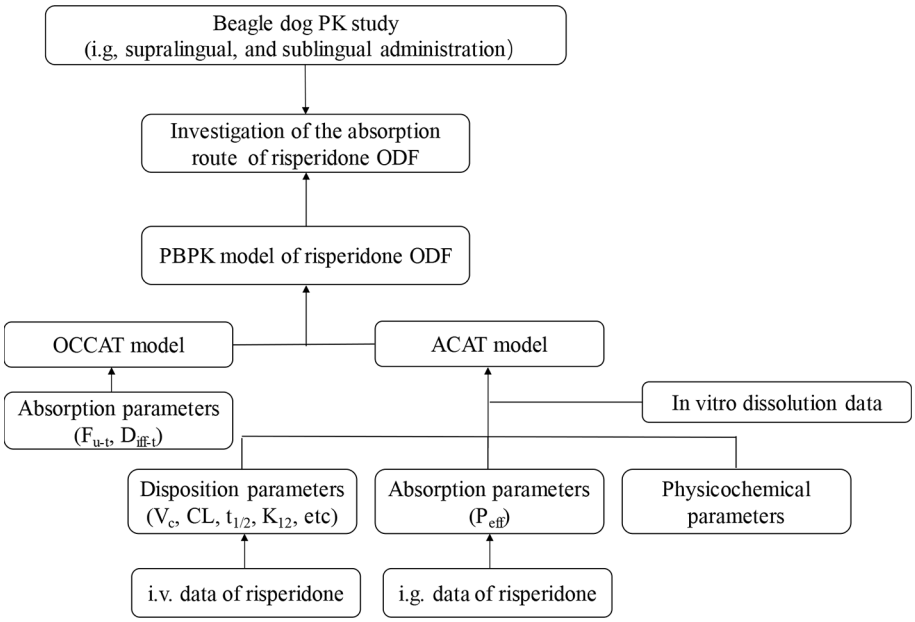

FIGURE 1 | Schematic diagram of the methodology adopted.

risperidone in 25 ml of 0.05% (m/v) tartaric acid water solution. For i.g. administration, risperidone ODFs which contained 5 mg of risperidone were dissolved in 25 ml of water solution. For supralingual administration, risperidone ODFs were put onto the tongue of Beagle dogs, and for sublingual administration, risperidone ODFs were put on the bottom of the tongue. The dogs were kept still for 2 min. A dose of 1 mg/body was administrated.

Four healthy Beagle dogs (male:female, 1:1) weighting 9.04 ± 1.88 kg (Certificate No. 20150005001131), purchased from Shanghai Jambo Biological Technology Co., Ltd (Shanghai, China), were used in this study. The study protocol was reviewed and approved by the Animal Management and Ethic Committee of the China State Institute of Pharmaceutical Industry. Dogs were housed individually in stainless steel cages. Tap water was given *ad-libitum* and food was provided once daily. Dogs were fasted for 12 h before drug administration. Blank blood samples were withdrawn prior to the administration of the drugs. Subsequently, blood samples were taken from forelimb vein at 0.167, 0.333, 0.5, 0.75, 1.0, 1.5, 2.0, 3.0, 4.0, 6.0, 8.0, 12, 24, and 32 h into heparin sodium-containing centrifuge tubes which were then centrifuged for 5 min at 3,000 rpm. The supernatant was collected and stored at -20 °C in the refrigerator until further analysis.

The main pharmacokinetic parameters of maximum plasma concentration (C_{max}), peak time (T_{max}), area under the concentration-time curve from 0 h to the time of last measurable concentration ($AUC_{0\text{-}t}$), and AUC from 0 to infinity ($AUC_{0\text{-}\infty}$), mean residue time (MRT), apparent volume of distribution (V_d), elimination half-life ($t_{1/2}$), and *in vivo* clearance (CL) were calculated by non-compartmental approach using the software of DAS 2.0 (Cheng et al., 2016). The results were summarized using their arithmetic means and standard deviations (SD). The statistically significant difference of the main pharmacokinetic parameters (C_{max}, T_{max}, AUC, MRT, V_d, $t_{1/2}$, and CL) between the administration routes were assessed by the one-way analysis of variance (ANOVA) model using the software of PASW Statistics 18 at a significance level of $\alpha = 0.05$.

Bioanalytical Method of Risperidone

A validated HPLC tandem mass spectrometry (HPLC-MS/MS) method for the determination of risperidone and the metabolite 9-OH risperidone in Beagle dog plasma were reported previously (Zhang et al., 2017). Calibration curves were constructed in the concentration range of 0.2–200 ng/ml with a lower limit of quantification (LLOQ) of 0.2 ng/ml. The intra-day precision ranged from 1.49% to 11.4% (n = 15) and the inter-day precisions ranged from 3.77% to 9.33% (n = 15). The HPLC system (Shimadzu Co. Ltd, Kyoto, Japan) equipped with a triple quadruple mass spectrometer (Shimadzu Co. Ltd, Kyoto, Japan) operating with ESI in the positive mode was used for the quantification of the analytes. Mobile phases consisted of methanol and water (35:65, v/v), both containing 0.05% formic acid and 5 mM ammonium formate. The flow rate was set at 0.3 ml/min. Ten µl of the aliquot was injected into the Inspire C_{18} column (2.1 mm×50 mm, 3 µm, Dikma Technologies Inc, Beijing, China) at a column oven of 40 °C. Multiple reaction monitoring (MRM) was utilized to determine risperidone, its metabolite 9-OH risperidone, and diphenhydramine (internal standard, IS) with transitions of *m/z* 411.10→191.10, *m/z* 427.10→207.15, and *m/z* 256.10→167.05, respectively. Direct protein precipitation using acetonitrile was used for the extraction of analytes from dog plasma.

Model Development

The PBPK model of risperidone in Beagle dog was conducted using GastroPlus™ (version 9.7, Simulation Plus, Inc., CA, USA). Extensive and systematic literature search was performed to collect physicochemical parameters (molecular weight, solubility, pKa, and log P), blood to plasma partition coefficient (B/P) of dogs, and dog plasma unbound fraction of risperidone (f_u) (PMDA label, 2018; Mannens et al., 1994). The diffusion coefficient of risperidone was predicted using GastroPlus™. Mean precipitation time, drug particle density, and particle size utilized default values in GastroPlus™.

The systemic clearance (CL), elimination rate constants, and volumes of distribution (V) were calculated by fitting the plasma concentration versus time profile of i.v. administration of risperidone in Beagle dogs using the empirical three-compartmental pharmacokinetic (PK) models in DAS 2.0. The obtained PK parameters were used to simulate the *in vivo* elimination of risperidone in PBPK model without further alteration.

The Advanced Compartment Absorption and Transit (ACAT) model implemented in GastroPlus™ defines the GI tract as one stomach, seven small intestine segment and one colon compartment(s), within each of which, drug can exist in several states simultaneously including unreleased, undissolved, dissolved, degraded, metabolized, and absorbed as it transits through successive compartments (Takano et al., 2006). The kinetics associated with these processes are modeled by a system of coupled linear and non-linear rate equations. The plasma concentration versus time profile of i.g. administration of risperidone in Beagle dogs was used to build the GastroPlus™ ACAT models. The effective permeability (P_{eff}) value of risperidone was optimized to match the plasma concentration-time curves.

The Oral Cavity Compartment Absorption and Transit (OCCAT) model divided the oral cavity into six physiological compartments: buccal, gingival, palate, top of the tongue, bottom of the tongue, and mouth floor, which accounts for drug dissolution in saliva, diffusion through the oral mucosa, and drug absorption into the systemic circulation (Xia et al., 2015). The parameters involved in the intraoral modeling settings, such as fraction unbound in oral tissue ($F_{u\text{-}t}$), and oral mucosa diffusivity ($D_{iff\text{-}t}$), were estimated using GastroPlus™. The OCCAT model is linked to the ACAT model for the prediction of the percentage of absorbed drug from oral cavity.

Z-factor model (Eq. 1) in the software of GastroPlus™ was chosen to describe the *in vivo* dissolution kinetics of risperidone ODF (Takano et al., 2006). Z is a dissolution parameter, which is independent of the saturated solubility, applied amount of drug, and the volume of medium, and is determined by fitting to the *in vitro* dissolution data (Takano et al., 2006).

$$\frac{dX_{d,vitro}}{dt} = z\left(C_s - \frac{X_{d,vitro(t)}}{V_{vitro}}\right)\left(\frac{X_{s,vitro(t)}}{X_{0,vitro}}\right)^{2/3} X_{0,vitro} \quad (1)$$

where $X_{d,vitro(t)}$ is the mass of dissolved drug at time t, r is the density of the drug, $X_{s,vitro(t)}$ is the mass of solid drug at time t, $X_{0,vitro}$ is the initial mass of solid drug, C_s is the saturated solubility of the drug, and V_{vitro} is the volume of the dissolution medium.

The predictive accuracy of the PBPK model was assessed by calculating the fold error based on the following formula:

$$\text{Fold error} = \left\{ \begin{array}{l} \frac{\text{observed value}}{\text{simulated value}}, \text{if observed value} > \text{simulated value} \\ \frac{\text{simulated value}}{\text{observed value}}, \text{if observed value} < \text{simulated value} \end{array} \right\} \quad (2)$$

An accurate prediction was achieved if fold error was within two (Li et al., 2009).

Parameter Sensitivity Analysis and Regional Absorption Prediction

In OCCAT model of GastroPlus™, there are three oral transit models designed for intraoral delivery system, namely, *Normal Swallowing*, *Hold & Swallow* as well as *Hold Rinse & Swallow*. Since ODFs can maintain some time of contact in mucosal surface, the option of *Hold & Swallow* was chosen. The hold time (residence time) of the drug in oral cavity is a main factor which may affect the absorption *via* oral mucosa for rapidly-disintegrating formulations. A sensitivity analysis was performed to investigate the impact of residence time on the *in vivo* performance of risperidone ODF. Since ODFs generally release the drug immediately, we conducted the sensitivity analysis of oral residence time in a range of 0–10 min. A sensitivity factor was calculated for each systemic parameter by Eq. 3 (Hens et al., 2018).

$$\text{Sensitivity factor} = \frac{\text{Maximum value} - \text{Minimum value}}{\text{Maximum value}} \quad (3)$$

The sensitivity value was between 0 and 1. The higher the value, the more sensitive it is. The percentage of absorbed drug from oral cavity was also evaluated.

RESULTS

In Vitro and *In Vivo* Dissolution Data

The *in vitro* dissolution results at different test conditions and *in vivo* dissolution curve fitted by Z-factor model are shown in **Figure 2**. The ODF all achieved a complete release of its risperidone contents in different medium within 2 min. This dissolution was generally unaffected by pH at the range of 1–7.

In Vivo Pharmacokinetic Data

The mean plasma concentration-time curves of i.v., i.g., supralingual, and sublingual administration of 1 mg/body risperidone in Beagle dogs are shown in **Figure 3**. The main pharmacokinetic parameters for risperidone are summarized in **Table 1**.

There were no statistically significant differences in the AUC_{0-t} ($P = 0.4327$), $AUC_{0-\infty}$ ($P = 0.3278$), C_{max} ($P = 0.0531$), T_{max} ($P = 0.2775$), MRT_{0-t} ($P = 0.2956$), $MRT_{0-\infty}$ ($P = 0.5141$), $t_{1/2}$($P = 0.2719$),

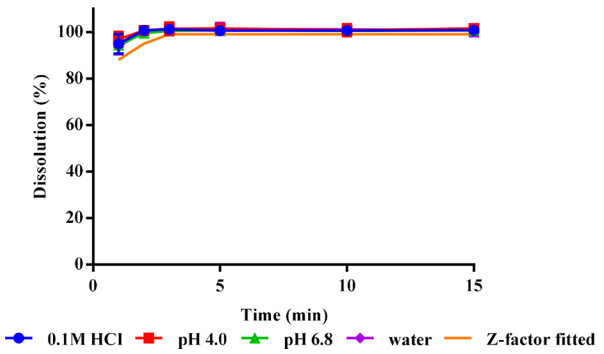

FIGURE 2 | *In vitro* dissolution profiles (n = 3) and *in vivo* fitted dissolution profile for risperidone ODF.

V_d (P = 0.5565), and CL (P = 0.3720) values among the sublingual, supralingual, and i.g. administration routes.

Model Development

The input parameters for GastroPlus™ modeling are summarized in **Table 2**.

Parameter Sensitivity Analysis

The parameter sensitivity assessed the influence of oral residence time in a range of 0–10 min on the T_{max}, C_{max}, $AUC_{0-\infty}$, and bioavailability of risperidone ODF, which is depicted in **Figure 4**. The C_{max}, $AUC_{0-\infty}$, and bioavailability of risperidone were almost unchanged when oral residence time increased from 0 to 10 min. The calculated sensitivity factor for T_{max}, C_{max}, $AUC_{0-\infty}$, and bioavailability were 0.26, 0.10, 0.11, and 0.11, respectively. All of the values were low. No obvious difference was observed for the C_{max}, $AUC_{0-\infty}$, and bioavailability of risperidone ODF when oral residence time increased within 10 min based on the calculated value and the graphic trend (**Figure 4**). The results indicated that oromucosal absorption might not be critical to risperidone ODF in short residence time.

Regional Absorption Prediction

The fraction absorbed of risperidone ODF in the oral cavity at an oral residence time of 2 min, 5 min, and 10 min was predicted to be 7.0%, 11.4%, and 19.5%, respectively. The extent of absorption increased slightly as the oral residence time prolonged. Since risperidone ODF dissolved completely in the oral cavity of Beagle dogs within 2 min, the absorption percentage *via* oral mucosa was almost negligible. Thus, the gastrointestine might be the main absorption route for risperidone ODF. The PBPK modeling of risperidone ODF could be simplified to include ACAT model solely.

The results indicated that the reason for the similar PK profiles following sublingual and supralingual administration of risperidone ODF was that the absorption routes of the two administration sites were the same and they were both mainly absorbed by gastrointestinal tract after entering with saliva

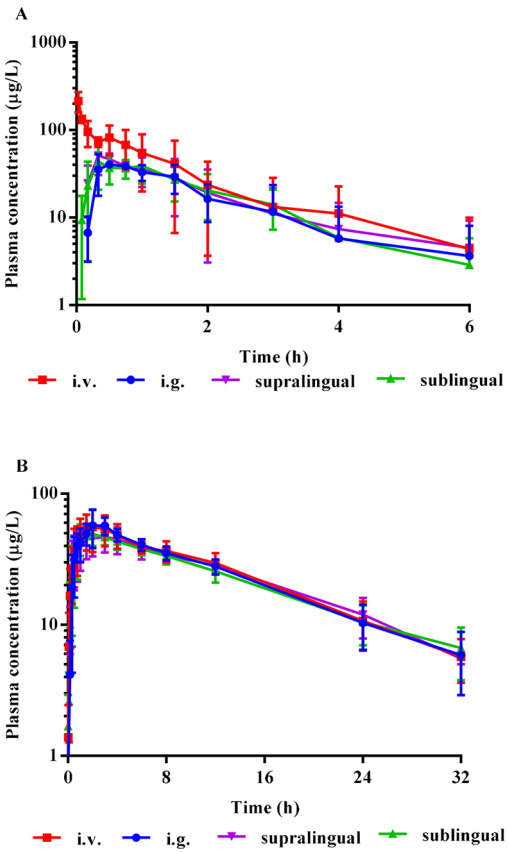

FIGURE 3 | Mean plasma concentration-time curves of risperidone **(A)**, and the metabolite 9-OH risperidone **(B)** in Beagle dogs (Mean ± SD, n = 4) after i.v., i.g., supralingual, and sublingual administration of 1 mg/body. The error bars represent standard deviation (SD) from the mean.

although sublingual mucosa has the better permeability and higher vascularization.

Model Validation

ODFs are usually designed for supralingual administration, and there are no difference of PK profile of risperidone between supralingual and sublingual administration route. Thus, only the PK data of supralingual administration of risperidone ODF was used for the model validation. The *in vivo* absorption of risperidone ODF following supralingual administration was predicted using the ACAT model, and was compared with observed data. The simulated plasma concentration-time profiles are described in **Figure 5**. There is a good match between the predicted plasma concentration-time curve and the observed one.

The predicted and observed main pharmacokinetic parameters are summarized in **Table 3**. The fold errors of T_{max}, C_{max}, and $AUC_{0-\infty}$ for risperidone were 1.17, 1.54, 1.11, respectively. All were within 2-fold, indicating the good prediction of the developed PBPK model for risperidone ODF.

TABLE 1 | Main pharmacokinetic parameters of risperidone (Mean ± SD) in Beagle dogs after i.v., i.g., supralingual, and sublingual administration (n = 4).

Parameters	Unit	i.v.	i.g.	Sublingual	Supralingual
AUC_{0-t}	μg/L·h	177.02 ± 113.04	89.99 ± 48.73	98.89 ± 40.89	97.31 ± 54.39
$AUC_{0-\infty}$	μg/L·h	179.10 ± 115.28	91.26 ± 48.58	101.57 ± 43.34	101.87 ± 57.42
T_{max}	h	0.03 ± 0	0.71 ± 0.53	0.67 ± 0.38	0.62 ± 0.58
C_{max}	μg/L	214.97 ± 56.43	45.85 ± 7.60	52.57 ± 10.60	59.38 ± 7.32
MRT_{0-t}	h	1.30 ± 0.80	1.71 ± 0.75	1.78 ± 0.41	1.50 ± 0.71
$MRT_{0-\infty}$	h	1.40 ± 0.89	1.79 ± 0.74	1.93 ± 0.52	1.73 ± 0.82
V_d	L	12.77 ± 9.79	14.93 ± 1.43	17.75 ± 3.06	17.22 ± 7.70
$t_{1/2}$	h	1.37 ± 0.82	0.92 ± 0.41	1.21 ± 0.40	1.13 ± 0.50
CL	L/h	7.69 ± 4.60	12.90 ± 5.07	11.03 ± 3.80	11.93 ± 5.24
F	%	/	57.04 ± 17.45	65.16 ± 20.16	61.98 ± 17.73

AUC_{0-t} area under the concentration-time curve from 0 h to the time of last measurable concentration, $AUC_{0-\infty}$ AUC from 0 to infinity, T_{max} peak time, C_{max} maximum plasma concentration, MRT mean residue time, V_d apparent volume of distribution, $t_{1/2}$ elimination half-life, CL clearance, F relative bioavailability.

TABLE 2 | Summary of input parameter for GastroPlus™ Simulation of risperidone.

Parameters		Value
Physiochemical parameters		
Mol Weight (g/mol)		410.49
log P		3.04[a]
Compound type		dibasic base
pKa		pKa_1 = 8.24 pKa_2 = 3.11[b]
B/P		0.506[c]
f_u		0.083[c]
Solubility (pH 6.8) (mg/ml)		0.9[d]
Diffusion coefficient (cm^2/s)		0.64×10^{-5}[e]
Mean Precipitation Time (s)		900[f]
Drug particle density (g/ml)		1.2[f]
Particle size (μm)		25[f]
Absorption parameters		
ACAT model	P_{eff} (10^{-4} cm/s)	5.3894[e]
OCCAT model	F_{u-t}	0.15382[e]
	D_{iff-t} (cm/s)	9.383×10^{-7}[e]
Disposition parameters		
First pass extraction (%)		51[e]
V_c (L/kg)		0.3139[e]
CL (L/h/kg)		0.5903[e]
$t_{1/2}$ (h)		2.43[e]
K_{12} (h^{-1})		16.352[e]
K_{21} (h^{-1})		9.007[e]
K_{13} (h^{-1})		0.4625[e]
K_{31} (h^{-1})		0.4103[e]
V_2 (L/kg)		0.56988[e]
V_3 (L/kg)		0.35383[e]
Dosing design		
Dose (mg)		1
Body weight (kg)		9.0425
No. of dogs		4

log P octanol/water partition coefficient, pKa dissociation constant, B/P blood to plasma partition coefficient, f_u plasma unbound fraction, P_{eff} effective permeability, F_{u-t} fraction unbound in oral tissue, D_{iff-t} oral mucosa diffusivity, V volumes of distribution, V_c volume of distribution of the central compartment,V_2 volume of distribution of the first peripheral compartment,V_3 volume of distribution of the second peripheral compartment, CL in vivo *clearance, $t_{1/2}$ elimination half-life, K elimination rate constants.*

[a]*Taken from Drugbank.*

[b]*Taken from Pubchem.*

[c]*Taken from Ref. (Mannens et al., 1994).*

[d]*Taken from Ref. (PMDA label, 2018).*

[e]*Estimated using GastroPlus™.*

[f]*Default value of GastroPlus™*

DISCUSSION

ODFs can maintain some time of contact in mucosal surface on which they dissolve rapidly and release drug into the saliva. The drugs may be absorbed into the systemic circulation either through oral mucosa, or intestinal mucosa, or both. It was found that the sildenafil ODF was bioequivalent to that of the conventional tablet (Viagra®). The plasma concentration-time profiles of sildenafil and the metabolite were nearly superimposable between the two dosage forms (Radicioni et al., 2017). However, after sublingual or buccal administration of the ropinirole ODF, a fast absorption was achieved within 15 min. The bioavailability was dramatically improved by about 7-fold compared to that of oral administration route (Lai et al., 2018). Similar result was also seen in selegiline. The bioavailability of 1.25 mg Zydis selegiline (Zelapar®), which was an oral lyophilisate (tablet) that dissolves rapidly when it was put into the oral cavity, was comparable to that of the standard oral tablets of 10 mg. But the principal metabolites were at least 90% lower compared with the oral tablet, leading to a reduction of the dose-related side effect (Poston and Waters, 2007). Therefore, it is important to investigate the mechanism of absorption in the development of these intraoral formulations.

Various models have been developed to investigate the permeability of the compounds in the intraoral formulations across the oral mucosa including *in vitro* models (animal/human tissue model, TR 146 cell culture, EpiOral™, PermeaPad®, et al), *in situ* model, *in vivo* pharmacokinetic study, and i*n silico* absorption model (Patel et al., 2012). The *in silico* absorption model integrates the compound and formulation properties as well as physiology and anatomy data, and is thus ideally suitable to investigate the *in vivo* absorption characteristics and mechanism of the intraoral formulations, providing important insights into the factors leading to the different bioavailability.

There are few reports on the application of PBPK modeling to aid the development of the intraoral drug delivery systems. A PBPK model has been built for buprenorphine to predict the pharmacokinetics of buprenorphine sublingual tablets *in vivo* under different dosing strength, guiding the clinical trial design and the rational use of the drug by Kalluri and his co-workers (Kalluri et al., 2017). Due to the lack of oral cavity physiology module in Simcyp™, the inhalation route was used to simulate the portion of sublingual absorbed. The *in vivo* absorption properties and quantitative contribution of each absorption route of buprenorphine were predicted using the validated

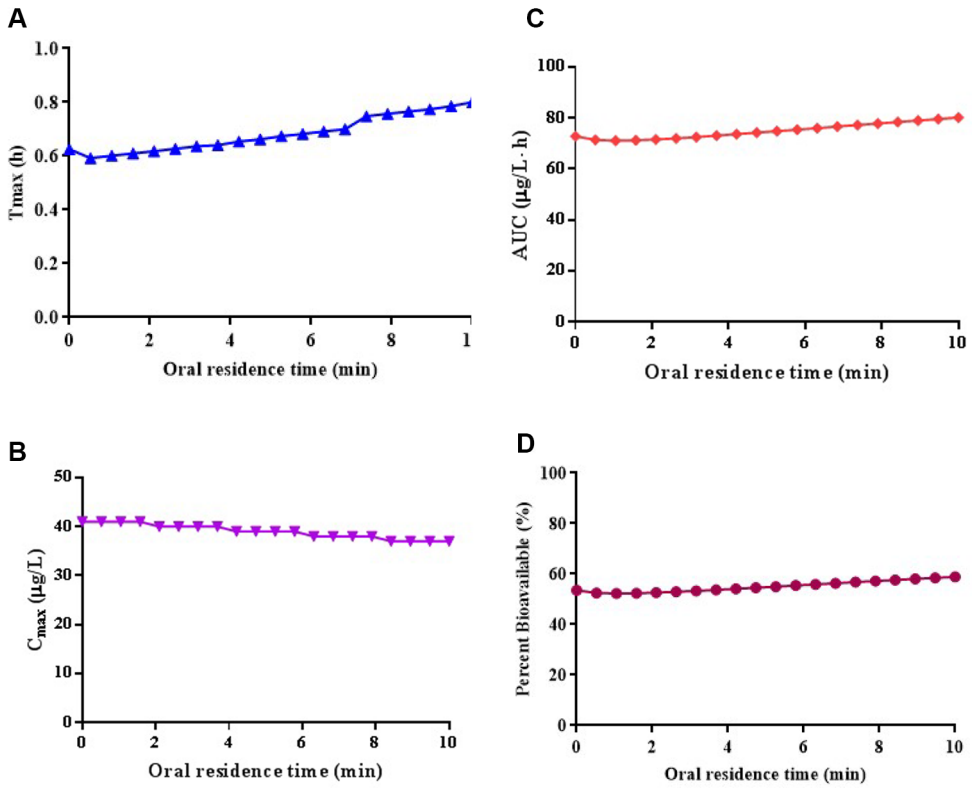

FIGURE 4 | Simulated the influence of oral residence time at a range of 0–10 min on the T_{max} **(A)**, C_{max} **(B)**, $AUC_{0-\infty}$ **(C)**, and bioavailability **(D)** of risperidone ODF.

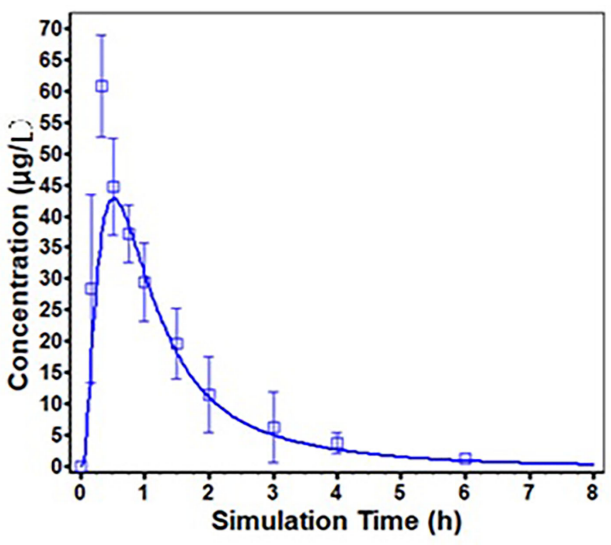

FIGURE 5 | Predicted (solid line) and Observed (square frame, error bars represent one standard deviation from the mean) mean plasma concentration profiles following supralingual administration of 1 mg/body risperidone ODF.

TABLE 3 | Comparison of main pharmacokinetic parameters of predicted and observed after supralingual administration of 1 mg/body risperidone ODF.

Parameters	Unit	Predicted	Observed	Fold error
T_{max}	h	0.53	0.62	1.17
C_{max}	μg/L	38.43	59.38	1.54
$AUC_{0-\infty}$	μg/L·h	91.56	101.87	1.11

PBPK model. The prediction of buprenorphine utilized a "top-down" strategy, for which the *in vivo* pharmacokinetic data was used to calculate the contribution percentage of each absorption route based on a great deal of pharmacokinetic data and the general understanding of the absorption mechanism. Additionally, they employed a simple first-order absorption process without the full consideration of the physiological difference between the oral cavity and lung. The oral transmucosal absorption is driven by a complicated partition between saliva and mucosa tissue, permeation through epithelium, absorption into the system circulation, and the portion of the compound swallowed unintentionally. The OCCAT model in GastroPlus™ takes into account the compound dissolution/precipitation in saliva, partition between saliva and mucosa tissue, diffusion through the oral mucosa, and

absorption into the blood, as well as the link with the ACAT model to determine gastrointestinal absorption of the swallowed portion. Thus it can directly estimate the oral transmucosal absorption proportion using the physicochemical data of compounds. The predictive capability of the OCCAT model has ever been evaluated by zolpidem sublingual tablets (Intermezzo®). The results showed that the OCCAT model well captured the observed pharmacokinetics of zolpidem ($R^2 > 0.9$). The estimated zolpidem absorption *via* the oral mucosa was about 18% (Xia et al., 2015). In addition, the validation of the OCCAT model was also conducted for other intraoral drug delivery systems, such as sublingual solution (verapamil), and sublingual tablets (propranolol, asenapine, and nicotine) (Xia et al., 2015). The simulated oral transmucosal absorption portion was comparable with the observed data, except nicotine, a small molecule of low lipophilicity and high solubility, which was underestimated (Xia et al., 2015). Therefore, more data for various kinds of compounds with different physicochemical properties are desired to evaluate and optimize the OCCAT model, so as to improve its utility.

In this study, the combination of OCCAT and ACAT model in the software of GastroPlus was used to investigate the absorption routes of risperidone ODF as well as the potential application of the oral transmucosal delivery. Our results showed the successful application of the OCCAT model to quantify the oromucosal absorption of risperidone, a compound of low solubility and high permeability, providing an example for the development of other ODFs. The OCCAT model has great potential to prospectively predict the intraoral drug products at various stage of the drug development, guide the selection of the lead compounds and dosage forms for oral transmucosal delivery, and replace some preclinical studies as well as clinical trials, which can save much time and cost.

The PBPK model of risperidone was established and validated by pharmacokinetic studies in Beagle dogs. Based on the developed PBPK model, the drug absorption routes were investigated, and the influence of formulation and physiological factors on drug absorption was assessed by parameter sensitivity analysis, which can determine the important physiological factors affecting the bioavailability of dosage forms and help the rational design of formulations. For example, if a drug is mainly absorbed through oral mucosa, we can improve the transport of drugs across the oral mucosa by formulation optimization, such as adding mucoadhesive polymers to prolong the residence time on the mucosal surface, or using permeation enhancer to enhance the drug permeation across the oral mucosa. If a drug is not easily absorbed through the oral mucosa and the gastrointestinal tract is the main absorption site, the formulation only needs to be dispersed in the oral cavity and its dissolution characteristics only needs to meet the requirements of common oral dosage forms. Moreover, in the research and development of the drug, the impact of formulation changes on bioavailability can also be predicted through PBPK, reducing the need for clinical trials and shortening the research process.

This method of PBPK modeling provides some insights for the research of intraoral drug delivery systems such as ODFs, ODTs, sublingual films and mucoadhesive buccal films. For drugs with the possibility of oral mucosa absorption, especially those can be rapidly absorbed through oral mucosa, the absorption model of PBPK which combines the OCCAT model with ACAT model can analyze the impact of dosage forms, formulation and the administration sites of the oral cavity on the oral absorption proportion, and suggest the methods to improve the absorption *via* oral mucosa and bioavailability. The optimal preparation design and clinical drug dosing strategy can be determined through modeling and simulation. Thus, the preclinical studies and clinical trials can be reduced. Finally, simplified drug development and supervision can be expected to achieve.

The results of PBPK modeling showed that the fraction absorbed *via* oral mucosa increased from 7.0% to 19.5% when the residence time changed from 2 min to 10 min while the bioavailability of risperidone was almost unchanged. It is not necessary to increase the residence time in formulation design for the fact that the bioavailability of risperidone cannot be significantly improved by prolonging the residence time in the oral cavity. The rapid dissolution and good compliance are the goals in formulation optimization. The slight change of the residence time caused by the change of the formulation will not affect its bioavailability. As risperidone is mainly absorbed through gastrointestine, the individual differences of oral physiological factors such as the amount of saliva and the flow rate of saliva have little effect on its bioavailability. Therefore, risperidone ODF can be developed according to the requirements of oral dosage forms. The quality indexes such as content, content uniformity, stability and dissolution rate can refer to the requirements of conventional oral dosage forms, and bioequivalence evaluation can choose conventional tablets or ODTs as reference formulations.

The absorption rate and extent of drugs *via* oral mucosa are closely related to the physicochemical properties of the drug including molecular weight, octanol-water partition coefficient, solubility, and ionization constant (Bredenberg et al., 2003; Nicolazzo et al., 2005; Pather et al., 2008). Drugs with fairly good lipophilicity and water solubility are favored to facilitate diffusion across the lipid-rich cytomembrane and the hydrophilic cytoplasm. Furthermore, the drugs in the unionized molecule form can be absorbed across the epithelial cells more effectively (Lam et al., 2014). Therefore, the pKa value, representing the extent of ionization at different pH is of great importance. Risperidone is a small molecule compound which has good lipophilicity and poor water solubility (Khames, 2017). It is a dibasic base with dissociation constants of 8.24 (pKa_1) and 3.11 (pKa_2) which is easy to ionize at the oral mucosa (Saibi et al., 2012). For these reasons, it's difficult for risperidone to permeate across the oral mucosa. In addition to the physicochemical

properties of the drug, the residence time of the formulation in mucosal surface also has an impact on the oral transmucosal absorption. Risperidone ODF dissolves rapidly in the oral cavity, the residence time of the formulation was within 2 min, which limited the absorption of risperidone *via* oral mucosa.

CONCLUSION

The PBPK modeling of risperidone ODF indicated that the majority of the absorption occurred in the gastrointestine, and the percent absorbed *via* oral mucosa was almost negligible as the fact that risperidone ODF dissolved completely in the mouth of Beagle dogs within 2 min. The PBPK mechanistic absorption model which combines OCCAT with ACAT model could be used for the prediction of the *in vivo* absorption to scientifically and rationally guide the development of the ODF product, accelerating the research and development process.

DATA AVAILABILITY STATEMENT

The datasets generated for this study are available on request to the corresponding authors.

ETHICS STATEMENT

This research was approved by the Animal Management and Ethic Committee of the China State Institute of Pharmaceutical Industry.

AUTHOR CONTRIBUTIONS

All authors listed have made substantial, direct, and intellectual contribution to the work and approved it for publication.

FUNDING

This work was supported by National Natural Science Foundation of China (81473409), Foundation of Shanghai Science and Technology Commission (18DZ2290500), PDH-SPFDU Joint Research Fund (RHJJ2017-05), and Shanghai Science and Technology Innovation Fund (18140900900).

REFERENCES

Bredenberg, S., Duberg, M., Lennernas, B., Lennernas, H., Pettersson, A., Westerberg, M., et al. (2003). *In vitro* and *in vivo* evaluation of a new sublingual tablet system for rapid oromucosal absorption using fentanyl citrate as the active substance. *Eur. J. Pharm. Sci.* 20 (3), 327–334. doi: 10.1016/j.ejps.2003.07.002

Cheng, Z., Ding, C., Li, Z., Song, D., Yuan, J., Hao, W., et al. (2016). Simultaneous determination of three triterpenes in rat plasma by LC-MS/MS and its application to a pharmacokinetic study of Rhizoma Alismatis extract. *J. Chromatogr. B. Analyt. Technol. BioMed. Life Sci.* 1008 (1), 32–37. doi: 10.1016/j.jchromb.2015.11.011

de Leon, J., Wynn, G., and Sandson, N. B. (2010). The pharmacokinetics of paliperidone versus risperidone. *Psychosomatics* 51 (1), 80–88. doi: 10.1176/appi.psy.51.1.80

Foo, W. C., Khong, Y. M., Gokhale, R., and Chan, S. Y. (2018). A novel unit-dose approach for the pharmaceutical compounding of an orodispersible film. *Int. J. Pharm.* 539 (1-2), 165–174. doi: 10.1016/j.ijpharm.2018.01.047

Gong, W., Liu, Y., Mei, D. Y., Yang, M., and Mei, X. G. (2015). Preparation, release and pharmacokinetics of a risperidone elementary osmotic pump system. *Drug Dev. Ind. Pharm.* 41 (3), 464–469. doi: 10.3109/03639045.2013.877923

Heemstra, L. B., Finnin, B. C., and Nicolazzo, J. A. (2010). The buccal mucosa as an alternative route for the systemic delivery of risperidone. *J. Pharm. Sci.* 99 (11), 4584–4592. doi: 10.1002/jps.22175

Hens, B., Talattof, A., Paixão, P., Bermejo, M., Tsume, Y., Löbenberg, R., et al. (2018). Measuring the impact of gastrointestinal variables on the systemic outcome of two suspensions of posaconazole by a PBPK model. *AAPS J.* 20 (3), 57–70. doi: 10.1208/s12248-018-0217-6

Hoffmann, E. M., Breitenbach, A., and Breitkreutz, J. (2011). Advances in orodispersible films for drug delivery. *Expert Opin. Drug Deliv.* 8 (3), 299–316. doi: 10.1517/17425247.2011.553217

Huang, M. L., Van Peer, A., Woestenborghs, R., De Coster, R., Heykants, J., Jansen, A. A., et al. (1993). Pharmacokinetics of the novel antipsychotic agent risperidone and the prolactin response in healthy subjects. *Clin. Pharmacol. Ther.* 54 (3), 257–268. doi: 10.1038/clpt.1993.146

Kalluri, H. V., Zhang, H., Caritis, S. N., and Venkataramanan, R. (2017). A physiologically based pharmacokinetic modeling approach to predict buprenorphine pharmacokinetics following intravenous &sublingual administration. *Br. J. ClinPharmacol.* 83 (11), 2458–2473. doi: 10.1111/bcp.13368

Khames, A. (2017). Investigation of the effect of solubility increase at the main absorption site on bioavailability of BCS class II drug (risperidone) using liquisolid technique. *Drug Deliv.* 24 (1), 328–338. doi: 10.1080/10717544.2016.1250140

Krampe, R., Sieber, D., Pein-Hackelbusch, M., and Breitkreutz, J. (2016). A new biorelevant dissolution method for orodispersible films. *Eur. J. Pharm. Biopharm.* 98 (1), 20–25. doi: 10.1016/j.ejpb.2015.10.012

Lai, K. L., Fang, Y., Han, H., Li, Q., Zhang, S., Li, H. Y., et al. (2018). Orally-dissolving film for sublingual and buccal delivery of ropinirole. *Colloids Surf B. Biointerfaces* ,1 (163), 9–18. doi: 10.1016/j.colsurfb.2017.12.015

Lam, J. K., Xu, Y., Worsley, A., and Wong, I. C. (2014). Oral transmucosal drug delivery for pediatric use. *Adv. Drug Delivery Rev.* 73 (6), 50–62. doi: 10.1016/j.addr.2013.08.011

Li, H., Sun, J., Sui, X., Yan, Z., Sun, Y., Liu, X., et al. (2009). Structure-based prediction of the nonspecific binding of drugs to hepatic microsomes. *AAPS J.* 11 (2), 364–370. doi: 10.1208/s12248-009-9113-4

Lin, L., and Wong, H.(2017) Predicting Oral Drug Absorption: Mini review on physiologically-based pharmacokinetic models. *Pharmaceutics* 9 (4), 41–54. doi: 10.3390/pharmaceutics9040041

Madhav, N. V., Shakya, A. K., Shakya, P., and Singh, K. (2009). Orotransmucosal drug delivery systems: a review. *J. Control Release* 140 (1), 2–11. doi: 10.1016/j.jconrel.2009.07.016

Mannens, G., Huang, M. L., Meuldermans, W., Hendrickx, J., Woestenborghs, R., and Heykants, J. (1993). Absorption, metabolism, and excretion of risperidone in humans. *Drug Metab. Dispos.* 21 (6), 1134–1141.

Mannens, G., Meuldermans, W., Snoeck, E., and Heykants, J. (1994). Plasma protein binding of risperidone and its distribution in blood. *Psychopharmacol. (Berl.)* 114 (4), 566–572. doi: 10.1007/BF02244986

Megens, A. A., Awouters, F. H., Schotte, A., Meert, T. F., Dugovic, C., Niemegeers, C. J., et al. (1994). Survey on the pharmacodynamics of the new antipsychotic risperidone. *Psychopharmacol. (Berl.)* 114 (1), 19–23. doi: 10.1007/BF02245439

Meuldermans, W., Hendrickx, J., Mannens, G., Lavrijsen, K., Janssen, C., Bracke, J., et al. (1994). The metabolism and excretion of risperidone after oral administration in rats and dogs. *Drug Metab. Dispos.* 22 (1), 129–138.

Narayan, R., Singh, M., Ranjan, O., Nayak, Y., Garg, S., Shavi, G. V., et al. (2016). Development of risperidone liposomes for brain targeting through intranasal route. *Life Sci.* 163, 38–45. doi: 10.1016/j.lfs.2016.08.033

Nicolazzo, J. A., Reed, B. L., and Finnin, B. C. (2005). Buccal penetration enhancers–how do they really work? *J. Control Release* 105 (1-2), 1–15. doi: 10.1016/j.jconrel.2005.01.024

Patel, V. F., Liu, F., and Brown, M. B. (2012). Modeling the oral cavity: *in vitro* and *in vivo* evaluations of buccal drug delivery systems. *J. Control Release* 161 (3), 746–756. doi: 10.1016/j.jconrel.2012.05.026

Pather, S. I., Rathbone, M. J., and Senel, S. (2008). Current status and the future of buccal drug delivery systems. *Expert Opin. Drug Deliv.* 5 (5), 531–542. doi: 10.1517/17425247.5.5.531

PMDA label. (2018). http://www.pmda.go.jp/PmdaSearch/iyakuDetail/ResultDataSetPDF/230127_1179038C1078_1_24

Poston, K. L., and Waters, C. (2007). Zydis Selegiline in the Management of Parkinson's Disease. *Expert Opin. Pharmacother.* 8 (15), 2615–2624. doi: 10.1517/14656566.8.15.2615

Poston, K. L., and Waters, C. (2007). Zydisselegiline in the management of Parkinson's disease. *Expert. Opin. Pharmacother.* 8 (15), 2615–2624. doi: 10.1517/14656566.8.15.2615

Radicioni, M., Castiglioni, C., Giori, A., Cupone, I., Frangione, V., and Rovati, S. (2017). Bioequivalence study of a new sildenafil 100 mg orodispersible film compared to the conventional film-coated 100 mg tablet administered to healthy male volunteers. *Drug Des. DevelTher.* 11 (11), 1183–1192. doi: 10.2147/DDDT.S124034

Saibi, Y., Sato, H., and Tachiki, H. (2012). Developing *in vitro-in vivo* correlation of risperidone immediate release tablet. *AAPS PharmSciTech.* 13 (3), 890–895. doi: 10.1208/s12249-012-9814-3

Shimizu, S., den Hoedt, S. M., Mangas-Sanjuan, V., Cristea, S., Geuer, J. K., van den Berg, D. J., et al. (2017). Target-site investigation for the plasma prolactin response: mechanism-based pharmacokinetic-pharmacodynamic analysis of risperidone and paliperidone in the rat. *Drug Metab. Dispos.* 45 (2), 152–159. doi: 10.1124/dmd.116.072306

Takano, R., Sugano, K., Higashida, A., Hayashi, Y., Machida, M., Aso, Y., et al. (2006). Oral absorption of poorly water-soluble drugs: computer simulation of fraction absorbed in humans from a miniscale dissolution test. *Pharm. Res.* 23 (6), 1144–1156. doi: 10.1007/s11095-006-0162-4

Upton, R. N., Foster, D. J., and Abuhelwa, A. Y. (2016). An introduction to physiologically-based pharmacokinetic models. *Paediatr. Anaesth.* 26 (11), 1036–1046. doi: 10.1111/pan.12995

Xia, B., Yang, Z., Zhou, H., Lukacova, V., Zhu, W., Milewski, M., et al. (2015). Development of a novel oral cavity compartmental absorption and transit model for sublingual administration: illustration with zolpidem. *AAPS J.* 17 (3), 631–642. doi: 10.1208/s12248-015-9727-7

Zhang, H., Wang, D. H., Wang, B., Yang, Q. M., and Chen, F. (2017). Preparation and *in vitro/in vivo* evaluation of risperidone orodispersible films. *Chin J. Pharm.* 48 (3), 406–412. doi: 10.16522/j.cnki.cjph.2017.03.014

Conflict of Interest: The authors declare that the research was conducted in the absence of any commercial or financial relationships that could be construed as a potential conflict of interest.

frontiers in Pharmacology

ORIGINAL RESEARCH
published: 26 February 2020
doi: 10.3389/fphar.2020.00085

Chemotherapeutic Nanoparticle-Based Liposomes Enhance the Efficiency of Mild Microwave Ablation in Hepatocellular Carcinoma Therapy

*Songsong Wu[1,2], Dongyun Zhang[1], Jie Yu[1], Jianping Dou[1], Xin Li[1], Mengjuan Mu[1] and Ping Liang[1]**

[1] Department of Interventional Ultrasound, Chinese PLA General Hospital, Beijing, China, [2] Department of Ultrasonography, Fujian Provincial Hospital, Shengli Clinical Medical College of Fujian Medical University, Fuzhou, China

OPEN ACCESS

Edited by:
Paul Chi-Lui Ho, National University of Singapore, Singapore

Reviewed by:
Qingyu Zhou, University of South Florida, United States
Eric Robinet, Centre Hospitalier Universitaire de Besançon, France

***Correspondence:**
Ping Liang
liangping301@hotmail.com

Specialty section:
This article was submitted to Experimental Pharmacology and Drug Discovery, a section of the journal Frontiers in Pharmacology

Received: *09 October 2019*
Accepted: *27 January 2020*
Published: *26 February 2020*

Citation:
Wu S, Zhang D, Yu J, Dou J, Li X, Mu M and Liang P (2020) Chemotherapeutic Nanoparticle-Based Liposomes Enhance the Efficiency of Mild Microwave Ablation in Hepatocellular Carcinoma Therapy. Front. Pharmacol. 11:85. doi: 10.3389/fphar.2020.00085

Hepatocellular carcinoma (HCC) is the third leading cause of death from cancer, and the 5-year overall survival (OS) rate for HCC remains unsatisfying worldwide. Microwave ablation (MWA) is a minimally invasive therapy that has made progress in treating HCC. However, HCC recurrence remains problematic. Therefore, combination therapy may offer better outcomes and enhance MWA efficiency through improved tumor control. We have developed doxorubicin-loaded liposomes (DNPs) as an efficient nanoplatform to enhance MWA of hepatocellular carcinoma even at the mild ablation condition. In this study, we demonstrated that the uptake of DNPs by HCC cells was increased 1.5-fold compared with that of free DOX. Enhanced synergism was observed in the combination of DNPs and MWA, which induced nearly 80% cell death. The combination of mild MWA and DNPs enhanced the ablation efficiency of HCC with significant inhibition of liver tumors and accounted for the longest survival rate among all groups. A much higher accumulation of the DNPs was observed in the transitional zone than in the ablation zone. No apparent systemic toxicity was observed for any of the treatments after 14 days. The present work demonstrates that DNPs combined with MWA could be a promising nanoparticle-based therapeutic approach for the treatment of hepatocellular carcinoma and shows potential for future clinical applications.

Keywords: hepatocellular carcinoma, liposomes, microwave ablation, combination therapy, enhance, nanoparticles

INTRODUCTION

Hepatocellular carcinoma (HCC) ranks as the sixth most common malignancy worldwide and is the fourth leading cause of cancer death (Siegel et al., 2019). The 5-year overall survival (OS) rate for HCC remains poor worldwide (Costentin, 2017). Surgery is not always an option among patients with liver cancer as concurrent liver cirrhosis, which many of these patients have, increases the risk of mortality (Johnson and Wright, 2019). Minimally invasive therapies, such as radiofrequency

ablation or microwave ablation (MWA) and high-intensity focused ultrasound ablation, offer new therapeutic approaches for HCC,(Zhu et al., 2018; Lyu et al., 2018; Mu et al., 2018; Huang et al., 2019) with the advantages of lower morbidity and mortality and broader indications compared with surgery (Shiina et al., 2018).

Rapid temperature, a larger ablation zone, and low susceptibility to the heat-sink effect are advantages that confer superiority to MWA for HCC therapy compared with other thermal modalities, (Facciorusso et al., 2016) particularly for early-stage HCC (Salati et al., 2017). These advantages overcome several challenges, including how the size of HCC can severely affect MWA efficacy, which may result in postsurgical recurrence or the development of unwanted lesions near important blood vessels and collateral biliary ducts that are difficult to ablate completely (Yu et al., 2017). High temperatures in the central zone near the antenna lead to necrosis and protein denaturation, whereas in the transitional zone, lower temperatures and the resulting energy insufficiency lead to a recurrence of more aggressive phenotypes and worse outcomes (Chu and Dupuy, 2014). Therefore, new strategies have been constantly researched.

Combination therapy may offer better outcomes to obtain an enhanced MWA efficiency with improved tumor control (Zhou et al., 2017). Previous studies have demonstrated that hyperthermia could augment chemotherapy, which in turn, enhanced ablation efficiency; therefore, temperature and chemotherapeutic agents acted to achieve tumor therapy (Yan et al., 2017). Nevertheless, liver cancer chemotherapy is not without its limitations, and the two major challenges are poor delivery efficiency and limited drug penetration into tumors (El Dika and Abou-Alfa, 2017). Nanoparticles as a drug delivery system has brought great improvements to cancer therapy (Dong et al., 2019). Nanoparticle therapeutics, based on natural or synthetic organic geo-macromolecules, have been developed as drug delivery systems by extending circulation times and facilitating uptake into tumors *via* enhanced permeability and retention (EPR) effect caused by leaky tumor vasculature (Yang et al., 2019). Liposomes were first approved by the US Food and Drug Administration and, since then, have attracted tremendous attention due to their high payload and easy synthesis, facilitating increased drug accumulation at tumor sites (Jha et al., 2016; Wang et al., 2019).

A combination therapy comprising ablation with chemotherapy offers several advantages over single ablation therapy, thereby decreasing ablation energy and enhancing tumor destruction (Fang et al., 2019; Xu et al., 2019). We therefore hypothesised that liposomes possessing optimal targeting properties and compatibility may transfer more necrosis-inducing drugs to the tumor and may thus be an effective chemical enhancer of MWA in HCC therapy. In this study, we used mild MWA energy, defined as small amounts of necrosis achieved through low microwave energy, to mimic the transitional zone. The literature on mild MWA combined with liposomes as an effective therapy to improve ablation outcomes and decrease recurrence is limited. We synthesised liposome-loading doxorubicin (DNPs), which enhanced the mild MWA effect and demonstrated that low microwave energy caused a relapse of all tumors, but a combination therapy could significantly reduce tumor growth and recurrence. Additionally, we provided evidence for the effectiveness of combination therapy in treating HCC or tumors located in difficult-to-access regions.

MATERIALS AND METHODS

Reagents

Disaturated-phosphatidylcholine (DSPC) and 1,2 distearoyl-sn-glycero-3-phosphoethanolamine-N-[methoxy (poly-ethylene-glycol)-2000] (DSPE-PEG2000) were purchased from Avanti Polar Lipids, Inc. (USA). Cholesterol (Sigma-Aldrich, USA), DMEM and penicillin/streptomycin (HyClone, USA), fetal bovine serum (Biological Industries, Israel), DOX (Tokyo Chemical Industry, Japan), Gd-DTPA-HPDP (Consun, Guangzhou, China), RIPA Lysis Buffer (Beyotime, Shanghai, China), and a Cell Counting Kit-8 (CCK-8) (Dojindo Laboratories, Japan) were purchased and used as indicated by the manufacturer. Deionized water (18.2 MΩ cm) from a Milli-Q purification system was used for all reagent preparations.

Synthesis and Characterisation of DNPs

The liposome formulation was composed of DSPC: cholesterol: DSPE-PEG-2000 dissolved in chloroform in a 55:40:5 molar ratio. The organic solvent was removed under nitrogen flow until a thin lipid film (10 mg) was formed. Then, the film was further dried for over 2 h under a vacuum. DOX was loaded *via* remote loading methods (Deng et al., 2014).The procedures were as follows: 1-ml $(NH_4)_2SO_4$ solution (300 mM) was mixed with the lipid film and then hydrated *via* sonication at 65°C for 15 min at a frequency of 20 kHz and a power of 130 W for 6 min. The obtained rough liposomes were dialysed for 6 h with degassed water to remove the unloading $(NH_4)_2SO_4$. Subsequently, the liposome suspension was mixed with 1.0-mg DOX and maintained at room temperature for 24 h. Finally, the particles were purified by centrifugation using 10-kDa molecular weight cutoff filters to remove unloading DOX. The dynamic light scattering (DLS) measurement of DNPs was performed using a Zetasizer (Malvern Nano ZS, UK). The Gd-DTPA-HPDP encapsulated DNPs were synthesised as mentioned above to capture images of the tumor uptake of DNPs. Liquids containing 1-ml $(NH_4)_2SO_4$ solution and 5-mM Gd-DTPA-HPDP were mixed with the lipid film, and the mixture was sonicated and purified to obtain the encapsulated Gd-DTPA-HPDP DNPs.

In Vitro Cellular Uptake and Ablation–Chemo Treatment

HepG2 and Huh7 cells were seeded into 24-well plates (3×10^5/well), incubated with various concentrations of DNPs and DOX for 1, 3, and 6 h. Cells were washed with PBS to remove the drugs and were harvested for measurement of DOX fluorescence through flow cytometry (Beckman CytoFLEX, USA). Chemotherapeutic efficacy of DNPs was quantitatively evaluated by exposing HepG2 and Huh7 cells seeded into 96-well plates (1×10^5/well) to various concentrations of DNPs and free DOX for 8 h. Cell viability was assessed using CCK-8

detection kits, and absorbance at 450 nm was measured using a multi-plate reader (Biotek, USA). All experiments were designed for three repeating groups.

To evaluate the combined cytotoxicity of DNPs with MWA, 1×10^4 HepG2 cells were seeded into 96-well plates and incubated with 6.0 μg/ml DNPs and 6.0 μg/ml free DOX as a control in a 100 μl fresh medium. Cells were washed with PBS twice after an 8-h incubation and replaced with a 250-μl fresh medium. A microwave antenna (Kangyou Medical, China) was placed into the well, and cells were exposed to MWA (2450 MHz, 1.2 W) for 4 min. Cell viability was determined as described above. MWA followed the DNPs experiment and was conducted further to compare the outcome of chemoablation and ablation chemotherapy. Cells with a 250-μl medium were exposed to MWA (2450 MHz, 1.2 W) for 4 min. Then, cells were incubated with 6.0 μg/ml DNPs and 6.0 μg/ml DOX as a control in a 100 μl fresh medium. Eight hours later, cell viability was determined.

Animal Experiments

Animals received care in accordance with the Guide for the Care and Use of Laboratory Animals published by the US National Institute of Health. The Chinese PLA General Hospital Animal Care and Use Committee approved all procedures employed in this study. Female BALB/c nude mice (6–8 weeks old) were maintained under aseptic conditions in a small animal isolator and were housed in groups of five in standard cages with access to food and water and a 12-h light/dark cycle. Animals were adapted to the animal facility for at least 7 days prior to the experiments. Mouse tumor models were established by subcutaneous injection of 2×10^6 HepG2 cells in the right abdomen, and the tumor volume (mm^3) was calculated as length × $(width)^2/2$.

Ablation–Chemo Combination Therapy in HCC Models

For tumor imaging, when the tumor size reached 10 × 10 mm, 100 μl of DNPs (100 μg/ml) was intravenously injected into tumor-bearing mice. An MRI examination (Bruker, Germany) was performed at various time points. To determine the efficiency of ablation–chemo, mice were divided into six groups (five per group), namely: (1) control group, (2) DOX group, (3) DNPs group, (4) MWA group, (5) MWA + DOX group, and (6) MWA + DNPs group. Mice were intravenously injected with 100 μl of PBS, DOX (100 μg/ml) or DNPs (containing 100 μg/ml of DOX), and 24 h later, mice were treated with MWA (2450 MHz, 1.0 W, 60 s). Thermal imaging was recorded through an infrared thermal imaging camera (Magnity Electronics Co., China). Three days later, intravenous injection of PBS, DOX, and DNPs were intravenously injected again, 24 h later, mice were treated with MWA, and the drug dose and MWA parameter were the same as in the first treatment. Changes in tumor volumes and body weight were recorded. Mice were sacrificed after 14 days, blood was collected for a biochemical panel evaluation (Mindary BC-5130, China), and tumors were collected for analysis. The survival experiments were repeated as aforementioned to calculate the survival of six groups. Considering the tumor burden of mice, a cutoff line was set, namely, a mouse burdened with a tumor volume larger than 1200 mm^3 was considered dearth.

Mild MWA Contributed to the Tumor Uptake of DNPs

HepG2 cells (1×10^4) were seeded into 96-well plates and treated with a 250-μl fresh medium containing 6.0 μg/ml DNPs with a similar concentration of free DOX as the control. The microwave antenna was placed into the well, and cells were exposed to mild MWA at 1.0 W for 4 min. After an hour, cells were washed and examined with a microscope (Olympus BX43, Japan); at the same time, cells were lysed for quantitative analysis of DOX fluorescence using a multi-plate reader at an excitation wavelength 480 nm and emission wavelength 580 nm.

For *in vivo* experiments, when the tumor size reached 10 × 10 mm, 100 μl of DNPs (100 μg/ml) was intravenously injected into tumor-bearing mice. Eight hours later, mice were treated with MWA (2450 MHz, 1.0 W, 60 s). Eight hours after that, tumors were harvested from mice and imaged by microscope-based fluorescence imaging.

In Vivo Toxicology Analysis

The blood of mice in the six groups on day 14 was collected for biochemical panel evaluation (Mindary BC-5130, China). Hepatic, heart, and kidney functional indicators of mice in the six groups on day 14 after treatment, such as alanine albumin (ALB), aspartate alkaline phosphatase aminotransferase (ALT), aminotransferase (AST), creatine kinase-MB (CK-MB), blood urine creatinine (Cr), blood urea nitrogen and urea, were tested to measure the responses of the experimental animals to the treatments.

Statistical Analysis

The results are presented as the mean ± SD. Cell viability, tumor volume and weight, and mouse body weight were compared using a one-way ANOVA test and a Student's t-test. A Student's t-test was used to compare the blood biochemistry panel and complete blood counts between treatments. Differences were considered significant for $p < 0.05$.

RESULTS

Synthesis and Cellular Uptake of DNPs and the Ablation–Chemo Effect

The mixture of DSPC, cholesterol, and DSPE-PEG2000 at a molar ratio of 55:40:5 generated efficient encapsulation of DOX (>90%) into the liposomes through the remote loading method. DOX encapsulation achieved was at 94.3% ± 1.81%. The DLS results showed the hydrodynamic sizes of DNPs to measure 95.5 ± 4.32 nm with adequate size distribution (**Figure 1A**) and a negative charge (-20.13 ± 1.04 mV). Cellular uptake of DNPs by HCC cells was evaluated by flow cytometry, which showed that liposome-mediated cellular uptake generated significantly higher DOX fluorescence intensity compared with free DOX ($p < 0.05$)

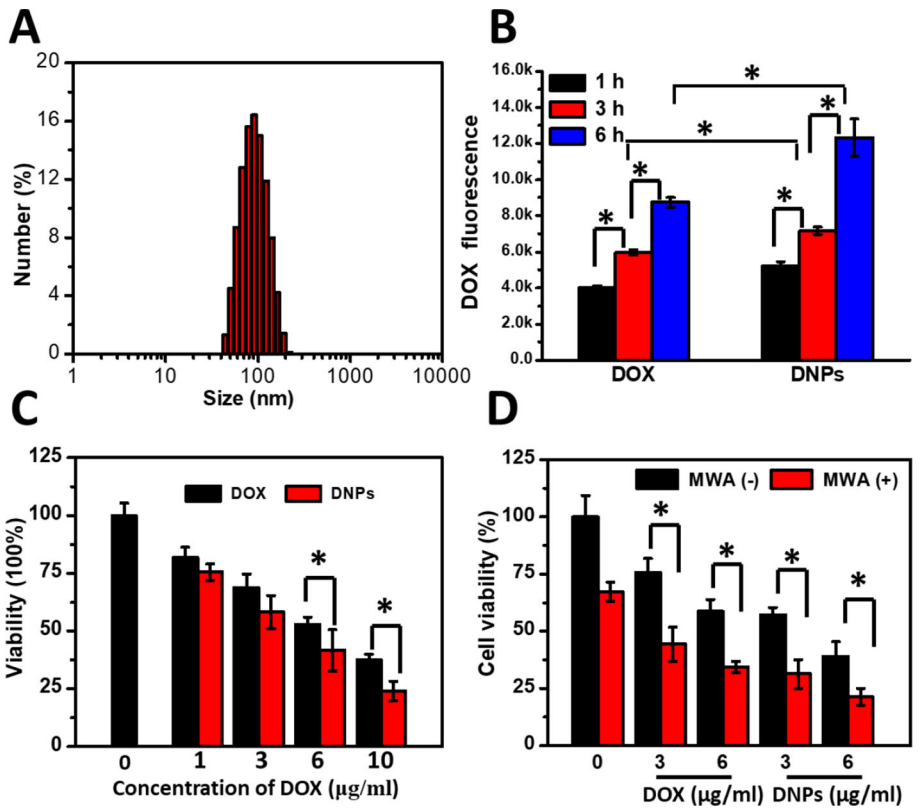

FIGURE 1 | Characterization and cellular uptake of DNPs and the ablation-chemo effect. **(A)** DLS distribution of DNPs. **(B)** Intracellular DOX fluorescence of HepG2 treated with DNPs by flow cytometry. **(C)** Cell survival of cells treated with DOX and DNPs for 8 h. **(D)** Survival of cells treated with MWA at 1.2 W for 4 min after free DOX and DNPs at different concentrations incubated for 8 h. *p < 0.05.

(**Figure 1B**). The difference was sustained over 1–6 h. The DOX uptake by DNPs increased 1.5-fold compared with that of free DOX (**Figure 1B**). The sensitivity of tumor cells to DNPs varied with the concentration when cell viability was tested using a standard Cell Counting Kit-8 (CCK-8) assay. The efficiency of cell death mediated by DNPs was positively correlated to the drug concentration and DOX encapsulation in liposomes showed better antitumor effects than DOX (**Figure 1C**). Cellular toxicity of DNPs was higher than free DOX, and cell viability of DNPs (41.65% ± 8.88%) was lower than that of DOX (52.77% ± 3.28%) at the concentration of 6.0 μg/ml, and the significance was obvious. Furthermore, another kind of human cancer cell, Huh7, was tested to validate the uptake and cytotoxicity experiments. The results showed that DNPs had higher fluorescence intensity compared with DOX (**Supporting S1**). The cytotoxicity of Huh7 was the same as the HepG2 result (**Supporting S2**).

To test whether MWA enhanced cellular toxicity mediated by DNPs, tumor cells were preincubated with DNPs and treated by MWA. MWA alone showed little cellular suppression at 1.2 W/cm^2 for 4 min, and cell viability was 67.3% ± 4.19% (**Figure 1D**). For the DNPs group, the viabilities were 57.15% ± 3.24% and 39.15% ± 6.24% at 3 μg/ml and 6 μg/ml, respectively. However, the combination of DOX and MWA enhanced cell death and the cell viability were 44.41% ± 7.52% and 34.41% ± 2.52% at 3 μg/ml and 6 μg/ml, respectively. An enhanced effect was observed with the combination of DNPs and MWA, the cell viability of 31.31% ± 6.18% and 21.31% ± 3.68% at 3 μg/ml and 6 μg/ml, respectively. Thus, chemoablation of DNPs exerted higher cellular toxicity than DOX, which is in accordance with the results of the cellular cytotoxicity test. In addition, we further tested MWA followed by DNPs. The results showed that DNPs followed by MWA had less viability than MWA followed by DNPs (**Supporting S3**). These experiments illustrated that chemoablation obtained better outcomes than ablation followed by chemotherapy.

In Vivo Imaging of DNPs in HCC by MRI

Gd-DTPA-HPDP encapsulated DNPs as MRI contrast agents can be easily tracked to visualise the drug delivery process through the measurement of T1 relaxation and various concentrations of liposomes. The corresponding quantitative analysis revealed that the MRI signal correlated linearly to the concentration of DNPs from 0 to 0.32 μM of Ga^{3+} (**Figure 2A**). An *in vivo* MRI scan was performed to investigate the accumulation of DNPs in tumors, and it showed a gradual increase in the MRI intensity of DNPs in the tumor, and over a 24 h continuous observation period, a sufficient amount of DNPs efficiently and passively targeted the tumor site (**Figure 2B**).

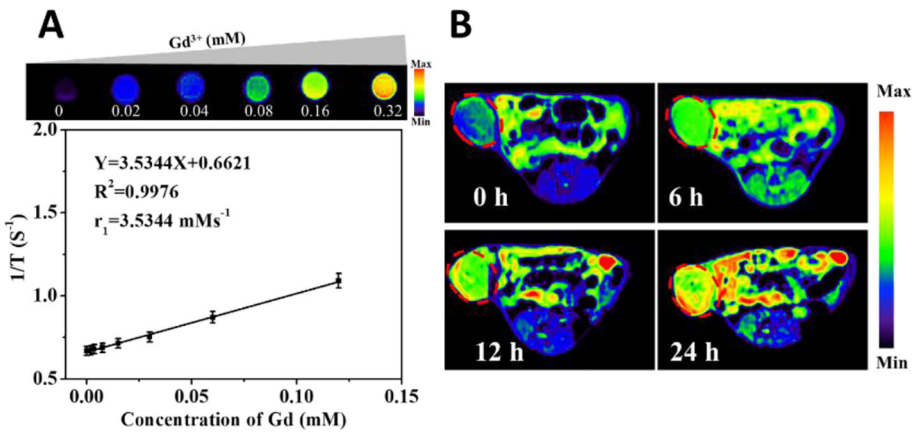

FIGURE 2 | MRI images of Gd-DTPA-HPDP encapsulated DNPs *in vivo*. **(A)** Quantitative curve of the MRI intensity of DNPs at different concentrations. **(B)** MRI images of mice at different time points after DNPs injection.

Ablation Chemotherapy in HCC Models

We measured the intra-tumoral temperature when MWA was carried out by 1 W/cm^2 for 60 s. The DNPs had a maximum temperature at 55.8°C, 56.3°C, and 58.3°C at 36, 48, and 60 s, respectively (**Figures 3A, B**). The maximum temperature of both the MWA and MWA + DOX group did not differ compared with the MWA + DNPs group (data not shown). Investigation of the antitumor properties of chemoablation in HCC models showed that tumors treated with DOX were not significantly different from the control group (1334.68 ± 420.15 mm^3 vs 1411.21 ± 209.71 mm^3) (**Figure 4A**). However, in the DNPs group, inhibition of tumor growth was significantly higher than that of the DOX group (969.37 ± 284.08 mm^3 vs 1411.21 ± 209.71 mm^3). Additionally, combination therapy of DNPs plus MWA injected twice led to a satisfactory tumor remission (256.44 ± 172.35 mm^3). It was noted that MWA and MWA + DOX inhibited tumor growth less effectively than MWA + DNPs, which was attributed to the ERP effect of DNPs (**Figure 4B**). Furthermore, the OS duration of mice treated with MWA, MWA + DOX, and MWA + DNPs significantly increased when compared with the control group. Survival of MWA + DNPs group was 100% on day 14.

On day 14 after MWA, the mean tumor weights were 750.46 ± 144.58 mg, 724.18 ± 189.99 mg, and 576.04 ± 170.4 mg for the control, DOX, and DNPs, respectively (**Figure 4C**). The reduction in tumor weight in the DNPs group confirmed that DNPs exerted a significant anticancer effect in HCC, owing to accumulated drug cytotoxicity. On the other hand, the mean tumor weights of MWA, MWA + DOX, and MWA + DNPs were 543.46 ± 129.64 mg, 275.98 ± 152.96 mg, and 129.7 ± 96.88 mg, respectively (**Figure 4C**), which shows that MWA treatment could significantly affect tumor growth. Since the weight curve

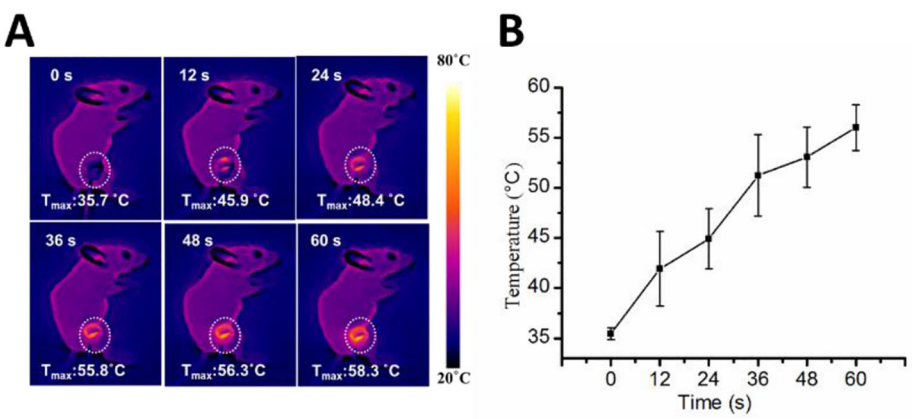

FIGURE 3 | Infrared thermo-graphic maps of the MWA process. **(A)** Infrared thermo-graphic maps of mice exposed to MWA for 1min at 1.2 W/cm^2. **(B)** Maximum temperature profiles of MWA after injection of DNPs after 24 h.

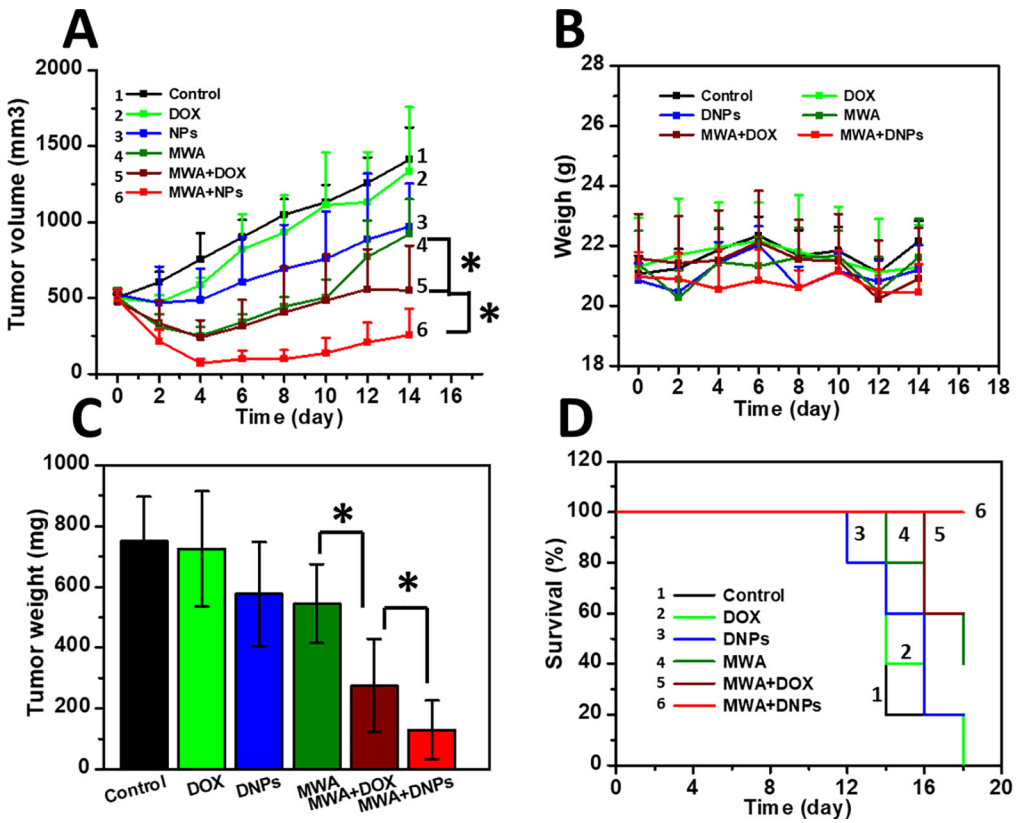

FIGURE 4 | Antitumor effect in HCC models. **(A)** Tumor growth curve of six mice groups after mild MWA treatment. **(B)** Survival curve of mice of six groups after mild MWA treatment. **(C)** tumor weights of all mice after being sacrificed on day 14. **(D)** Body weight change of mice curve for 14 days. *p < 0.05.

analysis showed no body weight loss during the observation period in all groups, there was no apparent systemic toxicity observed for any of the treatments after 14 days (**Figure 4D**).

Mild MWA Promoted Tumor Uptake of DNPs

Uptake of DNPs into the tumor and cells under mild MWA to mimic the transitional MWA condition showed increased tumor uptake of DNPs after MWA treatment. As shown in **Figure 5A**, an increase in fluorescence of DNPs with MWA duration was observed as fluorescence at 4 min after MWA was more intense than that at 3 min. This was true for both DOX and DNPs. DOX fluorescence was significantly lower than that of the DNPs, and quantitative analysis revealed that the cellular uptake of DNPs was increased 1.1-fold over DOX after mild MWA treatment for 4 min (**Figure 5B**). The cellular uptake of DNPs was significantly higher than that of DOX, as shown in the *in vivo* experiments (**Figure 5C**), where the DNPs in the transitional zone were much higher than those in the ablation zone.

In Vivo Toxicology Analysis

Toxicity associated with each treatment was investigated *via in vivo* blood biochemistry tests, and as shown in **Figures 6A–H**, MWA, DOX, DNPs, MWA + DOX, and MWA + DNPs showed no significant differences with the control group in the levels of these markers, indicating the favourable hepatic, heart, and renal safety profile of MWA, DOX, DNPs, MWA + DOX, and MWA + DNPs in mice.

DISCUSSION

There have been tremendous improvements in HCC therapy during the last two decades, especially in the use of minimal interventional therapies (Facciorusso et al., 2016; Salati et al., 2017; Shiina et al., 2018). Microwave ablation is one such method that has shown promising outcomes for HCC treatment, due to the rapid temperature increase and larger ablation compared with other modalities (Zhang et al., 2019). Despite being a promising technique for HCC ablation, MWA faces some challenges, including the limited ablation zone and the thermal injury risk for adjacent visceral tissues (Facciorusso et al., 2016). Since HCC tumors often recur after MWA, preventing or reducing HCC relapse after MWA is a major clinical challenge. However, we applied a combination therapy, which conferred more benefits than MWA alone, particularly for HCC or tumors adjacent to the gastrointestinal tract to surmount those challenges (Zhou et al., 2017).

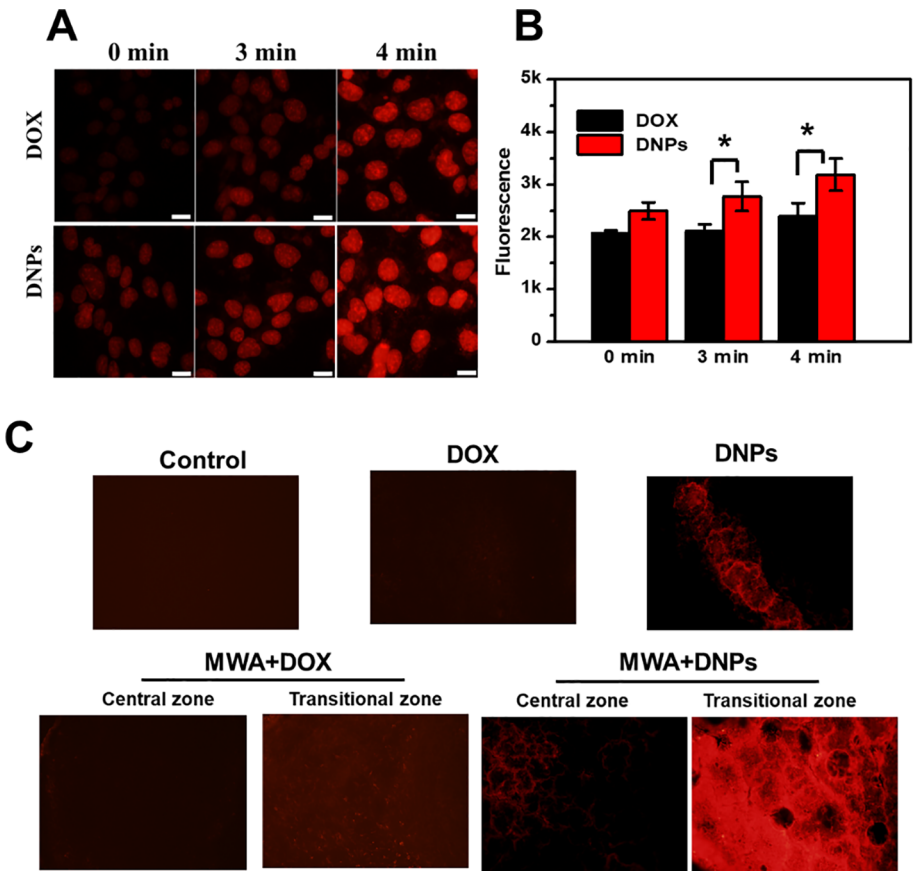

FIGURE 5 | Mild microwave ablation enhanced the tumor uptake of DNPs. **(A)** Cellular uptake of DNPs under mild MWA. **(B)** Quantitative cellular uptake of DOX and DNPs after mild MWA with multiplate reader. **(C)** Images of tumor tissue uptake of DNPs after mild MWA. *$p < 0.05$.

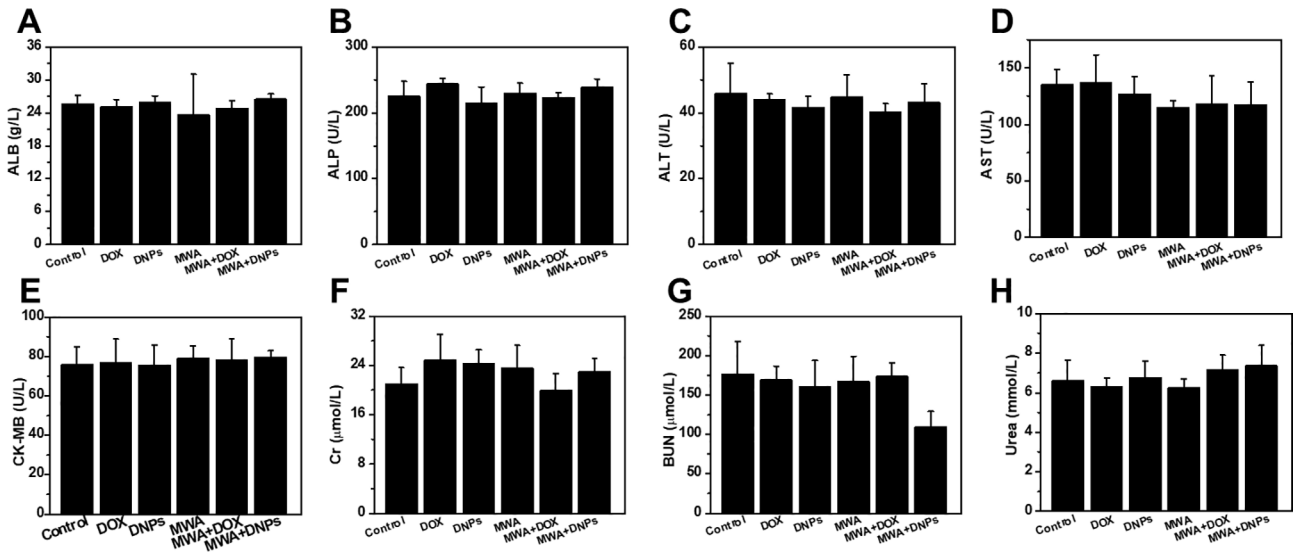

FIGURE 6 | Hepatic, heart, and kidney functional indicators of mice with different treatment. **(A)** ALB, **(B)** ALP, **(C)** ALT, **(D)** AST, **(E)** CK-MB, **(F)** Cr,**(G)** UN, **(H)** UREA vis blood biochemistry test.

The EPR effect endows nanoparticles with unique advantages over chemotherapy (Chen et al., 2018). In this study, we designed DNPs as an effective nanomedicine when combined with MWA to improve the outcome of HCC therapy. Intracellular DOX concentration of DNPs was higher than DOX by liposome-mediated cellular uptake, which led to higher cytotoxicity of DNPs than DOX. Chemotherapy in HCC often achieves underwhelming anticancer effects, and an urgent need for alternative approaches led to a combination therapy to treat HCC. The combination of ablation and nanoparticle-mediated chemotherapy has been demonstrated in several studies to significantly improve tumor control rates and prolong survival (Yang et al., 2012; Wang et al., 2016). We provided evidence in this study for the combination of MWA + DNPs to significantly suppress *in vivo* tumor growth compared with single treatment with DNPs and MWA, indicating that the combined effect was achieved. Our results suggest that the suppression mediated by MWA could be boosted by combination therapy. Thus, it is plausible that ablation with DNPs exceeded the outcome of MWA and increased its potency. Thus, combination therapy showed better antitumor properties than MWA alone.

Since tumor volume and weight in the MWA + DNPs group were significantly lower than that of other groups, it is plausible that the tumors were completely eradicated during treatment. For tumors larger than 5–10 cm, insufficient ablation of the periphery of the tumor often led to recurrent HCC. Therefore, in this study, we used mild MWA energy to mimic the transitional zone, where the resulting mild hyperthermia in the transitional zone increased tumor temperatures to 42°C, which could not kill all tumor cells (Chu and Dupuy, 2014). However, mild hyperthermia and its secondary effects may be directly lethal to some cancer cells and sensitise cells to chemotherapy (Solazzo et al., 2010). The tumor vascellums could be reconstructed by the thermal effect, and enhanced tumor uptake has been observed in previous photodynamic therapies. In our study, DNPs accumulated more in the transitional zone than in the ablation zone, which led to extravasation of nanoparticles at the site, (Zhen et al., 2014) resulting in a lethal effect on the tumors and an improvement in the outcome of MWA. This could be attributed to the open vasculature in the transitional zone that increased the accumulation of DNPs in the tumor. Our findings are robust and support the notion that further development of chemotherapeutic nanomedicine combined with MWA presents a promising and effective treatment strategy for HCC due to its optimal tumor-targeting properties and enhanced drug delivery efficacy.

CONCLUSION

In the present study, we described the development of DNPs, a nanoplatform comprising liposomes loaded with DOX that robustly enhance mild MWA therapy in HCC, indicating a substantial antitumor efficacy. Chemoablation therapy in the HCC model used in this study led to improved survival rates by enhancing the precision and efficiency of the targeted approach adopted. Thus, DNPs hold considerable promise for clinical HCC therapy as a result of its favourable HCC targeting properties.

DATA AVAILABILITY STATEMENT

All datasets generated for this study are included in the article/ **Supplementary Material**.

ETHICS STATEMENT

The animal study was reviewed and approved by the Chinese PLA General Hospital Animal Care and Use Committee.

AUTHOR CONTRIBUTIONS

PL designed the study. SW, DZ, JD, XL, and MM carried out the experiments. JY revised the manuscript. SW and PL wrote the manuscript.

ACKNOWLEDGMENTS

This work was supported by the National Natural Science Foundation of China (91859201)

SUPPLEMENTARY MATERIAL

The Supplementary Material for this article can be found online at: https://www.frontiersin.org/articles/10.3389/fphar.2020.00085/full#supplementary-material

REFERENCES

Chen, X., Fu, C., Wang, Y., Wu, Q., Meng, X., and Xu, K. (2018). Mitochondria-targeting nanoparticles for enhanced microwave ablation of cancer. *Nanoscale* 10, 15677–15685. doi: 10.1039/C8NR03927E

Chu, K. F., and Dupuy, D. E. (2014). Thermal ablation of tumors: biological mechanisms and advances in therapy. *Nat. Rev. Cancer* 14, 199–208. doi: 10.1038/nrc3672

Costentin, C. (2017). Hepatocellular carcinoma surveillance. *Presse Med.* 46, 381–385. doi: 10.1016/j.lpm.2016.11.006

Deng, Z., Yan, F., Jin, Q., Li, F., Wu, J., Liu, X., et al. (2014). Reversal of multidrug resistance phenotype in human breast cancer cells using doxorubicin-liposome-microbubble complexes assisted by ultrasound. *J. Control Release* 174, 109–116. doi: 10.1016/j.jconrel.2013.11.018

Dong, H., Pang, L., Cong, H., Shen, Y., and Yu, B. (2019). Application and design of esterase-responsive nanoparticles for cancer therapy. *Drug Delivery* 26, 416–432. doi: 10.1080/10717544.2019.1588424

El Dika, I., and Abou-Alfa, G. K. (2017). The role (if any) of chemotherapy in hepatocellular carcinoma. *Lancet Gastroenterol. Hepatol.* 2, 387–389. doi: 10.1016/S2468-1253(17)30104-8

Facciorusso, A., Di Maso, M., and Muscatiello, N. (2016). Microwave ablation versus radiofrequency ablation for the treatment of hepatocellular carcinoma: a systematic review and meta-analysis. *Int. J. Hyperthermia* 32, 339–344. doi: 10.3109/02656736.2015.1127434

Fang, Y., Li, H. Y., Yin, H. H., Xu, S. H., Ren, W. W., Ding, S. S., et al. (2019). Radiofrequency-sensitive longitudinal relaxation tuning strategy enabling the visualization of radiofrequency ablation intensified by magnetic composite. *ACS Appl. Mater Interfaces* 11, 11251–11261. doi: 10.1021/acsami.9b02401

Huang, L., Zhou, K., Zhang, J., Ma, Y., Yang, W., Ran, L., et al. (2019). Efficacy and safety of high-intensity focused ultrasound ablation for hepatocellular carcinoma by changing the acoustic environment: microbubble contrast agent (SonoVue) and transcatheter arterial chemoembolization. *Int. J. Hyperthermia* 36, 244–252. doi: 10.1080/02656736.2018.1558290

Jha, S., Sharma, P. K., and Malviya, R. (2016). Liposomal drug delivery system for cancer therapy: advancement and patents. *Recent Pat. Drug Delivery Formul.* 10, 177–183. doi: 10.2174/1872211310666161004155757

Johnson, B. W., and Wright, G. P. (2019). Regional therapies for the treatment of primary and metastatic hepatic tumors: a disease-based review of techniques and critical appraisal of current evidence. *Am. J. Surg.* 217, 541–545. doi: 10.1016/j.amjsurg.2018.10.018

Lyu, N., Kong, Y., Mu, L., Lin, Y., Li, J., Liu, Y., et al. (2018). Hepatic arterial infusion of oxaliplatin plus fluorouracil/leucovorin vs. sorafenib for advanced hepatocellular carcinoma. *J. Hepatol.* 69, 60–69. doi: 10.1016/j.jhep.2018.02.008

Mu, L., Sun, L., Pan, T., Lyu, N., Li, S., Li, X., et al. (2018). Percutaneous CT-guided radiofrequency ablation for patients with extrahepatic oligometastases of hepatocellular carcinoma: long-term results. *Int. J. Hyperthermia* 34, 59–67. doi: 10.1080/02656736.2017.1318332

Salati, U., Barry, A., Chou, F. Y., Ma, R., and Liu, D. M. (2017). State of the ablation nation: a review of ablative therapies for cure in the treatment of hepatocellular carcinoma. *Future Oncol.* 13, 1437–1448. doi: 10.2217/fon-2017-0061

Shiina, S., Sato, K., Tateishi, R., Shimizu, M., Ohama, H., Hatanaka, T., et al. (2018). Percutaneous ablation for hepatocellular carcinoma: comparison of various ablation techniques and surgery. *Can. J. Gastroenterol. Hepatol.* 2018, 4756147. doi: 10.1155/2018/4756147

Siegel, R. L., Miller, K. D., and Jemal, A. (2019). Cancer statistics, 2019. *CA Cancer J. Clin.* 69, 7–34. doi: 10.3322/caac.21551

Solazzo, S. A., Ahmed, M., Schor-Bardach, R., Yang, W., Girnun, G. D., Rahmanuddin, S., et al. (2010). Liposomal doxorubicin increases radiofrequency ablation-induced tumor destruction by increasing cellular oxidative and nitrative stress and accelerating apoptotic pathways. *Radiology* 255, 62–74. doi: 10.1148/radiol.09091196

Wang, S., Mei, X. G., Goldberg, S. N., Ahmed, M., Lee, J. C., Gong, W., et al. (2016). Does thermosensitive liposomal vinorelbine improve end-point survival after percutaneous radiofrequency ablation of liver tumors in a mouse model? *Radiology* 279, 762–772. doi: 10.1148/radiol.2015150787

Wang, Y., Huang, H., Zou, H., Tian, X., Hu, J., Qiu, P., et al. (2019). Liposome encapsulation of oncolytic virus M1 to reduce immunogenicity and immune clearance *in vivo*. *Mol. Pharm.* 16, 779–785. doi: 10.1021/acs.molpharmaceut.8b01046

Xu, J., Cheng, X., Tan, L., Fu, C., Ahmed, M., Tian, J., et al. (2019). Microwave responsive nanoplatform *via* P-selectin mediated drug delivery for treatment of hepatocellular carcinoma with distant metastasis. *Nano Lett.* 19, 2914–2927. doi: 10.1021/acs.nanolett.8b05202

Yan, F., Wang, S., Yang, W., Goldberg, S. N., Wu, H., Duan, W. L., et al. (2017). Tumor-penetrating peptide-integrated thermally sensitive liposomal doxorubicin enhances efficacy of radiofrequency ablation in liver tumors. *Radiology* 285, 462–471. doi: 10.1148/radiol.2017162405

Yang, W., Ahmed, M., Tasawwar, B., Levchenko, T., Sawant, R. R., Torchilin, V., et al. (2012). Combination radiofrequency (RF) ablation and IV liposomal heat shock protein suppression: reduced tumor growth and increased animal endpoint survival in a small animal tumor model. *J. Control Release* 160, 239–244. doi: 10.1016/j.jconrel.2011.12.031

Yang, R., Hou, M., Gao, Y., Zhang, L., Xu, Z., Kang, Y., et al. (2019). Indocyanine green-modified hollow mesoporous Prussian blue nanoparticles loading doxorubicin for fluorescence-guided tri-modal combination therapy of cancer. *Nanoscale* 11, 5717–5731. doi: 10.1039/C8NR10430A

Yu, J., Yu, X. L., Han, Z. Y., Cheng, Z. G., Liu, F. Y., Zhai, H. Y., et al. (2017). Percutaneous cooled-probe microwave versus radiofrequency ablation in early-stage hepatocellular carcinoma: a phase III randomised controlled trial. *Gut* 66, 1172–1173. doi: 10.1136/gutjnl-2016-312629

Zhang, D., Liang, W., Zhang, M., Liang, P., Gu, Y., Kuang, M., et al. (2019). Multiple antenna placement in microwave ablation assisted by a three-dimensional fusion image navigation system for hepatocellular carcinoma. *Int. J. Hyperthermia* 35, 122–132. doi: 10.1080/02656736.2018.1484183

Zhen, Z., Tang, W., Chuang, Y. J., Todd, T., Zhang, W., Lin, X., et al. (2014). Tumor vasculature targeted photodynamic therapy for enhanced delivery of nanoparticles. *ACS Nano* 8, 6004–6013. doi: 10.1021/nn501134q

Zhou, Q., Wu, S., Gong, N., Li, X., Dou, J., Mu, M., et al. (2017). Liposomes loading sodium chloride as effective thermo-seeds for microwave ablation of hepatocellular carcinoma. *Nanoscale* 9, 11068–11076. doi: 10.1039/C7NR02955A

Zhu, K., Huang, J., Lai, L., Huang, W., Cai, M., Zhou, J., et al. (2018). Medium or large hepatocellular carcinoma: sorafenib combined with transarterial chemoembolization and radiofrequency ablation. *Radiology* 288, 300–307. doi: 10.1148/radiol.2018172028

Conflict of Interest: The authors declare that the research was conducted in the absence of any commercial or financial relationships that could be construed as a potential conflict of interest.

frontiers in Pharmacology

REVIEW
published: 28 April 2020
doi: 10.3389/fphar.2020.00524

Advances in Oral Drug Delivery for Regional Targeting in the Gastrointestinal Tract - Influence of Physiological, Pathophysiological and Pharmaceutical Factors

Susan Hua [1,2]*

[1] Therapeutic Targeting Research Group, School of Biomedical Sciences and Pharmacy, University of Newcastle, Callaghan, NSW, Australia, [2] Hunter Medical Research Institute, New Lambton Heights, NSW, Australia

The oral route is by far the most common route of drug administration in the gastrointestinal tract and can be used for both systemic drug delivery and for treating local gastrointestinal diseases. It is the most preferred route by patients, due to its advantages, such as ease of use, non-invasiveness, and convenience for self-administration. Formulations can also be designed to enhance drug delivery to specific regions in the upper or lower gastrointestinal tract. Despite the clear advantages offered by the oral route, drug delivery can be challenging as the human gastrointestinal tract is complex and displays a number of physiological barriers that affect drug delivery. Among these challenges are poor drug stability, poor drug solubility, and low drug permeability across the mucosal barriers. Attempts to overcome these issues have focused on improved understanding of the physiology of the gastrointestinal tract in both healthy and diseased states. Innovative pharmaceutical approaches have also been explored to improve regional drug targeting in the gastrointestinal tract, including nanoparticulate formulations. This review will discuss the physiological, pathophysiological, and pharmaceutical considerations influencing drug delivery for the oral route of administration, as well as the conventional and novel drug delivery approaches. The translational challenges and development aspects of novel formulations will also be addressed.

Keywords: gastrointestinal, oral, drug delivery, gastroretentive, small intestine, colon, nanomedicine, formulation, translation

OPEN ACCESS

Edited by:
Salvatore Salomone, University of Catania, Italy

Reviewed by:
Juan M. Irache, University of Navarra, Spain
Maria Helena Andrade Santana, Campinas State University, Brazil

***Correspondence:**
Susan Hua
Susan.Hua@newcastle.edu.au

Specialty section:
This article was submitted to Experimental Pharmacology and Drug Discovery, a section of the journal Frontiers in Pharmacology

Received: *05 September 2019*
Accepted: *03 April 2020*
Published: *28 April 2020*

Citation:
Hua S (2020) Advances in Oral Drug Delivery for Regional Targeting in the Gastrointestinal Tract - Influence of Physiological, Pathophysiological and Pharmaceutical Factors. Front. Pharmacol. 11:524. doi: 10.3389/fphar.2020.00524

INTRODUCTION

The oral route is by far the most common route for drug administration in the gastrointestinal tract (GI tract) and can be used for both systemic drug delivery and for treating local gastrointestinal diseases. It is the most preferred route by patients, due to its advantages, such as ease of use, non-invasiveness, and convenience for self-administration (Shreya et al., 2018; Homayun et al., 2019).

Formulations can also be designed to enhance drug delivery to specific regions in the upper or lower GI tract. The upper GI tract consists of the mouth, pharynx, esophagus, stomach, and the first part of the small intestine (duodenum), whereas the lower GI tract includes the other parts of the small intestine (jejunum and ileum) and the large intestine (cecum, colon, and rectum) (Marieb and Hoehn, 2010; Reinus and Simon, 2014). Drugs administered *via* the oral route, however, generally have slower absorption, which is not preferred during an emergency (Homayun et al., 2019). They might also be unpleasant in taste, cause gastric irritation, and/or undergo first-pass drug elimination processes in both the intestine and liver (Martinez and Amidon, 2002; Homayun et al., 2019). In addition, the physiological environment in the GI tract can also affect the stability and solubility of drugs (Martinez and Amidon, 2002; Shreya et al., 2018; Homayun et al., 2019).

There are generally three main goals in formulation design for the oral route of gastrointestinal drug delivery (Martinez and Amidon, 2002): (i) local drug delivery to treat gastrointestinal disease, whereby the drug generally needs to be taken up into gastrointestinal mucosa but will not be systemically absorbed or will be poorly absorbed; (ii) systemic drug delivery, where drug absorption needs to be able to traverse the mucosal wall into the systemic circulation; and (iii) increase dissolution rate of poorly soluble drugs, which generally does not require the formulation to cross the mucosa or cells. Drug absorption in the GI tract is governed by many factors such as surface area for absorption, blood flow to the site of absorption, the physical state of the drug (such as a solution, suspension or solid dosage form), its water solubility, and the concentration of the drug at the site of absorption (Martinez and Amidon, 2002; Brunton et al., 2018). For absorption to occur, drugs must be able to penetrate the epithelium, which is the innermost layer that forms a continuous lining of the entire GI tract. This epithelial cell barrier selectively regulates transport from the lumen to the underlying tissue compartment. Drug molecules can be transported passively *via* paracellular diffusion (between cells) and transcellular diffusion (through the cell) or actively *via* receptor-mediated endocytosis and carrier-mediated transport. Of these pathways, the transcellular route is the main mechanism of drug absorption in the GI tract and is usually proportional to the lipid solubility of the drug (Brunton et al., 2018; Homayun et al., 2019). Therefore, absorption is favored when the drug molecule is in the non-ionized form, which is much more lipophilic than the ionized form.

Oral drug delivery is a significant area of formulation research due to the aforementioned advantages for patients. Significant pharmaceutical advances have been made to improve the regional targeting of drugs in the GI tract, however very few of them have translated to the clinical phase. This review will discuss the physiological, pathophysiological, and pharmaceutical considerations influencing drug delivery for the oral route of administration, as well as the conventional and novel drug delivery approaches. The translational challenges and development aspects of novel formulations will also be addressed.

FUNCTIONAL ANATOMY

The GI tract is a muscular tube that is approximately 9 meters in length with varying diameters. The main functions of the GI tract are the digestion of food, absorption of nutrients, and excretion of waste products (Marieb and Hoehn, 2010; Reinus and Simon, 2014). Following oral administration, food and pharmaceuticals transit through the esophagus to the stomach, aided by peristaltic contractions. Most of the digestion then takes place in the stomach by the action of acid and enzymes, especially peptidases (Reinus and Simon, 2014). The stomach also acts as a temporary reservoir for ingested food before it is delivered to the duodenum at a controlled rate. Very little drug absorption occurs in the stomach owing to its small surface area.

The small intestine is the longest (approximately 6 meters in length) and most convoluted part of the GI tract, where digestion is completed with enzymes from the liver and the pancreas, and most of the absorption of nutrients then takes place (Marieb and Hoehn, 2010; Reinus and Simon, 2014). The small intestine is also the major site of drug absorption, due to its large surface area. The surface area of the small intestine is increased enormously to approximately 200 m^2 in an adult owing to the presence of villi and microvilli that are well supplied with blood vessels (Marieb and Hoehn, 2010; Reinus and Simon, 2014). Villi are finger-like projections that protrude into the intestinal lumen and are covered by epithelial cells. Interestingly, Helander et al. recently recalculated the mucosal surface area of the intestine in humans using morphometric data obtained by light and electron microscopy on biopsies from healthy adult volunteers or patients with endoscopically normal mucosae. They reported a mean total mucosal surface area of approximately 32 m^2 for the interior of the GI tract, with approximately 2 m^2 representing the large intestine (Helander and Fandriks, 2014).

The large intestine is the final major part of the GI tract. Its primary function is to process the waste products and absorb any remaining nutrients and water back into the system, which is important for homeostasis (Reinus and Simon, 2014). The remaining waste is then sent to the rectum and discharged from the body as stool. The colon has been investigated as a site for both systemic and local drug delivery. Anatomically, it can be further divided into four parts — ascending, transverse, descending, and sigmoid colon. The mucosa of the colon is smooth and has no specialized villi, hence the surface area is vastly smaller than the small intestine (Marieb and Hoehn, 2010; Reinus and Simon, 2014). However, the surface area of the large intestinal epithelium is amplified by being arranged into crypt structures. The colon is permanently colonized by an extensive number and variety of bacteria, which form the microbiome (Consortium, 2012; Reinus and Simon, 2014).

PHYSIOLOGICAL FACTORS INFLUENCING ORAL DRUG DELIVERY

Despite the clear advantages offered by the oral route, drug delivery can be challenging as the human GI tract is complex and

displays a number of physiological barriers that affect drug delivery. Among these challenges are poor drug solubility, poor drug stability, and low drug permeability across the mucosal barriers (Martinez and Amidon, 2002). Even within healthy individuals, there is variability in the physiology of the GI tract (**Figure 1**). Therefore, considerations should be made during formulation design to the following factors (Martinez and Amidon, 2002; Hua et al., 2015): (i) how long the formulation resides in specific sections of the GI tract; (ii) the influence of the gastrointestinal environment on the delivery of the formulation at the site of action as well as on the stability and solubility of the drug; (iii) the intestinal fluid volume; and (iv) the degree of metabolism of the drug or formulation in the GI tract through microbial or enzymatic degradation.

Gastrointestinal Transit Time

Gastrointestinal transit time is an important factor for dosage forms and drugs that have region-specific targeting or absorption properties (**Figure 1**). The amount of time needed for a dosage form to leave the stomach is highly variable and can range from several minutes to several hours (Reinus and Simon, 2014). Gastric transit time depends on many physiological factors, including age, body posture, gender, osmolarity, and food intake (Timmermans and Moes, 1994; Kagan and Hoffman, 2008). For example, gastric transit can range from 0 to 2 h in the fasted state and can be prolonged up to 6 h in the fed state (Reinus and Simon, 2014). In general, the transit time in the small intestine is considered relatively constant at around 3 to 4 h (Hu et al., 2000). However, this can range from 2 to 6 h in healthy individuals (Reinus and Simon, 2014). Colonic transit times can be highly variable, with ranges from 6 to 70 h reported (Coupe et al., 1991; Rao et al., 2004). Additional confounders affecting gastrointestinal transit time include the time of dosing in relation to an individual's bowel movements (Sathyan et al., 2000) and gender, with females having significantly longer colonic transit times (Buhmann et al., 2007).

Gastrointestinal pH

With regards to the gastrointestinal environment, differences in pH along the GI tract have been exploited for the purposes of delayed release therapies (**Figure 1**). The highly acidic gastric environment (pH 1.5–2 in the fasted state) rises rapidly to pH 6 in the duodenum and increases along the small intestine to pH 7.4 at the terminal ileum (Fallingborg et al., 1993; Bratten and Jones, 2006). It should be noted that the pH in the cecum drops just below pH 6 and again rises in the colon reaching pH 6.7 at the rectum (Evans et al., 1988; Sasaki et al., 1997; Nugent et al., 2001). However, individuals can exhibit variability in pH ranges, with factors such as dietary intake (i.e., food and fluids) as well as microbial metabolism being major determinants (Ibekwe et al., 2008). For example, gastric pH can increase to 3–6 in the fed state. Gastrointestinal pH can also affect the ionization state of drug molecules, which in turn influences drug absorption (Brunton et al., 2018).

Gastrointestinal Mucus

The continuous secretion of mucus in the GI tract is another hurdle for the effective oral delivery of drugs. Mucus secretion acts as a lubricant to facilitate the passage of digestive matter and to protect the underlying epithelium from pathogens and mechanical stress (Atuma et al., 2001). The mucus is composed of water and mucin protein molecules coated with proteoglycans, which gives the mucus a negative charge (Homayun et al., 2019). The mouth and esophagus do not have a distinct mucus layer, but they are washed by mucus from the salivary glands (Johansson et al., 2013). The small

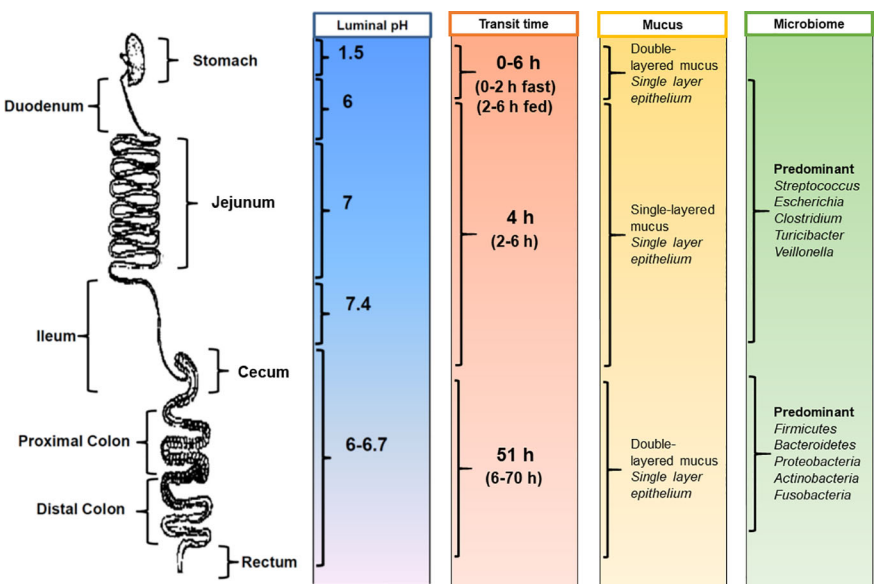

FIGURE 1 | Physiological factors in the gastrointestinal tract that influence oral drug delivery. [Adapted from (Hua et al., 2015)].

intestine has only one type of mucus that is unattached and loose (Atuma et al., 2001; Johansson et al., 2013). In contrast, the stomach and colon have the thickest mucus layer in the GI tract, with a two-layered mucus system comprising of: (i) an inner, attached mucus layer and (ii) an outer, unattached, loose mucus layer (Atuma et al., 2001; Johansson et al., 2013) (**Figure 1**). The thick mucus layer protects the mucosal tissue from gastric acid in the stomach and also provides a stable environment for the enteric microflora in the colon (Macfarlane et al., 1988; Atuma et al., 2001). It should be noted that mucus is continuously secreted by goblet cells along the GI tract and is subsequently shed and cleared from tissues due to the turnover of cells (Homayun et al., 2019). For drug delivery, the mucus layer acts as an important barrier for the permeability of drug molecules (especially hydrophobic molecules) and can also decrease the residence time of drugs and dosage forms.

Intestinal Fluid Volume

Control of luminal fluidity is central to gastrointestinal function (Chowdhury and Lobo, 2011; Reinus and Simon, 2014). For example, the fluid environment permits contact of digestive enzymes with food particles, assists in the transit of intestinal contents along the length of the GI tract without damage to the epithelial lining, and supports the dissolution and absorption of nutrients and drugs (Reinus and Simon, 2014). Daily water balance in the healthy adult human GI tract includes secretion from saliva (1.5 L), gastric juice (2.5 L), pancreatic juice (1.5 L) and other intestinal components (~1 L), as well as absorption from the small intestine (7 L) and large intestine (1.9 L) (Reinus and Simon, 2014). Fluid-to-matter ratios influence pH and may also affect drug delivery and drug absorption, particularly in the lower GI tract. For example, food intake can significantly alter free fluid volumes, bile salts, and digestive enzyme levels in the GI tract (Reinus and Simon, 2014). In addition, the viscosity of the mucous-gel layer is affected by intestinal fluid secretion (Johansson et al., 2013; Reinus and Simon, 2014), which may influence the ability of drugs to be taken up by cells at the site of action. Increased fluid secretion and decreased reabsorption can dilute digestive enzymes and alter the intestinal microbiome. This can affect carbohydrate and polysaccharide digestion (Yang, 2008) as well as contribute to changes in intestinal transit times (Van Citters and Lin, 2006). Therefore, changes in intestinal fluid volumes can influence the way conventional formulations are processed in the GI tract.

Gastrointestinal Enzymes and Microbiome

Enzymatic and microbial degradation of drugs and dosage forms can occur throughout the GI tract. **Table 1** shows the main enzymes in the saliva, gastric fluid, and intestinal fluid that are important in the metabolism of proteins, fats, and carbohydrates. The stomach and small intestine are the site of action for the major enzymes involved in the digestion of food (Marieb and Hoehn, 2010; Reinus and Simon, 2014). These enzymes can affect the stability of susceptible drugs and dosage forms, but they can also be exploited in formulation design for regional drug delivery in the GI tract.

TABLE 1 | Main enzymes in the gastrointestinal tract.

Enzyme	Produced by	Site of action
Salivary amylase	Salivary glands	Mouth
Pancreatic amylase	Pancreas	Small intestine
Maltase	Small intestine	Small intestine
Pepsin	Gastric glands	Stomach
Trypsin	Pancreas	Small intestine
Peptidases	Small intestine	Small intestine
Nuclease	Pancreas	Small intestine
Nucleosidases	Small intestine	Small intestine
Lipase	Pancreas	Small intestine

The intestinal microbiome, which contains over 500 distinct bacterial species (Sartor, 2008; Consortium, 2012), is also important for both digestion and intestinal health, including digestion and metabolism of carbohydrates, fatty acids, and proteins (Macfarlane and Macfarlane, 2011) (**Figure 1**). The majority of the intestinal microbiome resides in the anaerobic colon and fermentation of carbohydrates is the main source of nutrition for this population (Macfarlane and Macfarlane, 2011). This has been exploited in formulation design with the use of non-starch polysaccharide coatings, which undergo relatively exclusive fermentation by the colonic microbiome (Sinha and Kumria, 2001). Both genetic and environmental factors contribute to the considerable variation in the composition of the microbiome that is seen between individuals (Sartor, 2010). However, the dominant species (*Firmicutes*, *Bacteroidetes*, *Proteobacteria*, *Actinobacteria*, and *Fusobacteria*) appear to be consistent and represent the majority of the colonic flora (Frank et al., 2007; Consortium, 2012).

Interestingly, the gastrointestinal microbiome not only resides in the large intestine but is also found in the small intestine. In comparison to the large intestine, the density of the small intestinal microbiota is much lower, which is likely due to the rapid luminal flow, intestinal fluid volume, and the secretion of bactericidal compounds in this part of the GI tract (El Aidy et al., 2015). In addition, the composition of the microbiome in the small intestine can significantly fluctuate over a short period of time (e.g., within a day to several days) and is influenced by variations in dietary intake (Booijink et al., 2010). The small intestinal microbiota (El Aidy et al., 2015) is predominantly composed of subject-specific genera such as Clostridium, Escherichia, and Turicibacter in variable amounts. Streptococcus and Veillonella species are also consistently found in the small intestine. This endogenous microenvironment is thought to play a pivotal role in metabolic regulation (El Aidy et al., 2015). The effect of the small intestinal microbiota on oral dosage forms and drug absorption has not yet been elucidated.

PATHOPHYSIOLOGICAL FACTORS INFLUENCING ORAL DRUG DELIVERY

Adding to this complexity are the changes in gastrointestinal physiology associated with gastrointestinal or systemic disease, concurrent medications, and gastrointestinal surgery. These

factors are dynamic, inter-related, and can further affect the efficacy of orally administered formulations. Therefore, they remain an important challenge in formulation design.

Impact of Disease on Oral Drug Delivery

Depending on disease severity, gastrointestinal pathologies can affect some or all of the physiological variables for oral drug delivery (Hatton et al., 2018). For example, many acute gastrointestinal infections can cause temporal impairment in the microbiome (dysbiosis) (Britton and Young, 2014), drive increased intestinal fluid secretion (Patel and McCormick, 2014), and may increase or decrease bowel motility (Grover et al., 2008; Albenberg and Wu, 2014). These can affect the performance of locally acting dosage forms. For example, increased colonic motility in diarrhea can lead to reduced retention of locally acting dosage forms and incomplete drug release (Watts et al., 1992). In addition, toxins secreted by intestinal pathogens can cause intestinal inflammation and increased epithelial permeability, which may alter the concentration of drugs in the colonic mucosa (Hoque et al., 2012; Hatton et al., 2018).

In contrast, chronic diseases, such as inflammatory bowel disease (IBD), can cause significant changes to the physiology of the GI tract. IBD encompasses a group of chronic relapsing gastrointestinal diseases. The two main subtypes of IBD are Crohn's disease and ulcerative colitis (Podolsky, 2002). Both are considered distinct conditions, however, they can display many similar clinical features and typically result in cycles of remitting and relapsing inflammation of the mucosal tissue. The inflammation is continuous in UC and is confined to the colon (Podolsky, 2002). In some cases, the entire colon can also be affected (pancolitis). Crohn's inflammation, however, is generally discontinuous in manner and can affect any region of the GI tract. The commonly affected regions include the terminal ileum and the colon (Podolsky, 2002). The physiological changes associated with chronic inflammation of the GI tract should be considered in the development of improved oral delivery strategies for the management of IBD (Hua et al., 2015). Mucosal inflammation in IBD causes pathophysiological changes, such as: (i) increased mucus production; (ii) a disrupted intestinal barrier due to the presence of mucosal surface alterations, ulcers, and crypt distortions; and (iii) infiltration of immune cells (e.g., macrophages, lymphocytes, neutrophils, and dendritic cells) (Li and Thompson, 2003; Antoni et al., 2014). Together these changes can increase colonic epithelial permeability.

During relapse of IBD, patients suffering from severe mucosal inflammation may exhibit altered gastrointestinal motility and diarrhea, which in turn affects intestinal volume, pH, and mucosal integrity (Hua et al., 2015). In general, delayed orocecal transit times (i.e., the time taken for the meal to reach the cecum) have been reported in IBD patients, except when patients experience dysbiotic conditions (e.g., small intestinal bacterial overgrowth, SIBO) which can be associated with faster transit times (Kashyap et al., 2013; Rana et al., 2013). Studies have also shown that the colonic pH in IBD patients can be highly variable in terms of disease progression and severity, with some patients having more acidic colonic pH in the range of 2.3–5.5 (Fallingborg et al., 1993; Sasaki et al., 1997; Nugent et al., 2001). The inflammatory response at the mucosa, along with severe diarrhea, will also disrupt the resident microbiome by affecting the composition and diversity of the bacterial species (Linskens et al., 2001). This, in turn, can alter microbial metabolism in the GI tract and affect the secretion of enzymes. Therefore, active inflammation significantly alters the physiology of the GI tract, which can particularly affect the efficacy of conventional oral drug delivery approaches (Hua et al., 2015).

Furthermore, there is increasing evidence showing that non-gastrointestinal systemic diseases can also cause physiological and functional changes in the GI tract that can affect the performance of oral dosage forms and the absorption of drugs. This includes cystic fibrosis, Parkinson's disease, diabetes, HIV infection, and pain (Hatton et al., 2019). For example, pain can alter gastrointestinal physiology by affecting motility, secretion, intestinal permeability, mucosal blood flow, and the intestinal microbiome (Konturek et al., 2011).

Impact of Drugs on Oral Drug Delivery

Drugs can alter the physiology of the GI tract and affect the performance of other co-administered oral dosage forms and the absorption of other drugs. For example, drugs used to reduce gastric acid secretion (e.g., proton pump inhibitors and histamine H2-receptor antagonists) or modify pH (e.g., antacids) (Lahner et al., 2009; Brunton et al., 2018) can affect dosage forms that rely on the difference in pH in various regions of the GI tract to trigger drug release. Drugs that alter the motility of the GI tract can also have an impact on the effectiveness of oral drug delivery by affecting the time available for disintegration, dissolution, and/or drug absorption (Watts et al., 1992; Brunton et al., 2018). This includes the following: (i) drugs that act as prokinetics to stimulate gastrointestinal motility (e.g., metoclopramide, domperidone, and cisapride); (ii) drugs that can cause constipation (e.g., opioids, anticholinergic agents, antidiarrheal agents, antacids containing aluminium or calcium, iron/calcium supplements, diuretics, verapamil, and clonidine); and drugs that can cause diarrhea (e.g., laxatives, antibiotics, colchicine, cytotoxic agents, digoxin, magnesium, NSAIDs, orlistat, acarbose, and metformin). In addition, administration of antibiotics can cause dysbiosis (Sartor, 2010; Albenberg and Wu, 2014) and negatively affect biodegradable dosage forms that rely on enzymes of the microbiome for drug release. Therefore, co-administration of other drugs may cause inter-individual and intra-individual variability with respect to oral drug delivery and should be considered in oral formulation design, especially for specific disease indications.

Impact of Gastrointestinal Surgery on Oral Drug Delivery

Surgical resections of the stomach, small intestine or large intestine can significantly affect gastrointestinal anatomy and

physiology, as well as the effectiveness of oral dosage forms and drug absorption (Titus et al., 2013; Hua et al., 2015; Hatton et al., 2018). Partial gastric resection or bypass is performed for the treatment of peptic ulcer disease, malignancy, and as a means of weight loss. Although most drugs are minimally absorbed in the stomach, gastric resections and bariatric surgeries can affect gastric emptying and transit time (Titus et al., 2013). For example, vagotomy can delay gastric emptying, whereas resection of the pylorus can accelerate gastric emptying (Titus et al., 2013).

Intestinal resections can be the result of a number of diseases, including in severe IBD, malignancy, and in intestinal malrotation with ischemia. In general, small resections usually pose minimal issues for oral drug delivery, as the remaining intestine can compensate so that no functionality is lost (Kvietys, 1999; Titus et al., 2013). However, when large resections (usually greater than 50%) are performed, there may be profound changes in gastrointestinal function, including motility and drug absorption. For example, shortening of the intestine can reduce the transit distance through the GI tract, which potentially affects the way conventional oral formulations are processed (Kvietys, 1999; Titus et al., 2013). Resection can also significantly change the physiology of the intestinal tract by altering pH, digestion, transit, and nutrient absorption (Spiller et al., 1988; Schmidt et al., 1996; Fallingborg et al., 1998). For example, surgery is one of the main treatments for colorectal cancer which is defined as the development of malignant cells in the colonic epithelium (Patel, 2014; Banerjee et al., 2017). For more advanced disease, a colectomy (surgical procedure to remove all or part of the colon) is required, which will alter the local microenvironment and physiology of the GI tract (Titus et al., 2013). Many IBD patients also undergo surgical resection of intestinal tissues (Byrne et al., 2007). Consequences of these resections include a shortened bowel that may have associated implications for oral dosage form design. This includes altering luminal pH and transit times, impairing regulation of the ileal brake that controls food transit, and reduction of small chain fatty acid digestion (Kvietys, 1999; Titus et al., 2013; Hua et al., 2015).

Similarly, profound changes in gastrointestinal physiology and drug delivery can occur when specific segments of the GI tract are resected. In particular, resection of the terminal ileum alters water absorption and dilutes residual bile acids in the colon, thereby reducing net colonic fatty acid concentrations (Thompson et al., 1998; Gracie et al., 2012). The decrease in fatty acids reduces the ileal brake, which is a nutrient feedback mechanism that slows transit times to allow nutrient absorption (Van Citters and Lin, 1999; Van Citters and Lin, 2006). As fatty acids are the most potent stimulant of the ileal brake, a loss of both fatty acids from digestion and fatty acid receptors from resected tissue lead to a loss of the ileal brake (Lin et al., 2005) and, therefore, cause more rapid intestinal transit and less time for absorption. The terminal ileum is also responsible for bile salt reabsorption and, when removed, can become problematic and is generally manifested by choleretic diarrhea (Titus et al., 2013) that can significantly affect the therapeutic efficacy of conventional oral formulations.

CONVENTIONAL ORAL DRUG DELIVERY APPROACHES

The main formulations used for oral drug delivery are liquid dosage forms (such as solutions and suspensions) and solid dosage forms (such as tablets and capsules) (Allen et al., 2011). Because solid dosage forms need to disintegrate and then dissolve the drug before absorption can occur, dissolution rate determines availability of the drug for absorption (Martinez and Amidon, 2002). Manipulating the formulation can control the dissolution rate and where the drug is released in the GI tract for subsequent absorption. Their design is based on exploiting physiological conditions in the GI tract. By using modified formulations, it is possible to improve targeting to three different parts of the GI tract — namely the stomach, the small intestine, and the colon.

Gastroretentive Drug Delivery Systems

Prolonging the gastric residence time of dosage forms is particularly beneficial for drugs that are predominantly absorbed in the stomach or upper GI tract, or for drugs that suffer from solubility issues in the intestinal fluid (Mandal et al., 2016). This promotes the slow release of drug in the stomach, which subsequently extends the time available for drug dissolution and absorption in the stomach and/or small intestine. The benefit of this approach also includes sustained or controlled release drug delivery, which can reduce fluctuations in systemic drug concentrations as well as increase patient compliance to medications by minimizing the number of doses required (Awasthi and Kulkarni, 2016). Ideally, gastroretentive dosage forms should remain in the stomach for a specific duration and be able to undergo clearance from the body. For example, they should consist of components that are biodegradable or can undergo disintegration to smaller components after a predetermined time period. However, the prolonged nature of the dosage form would mean that immediate ceasing of a drug would be difficult, especially for patients experiencing adverse effects or hypersensitivity reactions.

The formulation approaches for gastroretention have been extensively reviewed (Streubel et al., 2006a; Mandal et al., 2016; Awasthi and Kulkarni, 2016; Tripathi et al., 2019) and include the following: (i) high-density dosage forms that sink into the folds of the antrum; (ii) floating dosage forms over gastric content; (iii) mucoadhesive dosage forms to gastric mucosa; and (iv) expandable dosage forms which expand or swell in the stomach to larger dimensions. Although there have been an extensive number of studies in the literature on gastroretentive dosage forms, the clinical translation of these technologies has not progressed as rapidly. Of these approaches, the floating dosage forms are the most common commercialized gastroretentive drug delivery system (Kumar and Kaushik, 2018). The major considerations for floating dosage forms are the susceptibility of the dosage form to body position (Timmermans and Moes, 1994) and the requirement to maintain a sufficient stomach content to allow an effective separation between the dosage form and the pyloric region (Whitehead et al., 1998; Kagan and Hoffman, 2008).

Expandable dosage forms have garnered particular attention in recent years. Ideally, these dosage forms should be small enough to swallow and be able to rapidly increase in size once in the stomach to prevent premature emptying through the pylorus (Streubel et al., 2006b). The diameter of the pylorus is approximately 12 ± 7 mm (Timmermans and Moes, 1993), which means that the size of the dosage form needs to be larger. It is generally accepted that a diameter >15 mm is required for prolonging gastric retention, especially during the fasted state (Timmermans and Moes, 1993; Bardonnet et al., 2006). The performance of these particular dosage forms is not dependent on the filling state of the stomach. There are several safety issues that need to be assessed for this type of dosage form, including the potential for accumulation of several dosage units in the stomach following multiple administrations, as well as possible occlusion of the esophagus or pylorus (Kagan and Hoffman, 2008).

Mucoadhesive and high-density dosage forms for gastroretention have translational limitations. For example, mucoadhesive dosage forms can be unpredictable regarding the site of adhesion (including the risk of esophageal binding) and can potentially suffer from elimination due to the high mucus turnover rate in the stomach (Rubinstein and Tirosh, 1994; Streubel et al., 2006b). The main disadvantage of high-density dosage forms is that they can be technically difficult to manufacture, generally requiring a large amount of drug due to the progressive decrease in the weight of the matrix as the drug gets released (Rouge et al., 1998; Awasthi and Kulkarni, 2016).

Regional Drug Targeting in the Small Intestine

Regional targeting of drugs to the small intestine is usually attained with gastroretentive dosage forms, pH-dependent dosage forms, or mucoadhesive dosage forms. Controlled drug delivery formulations with prolonged gastric residence time can be advantageous for drugs that are absorbed in the small intestine, especially those with an absorption window in the upper small intestine (Streubel et al., 2006b). Gastrointestinal transit time through the upper small intestine is rapid, thereby limiting the time available for absorption at this site. The advantages and disadvantages for each of the gastroretentive dosage forms have been discussed above *(refer to "Gastroretentive Drug Delivery Systems").*

Formulations that have pH-responsive coatings or matrices are particularly beneficial for drugs that are susceptible to degradation by gastric enzymes or by the acidity of the gastric fluid, as well as for drugs that can cause irritation to the gastric mucosa (Rouge et al., 1996; Thakral et al., 2013; Liu et al., 2017). In particular, enteric-coated solid dosage forms (e.g., tablets and capsules) are commonly used and are available clinically (Thakral et al., 2013; Al-Gousous et al., 2017). An enteric coating is defined as a material, usually a polymer, that forms a barrier over the surface of the dosage form that permits transit through the stomach to the small intestine before the drug is released (Felton and Porter, 2013; Thakral et al., 2013). However, disintegration and absorption from formulations containing enteric coatings or pH-responsive matrices may be erratic, due to the relatively slow dissolution or degradation of the polymers in comparison to the transit time of the formulation through the small intestine (Al-Gousous et al., 2017; Kang et al., 2018). Variability in gastric emptying time can also affect drug release in the small intestine (Al-Gousous et al., 2017). In addition, considerable intra- and inter-individual variability in the pH of the GI tract will affect drug release from pH-dependent dosage forms (Fallingborg et al., 1993; Sasaki et al., 1997; Nugent et al., 2001; Ibekwe et al., 2008; McConnell et al., 2008; Lahner et al., 2009; Brunton et al., 2018).

Mucoadhesive dosage forms, especially intestinal patches, have been investigated to prolong contact with the intestinal mucosa to improve drug absorption (Shen and Mitragotri, 2002; Toorisaka et al., 2012; Banerjee et al., 2016a; Gupta et al., 2016; Banerjee and Mitragotri, 2017). They are also able to protect the drug from degradation during transit in the upper GI tract. Drug release is influenced by formulation factors such as polymer composition, mucosal adhesive strength, drug concentration, drug release rate, and drug release direction (i.e., unidirectional or bidirectional) (Banerjee and Mitragotri, 2017; Homayun et al., 2019). These dosage forms are limited by the fact that they require sufficient binding with the intestinal wall to avoid being washed away by solid boluses of digested food, gastric and intestinal fluids, or by the continuous secretion and turnover of mucus (Banerjee and Mitragotri, 2017; Homayun et al., 2019). Being mucoadhesive in nature, there is a risk of adhesion with other mucosal surfaces following oral administration before entering the small intestine. This may lead to the release of drug into a region where it has minimal absorption capacity or is easily degraded. In addition, specificity in the site of binding in the small intestine, which is already extensive in length and highly convoluted, is also difficult to predict. Adhesion to the proximal region of the duodenum would be most ideal, as the latter regions are exposed to boluses of digested food that are more solid in form, which can more readily detach the patch from the luminal surface (Banerjee and Mitragotri, 2017; Homayun et al., 2019). However, some drugs are known to have preferential absorption sites in the small intestine (Murakami, 2017).

Regional Delivery of Drugs to the Colon

Colon targeted drug delivery is an active area of research, particularly for the treatment of local diseases affecting the colon, such as IBD and colorectal cancer. Improving the delivery of drugs to the colon not only improves the local effectiveness of therapeutics, but it can also reduce the risk of systemic adverse effects. Three main strategies are commonly used in conventional formulations for the regional delivery of drugs to the colon (Van den Mooter, 2006; Kagan and Hoffman, 2008; Vass et al., 2019): (i) utilization of a pH drop on entry into the colon; (ii) delayed release dosage forms that rely on gastrointestinal transit time; and (iii) exploitation of metabolic capabilities of the colonic microbiome.

pH-Responsive Dosage Forms

In general, the first approach uses pH-specific coatings and matrices that are soluble at neutral or slightly alkaline pH to

release the drug in the distal part of the small intestine or in the colon. **Table 2** shows some examples of pH-dependent polymer coatings that have been used for the purpose of colonic targeting either alone or in combination, including some methacrylic resins (commercially available as Eudragit®) (Khan et al., 1999; Goto et al., 2004; Thakral et al., 2013) and hydroxypropyl methylcellulose (HPMC) derivatives (Nykanen et al., 2001; Gareb et al., 2016). In addition to triggering release at a specific pH range, the enteric coating protects the incorporated active agents against the harsh GI tract environment (e.g., gastric juice, bile acid, and microbial degradation) and can create an extended and delayed drug release profile to enhance therapeutic efficiency (Yang et al., 2002; Van den Mooter, 2006). Targeting the colon with such polymers has proved difficult due to considerable intra- and inter-individual variability in the pH of the GI tract (McConnell et al., 2008), which is also influenced by diet (Ibekwe et al., 2008), disease (Fallingborg et al., 1993; Sasaki et al., 1997; Nugent et al., 2001), and co-administered drugs (Lahner et al., 2009; Brunton et al., 2018). Despite this variability, pH responsive approaches to colonic delivery have been used commercially. For example, mesalazine used for IBD is commercially available as oral tablets coated with Eudragit L-100 (Mesasal® and Colitofalk®) or Eudragit S (Asacol®).

Time-Dependent Dosage Forms

Time-dependent formulations essentially use gastrointestinal transit times as a guide to activate drug release into the colon. These formulations typically rely on the relatively constant transit time through the small intestine, and work on the assumption that a dosage form will spend approximately 6 h in the stomach and small intestine in the fasted state. They are typically composed of hydrophilic polymers (e.g., ethyl cellulose and HPMC) in the coating or matrix that are able to gradually swell over time, which creates a lag phase before releasing the drug (Sangalli et al., 2001; Gazzaniga et al., 2006; Gareb et al., 2016). In particular, drug release from hydrophilic matrices depends on several processes, including swelling of the polymer, penetration of water through the matrix, drug dissolution, drug transport through the swelled polymer, and erosion of the matrix (Colombo et al., 1995; Colombo et al., 2000; Caraballo, 2010). Hydration of the polymer when in contact with aqueous fluids changes the structure of the polymer to form a gel layer, which controls the drug release rate (Caraballo, 2010). Drug release is also influenced by formulation factors related to the polymer (e.g., composition, concentration, distribution, viscosity) and drug (e.g., loading, solubility, particle size) (Siepmann and Peppas, 2001; Miranda et al., 2007; Caraballo, 2010).

The main disadvantage of this approach is the huge variability seen in gastrointestinal transit time in the stomach, small intestine, and colon—with many physiological, pathophysiological, and pharmaceutical factors influencing these parameters (*refer to sections Physiological Factors Influencing Oral Drug Delivery and Pathophysiological Factors Influencing Oral Drug Delivery*). For example, gastric emptying time can be significantly prolonged after eating, which can lead to premature drug release in the small intestine instead of the colon (Ibekwe et al., 2008; Reinus and Simon, 2014). In addition, gastrointestinal transit time can be altered when associated with disease, such as IBD. Colonic transit is typically faster in IBD patients and is likely due to diarrhea, which is typically worse during active disease (Hebden et al., 2000; Podolsky, 2002). This can lead to difficulties in targeting specific regions of the colon with conventional formulations. For example, conventional delayed release formulations have been reported to show asymmetric drug distribution in the colon, with significantly lower drug concentrations in the distal colon and higher drug retention in the proximal colon (Hebden et al., 2000). Therefore, transit time may not be a reliable approach for targeted drug delivery in the colon when associated with some diseases.

TABLE 2 | Examples of pH-dependent polymer coatings used for colonic targeting.

Polymer	Optimum pH
Eudragit® S-100	7.0
Eudragit® FS 30D	7.0
Eudragit® L-100	6.0
Cellulose acetate phthalate	6.0
Cellulose acetate trimellitate	5.5
Eudragit® L 30D-55	5.5
Eudragit® L 100-55	5.5
Hydroxypropyl methylcellulose phthalate 55	5.5
Hydroxypropyl methylcellulose phthalate 50	5.0
Polyvinyl acetate phthalate	5.0

Biodegradable Dosage Forms

The consistently high levels of resident bacteria in the colon have been exploited for colon-specific drug delivery and is considered a much more reliable factor (McConnell et al., 2008). Numerous enzymes are produced by the colonic bacterial flora, such as polysaccharidases, azoreductases, and glycosidases (Scheline, 1973; Cummings and Macfarlane, 1991; Rubinstein, 2000), and have been utilized in drug delivery approaches. For example, biodegradable polymers in coatings and/or matrix formulations have been used for regional drug targeting in the colon. In particular, polysaccharide-based systems have shown promising results, with non-starch polysaccharides being commonly used (Hovgaard and Brondsted, 1996; Rubinstein, 2000; Shah et al., 2011). Non-starch polysaccharides are more resistant to digestion and absorption in the small intestine but are metabolized in the large intestine. These polymers are generally hydrophilic and are able to hydrate and swell during transit through the GI tract (hence they are also exploited in time-dependent dosage forms). The hydrated layers allow the penetration of colonic bacteria and enzymes, which lead to degradation and drug release within an acceptable duration (Van den Mooter, 2006; Shah et al., 2011). It should be noted that most of these polymers are strongly hydrophilic, which can lead to premature drug release before the colon is reached (Hovgaard and Brondsted, 1996; Van den Mooter, 2006; Patel, 2015). Premature drug release can also occur with the inter- and intra-individual variability in gastrointestinal transit times (Coupe et al., 1991; Watts et al., 1992; Timmermans and Moes, 1994; Rao et al., 2004; Kagan and Hoffman, 2008; Reinus and

Simon, 2014; Brunton et al., 2018). Therefore, few have reached the clinic due to lack of specificity in drug release. Chemical modification of polysaccharides or combining them with other conventional hydrophobic polymers have been investigated as a way to increase their hydrophobicity. It should be noted that a balance between hydrophilic and hydrophobic properties of the polysaccharides is required. Those that have low water solubility may have better capability for drug retention but can suffer from issues with low degradation (Hovgaard and Brondsted, 1996; Shah et al., 2011).

Similarly, azoreductase activity of colonic bacteria has been extensively studied for colon-targeting systems, especially in the development of prodrugs (Rafii et al., 1990; Oz and Ebersole, 2008; Marquez Ruiz et al., 2012). Prodrugs essentially rely on the enzymatic activity of colonic bacteria to break down an inactive precursor and release the active drug moiety. This approach is usually used to improve physicochemical properties of drugs (e.g., solubility, permeability, and stability) and/or to target drug release to a specific site in the GI tract. This occurs with the prodrugs of 5-aminosalicylic acid (5-ASA), such as sulfasalazine and olsalazine, which are used in the treatment of IBD (Oz and Ebersole, 2008). For example, sulfasalazine has low absorption in the upper GI tract and is cleaved by azoreductases of the microflora in the colon to release the active 5-ASA moiety, which is thought to have local actions in the colon. Azoreductase enzymes are largely produced by anaerobes present in the proximal part of the large intestine and onwards (Rafii et al., 1990; Oz and Ebersole, 2008; Marquez Ruiz et al., 2012).

Pathological changes in the microflora can occur in diseases, such as IBD and gastrointestinal infections, as well as with the use of drugs (e.g., antibiotics) (Linskens et al., 2001; Sartor, 2010; Hua et al., 2015). This can affect the composition and diversity of bacterial species and, therefore, the secretion of enzymes that are important in triggering drug release for microbial-dependent drug delivery systems. In addition, considerable loss of biodegradable dosage forms may occur in the case of diarrhea, due to insufficient time for activation or drug release (Sartor, 2010; Albenberg and Wu, 2014).

Combination of Strategies

To circumvent the issues with variability in gastrointestinal physiology, a combination of colon-targeting strategies has been utilized in conventional formulations. For example, both pH and time-dependent strategies are commonly used to improve drug delivery to the colon (Zema et al., 2007; Talaei et al., 2013; Patel, 2015). For example, one of the first formulations of this type was Pulsincap® (Wilding et al., 1992; Stevens et al., 2002; Jain et al., 2011; Patel et al., 2011). It consists of a capsule, half of which is enteric-coated and the other half is non-disintegrating. The enteric coat protects against gastric acid and avoids the problem of variable gastric emptying. This coat dissolves on entering the small intestine, revealing a hydrogel plug that then starts to swell. Timing of drug release is governed by the amount of hydrogel, in that the hydrogel plug is ejected from the bottom half of the capsule with extensive swelling.

In addition, Entocort® EC is another example of a dosage form that uses a combination of pH and gastrointestinal transit time (McKeage and Goa, 2002; Edsbacker and Andersson, 2004). The dosage form contains ethyl cellulose-based granules that are approximately 1 mm in size and contain budesonide (corticosteroid). Each granule is coated with Eudragit® L, which is a pH-dependent coating that dissolves at pH >5.5 to allow drug release in the ileum and ascending colon. The ethyl cellulose granules then ensure time-dependent drug release in the colon. This multiparticulate formulation is indicated for colonic inflammation, particularly for IBD (McKeage and Goa, 2002; Edsbacker and Andersson, 2004). The combination approach has shown promising results in improving drug release in the colon and reducing premature drug release in the upper GI tract. However, it can still suffer from the intra- and inter-individual variability that can occur with each of these gastrointestinal parameters.

NANOPARTICULATE ORAL DRUG DELIVERY APPROACHES

The development of novel gastrointestinal drug delivery systems has gained increasing interest, due to the inconsistent efficacy and inter-patient variability of conventional approaches that mostly rely on non-stable parameters in the GI tract. In particular, nanoparticulate dosage forms have shown promising results in drug delivery compared to conventional single-unit dosage forms. These formulations contain a number of separate nanoparticle subunits in which the dose of the drug is distributed across. This allows them to overcome the challenges faced by single-unit dosage forms, such as unpredictable disintegration and dissolution, nonspecific drug release, dose dumping, and stability issues in the GI tract (Talaei et al., 2013; Hua et al., 2015; Shahdadi Sardo et al., 2019). Nanoparticles have a larger surface-area-to-volume ratio, which provides a greater surface area for interaction with the mucosal surface and for the solubilization of drugs. Nanoparticulate dosage forms have shown the following advantages for gastrointestinal drug delivery, owing to their smaller size: (i) easier transport through the GI tract; (ii) more uniform distribution and drug release; (iii) increase in residence time of particles in the GI tract, even when colonic motility is increased in diarrhea; (iv) improved uptake into mucosal tissues and cells; and (v) specific accumulation to the site of disease, such as inflamed tissues (Hua et al., 2015; Moss et al., 2018; Reinholz et al., 2018). Nanoparticles generally undergo cellular uptake *via* the transcellular pathway in the GI tract (Yu et al., 2016; Reinholz et al., 2018). Translocation of nanoparticles can also occur by paracellular transport and persorption through gaps or holes at the villous tips (Hillyer and Albrecht, 2001; des Rieux et al., 2005).

Nanoparticulate Dosage Forms for Gastric Delivery

There are limited studies that have investigated the use of nanoparticulate formulations for gastric drug delivery. A major issue is the rapid passage of nanoparticles through the stomach to the intestine due to their small particle size (Sarparanta et al., 2012). Size is an important parameter for gastroretentive dosage forms, with particles less than 7 mm in diameter being efficiently evacuated (Timmermans and Moes, 1993; Bardonnet et al., 2006). However, the advantage of nanoparticulate formulations is the dispersion of the drug across multiple subunits and, therefore, the distribution of multiple subunits throughout the stomach. This avoids the limitations of single-unit dosage forms. The size of the nanoparticles may also improve mucosal interaction, with the potential for cellular uptake and/or close interaction for efficient drug delivery. The delivery of high drug concentrations in the stomach is particularly beneficial for the treatment of local diseases such as gastritis, gastric ulcer, and bacterial infections (e.g., *Helicobacter pylori*), as well as for drugs that have better absorption in the stomach (Rouge et al., 1996; Mandal et al., 2016).

To address the potential for rapid clearance from the stomach, studies have incorporated gastroretentive strategies to nanoparticulate formulations, especially mucoadhesive (Umamaheshwari et al., 2004; Ramteke et al., 2008; Ramteke and Jain, 2008; Jain et al., 2009; Ramteke et al., 2009; Sarparanta et al., 2012; Ngwuluka et al., 2015; Jain et al., 2016; Sunoqrot et al., 2017) and high-density systems (Ngwuluka et al., 2015; Sharma et al., 2018). The studies have shown promising results with regard to gastric retention and/or mucoadhesion in both *in vitro* and *ex vivo* experiments. However, extrapolation of these results to animals and humans is difficult, as there are a number of significant physiological and pathophysiological factors that affect gastric drug delivery. For example, the success of gastroretentive dosage forms has been limited due to high gastric motility and rapid mucus turnover. The stomach content is also highly hydrated, which can affect the adhesion of many mucoadhesive polymers (Pawar et al., 2011; Sunoqrot et al., 2017).

Initial *in vivo* biodistribution studies of nanoparticulate dosage forms have demonstrated prolonged gastroretention of up to 3 h in animals that have been fasted (Sarparanta et al., 2012). Although this parameter was not assessed in other *in vivo* studies on nanoparticles, those on microparticulate dosage forms have shown prolonged gastric retention of over 8 h in the fasted state (Hao et al., 2014). The difference is likely due to the gastroretentive strategy applied to the particles as well as the animal species used in the study. In rodents, the stomach is divided into the forestomach where ingested material is stored, and the glandular stomach where digestion continues (Gartner, 2002). Sarparanta et al. (Sarparanta et al., 2012) reported that the majority of the orally administered mucoadhesive nanoparticles were found to be mixed with material that the animals had ingested during the experiment (e.g., hair and bedding chips) in the forestomach. This is likely to interfere with the adhesion of the nanoparticles with the mucosa. However, sheets of nanoparticles and nanoparticle aggregates were found strongly adhered to the mucosa in the glandular stomach.

Most of the *in vivo* efficacy studies have been focused on using nanoparticulate formulations for treating *Helicobacter pylori* infection. Efficacy of drug-loaded nanoparticles have been demonstrated in *Helicobacter pylori* infected animals, even with once daily dosing, due to their mucoadhesive properties (Umamaheshwari et al., 2004; Ramteke et al., 2008; Jain et al., 2009; Ramteke et al., 2009). The results have been promising, however further *in vivo* investigations are required in more clinically relevant animal models to determine the translatability and reproducibility of nanoparticulate formulations for gastric drug delivery. It would also be important to understand the performance of nanoparticulate dosage forms under both fed and fasted conditions. For effective clinical translation, it is likely that the nanoparticles will also need to be loaded into a capsule that is able to dissolve rapidly in the stomach. This will ensure stability during transit in the oral cavity and esophagus, as well as maximal release of nanoparticles in the stomach.

Nanoparticulate Dosage Forms for Small Intestinal Delivery

Nanoparticulate formulations have been applied to the regional targeting of drugs in the small intestine to improve both local and systemic absorption. This is particularly beneficial for drugs that have poor solubility in the small intestine or are unstable in the harsh gastric environment (Lundquist and Artursson, 2016). By increasing the bioavailability of drugs into the small intestine, nanoparticles can be designed to: (i) trigger drug release in the lumen for subsequent absorption; (ii) adhere to the mucosal surface for effective drug release and absorption; (iii) enhance mucosal uptake of intact nanoparticles with subsequent drug release for local or systemic absorption; or (iv) enhance mucosal uptake and absorption of intact nanoparticles into the systemic circulation. There are a number of studies which have reported enhanced systemic absorption of drugs in the small intestine from nanoparticulate formulations (Bargoni et al., 1998; Fonte et al., 2011; Zhang et al., 2011; Reix et al., 2012; Zhang et al., 2013a; Tariq et al., 2016; Ahmad et al., 2018; Prajapati et al., 2018). However, in the majority of cases, the specific mechanism of action was not elucidated.

The mucosal uptake of intact nanoparticles is the most challenging, as the nanoparticles would need to cross multiple cellular barriers after penetrating the mucus layer (Reinholz et al., 2018). For example, nanoparticles would need to cross the intestinal epithelium to reach the lamina propria and then traverse a layer of endothelial cells of the blood vessels for systemic delivery. Nanoparticles can cross the intestinal epithelium *via* three main pathways — paracellular transport (between cells through tight junctions), transcellular transport (through the interior of cells with subsequent exocytosis), and M-cell-mediated transport (Yu et al., 2016; Reinholz et al., 2018). The advantages and limitations of each pathway are summarized in **Table 3**.

TABLE 3 | Summary of the main pathways that nanoparticles can take to cross the intestinal epithelium (Yu et al., 2016; Reinholz et al., 2018).

Paracellular	• Transport through the intercellular space between intestinal epithelial cells (enterocytes) • Intercellular spaces have an aqueous environment and rely on passive transport *Limitations* • Passage of nanoparticles is restricted by the narrow tight junction space (0.3 to 20 nm) • Potential for toxicity with the passage of other gastrointestinal content in the chyme
Transcellular	• Transport through epithelial cells (enterocytes) by transcytosis, which includes endocytosis, intracellular trafficking, and exocytosis • Enterocytes represent 90–95% of the cells lining the GI tract • Nanoparticles can potentially undergo indirect transport to the systemic circulation *via* the hepatic portal system or direct transport to the systemic circulation *via* the intestinal lymphatic system *Limitations* • Internalized nanoparticles are usually transported to lysosomes that contain a variety of enzymes for degradation • Enterocytes have enzymes in the microvilli of the brush border membrane and within the glycocalyx • Mucus layer and glycocalyx of enterocytes are thicker compared to M cells
M-cell-mediated	• Transport through M cells (microfold cells) by transcytosis, which includes endocytosis, intracellular trafficking, and exocytosis • M cells are mainly localized in Peyer's patches in the small intestine and have reduced intracellular enzymatic activity • Mucus layer and glycocalyx of M cells are considerably thinner compared to enterocytes, allowing easier access • Nanoparticles can potentially be captured by macrophages and dendritic cells in the Peyer's patches (beneficial for the development of oral vaccinations) or undergo passive lymphatic targeting followed by systemic drug delivery *Limitations* • Absorption of nanoparticles is restricted due to the low proportion of M cells (~1%) in the intestinal epithelium • Cellular uptake can be low due to a lack of specificity of nanoparticles towards M cells

Paracellular Transport

The passage of nanoparticles by paracellular transport is restricted by the narrow tight junction space, which can range from 0.3 nm to 20 nm, depending on the state (Madara, 1998; Camenisch et al., 1998; Acosta, 2009; Chen et al., 2013). Incorporation of charged polymers has been investigated as a means to reversibly open tight junctions and improve drug delivery across the intestinal epithelial barrier. For example, chitosan (cationic polymer) has been reported to facilitate the paracellular transport of nanoparticles (Zhang et al., 2014a; Liu et al., 2016). The rapid and reversible absorption-enhancing effect of chitosan was suggested to be due to changes in intracellular pH caused by the activation of a chloride-bicarbonate exchanger, thereby resulting in the opening of the tight junctions (Rosenthal et al., 2012). Peptides that have the capability of modulating the degree and kinetics of tight junctions have also demonstrated enhanced paracellular transport of drugs (Taverner et al., 2015). However, the size restriction needed for effective paracellular transport would limit most nanoparticulate formulations as well as the potential for toxicity with the passage of other gastrointestinal content in the chyme (Reinholz et al., 2018).

Transcellular Transport

Transcellular transport of nanoparticles across enterocytes is considered the most promising pathway for small intestinal drug delivery, owing to the large representation of these epithelial cells lining the GI tract (Reinus and Simon, 2014). Nanoparticles can then potentially undergo indirect transport to the systemic circulation *via* the hepatic portal system or direct transport to the systemic circulation *via* the intestinal lymphatic system. The intestinal lymphatic systemic can be targeted *via* lacteals, which are lymphatic capillary vessels in the villi of the small intestine (Reinus and Simon, 2014; Managuli et al., 2018). There are several challenges with this particular pathway, including the following: (i) the thick mucus layer overlaying the enterocytes; (ii) the thick glycocalyx coating the surface of the enterocytes; (iii) the luminal enzymes; and (iv) the enzymes in the microvilli of the brush border membrane and within the glycocalyx (Kyd and Cripps, 2008; Lundquist and Artursson, 2016; Yu et al., 2016). Together, these barriers help to prevent pathogens and potential toxins in the gastrointestinal content from entering the body.

Although intestinal barriers play a protective role in the body, they can also restrict the uptake of nanoparticulate formulations by enterocytes, which means that most of the nanoparticles are degraded or eliminated from the body (Yu et al., 2016). Nanoparticles that are internalized within enterocytes face additional challenges that restrict them from undergoing transcytosis. In particular, they are usually transported to lysosomes for degradation. This typically involves the transport of nanoparticles in endosomes, which can eventually fuse with the cell membrane for exocytosis or fuse with lysosomes for degradation (Hofmann et al., 2014; Hu et al., 2015). Lysosomes are intracellular vesicles with an acidic pH of 4.5–5 (Mindell, 2012) and contain a variety of enzymes that have a physiological role in degrading or recycling foreign molecules or cellular compounds (Saftig and Klumperman, 2009). Entrapment and degradation of nanoparticles within lysosomes prevent exocytosis at the basolateral membrane, which affects the efficacy of nanoparticulate formulations (Yu et al., 2016; Reinholz et al., 2018).

Several approaches have been utilized to improve the delivery and transcytosis of nanoparticles across enterocytes in the small intestine. The main parameters are particle size, nanoparticle composition, and surface modification. Studies have demonstrated an inverse correlation between particle size and cellular uptake, with improved uptake with smaller nanoparticles (50 nm > 200 nm > 500 nm > 1000 nm) (Desai et al., 1996; Bannunah et al., 2014; Banerjee et al., 2016b). Following uptake into enterocytes and subsequent basolateral secretion into the interstitial space, nanoparticle size can potentially influence whether they are selectively taken up by the lymphatic system or hepatic portal system, with larger particles having a preference for the lymphatic system (Griffin et al., 2016). In addition, a variety of materials have been used to construct nanoparticles, including lipids and polymers. Further stability studies are required to determine the *in vivo* small intestinal

bioavailability of these nanoparticles following oral administration. For example, the harsh enzymatic environment might be particularly detrimental to lipid-based nanoparticles due to lipolysis (Beloqui et al., 2016; Hu et al., 2016; Shreya et al., 2018). Incorporation of additional strategies may be required to protect nanoparticles from premature degradation in the GI tract (Makhlof et al., 2011a).

The effect of physicochemical parameters, other than particle size, is only beginning to be understood. Only a few studies have investigated the effect of surface charge, hydrophobicity, and shape on the bioavailability and absorption of nanoparticles after oral administration. In general, cationic nanoparticles showed enhanced uptake and transport by enterocytes compared to those with an anionic or neutral charge (Bannunah et al., 2014; Hellmund et al., 2015; Du et al., 2018) as well as significantly increased oral bioavailability *in vivo* (Du et al., 2018). Importantly, the cationic nanoparticles were not only internalized by the intestinal epithelial cells, but they were also transported through these cells into the lamina propria (Du et al., 2018). In addition, coating the surface of nanoparticles with polyethylene glycol (PEG) to create a hydrophilic surface chemistry minimized strong interaction with the mucus constituents and increased particle translocation through the mucus as well as mucosa (Maisel et al., 2015; Du et al., 2018). With regard to nanoparticle shape, initial studies have demonstrated higher cellular uptake and transcytosis of rod-shaped nanoparticles compared to sphere-shaped nanoparticles (Banerjee et al., 2016b). Nanorods also exhibited significantly longer retention time in the GI tract (especially in the jejunum and ileum) compared to nanospheres, which allowed more time for intestinal absorption (Li et al., 2017). They showed improved penetration into the space between the intestinal villi, with only low absorption of intact nanoparticles (Li et al., 2017).

Improvements in the translocation of nanoparticles within enterocytes have also been achieved with ligand-mediated active targeting. This strategy involves the conjugation of ligands to the surface of nanoparticles and exploits cell-specific differences or disease-induced changes in the expression of receptors, proteins, and adhesion molecules on the surface of tissues (Hua et al., 2015; Sercombe et al., 2015). Interactions between targeting ligands and specific receptors expressed at the site of action are expected to improve bioadhesion of the carrier to specific cells and increase the extent for cellular uptake. Various receptors expressed on the surface of enterocytes have demonstrated improved uptake and transcytosis of nanoparticles, with improve systemic bioavailability and therapeutic efficacy of encapsulated therapeutics (Zhang and Wu, 2014; Griffin et al., 2016). This includes the conjugation of ligands to the surface of nanoparticles that are specific for the following receptors—vitamin B12 (Chalasani et al., 2007), folate (Anderson et al., 2001; Ling et al., 2009; Jain et al., 2012), biotin (Zhang et al., 2014b), and lectins (Zhang et al., 2005; Yin et al., 2006; Zhang et al., 2006b; Makhlof et al., 2011b). Vitamin B12 ligand-mediated transport is limited by the relatively slow uptake of vitamin B12 in the GI tract as well as restricted site for absorption in the distal ileum (Hamman et al., 2007; Zhang and Wu, 2014). In addition, lectins can show nonspecific interactions with the mucus layer of the intestinal epithelium (Irache et al., 1994; Cornick et al., 2015; Managuli et al., 2018) and can have toxicity and stability issues (Zhang and Wu, 2014).

Enhancing the transcytosis of intact nanoparticles across enterocytes is a promising strategy to improve the systemic delivery of drugs that have poor stability or solubility in the GI tract. However, further studies are required to determine the optimal nanoparticulate design that provides translatable and reproducible outcomes in humans. As the small intestine is the target for these nanoparticulate formulations, considerations should also be given to the stability of the nanoparticles during transit in the upper GI tract.

M-Cell-Mediated Transport

Uptake of nanoparticles by M cells (microfold cells), which are mainly localized in Peyer's patches in the small intestine, have become attractive targets for drug delivery. M cells are specialized epithelial cells of the gut-associated lymphoid tissues (GALT) that have a sentinel role for the intestinal immune system by transporting luminal antigens through the follicle-associated epithelium to the underlying immune cells (Miller et al., 2007). The M-cell-mediated pathway has been exploited for nanoparticle drug delivery, as M cells have the advantages of reduced intracellular enzymatic activity as well as a considerably thinner mucus layer and glycocalyx in comparison to enterocytes (Frey et al., 1996; Kyd and Cripps, 2008). These factors promote easier access and intracellular transport. There are two main pathways following uptake into M cells: (i) nanoparticles can be captured by macrophages and dendritic cells in the Peyer's patches, which is beneficial for the development of oral vaccinations (Singh et al., 2015; Yu et al., 2019); and (ii) nanoparticles can undergo passive lymphatic targeting followed by systemic drug delivery (Cavalli et al., 2003; Joshi et al., 2014; Joshi et al., 2016; Managuli et al., 2018). However, the absorption of nanoparticles by M cells is limited due to the low proportion of M cells (~1%) in the intestinal epithelium. In addition, cellular uptake can be low due to a lack of specificity of nanoparticles towards M cells (des Rieux et al., 2006; Yu et al., 2016).

Studies have focused on determining the physicochemical characteristics of nanoparticles for optimal uptake by M cells. In general, nanoparticles larger than 5 μm are taken up by M cells but remain entrapped in Peyer's patches, whereas those smaller than 1 μm are taken up by M cells and transported through the efferent lymphatics within macrophages (Eldridge et al., 1989; Eldridge et al., 1990; Managuli et al., 2018). In addition, non-ionic nanoparticles composed of hydrophobic constituents have better uptake by M cells in comparison to hydrophilic and charged nanoparticles (Bargoni et al., 1998; Shakweh et al., 2004; Managuli et al., 2018).

Active targeting strategies have also been applied to improve specificity of targeting to M cells. Major ligands that have been conjugated to the surface of nanoparticles for targeting Peyer's

patches include mannose receptor binding ligands (Fievez et al., 2009; Singodia et al., 2012; Youngren et al., 2013; De Coen et al., 2016), lectin-based ligands (Foster et al., 1998; Clark et al., 2000; Clark et al., 2001; Manocha et al., 2005; Chionh et al., 2009), and integrin specific ligands (Frey et al., 1996; Fievez et al., 2009). It should be noted that there are limited M cell specific targets that have been identified (Zhao et al., 2014), with many also being expressed on other elements in the GI tract. For example, mannose receptors are localized on the apical surface of enterocytes (Fievez et al., 2009; Managuli et al., 2018). In addition, lectins can interact with the carbohydrate residue in the mucus layer of the intestinal epithelium (Irache et al., 1994; Diesner et al., 2012; Cornick et al., 2015; Managuli et al., 2018). Of the targets identified, integrin specific ligands appear to be the most promising target for M cells due to its specificity. However, further *in vivo* studies are required to determine the translatability of these platforms for clinical use. Common laboratory animal species have been reported to have significantly higher density of Peyer's patches in the intestine compared to humans (Kararli, 1995). This should be taken into account to avoid an overestimation of the nanoparticle transport capacity in humans (Lundquist and Artursson, 2016).

Nanoparticulate Dosage Forms for Colon Delivery

The use of nanoparticulate formulations have demonstrated promising results for colonic drug delivery (Hua, 2014; Hua et al., 2015; Zhang et al., 2017). Reduction in particle size can also enhance targeting and uptake within diseased tissue in the colon. For example, nanoparticles can promote enhanced and selective delivery of drugs into inflamed colonic tissue by exerting an epithelial enhanced permeability and retention (eEPR) effect (Collnot et al., 2012; Xiao and Merlin, 2012), as well as allowing preferential uptake by immune cells that are highly increased in inflamed tissue (Lamprecht et al., 2005a). In addition, nanoparticles are able to avoid rapid carrier elimination that occurs in diarrhea, as these smaller particles are readily taken up into inflamed tissue and cells (Beloqui et al., 2013). When compared to conventional formulations, nanoparticulate formulations have been demonstrated to have improved or similar therapeutic efficacy at lower drug concentrations (Hua et al., 2015).

Basic Physicochemical Strategies for Colon Delivery

Nanoparticulate formulations have been designed to passively or actively target the colon. With regards to the ideal particle size for targeting capability in the colon, there have been varying results (Hua et al., 2015). In healthy rats and rats with induced colitis, it was observed that 100 nm particles showed significantly increased accumulation in inflamed colon in comparison to healthy animals (Lamprecht et al., 2001a). Interestingly, initial studies in humans with IBD demonstrated that microparticles (3 μm) had better bioadhesion and accumulation in the inflamed rectal mucosal wall as well as less propensity for systemic absorption (Schmidt et al., 2013). Nanoparticles (250 nm), however, were translocated to the serosal compartment of IBD patients, possibly leading to systemic absorption (Schmidt et al., 2013). Importantly, the total fraction of particles penetrating the rectal mucosa was relatively low in the study (Schmidt et al., 2013). Further studies are required to determine the reason for the difference in particle size response in animals compared to humans.

Although passive targeting, through modifying particle size, enables prolonged retention and improved permeability of nanoparticles, there have been contradictory findings with regards to specificity to diseased versus healthy tissue in the colon (Lamprecht et al., 2005a; Wachsmann et al., 2013). Modification of the surface charge of nanoparticles has been investigated to improve mucosal retention and targeting to diseased tissue. For example, cationic systems are generally considered mucoadhesive, as they adhere to the mucosal surface within inflamed tissue due to the interaction between the negatively charged intestinal mucosa and the positively charged carrier (Liu et al., 2005; Thirawong et al., 2008; Han et al., 2012; Niebel et al., 2012; Coco et al., 2013; Lautenschlager et al., 2013). Colonic mucins have a negative charge since their carbohydrates are substituted with a number of sialic acid and sulfate residues (Larsson et al., 2009; Antoni et al., 2014). In contrast, anionic delivery systems are considered bioadhesive, as they preferentially adhere to inflamed tissue *via* electrostatic interaction with the higher concentration of positively charged proteins (Lamprecht et al., 2001b; Jubeh et al., 2004; Meissner et al., 2006; Beloqui et al., 2013). In particular, high amounts of eosinophil cationic protein and transferrin have been observed in the inflammatory tissue of the colon in IBD patients (Carlson et al., 1999; Peterson et al., 2002; Tirosh et al., 2009). Anionic nanoparticles are able to interdiffuse among the mucus network due to less electrostatic interaction with the mucus in comparison to cationic nanoparticles, which can suffer from immobilization following binding to the mucus (Hua et al., 2015).

Similarly, PEGylated nanoparticles have been demonstrated to improve particle translocation through the mucus as well as mucosa (Tobio et al., 2000; Vong et al., 2012; Lautenschlager et al., 2013). The hydrophilic surface has also been shown to accelerated drug delivery into the leaky inflamed intestinal epithelium (Lautenschlager et al., 2013). Both surface charge and PEGylation are promising pharmaceutical strategies for mucosal targeting, however it is likely that additional colon-specific pharmaceutical strategies are needed to localize the nanoparticles in the colon following oral administration and to further improve targeting to diseased tissue (Hua et al., 2015). It should be noted that there have been conflicting results on the effect of surface charge on colonic targeting, with results mainly based on *ex vivo* tissue binding studies or *in vivo* studies following rectal administration (Hua et al., 2015). There is also a potential for electrostatic interactions and subsequent binding of charged nanoparticles with other charge-modifying substances (e.g., soluble mucins and bile acids) during gastrointestinal transit following oral administration (Hua et al., 2015).

Colon-Specific Pharmaceutical Strategies

Colon-specific pharmaceutical strategies are likely required to improve nanoparticle accumulation, retention, and drug release in the colon, as well as minimize drug release in the upper GI tract. Colon-specific approaches can be applied to single-unit dosage forms (e.g., capsules) that are loaded with nanoparticles or applied to each of the individual nanoparticle subunits. The latter approach has been investigated in a number of studies, whereby nanoparticles are modified with components that are sensitive to pH, enzymes, reactive oxygen species (ROS), and overexpressed receptors (Hua et al., 2015). For example, pH-dependent nanoparticulate formulations typically involve coating nanoparticles with pH-sensitive biocompatible polymers to trigger drug release in the colon and protect the incorporated active agents against the harsh gastrointestinal environment in the upper GI tract (Lamprecht et al., 2005b; Makhlof et al., 2009; Kshirsagar et al., 2012; Ali et al., 2014; Beloqui et al., 2014). Although preclinical studies of pH-dependent carriers for colon targeting have been promising, a major concern has been the inherent intra-individual and inter-individual variability of pH and emptying times from the GI tract as well as the change in luminal pH due to disease state.

Biodegradable nanoparticulate formulations take advantage of the consistently high levels of resident bacteria and enzymes in the colon to trigger drug release (Bhavsar and Amiji, 2007; Moulari et al., 2008; Laroui et al., 2010; Kriegel and Amiji, 2011; Kriegel and Amiji, 2011; Laroui et al., 2014a; Xiao et al., 2014). These factors are known to be more consistent to allow efficient colon-targeted drug delivery. Biodegradable polymers have been used in the coatings or matrix of the nanoparticles, including poly-lactic acid (PLA), poly(lactic-co-glycolic acid) (PLGA), and chitosan. In addition, nanoparticles have also been embedded in hydrogel matrices containing polymers that have been shown to be specifically degraded by enzymes in the colon (Laroui et al., 2010; Laroui et al., 2014a; Laroui et al., 2014b; Xiao et al., 2014). Hydrogels are dosage forms that provide a platform for protecting therapeutics through the GI tract and can achieve site-specific delivery by including polymers that exploit fundamental physiological changes (Sharpe et al., 2014). As previously discussed for conventional formulations, biodegradable polymers can suffer from premature drug release or burst release based on their hydrophilicity and solubility in the upper GI tract.

Redox-based nanoparticulate formulations have shown promise for enhancing drug accumulation at sites of colonic inflammation (Wilson et al., 2010). They are able to target diseased tissue of the colon by taking advantage of the abnormally high levels of ROS that are produced at the sites of inflammation to trigger drug release. For example, 10- to 100-fold increase in mucosal ROS concentrations have been reported in biopsies taken from ulcerative colitis patients (Simmonds et al., 1992; Lih-Brody et al., 1996). These were found to be confined to sites of disease and correlated with disease progression (Simmonds et al., 1992; Lih-Brody et al., 1996). The high concentration of ROS is typically generated by activated phagocytes (Mahida et al., 1989). Although there are very few studies available, the initial *in vivo* results have demonstrated localization and efficacy of these nanoparticles to sites of intestinal inflammation in mice with colitis following oral administration (Wilson et al., 2010).

Ligand-mediated active targeting is another promising strategy to enhance drug accumulation and uptake to sites of disease within the colon. This includes the conjugation of ligands to the surface of nanoparticles that are specific for the following — macrophage receptors (e.g., mannose receptors and macrophage galactose-type lectin) (Coco et al., 2013; Xiao et al., 2013; Zhang et al., 2013b; Laroui et al., 2014b), intercellular adhesion molecule-1 (ICAM-1) (Mane and Muro, 2012), transferrin receptors (Harel et al., 2011), and glycoprotein CD98 (Xiao et al., 2014). Additional *in vivo* studies are required to evaluate the efficacy and stability of different targeting ligands and formulations in animal models of colitis (Hua et al., 2015). Commonly used targeting moieties include peptides and monoclonal antibodies, which have been shown to have high targeting specificity and potential mucopenetrative properties (Saltzman et al., 1994). However, oral administration of antibody and peptide-based formulations can suffer from degradation by gastric acid and enzymes in the GI tract. Therefore, further formulation design may be needed for effective oral administration.

CONSIDERATIONS FOR TRANSLATIONAL DEVELOPMENT

Significant advances in the development of oral formulations to improve the regional targeting of drugs in the GI tract have been reported in the literature. However, very few of them have translated to the clinical phase, which is likely due to a combination of biological and pharmaceutical factors. Understanding the relationship between biology and pharmaceutics are important determinants for the successful translation of new formulations (Hua et al., 2018). This includes understanding the effect of physiology and/or pathophysiology on the distribution, retention, disintegration, and release of drugs from oral dosage forms in the GI tract, as well as correlation with *in vivo* behavior (e.g., efficacy and safety) in animals and humans. Differences in the anatomy and/or physiology of the animal species used in *in vivo* studies compared to humans should also be taken into account when evaluating new formulations (Kararli, 1995; Hatton et al., 2015). Considerations should also be given to physiological heterogeneity in the GI tract of both healthy patients and those with specific pathological conditions (Titus et al., 2013; Hua et al., 2015; Hatton et al., 2018; Hatton et al., 2019).

For innovative platforms, such as nanoparticles, safety of the different carriers following uptake needs to be evaluated further. For example, there has been limited studies focused on the toxicology of nanoparticles in the GI tract of humans — this is likely to vary according to the size and composition of the particles (Bergin and Witzmann, 2013; Talkar et al., 2018; Vita et al., 2019). Preclinical studies should be conducted under appropriate blinding and randomization to reduce bias. In addition, assessment against proper controls, including the gold standard treatment and not just free drug solution, is

required to determine the potential place in therapy of the innovative platform (Hua et al., 2018). These factors are currently lacking in many published studies, which makes it difficult to assess clinical translatability of the results. Considerations should also be given to the "final product" for clinical use. Nanoparticles can either be delivered as an oral liquid suspension or loaded into solid-dosage forms (e.g., capsules). Depending on the target region in the GI tract, pharmaceutical strategies may need to be incorporated to protect the nanoparticles from premature interaction or degradation during transit. For example, coating capsules or nanoparticles with pH sensitive polymers.

Furthermore, the complexity in the design and development of new formulations should be minimized as much as possible for clinical translation to be justified (Hua et al., 2015; Hua et al., 2018). Platforms that require complex and/or laborious synthesis procedures generally have limited clinical translation potential, as they can be quite problematic and costly to pharmaceutically manufacture on a large scale. Other considerations include availability of materials and industrial equipment, insufficient batch-to-batch reproducibility to set specifications, and overall cost of dosage form development (Hua et al., 2018). Last but not least, there needs to be a clear benefit of efficacy and/or safety with any new oral formulation compared to clinically available dosage forms.

CONCLUSION

The oral route of administration is the most preferred route by patients for gastrointestinal drug delivery. However, the performance of the dosage forms and drug absorption are highly dependent on the physiology of the GI tract. Gastrointestinal physiology is complex and can display both large intra- and inter-individual variability. Attempts to overcome these issues have focused on improved understanding of the physiology of the GI tract in both healthy and diseased states. Innovative pharmaceutical approaches are also being explored to improve regional drug targeting in the GI tract, with the majority still in the infancy stages of translational development. For example, the use of multiparticulate dosage systems, such as nanoparticles, has shown promising results in improving gastrointestinal drug delivery compared to single-unit dose formulations. Effective translation will depend on rational dosage form design to enable improvements in gastrointestinal drug delivery for the treatment of both systemic diseases and local gastrointestinal diseases.

AUTHOR CONTRIBUTIONS

SH was involved in conception of the idea for the review, drafted the manuscript, and approved the final version of the manuscript.

ACKNOWLEDGMENTS

The author wishes to thank the University of Newcastle, Pharmacy Research Trust of New South Wales, Rebecca L. Cooper Medical Research Foundation, Gladys M Brawn Fellowship, and ausEE Research Foundation for providing financial support for this work.

REFERENCES

Acosta, E. (2009). Bioavailability of nanoparticles in nutrient and nutraceutical delivery. *Curr. Opin. Colloid Interface Sci.* 14, 3–15. doi: 10.1016/j.cocis.2008.01.002

Ahmad, N., Alam, M. A., Ahmad, R., Umar, S., and Jalees Ahmad, F. (2018). Improvement of oral efficacy of Irinotecan through biodegradable polymeric nanoparticles through *in vitro* and *in vivo* investigations. *J. Microencapsul.* 35 (4), 327–343. doi: 10.1080/02652048.2018.1485755

Albenberg, L. G., and Wu, G. D. (2014). Diet and the intestinal microbiome: associations, functions, and implications for health and disease. *Gastroenterology* 146 (6), 1564–1572. doi: 10.1053/j.gastro.2014.01.058

Al-Gousous, J., Tsume, Y., Fu, M., Salem, I. I., and Langguth, P. (2017). Unpredictable Performance of pH-Dependent Coatings Accentuates the Need for Improved Predictive in Vitro Test Systems. *Mol. Pharm.* 14 (12), 4209–4219. doi: 10.1021/acs.molpharmaceut.6b00877

Ali, H., Weigmann, B., Neurath, M. F., Collnot, E. M., Windbergs, M., and Lehr, C. M. (2014). Budesonide loaded nanoparticles with pH-sensitive coating for improved mucosal targeting in mouse models of inflammatory bowel diseases. *J. Control Release* 183, 167–177. doi: 10.1016/j.jconrel.2014.03.039

Allen, L. V., Popovich, N. G., and Ansel, H. C. (2011). *Ansel"s pharmaceutical dosage forms and drug delivery systems. 9th ed.* (Philadelphia: Lippincott Williams & Wilkins).

Anderson, K. E., Eliot, L. A., Stevenson, B. R., and Rogers, J. A. (2001). Formulation and evaluation of a folic acid receptor-targeted oral vancomycin liposomal dosage form. *Pharmaceut. Res.* 18 (3), 316–322. doi: 10.1023/A:1011002913601

Antoni, L., Nuding, S., Wehkamp, J., and Stange, E. F. (2014). Intestinal barrier in inflammatory bowel disease. *World J. Gastroenterol.* 20 (5), 1165–1179. doi: 10.3748/wjg.v20.i5.1165

Atuma, C., Strugala, V., Allen, A., and Holm, L. (2001). The adherent gastrointestinal mucus gel layer: thickness and physical state *in vivo*. *Am. J. Physiol. Gastrointest Liver Physiol.* 280 (5), G922–G929. doi: 10.1152/ajpgi.2001.280.5.G922

Awasthi, R., and Kulkarni, G. T. (2016). Decades of research in drug targeting to the upper gastrointestinal tract using gastroretention technologies: where do we stand? *Drug Deliv.* 23 (2), 378–394. doi: 10.3109/10717544.2014.936535

Banerjee, A., and Mitragotri, S. (2017). Intestinal patch systems for oral drug delivery. *Curr. Opin. Pharmacol.* 36, 58–65. doi: 10.1016/j.coph.2017.08.005

Banerjee, A., Lee, J., and Mitragotri, S. (2016a). Intestinal mucoadhesive devices for oral delivery of insulin. *Bioengineering Trans. Med.* 1 (3), 338–346. doi: 10.1002/btm2.10015

Banerjee, A., Qi, J., Gogoi, R., Wong, J., and Mitragotri, S. (2016b). Role of nanoparticle size, shape and surface chemistry in oral drug delivery. *J. Control Release* 238, 176–185. doi: 10.1016/j.jconrel.2016.07.051

Banerjee, A., Pathak, S., Subramanium, V. D., Dharanivasan, G., Murugesan, R., and Verma, R. S. (2017). Strategies for targeted drug delivery in treatment of colon cancer: current trends and future perspectives. *Drug Discovery Today* 22 (8), 1224–1232. doi: 10.1016/j.drudis.2017.05.006

Bannunah, A. M., Vllasaliu, D., Lord, J., and Stolnik, S. (2014). Mechanisms of nanoparticle internalization and transport across an intestinal epithelial cell model: effect of size and surface charge. *Mol. Pharm.* 11 (12), 4363–4373. doi: 10.1021/mp500439c

Bardonnet, P. L., Faivre, V., Pugh, W. J., Piffaretti, J. C., and Falson, F. (2006). Gastroretentive dosage forms: overview and special case of Helicobacter pylori. *J. Control Release* 111 (1-2), 1–18. doi: 10.1016/j.jconrel.2005.10.031

Bargoni, A., Cavalli, R., Caputo, O., Fundaro, A., Gasco, M. R., and Zara, G. P. (1998). Solid lipid nanoparticles in lymph and plasma after duodenal administration to rats. *Pharmaceut. Res.* 15 (5), 745–750. doi: 10.1023/A:1011975120776

Beloqui, A., Coco, R., Alhouayek, M., Solinis, M. A., Rodriguez-Gascon, A., Muccioli, G. G., et al. (2013). Budesonide-loaded nanostructured lipid carriers reduce inflammation in murine DSS-induced colitis. *Int. J. Pharm.* 454 (2), 775–783. doi: 10.1016/j.ijpharm.2013.05.017

Beloqui, A., Coco, R., Memvanga, P. B., Ucakar, B., des Rieux, A., and Preat, V. (2014). pH-sensitive nanoparticles for colonic delivery of curcumin in inflammatory bowel disease. *Int. J. Pharm.* ;473 (1-2), 203–212. doi: 10.1016/j.ijpharm.2014.07.009

Beloqui, A., des Rieux, A., and Preat, V. (2016). Mechanisms of transport of polymeric and lipidic nanoparticles across the intestinal barrier. *Adv. Drug Delivery Rev.* 106 (Pt B), 242–255. doi: 10.1016/j.addr.2016.04.014

Bergin, I. L., and Witzmann, F. A. (2013). Nanoparticle toxicity by the gastrointestinal route: evidence and knowledge gaps. *Int. J. BioMed. Nanosci. Nanotechnol.* 3 (1-2), 1–44. doi: 10.1504/IJBNN.2013.054515

Bhavsar, M. D., and Amiji, M. M. (2007). Gastrointestinal distribution and *in vivo* gene transfection studies with nanoparticles-in-microsphere oral system (NiMOS). *J. Control Release* 119 (3), 339–348. doi: 10.1016/j.jconrel.2007.03.006

Booijink, C. C., El-Aidy, S., Rajilic-Stojanovic, M., Heilig, H. G., Troost, F. J., Smidt, H., et al. (2010). High temporal and inter-individual variation detected in the human ileal microbiota. *Environ. Microbiol.* 12, 3213–3227. doi: 10.1111/j.1462-2920.2010.02294.x

Bratten, J., and Jones, M. P. (2006). New directions in the assessment of gastric function: clinical applications of physiologic measurements. *Digestive Dis.* 24 (3-4), 252–259. doi: 10.1159/000092878

Britton, R. A., and Young, V. B. (2014). Role of the intestinal microbiota in resistance to colonization by Clostridium difficile. *Gastroenterology* 146 (6), 1547–1553. doi: 10.1053/j.gastro.2014.01.059

Brunton, L. L., Knollmann, B. C., and Hilal-Dandan, R. (2018). *Goodman & Gilman's: The Pharmacological Basis of Therapeutics. 13th edition* (New York: McGraw-Hill Education).

Buhmann, S., Kirchhoff, C., Ladurner, R., Mussack, T., Reiser, M. F., and Lienemann, A. (2007). Assessment of colonic transit time using MRI: a feasibility study. *Eur. Radiol.* 17 (3), 669–674. doi: 10.1007/s00330-006-0414-z

Byrne, C. M., Solomon, M. J., Young, J. M., Selby, W., and Harrison, J. D. (2007). Patient preferences between surgical and medical treatment in Crohn's disease. *Dis. Colon Rectum.* 50 (5), 586–597. doi: 10.1007/s10350-006-0847-0

Camenisch, G., Alsenz, J., van de Waterbeemd, H., and Folkers, G. (1998). Estimation of permeability by passive diffusion through Caco-2 cell monolayers using the drugs' lipophilicity and molecular weight. *Eur. J. Pharmaceut. Sci.* 6 (4), 317–324. doi: 10.1016/S0928-0987(97)10019-7

Caraballo, I. (2010). Factors affecting drug release from hydroxypropyl methylcellulose matrix systems in the light of classical and percolation theories. *Expert Opin. Drug Delivery* 7 (11), 1291–1301. doi: 10.1517/17425247.2010.528199

Carlson, M., Raab, Y., Peterson, C., Hallgren, R., and Venge, P. (1999). Increased intraluminal release of eosinophil granule proteins EPO, ECP, EPX, and cytokines in ulcerative colitis and proctitis in segmental perfusion. *Am. J. Gastroenterol.* 94 (7), 1876–1883. doi: 10.1111/j.1572-0241.1999.01223.x

Cavalli, R., Bargoni, A., Podio, V., Muntoni, E., Zara, G. P., and Gasco, M. R. (2003). Duodenal administration of solid lipid nanoparticles loaded with different percentages of tobramycin. *J. Pharm. Sci.* 92 (5), 1085–1094. doi: 10.1002/jps.10368

Chalasani, K. B., Russell-Jones, G. J., Jain, A. K., Diwan, P. V., and Jain, S. K. (2007). Effective oral delivery of insulin in animal models using vitamin B12-coated dextran nanoparticles. *J. Control Release* Sep 26122 (2), 141–150. doi: 10.1016/j.jconrel.2007.05.019

Chen, M. C., Mi, F. L., Liao, Z. X., Hsiao, C. W., Sonaje, K., Chung, M. F., et al. (2013). Recent advances in chitosan-based nanoparticles for oral delivery of macromolecules. *Adv. Drug Delivery Rev.* 65 (6), 865–879. doi: 10.1016/j.addr.2012.10.010

Chionh, Y. T., Wee, J. L., Every, A. L., Ng, G. Z., and Sutton, P. (2009). M-cell targeting of whole killed bacteria induces protective immunity against gastrointestinal pathogens. *Infect. Immun.* 77 (7), 2962–2970. doi: 10.1128/IAI.01522-08

Chowdhury, A. H., and Lobo, D. N. (2011). Fluids and gastrointestinal function. *Curr. Opin. Clin. Nutr. Metab. Care* 14 (5), 469–476. doi: 10.1097/MCO.0b013e328348c084

Clark, M. A., Hirst, B. H., and Jepson, M. A. (2000). Lectin-mediated mucosal delivery of drugs and microparticles. *Adv. Drug Delivery Rev.* 43 (2-3), 207–223. doi: 10.1016/S0169-409X(00)00070-3

Clark, M. A., Blair, H., Liang, L., Brey, R. N., Brayden, D., and Hirst, B. H. (2001). Targeting polymerised liposome vaccine carriers to intestinal M cells. *Vaccine* 20 (1-2), 208–217. doi: 10.1016/S0264-410X(01)00258-4

Coco, R., Plapied, L., Pourcelle, V., Jerome, C., Brayden, D. J., Schneider, Y. J., et al. (2013). Drug delivery to inflamed colon by nanoparticles: comparison of different strategies. *Int. J. Pharm.* 440 (1), 3–12. doi: 10.1016/j.ijpharm.2012.07.017

Collnot, E. M., Ali, H., and Lehr, C. M. (2012). Nano- and microparticulate drug carriers for targeting of the inflamed intestinal mucosa. *J. Control Release* 20161 (2), 235–246. doi: 10.1016/j.jconrel.2012.01.028

Colombo, P., Bettini, R., Massimo, G., Catellani, P. L., Santi, P., and Peppas, N. A. (1995). Drug diffusion front movement is important in drug release control from swellable matrix tablets. *J. Pharm. Sci.* 84 (8), 991–997. doi: 10.1002/jps.2600840816

Colombo, P., Bettini, R., Santi, P., and Peppas, N. A. (2000). Swellable matrices for controlled drug delivery: gel-layer behaviour, mechanisms and optimal performance. *Pharmaceut. Sci. Technol. Today* 3 (6), 198–204. doi: 10.1016/S1461-5347(00)00269-8

Consortium, T. H. M. P. (2012). Structure, Function and Diversity of the Healthy Human Microbiome. *Nature* 486, 207–214. doi: 10.1038/nature11234

Cornick, S., Tawiah, A., and Chadee, K. (2015). Roles and regulation of the mucus barrier in the gut. *Tissue Barriers* 3 (1-2), e982426. doi: 10.4161/21688370.2014.982426

Coupe, A. J., Davis, S. S., and Wilding, I. R. (1991). Variation in gastrointestinal transit of pharmaceutical dosage forms in healthy subjects. *Pharmaceut. Res.* 8 (3), 360–364. doi: 10.1023/A:1015849700421

Cummings, J. H., and Macfarlane, G. T. (1991). The control and consequences of bacterial fermentation in the human colon. *J. Appl. Bacteriol.* 70 (6), 443–459. doi: 10.1111/j.1365-2672.1991.tb02739.x

De Coen, R., Vanparijs, N., Risseeuw, M. D., Lybaert, L., Louage, B., De Koker, S., et al. (2016). pH-Degradable Mannosylated Nanogels for Dendritic Cell Targeting. *Biomacromolecules* 17 (7), 2479–2488. doi: 10.1021/acs.biomac.6b00685

des Rieux, A., Ragnarsson, E. G., Gullberg, E., Preat, V., Schneider, Y. J., and Artursson, P. (2005). Transport of nanoparticles across an *in vitro* model of the human intestinal follicle associated epithelium. *Eur. J. Pharmaceut. Sci.* 25 (4-5), 455–465. doi: 10.1016/j.ejps.2005.04.015

des Rieux, A., Fievez, V., Garinot, M., Schneider, Y. J., and Preat, V. (2006). Nanoparticles as potential oral delivery systems of proteins and vaccines: a mechanistic approach. *J. Control Release* 116 (1), 1–27. doi: 10.1016/j.jconrel.2006.08.013

Desai, M. P., Labhasetwar, V., Amidon, G. L., and Levy, R. J. (1996). Gastrointestinal uptake of biodegradable microparticles: effect of particle size. *Pharmaceut. Res.* 13 (12), 1838–1845. doi: 10.1023/A:1016085108889

Diesner, S. C., Wang, X. Y., Jensen-Jarolim, E., Untersmayr, E., and Gabor, F. (2012). Use of lectin-functionalized particles for oral immunotherapy. *Ther. Deliv.* 3 (2), 277–290. doi: 10.4155/tde.11.146

Du, X. J., Wang, J. L., Iqbal, S., Li, H. J., Cao, Z. T., Wang, Y. C., et al. (2018). The effect of surface charge on oral absorption of polymeric nanoparticles. *Biomater. Sci.* 6 (3), 642–650. doi: 10.1039/C7BM01096F

Edsbacker, S., and Andersson, T. (2004). Pharmacokinetics of budesonide (Entocort EC) capsules for Crohn's disease. *Clin. Pharmacokinet.* 43 (12), 803–821. doi: 10.2165/00003088-200443120-00003

El Aidy, S., van den Bogert, B., and Kleerebezem, M. (2015). The small intestine microbiota, nutritional modulation and relevance for health. *Curr. Opin. Biotechnol.* 32, 14–20. doi: 10.1016/j.copbio.2014.09.005

Eldridge, J. H., Meulbroek, J. A., Staas, J. K., Tice, T. R., and Gilley, R. M. (1989). Vaccine-containing biodegradable microspheres specifically enter the gut-

associated lymphoid tissue following oral administration and induce a disseminated mucosal immune response. *Adv. Exp. Med. Biol.* 251, 191–202. doi: 10.1007/978-1-4757-2046-4_18

Eldridge, J. H., Hammond, C. J., Meulbroek, J. A., Staas, J. K., Gilley, R. M., and Tice, T. R. (1990). Controlled vaccine release in the gut-associated lymphoid tissues. I. Orally administered biodegradable microspheres target the peyer's patches. *J. Control Release* 11, 205–214. doi: 10.1016/0168-3659(90)90133-E

Evans, D. F., Pye, G., Bramley, R., Clark, A. G., Dyson, T. J., and Hardcastle, J. D. (1988). Measurement of gastrointestinal pH profiles in normal ambulant human subjects. *Gut* 29 (8), 1035–1041. doi: 10.1136/gut.29.8.1035

Fallingborg, J., Christensen, L. A., Jacobsen, B. A., and Rasmussen, S. N. (1993). Very low intraluminal colonic pH in patients with active ulcerative colitis. *Digestive Dis. Sci.* 38 (11), 1989–1993. doi: 10.1007/BF01297074

Fallingborg, J., Pedersen, P., and Jacobsen, B. A. (1998). Small intestinal transit time and intraluminal pH in ileocecal resected patients with Crohn's disease. *Digestive Dis. Sci.* 43 (4), 702–705. doi: 10.1023/A:1018893409596

Felton, L. A., and Porter, S. C. (2013). An update on pharmaceutical film coating for drug delivery. *Expert Opin. Drug Deliv.* 10 (4), 421–435. doi: 10.1517/17425247.2013.763792

Fievez, V., Plapied, L., des Rieux, A., Pourcelle, V., Freichels, H., Wascotte, V., et al. (2009). Targeting nanoparticles to M cells with non-peptidic ligands for oral vaccination. *Eur. J. Pharm. Biopharm* 73 (1), 16–24. doi: 10.1016/j.ejpb.2009.04.009

Fonte, P., Nogueira, T., Gehm, C., Ferreira, D., and Sarmento, B. (2011). Chitosan-coated solid lipid nanoparticles enhance the oral absorption of insulin. *Drug Deliv. Trans. Res.* 1 (4), 299–308. doi: 10.1007/s13346-011-0023-5

Foster, N., Clark, M. A., Jepson, M. A., and Hirst, B. H. (1998). Ulex europaeus 1 lectin targets microspheres to mouse Peyer's patch M-cells *in vivo*. *Vaccine* 16 (5), 536–541. doi: 10.1016/S0264-410X(97)00222-3

Frank, D. N., St Amand, A. L., Feldman, R. A., Boedeker, E. C., Harpaz, N., and Pace, N. R. (2007). Molecular-phylogenetic characterization of microbial community imbalances in human inflammatory bowel diseases. *Proc. Natl. Acad. Sci. U. States A.* 104 (34), 13780–13785. doi: 10.1073/pnas.0706625104

Frey, A., Giannasca, K. T., Weltzin, R., Giannasca, P. J., Reggio, H., Lencer, W. I., et al. (1996). Role of the glycocalyx in regulating access of microparticles to apical plasma membranes of intestinal epithelial cells: implications for microbial attachment and oral vaccine targeting. *J. Exp. Med.* 184 (3), 1045–1059. doi: 10.1084/jem.184.3.1045

Gareb, B., Eissens, A. C., Kosterink, J. G. W., and Frijlink, H. W. (2016). Development of a zero-order sustained-release tablet containing mesalazine and budesonide intended to treat the distal gastrointestinal tract in inflammatory bowel disease. *Eur. J. Pharm. Biopharm.* 103, 32–42. doi: 10.1016/j.ejpb.2016.03.018

Gartner, G. K. (2002). The forestomach of rats and mice, an effective device supporting digestive metabolism in muridae. *J. Exp. Anim. Sci.* 42, 1–20. doi: 10.1016/S0939-8600(02)80002-5

Gazzaniga, A., Maroni, A., Sangalli, M. E., and Zema, L. (2006). Time-controlled oral delivery systems for colon targeting. *Expert Opin. Drug Deliv.* 3 (5), 583–597. doi: 10.1517/17425247.3.5.583

Goto, T., Tanida, N., Yoshinaga, T., Sato, S., Ball, D. J., Wilding, I. R., et al. (2004). Pharmaceutical design of a novel colon-targeted delivery system using two-layer-coated tablets of three different pharmaceutical formulations, supported by clinical evidence in humans. *J. Control Release* 97 (1), 31–42. doi: 10.1016/j.jconrel.2004.02.023

Gracie, D. J., Kane, J. S., Mumtaz, S., Scarsbrook, A. F., Chowdhury, F. U., and Ford, A. C. (2012). Prevalence of, and predictors of, bile acid malabsorption in outpatients with chronic diarrhea. *Neurogastroenterol. Motil.* 24 (11), 983–e538. doi: 10.1111/j.1365-2982.2012.01953.x

Griffin, B. T., Guo, J., Presas, E., Donovan, M. D., Alonso, M. J., and O'Driscoll, C. M. (2016). Pharmacokinetic, pharmacodynamic and biodistribution following oral administration of nanocarriers containing peptide and protein drugs. *Adv. Drug Delivery Rev.* 106 (Pt B), 367–380. doi: 10.1016/j.addr.2016.06.006

Grover, M., Kanazawa, M., Palsson, O. S., Chitkara, D. K., Gangarosa, L. M., Drossman, D. A., et al. (2008). Small intestinal bacterial overgrowth in irritable bowel syndrome: association with colon motility, bowel symptoms, and psychological distress. *Neurogastroenterol. Motil.* 20 (9), 998–1008. doi: 10.1111/j.1365-2982.2008.01142.x

Gupta, V., Hwang, B. H., Doshi, N., Banerjee, A., Anselmo, A. C., and Mitragotri, S. (2016). Delivery of Exenatide and Insulin Using Mucoadhesive Intestinal Devices. *Ann. Biomed. Engineering* 44 (6), 1993–2007. doi: 10.1007/s10439-016-1558-x

Hamman, J. H., Demana, P. H., and Olivier, E. I. (2007). Targeting receptors, transporters and site of absorption to improve oral drug delivery. *Drug Target Insights* 2, 71–81. doi: 10.1177/117739280700200003

Han, H. K., Shin, H. J., and Ha, D. H. (2012). Improved oral bioavailability of alendronate *via the* mucoadhesive liposomal delivery system. *Eur. J. Pharmaceut. Sci.* 46 (5), 500–507. doi: 10.1016/j.ejps.2012.04.002

Hao, S., Wang, Y., and Wang, B. (2014). Sinking-magnetic microparticles prepared by the electrospray method for enhanced gastric antimicrobial delivery. *Mol. Pharm.* 11 (5), 1640–1650. doi: 10.1021/mp5000339

Harel, E., Rubinstein, A., Nissan, A., Khazanov, E., Nadler Milbauer, M., Barenholz, Y., et al. (2011). Enhanced transferrin receptor expression by proinflammatory cytokines in enterocytes as a means for local delivery of drugs to inflamed gut mucosa. *PloS One* 6 (9), e24202. doi: 10.1371/journal.pone.0024202

Hatton, G. B., Yadav, V., Basit, A. W., and Merchant, H. A. (2015). Animal Farm: Considerations in Animal Gastrointestinal Physiology and Relevance to Drug Delivery in Humans. *J. Pharm. Sci.* 104 (9), 2747–2776. doi: 10.1002/jps.24365

Hatton, G. B., Madla, C. M., Rabbie, S. C., and Basit, A. W. (2018). All disease begins in the gut: Influence of gastrointestinal disorders and surgery on oral drug performance. *Int. J. Pharm.* 548 (1), 408–422. doi: 10.1016/j.ijpharm.2018.06.054

Hatton, G. B., Madla, C. M., Rabbie, S. C., and Basit, A. W. (2019). Gut reaction: impact of systemic diseases on gastrointestinal physiology and drug absorption. *Drug Discovery Today* 24 (2), 417–427. doi: 10.1016/j.drudis.2018.11.009

Hebden, J. M., Blackshaw, P. E., Perkins, A. C., Wilson, C. G., and Spiller, R. C. (2000). Limited exposure of the healthy distal colon to orally-dosed formulation is further exaggerated in active left-sided ulcerative colitis. *Alimentary Pharmacol. Ther.* 14 (2), 155–161. doi: 10.1046/j.1365-2036.2000.00697.x

Helander, H. F., and Fandriks, L. (2014). Surface area of the digestive tract - revisited. *Scand. J. Gastroenterol.* 49 (6), 681–689. doi: 10.3109/00365521.2014.898326

Hellmund, M., Achazi, K., Neumann, F., Thota, B. N., Ma, N., and Haag, R. (2015). Systematic adjustment of charge densities and size of polyglycerol amines reduces cytotoxic effects and enhances cellular uptake. *Biomater. Sci.* 3 (11), 1459–1465. doi: 10.1039/C5BM00187K

Hillyer, J. F., and Albrecht, R. M. (2001). Gastrointestinal persorption and tissue distribution of differently sized colloidal gold nanoparticles. *J. Pharm. Sci.* 90 (12), 1927–1936. doi: 10.1002/jps.1143

Hofmann, D., Tenzer, S., Bannwarth, M. B., Messerschmidt, C., Glaser, S. F., Schild, H., et al. (2014). Mass spectrometry and imaging analysis of nanoparticle-containing vesicles provide a mechanistic insight into cellular trafficking. *ACS Nano* 8 (10), 10077–10088. doi: 10.1021/nn502754c

Homayun, B., Lin, X., and Choi, H. J. (2019). Challenges and Recent Progress in Oral Drug Delivery Systems for Biopharmaceuticals. *Pharmaceutics* 11 (3), 129. doi: 10.3390/pharmaceutics11030129

Hoque, K. M., Chakraborty, S., Sheikh, I. A., and Woodward, O. M. (2012). New advances in the pathophysiology of intestinal ion transport and barrier function in diarrhea and the impact on therapy. *Expert Rev. Anti-infect. Ther.* 10 (6), 687–699. doi: 10.1586/eri.12.47

Hovgaard, L., and Brondsted, H. (1996). Current applications of polysaccharides in colon targeting. *Crit. Rev. Ther. Drug Carrier Syst.* 13 (3-4), 185–223. doi: 10.1615/CritRevTherDrugCarrierSyst.v13.i3-4.10

Hu, Z., Mawatari, S., Shibata, N., Takada, K., Yoshikawa, H., Arakawa, A., et al. (2000). Application of a biomagnetic measurement system (BMS) to the evaluation of gastrointestinal transit of intestinal pressure-controlled colon delivery capsules (PCDCs) in human subjects. *Pharmaceut. Res.* 17 (2), 160–167. doi: 10.1023/A:1007561129221

Hu, Y. B., Dammer, E. B., Ren, R. J., and Wang, G. (2015). The endosomal-lysosomal system: from acidification and cargo sorting to neurodegeneration. *Trans. Neurodegeneration* 4, 18. doi: 10.1186/s40035-015-0041-1

Hu, X., Fan, W., Yu, Z., Lu, Y., Qi, J., Zhang, J., et al. (2016). Evidence does not support absorption of intact solid lipid nanoparticles *via* oral delivery. *Nanoscale* 8 (13), 7024–7035. doi: 10.1039/C5NR07474F

Hua, S., Marks, E., Schneider, J. J., and Keely, S. (2015). Advances in oral nano-delivery systems for colon targeted drug delivery in inflammatory bowel disease: selective targeting to diseased versus healthy tissue. *Nanomedicine* 11 (5), 1117–1132. doi: 10.1016/j.nano.2015.02.018

Hua, S., de Matos, M. B. C., Metselaar, J. M., and Storm, G. (2018). Current Trends and Challenges in the Clinical Translation of Nanoparticulate Nanomedicines: Pathways for Translational Development and Commercialization. *Front. Pharmacol.* 9, 790. doi: 10.3389/fphar.2018.00790

Hua, S. (2014). Orally administered liposomal formulations for colon targeted drug delivery. *Front. Pharmacol.* 5, 138. doi: 10.3389/fphar.2014.00138

Ibekwe, V. C., Fadda, H. M., McConnell, E. L., Khela, M. K., Evans, D. F., and Basit, A. W. (2008). Interplay between intestinal pH, transit time and feed status on the *in vivo* performance of pH responsive ileo-colonic release systems. *Pharmaceut. Res.* 25 (8), 1828–1835. doi: 10.1007/s11095-008-9580-9

Irache, J. M., Durrer, C., Duchene, D., and Ponchel, G. (1994). In vitro study of lectin-latex conjugates for specific bioadhesion. *J. Control Release* 31, 181–188. doi: 10.1016/0168-3659(94)00033-6

Jain, P., Jain, S., Prasad, K. N., Jain, S. K., and Vyas, S. P. (2009). Polyelectrolyte coated multilayered liposomes (nanocapsules) for the treatment of Helicobacter pylori infection. *Mol. Pharm.* 6 (2), 593–603. doi: 10.1021/mp8002539

Jain, D., Raturi, R., Jain, V., Bansal, P., and Singh, R. (2011). Recent technologies in pulsatile drug delivery systems. *Biomatter* 1 (1), 57–65. doi: 10.4161/biom.1.1.17717

Jain, S., Rathi, V. V., Jain, A. K., Das, M., and Godugu, C. (2012). Folate-decorated PLGA nanoparticles as a rationally designed vehicle for the oral delivery of insulin. *Nanomed. (Lond)* 7 (9), 1311–1337. doi: 10.2217/nnm.12.31

Jain, S. K., Haider, T., Kumar, A., and Jain, A. (2016). Lectin-Conjugated Clarithromycin and Acetohydroxamic Acid-Loaded PLGA Nanoparticles: a Novel Approach for Effective Treatment of H. pylori. *AAPS PharmSciTech.* 17 (5), 1131–1140. doi: 10.1208/s12249-015-0443-5

Johansson, M. E., Sjovall, H., and Hansson, G. C. (2013). The gastrointestinal mucus system in health and disease. *Nat. Rev. Gastroenterol. Hepatol.* 10 (6), 352–361. doi: 10.1038/nrgastro.2013.35

Joshi, G., Kumar, A., and Sawant, K. (2014). Enhanced bioavailability and intestinal uptake of Gemcitabine HCl loaded PLGA nanoparticles after oral delivery. *Eur. J. Pharmaceut. Sci.* 60, 80–89. doi: 10.1016/j.ejps.2014.04.014

Joshi, G., Kumar, A., and Sawant, K. (2016). Bioavailability enhancement, Caco-2 cells uptake and intestinal transport of orally administered lopinavir-loaded PLGA nanoparticles. *Drug Delivery* 23 (9), 3492–3504. doi: 10.1080/10717544.2016.1199605

Jubeh, T., Barenholz, Y., and Rubinstein, A. (2004). Differential Adhesion of Normal and Inflamed Rat Colonic Mucosa by Charged Liposomes. *Pharmaceut. Res.* 21 (3), 447–453. doi: 10.1023/B:PHAM.0000019298.29561.cd

Kagan, L., and Hoffman, A. (2008). Systems for region selective drug delivery in the gastrointestinal tract: biopharmaceutical considerations. *Expert Opin. Drug Deliv.* 5 (6), 681–692. doi: 10.1517/17425247.5.6.681

Kang, J. H., Hwang, J. Y., Seo, J. W., Kim, H. S., and Shin, U. S. (2018). Small intestine- and colon-specific smart oral drug delivery system with controlled release characteristic. *Mater. Sci. Eng. C Mater. Biol. Appl.* 91, 247–254. doi: 10.1016/j.msec.2018.05.052

Kararli, T. T. (1995). Comparison of the gastrointestinal anatomy, physiology, and biochemistry of humans and commonly used laboratory animals. *Biopharm Drug Dispos.* 16 (5), 351–380. doi: 10.1002/bdd.2510160502

Kashyap, P. C., Marcobal, A., Ursell, L. K., Larauche, M., Duboc, H., Earle, K. A., et al. (2013). Complex interactions among diet, gastrointestinal transit, and gut microbiota in humanized mice. *Gastroenterology* 144 (5), 967–977. doi: 10.1053/j.gastro.2013.01.047

Khan, M. Z., Prebeg, Z., and Kurjakovic, N. (1999). A pH-dependent colon targeted oral drug delivery system using methacrylic acid copolymers. I. Manipulation Of drug release using Eudragit L100-55 and Eudragit S100 combinations. *J. Control Release* 58 (2), 215–222. doi: 10.1016/S0168-3659(98)00151-5

Konturek, P. C., Brzozowski, T., and Konturek, S. J. (2011). Stress and the gut: pathophysiology, clinical consequences, diagnostic approach and treatment options. *J. Physiol. Pharmacol.* 62 (6), 591–599.

Kriegel, C., and Amiji, M. (2011). Oral TNF-alpha gene silencing using a polymeric microsphere-based delivery system for the treatment of inflammatory bowel disease. *J. Control Release* 150 (1), 77–86. doi: 10.1016/j.jconrel.2010.10.002

Kriegel, C., and Amiji, M. M. (2011). Dual TNF-alpha/Cyclin D1 Gene Silencing With an Oral Polymeric Microparticle System as a Novel Strategy for the Treatment of Inflammatory Bowel Disease. *Clin. Transl. Gastroenterol.* 2, e2. doi: 10.1038/ctg.2011.1

Kshirsagar, S. J., Bhalekar, M. R., Patel, J. N., Mohapatra, S. K., and Shewale, N. S. (2012). Preparation and characterization of nanocapsules for colon-targeted drug delivery system. *Pharm. Dev. Technol.* 17 (5), 607–613. doi: 10.3109/10837450.2011.557732

Kumar, M., and Kaushik, D. (2018). An Overview on Various Approaches and Recent Patents on Gastroretentive Drug Delivery Systems. *Recent Pat. Drug Delivery Formul.* 12 (2), 84–92. doi: 10.2174/1872211312666180308150218

Kvietys, P. R. (1999). Intestinal physiology relevant to short-bowel syndrome. *Eur. J. Pediatr. Surg.* 9 (4), 196–199. doi: 10.1055/s-2008-1072243

Kyd, J. M., and Cripps, A. W. (2008). Functional differences between M cells and enterocytes in sampling luminal antigens. *Vaccine* 26 (49), 6221–6224. doi: 10.1016/j.vaccine.2008.09.061

Lahner, E., Annibale, B., and Delle Fave, G. (2009). Systematic review: impaired drug absorption related to the co-administration of antisecretory therapy. *Alimentary Pharmacol. Ther.* 29 (12), 1219–1229. doi: 10.1111/j.1365-2036.2009.03993.x

Lamprecht, A., Schäfer, U., and Lehr, C.-M. (2001a). Size-Dependent Bioadhesion of Micro- and Nanoparticulate Carriers to the Inflamed Colonic Mucosa. *Pharmaceut. Res.* 18 (6), 788–793. doi: 10.1023/A:1011032328064

Lamprecht, A., Ubrich, N., Yamamoto, H., Schafer, U., Takeuchi, H., Maincent, P., et al. (2001b). Biodegradable nanoparticles for targeted drug delivery in treatment of inflammatory bowel disease. *J. Pharmacol. Exp. Ther.* 299 (2), 775–781.

Lamprecht, A., Yamamoto, H., Takeuchi, H., and Kawashima, Y. (2005a). Nanoparticles enhance therapeutic efficiency by selectively increased local drug dose in experimental colitis in rats. *J. Pharmacol. Exp. Ther.* 315 (1), 196–202. doi: 10.1124/jpet.105.088146

Lamprecht, A., Yamamoto, H., Takeuchi, H., and Kawashima, Y. (2005b). A pH-sensitive microsphere system for the colon delivery of tacrolimus containing nanoparticles. *J. Control Release* 104 (2), 337–346. doi: 10.1016/j.jconrel.2005.02.011

Laroui, H., Dalmasso, G., Nguyen, H. T., Yan, Y., Sitaraman, S. V., and Merlin, D. (2010). Drug-loaded nanoparticles targeted to the colon with polysaccharide hydrogel reduce colitis in a mouse model. *Gastroenterology* 138 (3), 843–53 e1-2. doi: 10.1053/j.gastro.2009.11.003

Laroui, H., Geem, D., Xiao, B., Viennois, E., Rakhya, P., Denning, T., et al. (2014a). Targeting intestinal inflammation with CD98 siRNA/PEI-loaded nanoparticles. *Mol. Ther.* 22 (1), 69–80. doi: 10.1038/mt.2013.214

Laroui, H., Viennois, E., Xiao, B., Canup, B. S., Geem, D., Denning, T. L., et al. (2014b). Fab'-bearing siRNA TNFalpha-loaded nanoparticles targeted to colonic macrophages offer an effective therapy for experimental colitis. *J. Control Release* 186, 41–53. doi: 10.1016/j.jconrel.2014.04.046

Larsson, J. M., Karlsson, H., Sjovall, H., and Hansson, G. C. (2009). A complex, but uniform O-glycosylation of the human MUC2 mucin from colonic biopsies analyzed by nanoLC/MSn. *Glycobiology* 19 (7), 756–766. doi: 10.1093/glycob/cwp048

Lautenschlager, C., Schmidt, C., Lehr, C. M., Fischer, D., and Stallmach, A. (2013). PEG-functionalized microparticles selectively target inflamed mucosa in inflammatory bowel disease. *Eur. J. Pharm. Biopharm.* 85 (3 Pt A), 578–586. doi: 10.1016/j.ejpb.2013.09.016

Li, A. C., and Thompson, R. P. (2003). Basement membrane components. *J. Clin. Pathol.* 56 (12), 885–887. doi: 10.1136/jcp.56.12.885

Li, D., Zhuang, J., He, H., Jiang, S., Banerjee, A., Lu, Y., et al. (2017). Influence of Particle Geometry on Gastrointestinal Transit and Absorption following Oral Administration. *ACS Appl. Mater. Interf.* 9 (49), 42492–42502. doi: 10.1021/acsami.7b11821

Lih-Brody, L., Powell, S. R., Collier, K. P., Reddy, G. M., Cerchia, R., Kahn, E., et al. (1996). Increased oxidative stress and decreased antioxidant defenses in mucosa of inflammatory bowel disease. *Digestive Dis. Sci.* 41 (10), 2078–2086. doi: 10.1007/BF02093613

Lin, H. C., Prather, C., Fisher, R. S., Meyer, J. H., Summers, R. W., Pimentel, M., et al. (2005). Measurement of gastrointestinal transit. *Digestive Dis. Sci.* 50 (6), 989–1004. doi: 10.1007/s10620-005-2694-6

Ling, S. S., Yuen, K. H., Magosso, E., and Barker, S. A. (2009). Oral bioavailability enhancement of a hydrophilic drug delivered *via* folic acid-coupled liposomes in rats. *J. Pharm. Pharmacol.* 61 (4), 445–449. doi: 10.1211/jpp.61.04.0005

Linskens, R. K., Huijsdens, X. W., Savelkoul, P. H., Vandenbroucke-Grauls, C. M., and Meuwissen, S. G. (2001). The bacterial flora in inflammatory bowel disease: current insights in pathogenesis and the influence of antibiotics and probiotics. *Scand. J. Gastroenterol. Suppl.* 36 (234), 29–40. doi: 10.1080/003655201753265082

Liu, L., Fishman, M. L., Hicks, K. B., and Kende, M. (2005). Interaction of various pectin formulations with porcine colonic tissues. *Biomaterials* 26 (29), 5907–5916. doi: 10.1016/j.biomaterials.2005.03.005

Liu, M., Zhang, J., Zhu, X., Shan, W., Li, L., Zhong, J., et al. (2016). Efficient mucus permeation and tight junction opening by dissociable "mucus-inert" agent coated trimethyl chitosan nanoparticles for oral insulin delivery. *J. Control Release* 222, 67–77. doi: 10.1016/j.jconrel.2015.12.008

Liu, L., Yao, W., Rao, Y., Lu, X., and Gao, J. (2017). pH-Responsive carriers for oral drug delivery: challenges and opportunities of current platforms. *Drug Delivery* 24 (1), 569–581. doi: 10.1080/10717544.2017.1279238

Lundquist, P., and Artursson, P. (2016). Oral absorption of peptides and nanoparticles across the human intestine: Opportunities, limitations and studies in human tissues. *Adv. Drug Delivery Rev.* 106 (Pt B), 256–276. doi: 10.1016/j.addr.2016.07.007

Macfarlane, G. T., and Macfarlane, S. (2011). Fermentation in the human large intestine: its physiologic consequences and the potential contribution of prebiotics. *J. Clin. Gastroenterol.* 45 Suppl, S120–S127. doi: 10.1097/MCG.0b013e31822fecfe

Macfarlane, G. T., Allison, C., Gibson, S. A., and Cummings, J. H. (1988). Contribution of the microflora to proteolysis in the human large intestine. *J. Appl. Bacteriol.* 64 (1), 37–46. doi: 10.1111/j.1365-2672.1988.tb02427.x

Madara, J. L. (1998). Regulation of the movement of solutes across tight junctions. *Annu. Rev. Physiol.* 60, 143–159. doi: 10.1146/annurev.physiol.60.1.143

Mahida, Y. R., Wu, K. C., and Jewell, D. P. (1989). Respiratory burst activity of intestinal macrophages in normal and inflammatory bowel disease. *Gut* 30 (10), 1362–1370. doi: 10.1136/gut.30.10.1362

Maisel, K., Ensign, L., Reddy, M., Cone, R., and Hanes, J. (2015). Effect of surface chemistry on nanoparticle interaction with gastrointestinal mucus and distribution in the gastrointestinal tract following oral and rectal administration in the mouse. *J. Control Release* 197, 48–57. doi: 10.1016/j.jconrel.2014.10.026

Makhlof, A., Tozuka, Y., and Takeuchi, H. (2009). pH-Sensitive nanospheres for colon-specific drug delivery in experimentally induced colitis rat model. *Eur. J. Pharm. Biopharm.* 72 (1), 1–8. doi: 10.1016/j.ejpb.2008.12.013

Makhlof, A., Tozuka, Y., and Takeuchi, H. (2011a). Design and evaluation of novel pH-sensitive chitosan nanoparticles for oral insulin delivery. *Eur. J. Pharmaceut. Sci.* 42 (5), 445–451. doi: 10.1016/j.ejps.2010.12.007

Makhlof, A., Fujimoto, S., Tozuka, Y., and Takeuchi, H. (2011b). In vitro and *in vivo* evaluation of WGA-carbopol modified liposomes as carriers for oral peptide delivery. *Eur. J. Pharm. Biopharm.* 77 (2), 216–224. doi: 10.1016/j.ejpb.2010.12.008

Managuli, R. S., Raut, S. Y., Reddy, M. S., and Mutalik, S. (2018). Targeting the intestinal lymphatic system: a versatile path for enhanced oral bioavailability of drugs. *Expert Opin. Drug Deliv.* 15 (8), 787–804. doi: 10.1080/17425247.2018.1503249

Mandal, U. K., Chatterjee, B., and Senjoti, F. G. (2016). Gastro-retentive drug delivery systems and their *in vivo* success: a recent update. *Asian J. Pharmaceut. Sci.* 11, 575–584. doi: 10.1016/j.ajps.2016.04.007

Mane, V., and Muro, S. (2012). Biodistribution and endocytosis of ICAM-1-targeting antibodies versus nanocarriers in the gastrointestinal tract in mice. *Int. J. Nanomed.* 7, 4223–4237. doi: 10.2147/ijn.s34105

Manocha, M., Pal, P. C., Chitralekha, K. T., Thomas, B. E., Tripathi, V., Gupta, S. D., et al. (2005). Enhanced mucosal and systemic immune response with intranasal immunization of mice with HIV peptides entrapped in PLG microparticles in combination with Ulex Europaeus-I lectin as M cell target. *Vaccine* 23 (48-49), 5599–5617. doi: 10.1016/j.vaccine.2005.06.031

Marieb, E. N., and Hoehn, K. (2010). *Human Anatomy and Physiology. 8th ed.* (USA: Pearson Benjamin Cummings).

Marquez Ruiz, J. F., Kedziora, K., O'Reilly, M., Maguire, J., Keogh, B., Windle, H., et al. (2012). Azo-reductase activated budesodine prodrugs for colon targeting. *Bioorg. Med. Chem. Lett.* 22 (24), 7573–7577. doi: 10.1016/j.bmcl.2012.10.006

Martinez, M. N., and Amidon, G. L. (2002). A mechanistic approach to understanding the factors affecting drug absorption: a review of fundamentals. *J. Clin. Pharmacol.* 42 (6), 620–643. doi: 10.1177/00970002042006005

McConnell, E. L., Short, M. D., and Basit, A. W. (2008). An *in vivo* comparison of intestinal pH and bacteria as physiological trigger mechanisms for colonic targeting in man. *J. Controlled Release* 130 (2), 154–160. doi: 10.1016/j.jconrel.2008.05.022

McKeage, K., and Goa, K. L. (2002). Budesonide (Entocort EC Capsules): a review of its therapeutic use in the management of active Crohn's disease in adults. *Drugs* 62 (15), 2263–2282. doi: 10.2165/00003495-200262150-00015

Meissner, Y., Pellequer, Y., and Lamprecht, A. (2006). Nanoparticles in inflammatory bowel disease: particle targeting versus pH-sensitive delivery. *Int. J. Pharm.* 316 (1-2), 138–143. doi: 10.1016/j.ijpharm.2006.01.032

Miller, H., Zhang, J., Kuolee, R., Patel, G. B., and Chen, W. (2007). Intestinal M cells: the fallible sentinels? *World J. Gastroenterol.* 13 (10), 1477–1486. doi: 10.3748/wjg.v13.i10.1477

Mindell, J. A. (2012). Lysosomal acidification mechanisms. *Annu. Rev. Physiol.* 74, 69–86. doi: 10.1146/annurev-physiol-012110-142317

Miranda, A., Millan, M., and Caraballo, I. (2007). Investigation of the influence of particle size on the excipient percolation thresholds of HPMC hydrophilic matrix tablets. *J. Pharm. Sci.* 96 (10), 2746–2756. doi: 10.1002/jps.20912

Moss, D. M., Curley, P., Kinvig, H., Hoskins, C., and Owen, A. (2018). The biological challenges and pharmacological opportunities of orally administered nanomedicine delivery. *Expert Rev. Gastroenterol. Hepatol.* 12 (3), 223–236. doi: 10.1080/17474124.2018.1399794

Moulari, B., Pertuit, D., Pellequer, Y., and Lamprecht, A. (2008). The targeting of surface modified silica nanoparticles to inflamed tissue in experimental colitis. *Biomaterials* 29 (34), 4554–4560. doi: 10.1016/j.biomaterials.2008.08.009

Murakami, T. (2017). Absorption sites of orally administered drugs in the small intestine. *Expert Opin. Drug Discovery* 12 (12), 1219–1232. doi: 10.1080/17460441.2017.1378176

Ngwuluka, N. C., Choonara, Y. E., Kumar, P., du Toit, L. C., Modi, G., and Pillay, V. (2015). An optimized gastroretentive nanosystem for the delivery of levodopa. *Int. J. Pharm.* 494 (1), 49–65. doi: 10.1016/j.ijpharm.2015.08.014

Niebel, W., Walkenbach, K., Beduneau, A., Pellequer, Y., and Lamprecht, A. (2012). Nanoparticle-based clodronate delivery mitigates murine experimental colitis. *J. Control Release* 160 (3), 659–665. doi: 10.1016/j.jconrel.2012.03.004

Nugent, S. G., Kumar, D., Rampton, D. S., and Evans, D. F. (2001). Intestinal luminal pH in inflammatory bowel disease: possible determinants and implications for therapy with aminosalicylates and other drugs. *Gut* 48 (4), 571–577. doi: 10.1136/gut.48.4.571

Nykanen, P., Lempaa, S., Aaltonen, M. L., Jurjenson, H., Veski, P., and Marvola, M. (2001). Citric acid as excipient in multiple-unit enteric-coated tablets for targeting drugs on the colon. *Int. J. Pharm.* 229 (1-2), 155–162. doi: 10.1016/S0378-5173(01)00839-0

Oz, H. S., and Ebersole, J. L. (2008). Application of prodrugs to inflammatory diseases of the gut. *Molecules* 13 (2), 452–474. doi: 10.3390/molecules13020452

Patel, S., and McCormick, B. A. (2014). Mucosal Inflammatory Response to Salmonella typhimurium Infection. *Front. Immunol.* 5, 311. doi: 10.3389/fimmu.2014.00311

Patel, D. M., Jani, R. H., and Patel, C. N. (2011). Design and evaluation of colon targeted modified pulsincap delivery of 5-fluorouracil according to circadian rhythm. *Int. J. Pharmaceut. Invest.* 1 (3), 172–181. doi: 10.4103/2230-973X.85969

Patel, M. M. (2014). Getting into the colon: approaches to target colorectal cancer. *Expert Opin. Drug Delivery* 11 (9), 1343–1350. doi: 10.1517/17425247.2014.927440

Patel, M. M. (2015). Colon: a gateway for chronotherapeutic drug delivery systems. *Expert Opin. Drug Delivery* 12 (9), 1389–1395. doi: 10.1517/17425247.2015.1060217

Pawar, V. K., Kansal, S., Garg, G., Awasthi, R., Singodia, D., and Kulkarni, G. T. (2011). Gastroretentive dosage forms: a review with special emphasis on floating drug delivery systems. *Drug Deliv.* 18 (2), 97–110. doi: 10.3109/10717544.2010.520354

Peterson, C. G., Eklund, E., Taha, Y., Raab, Y., and Carlson, M. (2002). A new method for the quantification of neutrophil and eosinophil cationic proteins in feces: establishment of normal levels and clinical application in patients with inflammatory bowel disease. *Am. J. Gastroenterol.* 97 (7), 1755–1762. doi: 10.1111/j.1572-0241.2002.05837.x

Podolsky, D. K. (2002). Inflammatory bowel disease. *New Engl. J. Med.* 347 (6), 417–429. doi: 10.1056/NEJMra020831

Prajapati, J. B., Verma, S. D., and Patel, A. A. (2018). Oral bioavailability enhancement of agomelatine by loading into nanostructured lipid carriers: Peyer's patch targeting approach. *Int. J. Nanomed.* 13 (T-NANO 2014 Abstracts), 35–38. doi: 10.2147/IJN.S124703

Rafii, F., Franklin, W., and Cerniglia, C. E. (1990). Azoreductase activity of anaerobic bacteria isolated from human intestinal microflora. *Appl. Environ. Microbiol.* 56 (7), 2146–2151. doi: 10.1128/AEM.56.7.2146-2151.1990

Ramteke, S., and Jain, N. K. (2008). Clarithromycin- and omeprazole-containing gliadin nanoparticles for the treatment of Helicobacter pylori. *J. Drug Targeting* 16 (1), 65–72. doi: 10.1080/10611860701733278

Ramteke, S., Ganesh, N., Bhattacharya, S., and Jain, N. K. (2008). Triple therapy-based targeted nanoparticles for the treatment of Helicobacter pylori. *J. Drug Targeting* 16 (9), 694–705. doi: 10.1080/10611860802295839

Ramteke, S., Ganesh, N., Bhattacharya, S., and Jain, N. K. (2009). Amoxicillin, clarithromycin, and omeprazole based targeted nanoparticles for the treatment of H. pylori. *J. Drug Targeting* 17 (3), 225–234. doi: 10.1080/10611860902718649

Rana, S. V., Sharma, S., Malik, A., Kaur, J., Prasad, K. K., Sinha, S. K., et al. (2013). Small intestinal bacterial overgrowth and orocecal transit time in patients of inflammatory bowel disease. *Digestive Dis. Sci.* 58 (9), 2594–2598. doi: 10.1007/s10620-013-2694-x

Rao, K. A., Yazaki, E., Evans, D. F., and Carbon, R. (2004). Objective evaluation of small bowel and colonic transit time using pH telemetry in athletes with gastrointestinal symptoms. *Br. J. Sports Med.* 38 (4), 482–487. doi: 10.1136/bjsm.2003.006825

Reinholz, J., Landfester, K., and Mailander, V. (2018). The challenges of oral drug delivery *via* nanocarriers. *Drug Delivery* 25 (1), 1694–1705. doi: 10.1080/10717544.2018.1501119

Reinus, J. F., and Simon, D. (2014). *Gastrointestinal Anatomy and Physiology: The Essentials* (UK: John Wiley & Sons).

Reix, N., Parat, A., Seyfritz, E., Van der Werf, R., Epure, V., Ebel, N., et al. (2012). In vitro uptake evaluation in Caco-2 cells and *in vivo* results in diabetic rats of insulin-loaded PLGA nanoparticles. *Int. J. Pharm.* 437 (1-2), 213–220. doi: 10.1016/j.ijpharm.2012.08.024

Rosenthal, R., Gunzel, D., Finger, C., Krug, S. M., Richter, J. F., Schulzke, J. D., et al. (2012). The effect of chitosan on transcellular and paracellular mechanisms in the intestinal epithelial barrier. *Biomaterials* 33 (9), 2791–2800. doi: 10.1016/j.biomaterials.2011.12.034

Rouge, N., Buri, P., and Doelker, E. (1996). Drug absorption sites in the gastrointestinal tract and dosage forms for site-specific delivery. *Int. J. Pharmaceut.* 136, 117–139. doi: 10.1016/0378-5173(96)85200-8

Rouge, N., Allemann, E., Gex-Fabry, M., Balant, L., Cole, E. T., Buri, P., et al. (1998). Comparative pharmacokinetic study of a floating multiple-unit capsule, a high-density multiple-unit capsule and an immediate-release tablet containing 25 mg atenolol. *Pharm. Acta Helvetiae* 73 (2), 81–87. doi: 10.1016/S0031-6865(97)00050-2

Rubinstein, A., and Tirosh, B. (1994). Mucus gel thickness and turnover in the gastrointestinal tract of the rat: response to cholinergic stimulus and implication for mucoadhesion. *Pharmaceut. Res.* 11 (6), 794–799. doi: 10.1023/A:1018961204325

Rubinstein, A. (2000). Natural polysaccharides as targeting tools of drugs to the human colon. *Drug Dev. Res.* 50, 435–439. doi: 10.1002/1098-2299(200007/08)50:3/4<435::AID-DDR26>3.0.CO;2-5

Saftig, P., and Klumperman, J. (2009). Lysosome biogenesis and lysosomal membrane proteins: trafficking meets function. *Nat. Rev. Mol. Cell Biol.* 10 (9), 623–635. doi: 10.1038/nrm2745

Saltzman, W. M., Radomsky, M. L., Whaley, K. J., and Cone, R. A. (1994). Antibody diffusion in human cervical mucus. *Biophys. J.* 66 (2 Pt 1), 508–515. doi: 10.1016/S0006-3495(94)80802-1

Sangalli, M. E., Maroni, A., Zema, L., Busetti, C., Giordano, F., and Gazzaniga, A. (2001). In vitro and *in vivo* evaluation of an oral system for time and/or site-specific drug delivery. *J. Control Release* 73 (1), 103–110. doi: 10.1016/S0168-3659(01)00291-7

Sarparanta, M. P., Bimbo, L. M., Makila, E. M., Salonen, J. J., Laaksonen, P. H., Helariutta, A. M., et al. (2012). The mucoadhesive and gastroretentive properties of hydrophobin-coated porous silicon nanoparticle oral drug delivery systems. *Biomaterials* 33 (11), 3353–3362. doi: 10.1016/j.biomaterials.2012.01.029

Sartor, R. B. (2008). Microbial influences in inflammatory bowel diseases. *Gastroenterology* 134 (2), 577–594. doi: 10.1053/j.gastro.2007.11.059

Sartor, R. B. (2010). Genetics and environmental interactions shape the intestinal microbiome to promote inflammatory bowel disease versus mucosal homeostasis. *Gastroenterology* 139 (6), 1816–1819. doi: 10.1053/j.gastro.2010.10.036

Sasaki, Y., Hada, R., Nakajima, H., Fukuda, S., and Munakata, A. (1997). Improved localizing method of radiopill in measurement of entire gastrointestinal pH profiles: colonic luminal pH in normal subjects and patients with Crohn's disease. *Am. J. Gastroenterol.* 92 (1), 114–118.

Sathyan, G., Hwang, S., and Gupta, S. K. (2000). Effect of dosing time on the total intestinal transit time of non-disintegrating systems. *Int. J. Pharm.* 204 (1-2), 47–51. doi: 10.1016/S0378-5173(00)00472-5

Scheline, R. R. (1973). Metabolism of foreign compounds by gastrointestinal microorganisms. *Pharmacol. Rev.* 25 (4), 451–523.

Schmidt, T., Pfeiffer, A., Hackelsberger, N., Widmer, R., Meisel, C., and Kaess, H. (1996). Effect of intestinal resection on human small bowel motility. *Gut* 38 (6), 859–863. doi: 10.1136/gut.38.6.859

Schmidt, C., Lautenschlaeger, C., Collnot, E. M., Schumann, M., Bojarski, C., Schulzke, J. D., et al. (2013). Nano- and microscaled particles for drug targeting to inflamed intestinal mucosa: a first *in vivo* study in human patients. *J. Control Release* 165 (2), 139–145. doi: 10.1016/j.jconrel.2012.10.019

Sercombe, L., Veerati, T., Moheimani, F., Wu, S. Y., Sood, A. K., and Hua, S. (2015). Advances and Challenges of Liposome Assisted Drug Delivery. *Front. Pharmacol.* 6, 286. doi: 10.3389/fphar.2015.00286

Shah, N., Shah, T., and Amin, A. (2011). Polysaccharides: a targeting strategy for colonic drug delivery. *Expert Opin. Drug Deliv.* 8 (6), 779–796. doi: 10.1517/17425247.2011.574121

Shahdadi Sardo, H., Saremnejad, F., Bagheri, S., Akhgari, A., Afrasiabi Garekani, H., and Sadeghi, F. (2019). A review on 5-aminosalicylic acid colon-targeted oral drug delivery systems. *Int. J. Pharm.* 558, 367–379. doi: 10.1016/j.ijpharm.2019.01.022

Shakweh, M., Ponchel, G., and Fattal, E. (2004). Particle uptake by Peyer's patches: a pathway for drug and vaccine delivery. *Expert Opin. Drug Delivery* 1 (1), 141–163. doi: 10.1517/17425247.1.1.141

Sharma, A., Goyal, A. K., and Rath, G. (2018). Development and Characterization of Gastroretentive High-Density Pellets Lodged With Zero Valent Iron Nanoparticles. *J. Pharm. Sci.* 107 (10), 2663–2673. doi: 10.1016/j.xphs.2018.06.014

Sharpe, L. A., Daily, A. M., Horava, S. D., and Peppas, N. A. (2014). Therapeutic applications of hydrogels in oral drug delivery. *Expert Opin. Drug Deliv.* 11 (6), 901–915. doi: 10.1517/17425247.2014.902047

Shen, Z., and Mitragotri, S. (2002). Intestinal patches for oral drug delivery. *Pharmaceut. Res.* 19 (4), 391–395. doi: 10.1023/A:1015118923204

Shreya, A. B., Raut, S. Y., Managuli, R. S., Udupa, N., and Mutalik, S. (2018). Active Targeting of Drugs and Bioactive Molecules *via* Oral Administration by Ligand-Conjugated Lipidic Nanocarriers: Recent Advances. *AAPS PharmSciTech.* 20 (1), 15. doi: 10.1208/s12249-018-1262-2

Siepmann, J., and Peppas, N. A. (2001). Modeling of drug release from delivery systems based on hydroxypropyl methylcellulose (HPMC). *Adv. Drug Delivery Rev.* 48 (2-3), 139–157. doi: 10.1016/S0169-409X(01)00112-0

Simmonds, N. J., Allen, R. E., Stevens, T. R., Van Someren, R. N., Blake, D. R., and Rampton, D. S. (1992). Chemiluminescence assay of mucosal reactive oxygen metabolites in inflammatory bowel disease. *Gastroenterology* 103 (1), 186–196. doi: 10.1016/0016-5085(92)91112-H

Singh, B., Maharjan, S., Jiang, T., Kang, S. K., Choi, Y. J., and Cho, C. S. (2015). Combinatorial Approach of Antigen Delivery Using M Cell-Homing Peptide and Mucoadhesive Vehicle to Enhance the Efficacy of Oral Vaccine. *Mol. Pharm.* 12 (11), 3816–3828. doi: 10.1021/acs.molpharmaceut.5b00265

Singodia, D., Verma, A., Verma, R. K., and Mishra, P. R. (2012). Investigations into an alternate approach to target mannose receptors on macrophages using 4-sulfated N-acetyl galactosamine more efficiently in comparison with mannose-decorated liposomes: an application in drug delivery. *Nanomedicine* 8 (4), 468–477. doi: 10.1016/j.nano.2011.07.002

Sinha, V. R., and Kumria, R. (2001). Polysaccharides in colon-specific drug delivery. *Int. J. Pharm.* 224 (1-2), 19–38. doi: 10.1016/S0378-5173(01)00720-7

Spiller, R. C., Trotman, I. F., Adrian, T. E., Bloom, S. R., Misiewicz, J. J., and Silk, D. B. (1988). Further characterisation of the 'ileal brake' reflex in man–effect of ileal infusion of partial digests of fat, protein, and starch on jejunal motility and release of neurotensin, enteroglucagon, and peptide YY. *Gut* 29 (8), 1042–1051. doi: 10.1136/gut.29.8.1042

Stevens, H. N., Wilson, C. G., Welling, P. G., Bakhshaee, M., Binns, J. S., Perkins, A. C., et al. (2002). Evaluation of Pulsincap to provide regional delivery of dofetilide to the human GI tract. *Int. J. Pharm.* 236 (1-2), 27–34. doi: 10.1016/S0378-5173(02)00012-1

Streubel, A., Siepmann, J., and Bodmeier, R. (2006a). Gastroretentive drug delivery systems. *Expert Opin. Drug Deliv.* 3 (2), 217–233. doi: 10.1517/17425247.3.2.217

Streubel, A., Siepmann, J., and Bodmeier, R. (2006b). Drug delivery to the upper small intestine window using gastroretentive technologies. *Curr. Opin. Pharmacol.* 6 (5), 501–508. doi: 10.1016/j.coph.2006.04.007

Sunoqrot, S., Hasan, L., Alsadi, A., Hamed, R., and Tarawneh, O. (2017). Interactions of mussel-inspired polymeric nanoparticles with gastric mucin: Implications for gastro-retentive drug delivery. *Colloids Surf B Biointerf.* 156, 1–8. doi: 10.1016/j.colsurfb.2017.05.005

Talaei, F., Atyabi, F., Azhdarzadeh, M., Dinarvand, R., and Saadatzadeh, A. (2013). Overcoming therapeutic obstacles in inflammatory bowel diseases: a comprehensive review on novel drug delivery strategies. *Eur. J. Pharmaceut. Sci.* 49 (4), 712–722. doi: 10.1016/j.ejps.2013.04.031

Talkar, S., Dhoble, S., Majumdar, A., and Patravale, V. (2018). Transmucosal Nanoparticles: Toxicological Overview. *Adv. Exp. Med. Biol.* 1048, 37–57. doi: 10.1007/978-3-319-72041-8_3

Tariq, M., Alam, M. A., Singh, A. T., Panda, A. K., and Talegaonkar, S. (2016). Surface decorated nanoparticles as surrogate carriers for improved transport and absorption of epirubicin across the gastrointestinal tract: Pharmacokinetic and pharmacodynamic investigations. *Int. J. Pharm.* 501 (1-2), 18–31. doi: 10.1016/j.ijpharm.2016.01.054

Taverner, A., Dondi, R., Almansour, K., Laurent, F., Owens, S. E., Eggleston, I. M., et al. (2015). Enhanced paracellular transport of insulin can be achieved *via* transient induction of myosin light chain phosphorylation. *J. Control Release* 210, 189–197. doi: 10.1016/j.jconrel.2015.05.270

Thakral, S., Thakral, N. K., and Majumdar, D. K. (2013). Eudragit: a technology evaluation. *Expert Opin. Drug Deliv.* 10 (1), 131–149. doi: 10.1517/17425247.2013.736962

Thirawong, N., Thongborisute, J., Takeuchi, H., and Sriamornsak, P. (2008). Improved intestinal absorption of calcitonin by mucoadhesive delivery of novel pectin–liposome nanocomplexes. *J. Controlled Release* 125 (3), 236–245. doi: 10.1016/j.jconrel.2007.10.023

Thompson, J. S., Quigley, E. M., Adrian, T. E., and Path, F. R. (1998). Role of the ileocecal junction in the motor response to intestinal resection. *J. Gastrointestinal Surg.* 2 (2), 174–185. doi: 10.1016/S1091-255X(98)80010-3

Timmermans, J., and Moes, A. J. (1993). The cutoff size for gastric emptying of dosage forms. *J. Pharm. Sci.* 82 (8), 854. doi: 10.1002/jps.2600820821

Timmermans, J., and Moes, A. J. (1994). Factors controlling the buoyancy and gastric retention capabilities of floating matrix capsules: new data for reconsidering the controversy. *J. Pharm. Sci.* 83 (1), 18–24. doi: 10.1002/jps.2600830106

Tirosh, B., Khatib, N., Barenholz, Y., Nissan, A., and Rubinstein, A. (2009). Transferrin as a luminal target for negatively charged liposomes in the inflamed colonic mucosa. *Mol. Pharm.* 6 (4), 1083–1091. doi: 10.1021/mp9000926

Titus, R., Kastenmeier, A., and Otterson, M. F. (2013). Consequences of gastrointestinal surgery on drug absorption. *Nutr. Clin. Pract.* 28 (4), 429–436. doi: 10.1177/0884533613490740

Tobio, M., Sanchez, A., Vila, A., Soriano, I. I., Evora, C., Vila-Jato, J. L., et al. (2000). The role of PEG on the stability in digestive fluids and *in vivo* fate of PEG-PLA nanoparticles following oral administration. *Colloids Surf B Biointerf.* 18 (3-4), 315–323. doi: 10.1016/S0927-7765(99)00157-5

Toorisaka, E., Watanabe, K., Ono, H., Hirata, M., Kamiya, N., and Goto, M. (2012). Intestinal patches with an immobilized solid-in-oil formulation for oral protein delivery. *Acta Biomater.* 8 (2), 653–658. doi: 10.1016/j.actbio.2011.09.023

Tripathi, J., Thapa, P., Maharjan, R., and Jeong, S. H. (2019). Current State and Future Perspectives on Gastroretentive Drug Delivery Systems. *Pharmaceutics* 11 (4), 193. doi: 10.3390/pharmaceutics11040193

Umamaheshwari, R. B., Ramteke, S., and Jain, N. K. (2004). Anti-Helicobacter pylori effect of mucoadhesive nanoparticles bearing amoxicillin in experimental gerbils model. *AAPS PharmSciTech.* 5 (2), e32. doi: 10.1208/pt050232

Van Citters, G. W., and Lin, H. C. (1999). The ileal brake: a fifteen-year progress report. *Curr. Gastroenterol. Rep.* 1 (5), 404–409. doi: 10.1007/s11894-999-0022-6

Van Citters, G. W., and Lin, H. C. (2006). Ileal brake: neuropeptidergic control of intestinal transit. *Curr. Gastroenterol. Rep.* 8 (5), 367–373. doi: 10.1007/s11894-006-0021-9

Van den Mooter, G. (2006). Colon drug delivery. *Expert Opin. Drug Delivery* 3 (1), 111–125. doi: 10.1517/17425247.3.1.111

Vass, P., Demuth, B., Hirsch, E., Nagy, B., Andersen, S. K., Vigh, T., et al. (2019). Drying technology strategies for colon-targeted oral delivery of biopharmaceuticals. *J. Control Release* 296, 162–178. doi: 10.1016/j.jconrel.2019.01.023

Vita, A. A., Royse, E. A., and Pullen, N. A. (2019). Nanoparticles and danger signals: Oral delivery vehicles as potential disruptors of intestinal barrier homeostasis. *J. Leukocyte Biol.* 106 (1), 95–103. doi: 10.1002/JLB.3MIR1118-414RR

Vong, L. B., Tomita, T., Yoshitomi, T., Matsui, H., and Nagasaki, Y. (2012). An orally administered redox nanoparticle that accumulates in the colonic mucosa and reduces colitis in mice. *Gastroenterology* 143 (4), 1027–36 e3. doi: 10.1053/j.gastro.2012.06.043

Wachsmann, P., Moulari, B., Beduneau, A., Pellequer, Y., and Lamprecht, A. (2013). Surfactant-dependence of nanoparticle treatment in murine experimental colitis. *J. Control Release* 172 (1), 62–68. doi: 10.1016/j.jconrel.2013.07.031

Watts, P. J., Barrow, L., Steed, K. P., Wilson, C. G., Spiller, R. C., Melia, C. D., et al. (1992). The transit rate of different-sized model dosage forms through the human colon and the effects of a lactulose-induced catharsis. *Int. J. Pharm.* 87, 215–221. doi: 10.1016/0378-5173(92)90245-W

Whitehead, L., Fell, J. T., Collett, J. H., Sharma, H. L., and Smith, A. (1998). Floating dosage forms: an *in vivo* study demonstrating prolonged gastric retention. *J. Control Release* 55 (1), 3–12. doi: 10.1016/S0168-3659(97)00266-6

Wilding, I. R., Davis, S. S., Bakhshaee, M., Stevens, H. N., Sparrow, R. A., and Brennan, J. (1992). Gastrointestinal transit and systemic absorption of captopril from a pulsed-release formulation. *Pharmaceut. Res.* 9 (5), 654–657. doi: 10.1023/A:1015806211556

Wilson, D. S., Dalmasso, G., Wang, L., Sitaraman, S. V., Merlin, D., and Murthy, N. (2010). Orally delivered thioketal nanoparticles loaded with TNF-alpha-siRNA target inflammation and inhibit gene expression in the intestines. *Nat. Mater.* 9 (11), 923–928. doi: 10.1038/nmat2859

Xiao, B., and Merlin, D. (2012). Oral colon-specific therapeutic approaches toward treatment of inflammatory bowel disease. *Expert Opin. Drug Deliv.* 9 (11), 1393–1407. doi: 10.1517/17425247.2012.730517

Xiao, B., Laroui, H., Ayyadurai, S., Viennois, E., Charania, M. A., Zhang, Y., et al. (2013). Mannosylated bioreducible nanoparticle-mediated macrophage-specific TNF-alpha RNA interference for IBD therapy. *Biomaterials* 34 (30), 7471–7482. doi: 10.1016/j.biomaterials.2013.06.008

Xiao, B., Laroui, H., Viennois, E., Ayyadurai, S., Charania, M. A., Zhang, Y., et al. (2014). Nanoparticles with surface antibody against CD98 and carrying CD98

small interfering RNA reduce colitis in mice. *Gastroenterology* 146 (5), 1289–300 e1-19. doi: 10.1053/j.gastro.2014.01.056

Xiao, B., Yang, Y., Viennois, E., Zhang, Y., Ayyadurai, S., Baker, M., et al. (2014). Glycoprotein CD98 as a receptor for colitis-targeted delivery of nanoparticle. *J. Mater. Chem. B Mater. Biol. Med.* 2 (11), 1499–1508. doi: 10.1039/c3tb21564d

Yang, L., Chu, J. S., and Fix, J. A. (2002). Colon-specific drug delivery: new approaches and *in vitro*/*in vivo* evaluation. *Int. J. Pharm.* 235 (1-2), 1–15. doi: 10.1016/S0378-5173(02)00004-2

Yang, L. (2008). Biorelevant dissolution testing of colon-specific delivery systems activated by colonic microflora. *J. Control Release* 125 (2), 77–86. doi: 10.1016/j.jconrel.2007.10.026

Yin, Y., Chen, D., Qiao, M., Lu, Z., and Hu, H. (2006). Preparation and evaluation of lectin-conjugated PLGA nanoparticles for oral delivery of thymopentin. *J. Control Release* 116 (3), 337–345. doi: 10.1016/j.jconrel.2006.09.015

Youngren, S. R., Mulik, R., Jun, B., Hoffmann, P. R., Morris, K. R., and Chougule, M. B. (2013). Freeze-dried targeted mannosylated selenium-loaded nanoliposomes: development and evaluation. *AAPS PharmSciTech.* 14 (3), 1012–1024. doi: 10.1208/s12249-013-9988-3

Yu, M., Yang, Y., Zhu, C., Guo, S., and Gan, Y. (2016). Advances in the transepithelial transport of nanoparticles. *Drug Discovery Today* 21 (7), 1155–1161. doi: 10.1016/j.drudis.2016.05.007

Yu, X., Wen, T., Cao, P., Shan, L., and Li, L. (2019). Alginate-chitosan coated layered double hydroxide nanocomposites for enhanced oral vaccine delivery. *J. Colloid Interface Sci.* 556, 258–265. doi: 10.1016/j.jcis.2019.08.027

Zema, L., Maroni, A., Foppoli, A., Palugan, L., Sangalli, M. E., and Gazzaniga, A. (2007). Different HPMC viscosity grades as coating agents for an oral time and/or site-controlled delivery system: an investigation into the mechanisms governing drug release. *J. Pharm. Sci.* 96 (6), 1527–1536. doi: 10.1002/jps.20802

Zhang, X., and Wu, W. (2014). Ligand-mediated active targeting for enhanced oral absorption. *Drug Discovery Today* 19 (7), 898–904. doi: 10.1016/j.drudis.2014.03.001

Zhang, N., Ping, Q. N., Huang, G. H., and Xu, W. F. (2005). Investigation of lectin-modified insulin liposomes as carriers for oral administration. *Int. J. Pharm.* 294 (1-2), 247–259. doi: 10.1016/j.ijpharm.2005.01.018

Zhang, N., Ping, Q., Huang, G., Xu, W., Cheng, Y., and Han, X. (2006). Lectin-modified solid lipid nanoparticles as carriers for oral administration of insulin. *Int. J. Pharm.* 327 (1-2), 153–159. doi: 10.1016/j.ijpharm.2006.07.026

Zhang, Z., Huang, Y., Gao, F., Bu, H., Gu, W., and Li, Y. (2011). Daidzein-phospholipid complex loaded lipid nanocarriers improved oral absorption: *in vitro* characteristics and *in vivo* behavior in rats. *Nanoscale* 3 (4), 1780–1787. doi: 10.1039/c0nr00879f

Zhang, Z., Huang, J., Jiang, S., Liu, Z., Gu, W., Yu, H., et al. (2013a). Porous starch based self-assembled nano-delivery system improves the oral absorption of lipophilic drug. *Int. J. Pharm.* 444 (1-2), 162–168. doi: 10.1016/j.ijpharm.2013.01.021

Zhang, J., Tang, C., and Yin, C. (2013b). Galactosylated trimethyl chitosan-cysteine nanoparticles loaded with Map4k4 siRNA for targeting activated macrophages. *Biomaterials* 34 (14), 3667–3677. doi: 10.1016/j.biomaterials.2013.01.079

Zhang, J., Zhu, X., Jin, Y., Shan, W., and Huang, Y. (2014). Mechanism study of cellular uptake and tight junction opening mediated by goblet cell-specific trimethyl chitosan nanoparticles. *Mol. Pharm.* 11 (5), 1520–1532. doi: 10.1021/mp400685v

Zhang, X., Qi, J., Lu, Y., He, W., Li, X., and Wu, W. (2014). Biotinylated liposomes as potential carriers for the oral delivery of insulin. *Nanomedicine* 10 (1), 167–176. doi: 10.1016/j.nano.2013.07.011

Zhang, S., Langer, R., and Traverso, G. (2017). Nanoparticulate Drug Delivery Systems Targeting Inflammation for Treatment of Inflammatory Bowel Disease. *Nano Today* 16, 82–96. doi: 10.1016/j.nantod.2017.08.006

Zhao, J., Li, X., Luo, Q., Xu, L., Chen, L., Chai, L., et al. (2014). Screening of surface markers on rat intestinal mucosa microfold cells by using laser capture microdissection combined with protein chip technology. *Int. J. Clin. Exp. Med.* 7 (4), 932–939.

Conflict of Interest: The author declares that the research was conducted in the absence of any commercial or financial relationships that could be construed as a potential conflict of interest.

Advantages of publishing in Frontiers

OPEN ACCESS
Articles are free to read for greatest visibility and readership

FAST PUBLICATION
Around 90 days from submission to decision

HIGH QUALITY PEER-REVIEW
Rigorous, collaborative, and constructive peer-review

TRANSPARENT PEER-REVIEW
Editors and reviewers acknowledged by name on published articles

Frontiers
Avenue du Tribunal-Fédéral 34
1005 Lausanne | Switzerland

Visit us: www.frontiersin.org
Contact us: info@frontiersin.org | +41 21 510 17 00

REPRODUCIBILITY OF RESEARCH
Support open data and methods to enhance research reproducibility

DIGITAL PUBLISHING
Articles designed for optimal readership across devices

FOLLOW US
@frontiersin

IMPACT METRICS
Advanced article metrics track visibility across digital media

EXTENSIVE PROMOTION
Marketing and promotion of impactful research

LOOP RESEARCH NETWORK
Our network increases your article's readership